Studies on Electron Swarms in Gases using a Propagator Method

プロパゲータ法による気体中電子スオームに関する研究

Hirotake SUGAWARA
菅 原 広 剛

(1)

Studies on Electron Swarms in Gases using a Propagator Method

プロパゲータ法による 気体中電子スオームに関する研究

by
Hirotake Sugawara
菅原広剛

Hokkaido University, Japan
December, 1996

ACKNOWLEDGMENTS

The author would sincerely wish to thank his supervisor, Professor Yosuke Sakai of Hokkaido University, for his helpful guidance and support.

The author would also like to thank Professors Hiroaki Tagashira and Peter Lowel George Ventzek of Hokkaido University for their stimulating suggestion and kind support.

Thanks are also due to Professor Mitsuo Shimozuma and Doctor Hiroyuki Date of Medical College of Hokkaido University, Professor Kazutaka Kitamori of Hokkaido Institute of Technology, Professors Yoshiyuki Ohmori and Satoru Nakamura of Hokkaido Polytechnic College, Professors Hidenori Itoh and Kohki Satoh of Muroran Institute of Technology, Professor Toshiyuki Taniguchi, Professor Masafumi Suzuki and Doctor Takeshi Miura of Akita University, Professor Gen Tochitani of Saga University, Doctor Haruaki Akashi of National Defence Academy, and other colleagues in the author's laboratory for their interest and valuable discussion.

Last, but not least, the author would like to thank those dearest to him, his family and his wife for their constant encouragement and support.

Contents

1 Introduction 1
- 1.1 Motivation · · · 1
- 1.2 Analysis Techniques of Electron Swarms · · · 2
  - 1.2.1 Particle Model · · · 2
  - 1.2.2 Continuum Model · · · 3
  - 1.2.3 Hybrid Model · · · 4
- 1.3 Requirements for Analysis Techniques · · · 5
- 1.4 Objective of the Present Work · · · 6
- 1.5 Synopsis of Each Chapter · · · 6

References · · · 8

2 Propagator Method 9
- 2.1 Introduction · · · 9
- 2.2 Electron Distribution in Phase Space · · · 10
- 2.3 The Boltzmann Equation · · · 11
  - 2.3.1 Drift and Acceleration · · · 11
  - 2.3.2 Collision and Scattering · · · 12
- 2.4 Cells in Phase Space · · · 14
- 2.5 Propagator · · · 15
  - 2.5.1 Drift Propagator · · · 15
  - 2.5.2 Collision Propagator · · · 17
- 2.6 Computational Scheme · · · 18
- 2.7 Chapter Summary · · · 20

References · · · 21

3 Spatial Relaxation Processes of Electron Swarms under Steady-State Townsend Conditions 22
- 3.1 Introduction · · · 22
- 3.2 Computational Conditions · · · 23
  - 3.2.1 Analysis Model · · · 23
  - 3.2.2 The Law of Energy Conservation · · · 23
  - 3.2.3 Electron Flow in Velocity Space · · · 25
  - 3.2.4 Collision and Scattering · · · 27
- 3.3 Simulation Conditions · · · 29
  - 3.3.1 Steady-State Townsend Condition · · · 29
  - 3.3.2 Gases, Electric Fields, and Other Conditions · · · 30
- 3.4 Results and Discussion · · · 31
  - 3.4.1 Swarm Parameters · · · 31
  - 3.4.2 Electron Energy Distribution · · · 34
  - 3.4.3 Numerical Diffusion · · · 37

3.5 Chapter Summary 38
References 39

4 The Electron Energy Distributions under Steady-State Townsend and Pulsed Townsend Conditions 40
4.1 Introduction 40
4.2 Simulation Model and Conditions 41
4.2.1 Steady-State Townsend Condition 41
4.2.2 Calculation Model 42
4.2.3 Calculation Scheme 43
4.2.4 Simulation Conditions 45
4.3 Results and Discussion 45
4.3.1 Swarm Parameters in Argon 46
4.3.2 Swarm Parameters in Argon / Fluorine Mixture 48
4.3.3 Features of the Present Propagator Method 48
4.4 Observation-System-Dependent Configurations 49
4.5 Chapter Summary 50
References 51

5 Properties of Electron Swarms in the Upstream Region of an Electron Source 52
5.1 Introduction 52
5.2 Analysis Model 53
5.3 Relations among Swarm Parameters 54
5.3.1 Relative Density Gradient Coefficient 54
5.3.2 Drift Velocity 55
5.4 Calculation for the Electron Velocity Distribution 56
5.4.1 Computational Configuration for the Upstream Region 56
5.4.2 Gases and Electric Fields 57
5.5 Results and Discussion 58
5.5.1 Electron Energy Distribution 58
5.5.2 Electron Swarm Parameters 60
5.6 A Practical Example of Backward Diffusion 61
5.6.1 Effect of Absorbing Anode 61
5.6.2 Monte Carlo Simulation 62
5.7 Chapter Summary 64
References 65

6 Evaluation of the Centroid Drift Velocity of an Electron Swarm using Moment Equations 66
6.1 Introduction 66
6.2 Effects of Ionization and Electron Attachment 67
6.3 Calculation Method 68
6.3.1 Moment Equations 68
6.3.2 Propagator Method 70
6.4 Simulation Conditions 70
6.5 Results and Discussion 71
6.5.1 The Energy and Centroid Distributions 71
6.5.2 Moment Distribution 71
6.5.3 The Moment Generation Rate 71

6.5.4 Computational Load and Stability of the Present Propagator Method 77
6.6 Chapter Summary 79
References 80

7 Conclusions **81**
7.1 Summary of the Present Work 81
7.2 Future Orientation of the Study 83

Author's Publications Related to the Present Work **85**

A Derivation of Relations between Drift Velocities **88**
A.1 Relation Described in Real Space 88
A.2 Relation Described in Velocity Space 90

B FORTRAN 77 Programs of Propagator Method **92**
B.1 Spatial Relaxation Processes in He 92
B.2 Drift Equilibrium $F(\epsilon)$ in Ar/F_2 (steady-state Townsend condition) . . . 97
B.3 Drift Equilibrium $F(\epsilon)$ in Ar (pulsed Townsend condition) 106
B.4 $F(\epsilon)$ in SF_6 in the Upstream Region 111
B.5 Moment Equations for Wr in a Model Gas 117

List of Figures

2.1 Six-Dimensional Phase Space 10
2.2 Electron Drift 16
2.3 Electron Distribution after Energy Loss 18
2.4 Electron Collision and Scattering 19

3.1 Parallel Plane Electrodes Model 24
3.2 Cells for Parallel Plane Electrodes Model 24
3.3 Cells in Three-Dimensional Velocity Space 26
3.4 Evaluation of Electron Flow out of a Cell 26
3.5 Electron Distribution after Ionization 28
3.6 The Electron Collision Cross Sections of He 30
3.7 The Electron Collision Cross Sections of Ar 31
3.8 Electron Swarm Parameters in He 33
3.9 Electron Swarm Parameters in Ar 34
3.10 The Electron Energy Distribution in He 35
3.11 The Electron Energy Distribution in Ar 36
3.12 Treatment of Electron Drift 37

4.1 Systems of Electron Swarm Observation 40
4.2 Exponential Spatial Growth of Electron Flow 42
4.3 Electron Inflow and Outflow for a Slab 45
4.4 The Electron Collision Cross Sections of F_2 46
4.5 The SST Electron Energy Distribution in Ar 47
4.6 The SST Electron Energy Distribution in Ar / F_2 Mixture 47
4.7 Differential Operators for SST / PT Conditions 50
4.8 The PT Electron Energy Distribution in Ar 51

5.1 Definitions of Upstream and Downstream Regions 53
5.2 The Electron Collision Cross Sections of SF_6 57
5.3 The Electron Collision Cross Sections of a Ramp Model Gas 58
5.4 The Electron Energy Distributions in the Upstream and Downstream Regions 59
5.5 The Parity of the Number of Crossings 61
5.6 Complementarity Theorem 61
5.7 Effects of Absorbing Anode 62
5.8 The Electron Energy Distribution in front of Anode 63
5.9 The Electron Number Density Gradient in front of Anode 63

6.1 Motion of the Centroid of an Electron Swarm 68
6.2 Cell Configuration for Simultaneous Calculations 70
6.3 The Electron Drift Velocities in F_2, SF_6 and Ar 72

6.4 The Moment Distribution in F_2 73
6.5 The Moment Distribution in SF_6 73
6.6 The Moment Distribution in Ar 74
6.7 The Moment Generation Rate in SF_6 75
6.8 The Moment Generation Rate in Ar 76
6.9 The Moment Generation Rate in a Model Gas 78

List of Tables

1.1 Approaches for Categorization of Analysis Methods 2
1.2 Categories of Typical Electron Swarm Analyses 3

2.1 Collision Processes Considered in Electron Swarm Analyses 13
2.2 Coordinate Systems 14

3.1 Electron Displacement between Cells in Drift Process 27
3.2 Simulation Conditions for Parallel Plane Electrodes Model 31
3.3 Electron Swarm Parameters in He and Ar 33

4.1 The Numbers of Electrons Representing Electron Increase and Decrease . 42
4.2 Drift Equilibrium Electron Swarm Parameters 48
4.3 Differential Operators for SST / PT Conditions 49

5.1 Conditions for Electron Swarm Analyses in the Upstream Region 57
5.2 Electron Swarm Parameters in Upstream and Downstream Regions . . . 60

Chapter 1

Introduction

1.1 Motivation

Weakly ionized plasmas have found applications in a number of industrial technologies; *e.g.* as plasma sources for manufacturing electronic devices such as solar cells and ULSIs, ion sources, gas lasers, light sources, plasma displays, ozonizers and pollution control. Weakly ionized plasmas are also called thermally non-equilibrium discharge plasmas because the electron temperature, which is usually more than tens of thousands K, is much higher than those of the other species in the plasmas. It is this fact that enables us to efficiently utilize the electron energy to induce physical and chemical reactions in industrial applications that would require either prohibitively high gas temperatures or could not be achieved any other way.

Since plasma-chemical reactions are induced by electrons, it is important to understand their behavior. Electron behavior in plasmas is subject to some fundamental physical principles known as Newton's equation of motion and Maxwell's electro-magnetic equations. However, plasmas contain very large numbers of electrons. This allows the use of statistics to describe electron behavior macroscopically. The study of electron swarms, or groups of huge numbers of electrons, has the goal of deriving the macroscopic characteristics of electrons in plasmas based on the microscopic electron behavior under the action of the electric field, which is one of the most important basis of the plasma phenomena.

Properties of an electron swarm are described by quantities known as electron swarm parameters or simply electron transport coefficients. Some are the mean electron energy or the electron temperature, the ionization frequency and coefficient, the electron attachment frequency and coefficient, the electron drift velocities and the electron diffusion coefficients. Electron swarm parameters not only represent characteristics of an electron swarm itself, but can be used to quantify physical phenomena in industrial plasma applications. Examples of such quantities are the rate coefficients of chemical dissociation for generating reactive species in plasma processes and the excitation frequencies for producing excited species for photon emission in light sources. These physical and chemical processes of electrons in plasmas depend strongly on the electron energy, and most of the swarm parameters are derived from the electron energy distribution. Therefore, the electron energy distribution is one of the most important profiles of electron swarms for developing and optimizing plasma applications.

Computer simulation is an influential technique for analyzing electron behavior in plasmas. An advantage of computer simulation is that various experimental conditions to determine the electron behavior can be easily examined; *e.g.* kind of gas medium, the gas pressure, the applied electric field and initial and boundary conditions. Even an

experimentally difficult condition may be investigated by means of computer simulation.

On the other hand, the computational load required for plasma investigations tends to increase in some cases. Industrial plasma systems includes much complicated physical processes such as the effects of space charge, ions, magnetic field and photo-reactions. In addition, some of them have quite different time scales which may be from the order of nano seconds to more than the order of a second. In spite of the remarkable development of recent computer hardware, computational efficiency is still one of the primary requirements for plasma simulations as well as their accuracy and generality.

Utilizing parallel processing techniques is a way of obtaining high efficiency. However, efforts to introduce the parallel processing techniques to plasma analyses have just started, and their future orientation is still under exploration.

A simulation technique named propagator method (PM) is focused on here. PM is expected to be suitable for vector processing which is a kind of parallel computing technique. In the present thesis, basic implementation techniques of a PM are investigated based on some typical models for electron swarm analyses. Then, advantages of the PM are demonstrated by performing electron swarm analyses under various conditions which include severe ones for conventional simulation techniques. The primary objective of the present work is to obtain new knowledge of properties of electron swarms in order to contribute the plasma investigation. At the same time, it is considered as a future orientation of the present work to establish a PM as a general plasma analysis method which can perform accurate and efficient simulations by utilizing vector processing technique as well.

1.2 Analysis Techniques of Electron Swarms

There are many approaches to categorize techniques of computer simulations for electron swarm analysis. Some points of view for the categorization are listed in table 1.1. Monte Carlo simulation, Boltzmann equation analysis, continuity equation analysis and propagator method, which are typical techniques of electron swarm analysis, can be characterized as shown in table 1.2. Characteristics of these techniques are mentioned briefly in the following subsections.

Table 1.1: Approaches for categorization of electron swarm analysis methods.

treatment of medium	particle model / continuum model
occurrence of event	stochastic model / deterministic model
description of motion	Eulerian description / Lagrangian description (spatial description) / (material description)
principle of motion	kinetic model / fluid model / hybrid model
field of motion	phase space / velocity space / real space

1.2.1 Particle Model

In a particle model simulation, an electron swarm is regarded as a group of discrete electrons. The electrons are assumed to behave more or less individually. Microscopic motion of each individual particle is treated as free flight under the electric field and collision with other particles. A Monte Carlo simulation (MCS), introduced by Itoh and Musha (1960)

Table 1.2: Categories of typical electron swarm analyses. MCS, Monte Carlo simulation; BEq, Boltzmann equation analysis; PM, propagator method; ContEq, continuity equation.

method	medium	event	description	motion	field
MCS	particle	stochastic	Lagrangian	kinetic	phase space
BEq, PM	continuum	deterministic	Eulerian	kinetic	phase space
ContEq	continuum	deterministic	Eulerian	fluid	real space

for electron swarm analyses, is a typical example of a particle model. Random motion of charged particles is simulated using pseudo-random numbers to determine occurrence and kind of collision and the scattering angles. Stochastic behavior of charged particles can be simulated by MCS. Each particle is labeled and traced, thus, a point under observation in a particle model simulation accompanies with a moving particle. This kind of simulation methods that trace varying positions of particles is generically called material description or Lagrangian description.

Particle model simulations have some advantages; microscopic behavior can be simulated individually, boundary conditions can be treated keeping their physical aspect, and statistical approach is available in case analytical calculation is difficult. However, since a typical plasma contains a prohibitively large number of charged particles more than 10^8 cm^{-3} to 10^{12} cm^{-3}, it is actually impossible to simulate all of the electrons in the plasma. Then, statistical sampling technique and a scaling (weighting) method are usually adopted in MCS. Nonetheless, a large enough number of particle samples are required in order to avoid statistical fluctuation. This requirement results in increasing calculation time. Despite several improving techniques for efficient MCS have been proposed (*e.g.* Skullerud and Kuhn 1983, Nanbu 1994), the individual random motion of particles is a bottleneck in the way of vector processing. The problem of calculation time is still a primary difficulty of MCS.

1.2.2 Continuum Model

In a continuum model (*e.g.* Graves and Jensen 1986), species constituting a plasma are treated as continuous mediums. Their homogeneities are assumed in a volume element which is macroscopically small enough to obtain sufficient resolution and microscopically large enough so that the atomic-ordered fluctuation of the number density of a plasma species does not appear (Tanahashi 1991). In case a point under observation is fixed on a volume defined at a position and motion of the continuum is treated as inflow and outflow through the volume surface, this kind of treatment is called spatial description or Eulerian description, which is in dual or complementary relation with Lagrangian description.

Simulation techniques of electron swarms based on continuum model are originally described by the Boltzmann equation (BEq), which represents flow of charged particles in six-dimensional phase space in a manner of differential equation. Here, phase space means the direct product of real space and velocity space. A variety of analysis techniques have been proposed based on the BEq. These techniques can be classified according to their mathematical approach and the field of electron motion in which the BEq is described.

Most generally, electron motion is described in phase space, in which the position-dependent electron energy distribution can be defined. Simulation methods treating phase space involve "full" information on the electron motion; the position and velocity. Electron motion is described by kinetics based on the electron velocity distribution.

A mathematical way of solving the BEq in phase space is series expansion using orthogonal systems of function. The BEq is represented as a series of simultaneous differential equations in this technique. Typically, Legendre's polynomials (Ginzburg and Gurevich 1960) and Fourier transform (Parker and Lowke 1969, Tagashira *et al.* 1977, Date *et al.* 1992) are chosen for expanding the BEq in velocity space and real space, respectively. Kitamori *et al.* (1980) proposed a method of "direct estimation of moment", in which a series of moment equations representing the relation between electron swarm parameters are derived from the BEq. Kondo and Tagashira (1990, 1993) treated the BEq as an eigenvalue problem expressed in a matrix form of Burnett function expansion. Other mathematical approaches to the BEq are "path integral method" (Skullerud 1983, Segur *et al.* 1986) and "flight time integral method" (Ikuta and Murakami 1987). These methods are based on the integral of the dispersion function which represents the propagation of charged particles in phase space. These methods are oriented to analytic solution. In contrast, "propagator method" (*e.g.* Drallos and Wadehra 1989, Sommerer *et al.* 1989) is a dynamic numerical calculation method based on Green's function representing the electron propagation.

Simulations performed in velocity space misses position-dependent information of electron energy distribution. However, they still can perform self-consistent calculation based on kinetics described in velocity space when the physical processes under consideration are position-independent. All of the simulation methods mentioned in the preceding paragraph can be modified for calculation in velocity space by integrating the electron energy distribution with respect to the position. Simulations performed in phase space or velocity space are called kinetic models.

An example of the simulation methods treating only the spatial electron distribution in real space, which is no longer the "energy" distribution, is continuity equation (ContEq) analysis. ContEq analyses are traditionally called fluid models as well. A fluid model simulation has an advantage that their calculation scheme is simple and traditionally well-studied. However, it is difficult to perform self-consistent and stand-alone simulations by itself. Some electron transport coefficients, which is not derived by ContEq, must be imported from external calculations by another kinetic model in order to quantify the electron flow in real space. In the simplest cases, the transport coefficients under drift equilibrium conditions, under which the energy gain and loss of an electron swarm balance, are applied to ContEq analyses as a function of the electric field or the mean electron energy. However, the electron energy distribution is not unique for a value of those variables when the electron swarm is under transient, and most of plasma-chemical processes have dependence on the electron energy distribution which is missing in ContEq analyses. Validity of applying the drift equilibrium transport coefficients to a ContEq analysis must be verified elsewhere. Correspondence between mathematical expressions of boundary conditions required to solve the ContEq and their physical aspects must be validated as well.

1.2.3 Hybrid Model

The aim of a simulation based on hybrid model is to combine advantages of different kinds of simulation models. Combination of these models can be chosen depending on the purpose of a simulation.

Examples of the hybrid model simulations can be found in Belenguer and Boeuf (1990) and Sato and Tagashira (1991), in which position-dependent electron behavior is analyzed. MCS is performed to obtain the local electron energy distribution, and ContEq are combined for calculation of the spatial aspect. Self-consistency of the MCS and calculation

speed of ContEq are the advantages in this case. Their work also attempted to take thermally non-equilibrium effects into account of ContEq analysis techniques.

1.3 Requirements for Analysis Techniques

In general, properties required for techniques of plasma analyses would be physical exactitude, self-consistency, simplicity of treatment for boundary conditions, statistical and numerical stability, computational efficiency, generality for extension of simulation models, and so forth. Although various orders of priority for these properties can be considered depending on the simulation objectives, the orientation of the development of the analysis techniques are determined by these requirements.

For physical exactitude, a rigid description for the simulated object is required. Mathematical approximation should be chosen as carefully as possible. In case of highly mathematical approach, it is important that the correspondence between a mathematical expression and its physical meaning is always kept clear to verify the physical validity of the expression. Energy balance (Thomas 1969), a kind of the law of energy conservation, and conservation of the number of particles are typical examples of items to confirm the physical validity of simulation results.

Self-consistency is also important for any simulations since it enables stand-alone performance and proves the validity of the simulation results. Self-consistency will be guaranteed by considering kinetics of the electrons. A calculation of the electron energy distribution performed at least in velocity space can be qualified as a stand-alone and self-consistent simulation.

Statistical instability is a problem for MCS. As long as pseudo-random numbers are referred to for choosing one of the possible events, it is difficult to completely remove statistical fluctuation from the sampling in principle. However, some countermeasures such as particle-in-cell method (*e.g.* Boswell and Morey 1988, Surendra and Graves 1991) have been proposed to obtain well-averaged results. On the other hand, in continuum model simulations which assume homogeneity of the continuum and a large enough number of real physical particles in a volume, all possible processes under consideration are treated to occur in proportion to their probabilities deterministically.

The numerical stability of a simulation method including the stability for convergence of solution depends on its characteristics particular to the mathematical approach. Some kinds of instabilities in numerical calculation often appears in simulations using differential operations mainly. Simulation techniques based on integral calculation would be a safer way to avoid this kinds of instabilities.

For computational efficiency, it would be the most promising and steady way to fully utilize parallel processing techniques. Continuum models are suitable for vector processing since most part of the calculation can be described by a common expression form for fluid equations generalized for each position in phase space. Another advantage of continuum model is that the computational load is independent of the number of particles under consideration while the load of MCS is proportional to the number of traced particles. A simulation technique based on continuum model can obtain statistically stable results in case of electro-negative conditions under which the number of particles decreases due to electron attachment, and it can avoid the increase in calculation time even in case of steeply increasing particle population.

1.4 Objective of the Present Work

Propagator method (PM), which is focused on in the present work, is one of the continuum model simulations. This technique is expected to have the possibility to satisfy the requirements mentioned in the preceding section.

PM is originally a general-purpose simulation method for any physical phenomena including penetration processes which are described by Green's function (*e.g.* Hitchon *et al.* 1989). When this method is applied to weakly ionized plasma analyses, it is necessary to modify the PM appropriately based on conditions particular to the plasma phenomena. An objective of the present work is to establish the basis of the PM as an accurate and efficient simulation method of the plasma analyses.

In the present work, physical conditions to be concerned with especially in electron swarm analyses by PM are investigated. Using the PM developed in the present work, properties of electron swarms are investigated under some conditions, including ones severe for conventional simulation methods, in order to demonstrate advantages of the PM.

1.5 Synopsis of Each Chapter

This thesis consists of seven chapters.

Chapter 1, this chapter, is the introduction of this thesis. Background and objectives of the present studies are presented.

In chapter 2, detailed explanations for numerical scheme of the present propagator method (PM) is presented in a generalized form. This chapter involves definitions of terminologies, observation principles, physical processes under consideration, and their numerical treatment.

In chapters 3 through 6, analyses of electron swarm properties are investigated using the present PM.

In chapter 3, spatial relaxation processes of the electron energy distribution between parallel plane electrodes under steady-state Townsend conditions are analyzed. In order to describe the relation between the position and the energy of an electron under the electric field, an appropriate numerical treatment of the law of energy conservation is introduced to the present PM. Position-dependent profiles of the electron energy distribution and electron swarm parameters are clearly reproduced by the present PM.

In chapter 4, a new calculation technique based on PM for obtaining the drift equilibrium electron energy distributions under steady-state Townsend conditions in boundaryless free space is developed. Such electron energy distributions are, experimentally, observed at a position apart from the electron source since long enough distance for spatial relaxation processes is needed. The present PM derives drift equilibrium solutions of the electron energy distribution from calculations for electrons in a slab defined in the drift equilibrium region. Consideration for the relaxation distance required in conventional PM is omitted in the present technique. This calculation technique for steady-state Townsend conditions is deeply related to one for pulsed Townsend conditions. Correspondence of the present calculation methods and the observation systems of electron swarms is discussed compared with the treatment in the Boltzmann equation analyses.

Using this new technique developed in chapter 4, backward diffusion of an electron swarm toward the upstream region of an electron source is investigated in chapter 5. Properties of electron swarms particular to the upstream region are presented. An implicit effect of backward diffusion of electron swarms can be found in behavior of electron swarms in front of absorbing anode as the influence of the anode to the bulk region of a plasma. It

is demonstrated that the effect of the absorbing anode can be explained by the diffusion of electrons toward the upstream direction.

In chapter 6, the centroid drift velocity of an electron swarm is derived from moment equations and calculated using a PM. The centroid drift velocity is calculated only in velocity space while this velocity is originally defined based on the motion of the electron swarm in real space. In the PM developed in this investigation, calculations for the moment equations are performed simultaneously. This calculation scheme suggests a possibility of the PM for parallel processing in addition to simple vector processing.

Chapter 7 is the conclusions of the present work. The present investigations and their results are summarized, and the future orientation of this work is presented.

References

Belenguer Ph and Boeuf J P 1990 *Phys.Rev.A* **41** 4447-59
Boswell R W and Morey I J 1988 *Appl.Phys.Lett.* **52** 21-3
Date H, Kondo K, Yachi S and Tagashira H 1992 *J.Phys.D: Appl.Phys.* **25** 1330-4
Drallos P J and Wadehra 1989 *Phys.Rev.A* **40** 1967-75
Ginzburg V L and Curevich A V 1960 *Sov.Phys.Usp.* **3** 115-46
Graves D B and Jensen K F 1986 *IEEE Trans.Plasma Sci.* **14** 78-91
Hitchon W N G, Koch D J and Adams J B 1989 *J.Comput.Phys.* **83** 79-95
Huxley L G and Crompton R W
1974 *"The Diffusion and Drift of Electrons in Gases"*, *Wiley*, New York
Ikuta N and Murakami Y 1987 *J.Phys.Soc.Jpn.* **56** 115-27
Itoh T and Musha T 1960 *J.Phys.Soc.Jpn.* **15** 1675-80
Kitamori K, Tagashira H and Sakai Y 1980 *J.Phys.D: Appl.Phys.* **13** 535-50
Kondo K and Tagashira H 1990 *J.Phys.D: Appl.Phys.* **23** 1175-83
Kondo K and Tagashira H 1993 *J.Phys.D: Appl.Phys.* **26** 1948-56
Nanbu K 1994 *Jpn.J.Appl.Phys.* **33** 4752-3
Parker J H Jr and Lowke J J 1969 *Phys.Rev.* **181** 290-301
Pitchford L C, O'Neil S V and Rumble J R 1981 *Phys.Rev.A* **23** 294-304
Sato N and Tagashira H 1991 *IEEE Trans.Plasma Sci.* **19** 102-12
Segur P, Yousfi M, Kadri M H and Bordage M C
1986 *Transp.Theory and Stat.Phys.* **15** 705-57
Skullerud H R and Kuhn S 1983 *J.Phys.D: Appl.Phys.* **16** 1225-34
Skullerud H R 1968 *Brit.J.Appl.Phys.* **1** 1567-8
Sommerer T J, Hitchon W N G and Lawler J E 1989 *Phys.Rev.A* **39** 6356-66
Surendra M and Graves D B 1991 *IEEE Trans.Plasma Sci.* **19** 144-57
Tanahashi T 1991 *"GSMAC-FEM;*
Fundamental and Application of Numerical Fluid Dynamics", *IPC*, Tokyo
Tagashira H, Sakai Y and Sakamoto S 1977 *J.Phys.D: Appl.Phys.* **10** 1051-63
Thomas W R L 1969 *J.Phys.B: At.Mol.Phys.* **2** 551-61

Chapter 2

Propagator Method

2.1 Introduction

A term "propagator" means an operator or function that represents the motions of particles, fluid, wave, heat, or any phenomena which propagates or penetrates through space and media. Mathematically, propagators are called Green's function as well. Early examples of analyses using the propagator technique can be found in wave function studies for electron-impact excitation and electron scattering (*e.g.* Kang 1969, Schneider *et al.* 1969). Historically, early approaches were analytic in nature, since early computational resources were rather limited.

In the recent decade, Hitchon *et al.* (1989) described a generalized implementation of a propagator method (PM) for general transport phenomena calculations. Its numerical technique is based on iterative calculations of transport phenomena applied to many small volumes defined in space. In contrast to early analytic approaches, PM is a primitive calculation technique in a sense. The numerical procedure of the PM is simple iterative calculations, instead, PM requires large memory storage for spatial resolution. For this drawback, the PM has just become a practical simulation method in the latest decade due to the remarkable development in computational technology and the increase in computer memory capacity.

In analyses of electron swarms, PM is a numerical technique to solve the Boltzmann equation (BEq) for the electron flow in phase space. Propagator represents the transition probability of electrons from a set of position and velocity coordinates to another set of coordinates. The transition can happen via two kinds of processes; free flight under the influence of an electric field and collisions with gas molecules. Calculation in a PM is performed based on kinetic continuum model. The electron number density as functions of the position in phase space is expressed in Eulerian description. Small sections called cells are defined in phase space and the electron transition between the cells is calculated by the propagator.

Examples of applications of PM for weakly ionized plasma analyses can be found in many references. Drallos and Wadehra (1988, 1989) investigated the electron velocity distribution under a uniform electric field. Sommerer *et al.* (1989) and Mankelevich *et al.* (1991) applied a PM to analyses of cathode fall region of a glow discharge in helium between parallel plate electrodes. Simulations under time-varying RF (radio frequency; 13.56 MHz) electric fields in processing plasmas were presented by Sommerer *et al.* (1991) and Yamanashi *et al.* (1991). Parker *et al.* (1993) and Hitchon *et al.* (1993) verified the validity of kinetics of PM by comparisons with results obtained by other simulation methods.

In the present chapter, description of the electron energy distribution, the physical processes of electrons considered in electron swarm analyses, and their schematic treatment in PM are explained.

2.2 Electron Distribution in Phase Space

The motion of an electron is generally described by the following variables; the position $\boldsymbol{r} = (x, y, z)$, the electron velocity $\boldsymbol{v} = (v_x, v_y, v_z)$, and time t. These six variables except for t constitute a six-dimensional coordinate system of $(\boldsymbol{r}, \boldsymbol{v}) = (x, y, z; v_x, v_y, v_z)$, which is called phase space. The position in real space and the vector of the velocity of an electron are represented as the coordinates in phase space, and the temporal variations of these values is treated as motion in phase space. Since electrons with different velocities can be present at the same position, velocity space is defined independently for each position. Here, three-dimensional real space and three-dimensional velocity space are treated as independent of each other.

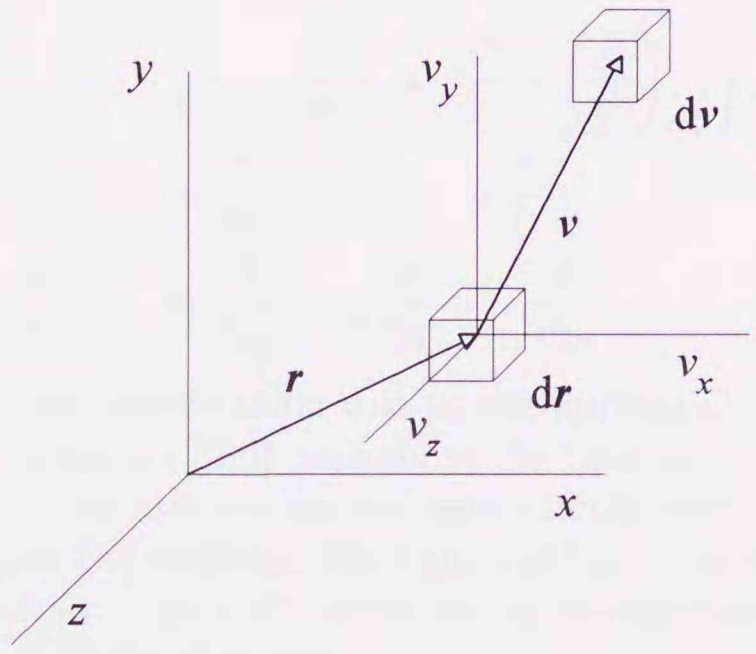

Figure 2.1: Six-dimensional phase space consisting of real space and velocity space $(\boldsymbol{r}, \boldsymbol{v}) = (x, y, z; v_x, v_y, v_z)$. The coordinates of an electron are represented by the position $\boldsymbol{r}$ and the velocity $\boldsymbol{v}$. Different electron behavior can be allowed even at the same position, therefore, velocity space (v_x, v_y, v_z) is defined for each position in real space (x, y, z).

The electron distribution function $f(\boldsymbol{r}, \boldsymbol{v}, t)$ is defined as the electron number density at a position $(\boldsymbol{r}, \boldsymbol{v})$ in phase space at a moment t. $f(\boldsymbol{r}, \boldsymbol{v}, t)$ represents the probability density of presence of electrons. The number of electrons $\mathrm{d}n$ in a volume element $\mathrm{d}\boldsymbol{r}\mathrm{d}\boldsymbol{v}$ at $(\boldsymbol{r}, \boldsymbol{v})$ is described as

$$\mathrm{d}n = f(\boldsymbol{r}, \boldsymbol{v}, t)\mathrm{d}\boldsymbol{r}\mathrm{d}\boldsymbol{v}. \tag{2.1}$$

Electron swarm parameters are derived from $f(\boldsymbol{r}, \boldsymbol{v}, t)$ by integrating $\mathrm{d}n$ with appropriate weighting functions to represent the average values of certain physical quantities. For example, the electron energy $\frac{1}{2}m|\boldsymbol{v}|^2$ is a weighting function for obtaining the mean electron energy $\bar{\epsilon}$ as

$$\bar{\epsilon} = \frac{\int \frac{1}{2}m|\boldsymbol{v}|^2 \mathrm{d}n}{\int \mathrm{d}n}. \tag{2.2}$$

$f(\boldsymbol{r}, \boldsymbol{v}, t)$ may be represented in other forms of the electron distribution function such as $f(\boldsymbol{v}, t)$, $f(v, t)$, and $F(\epsilon, t)$. They are the electron number densities as functions of the

vector electron velocity $\boldsymbol{v}$, the modules of the electron velocity or the electron speed v, and the electron energy ϵ, respectively. Relations among these distributions are

$$f(\boldsymbol{v},t) = \int_{\boldsymbol{r}} f(\boldsymbol{r},\boldsymbol{v},t)\mathrm{d}\boldsymbol{r} \tag{2.3}$$

$$f(v,t) = f(\boldsymbol{v},t)\frac{\mathrm{d}\boldsymbol{v}}{\mathrm{d}v} = 4\pi v^2 f(\boldsymbol{v},t) \tag{2.4}$$

$$F(\epsilon,t) = f(v,t)\frac{\mathrm{d}v}{\mathrm{d}\epsilon} = \frac{1}{mv}f(v,t) \tag{2.5}$$

where $v = |\boldsymbol{v}| = \sqrt{v_x^2 + v_y^2 + v_z^2}$, $\epsilon = \frac{1}{2}mv^2$, and m is the mass of an electron. The terms "the electron energy distribution" and "the electron velocity distribution" are often used equivalently, and "the electron distribution" implies both of the energy distribution and the spatial distribution of electrons in this thesis.

2.3 The Boltzmann Equation

Electron motion as a fluid in phase space is described by the BEq as

$$\frac{\partial}{\partial t}f(\boldsymbol{r},\boldsymbol{v},t) = \left\{-\boldsymbol{v}\cdot\frac{\partial}{\partial \boldsymbol{r}} - \boldsymbol{a}\cdot\frac{\partial}{\partial \boldsymbol{v}} + \left(\frac{\partial}{\partial t}\right)_{\mathrm{coll}}\right\} f(\boldsymbol{r},\boldsymbol{v},t) \tag{2.6}$$

$$\boldsymbol{v}\cdot\frac{\partial}{\partial \boldsymbol{r}} = v_x\frac{\partial}{\partial x} + v_y\frac{\partial}{\partial y} + v_z\frac{\partial}{\partial z} \tag{2.7}$$

$$\boldsymbol{a}\cdot\frac{\partial}{\partial \boldsymbol{v}} = a_x\frac{\partial}{\partial v_x} + a_y\frac{\partial}{\partial v_y} + a_z\frac{\partial}{\partial v_z} \tag{2.8}$$

where $\boldsymbol{a} = (a_x, a_y, a_z)$ is the acceleration due to the applied electric field $\boldsymbol{E}$. The term in the left hand side in equation (2.6) represents the temporal variation of the electron number density at $(\boldsymbol{r},\boldsymbol{v})$. The first and second terms in the right hand side are called the drift terms. They represent the electron inflow and outflow for a cell due to spatial motion and acceleration of electrons. The drift terms are an alternative Eulerian description of Newton's equation of motion for electrons.

The third term in the right hand side is called the collision term. It represents the electron flow in velocity space due to the change of the electron velocity at collisions with other particles in a plasma. For the present analyses of electron swarms, only binary collision with short range forces between an electron and a gas molecule is considered. It is assumed that there is no magnetic field and that the electron number density is low enough so that the space charge field is negligibly small compared to $\boldsymbol{E}$. Mutual interaction between electrons is also neglected.

Physical processes considered in electron swarm analyses are explained in detail in the following subsections.

2.3.1 Drift and Acceleration

The drift process of an electron between two succeeding collisions with gas molecules is a result of free flight between collisions under the acceleration $\boldsymbol{a}$ due to $\boldsymbol{E}$. The electron motion during a free flight is treated as a flow in phase space.

The drift terms in equation (2.6) are typical expressions for a flow in vector field written in Eulerian description:

$$\left(\frac{\partial}{\partial t}\right)_{\mathrm{drift}} f(\boldsymbol{r},\boldsymbol{v},t) = -\boldsymbol{v}\cdot\frac{\partial}{\partial \boldsymbol{r}}f(\boldsymbol{r},\boldsymbol{v},t) - \boldsymbol{a}\cdot\frac{\partial}{\partial \boldsymbol{v}}f(\boldsymbol{r},\boldsymbol{v},t). \tag{2.9}$$

The position-differential and velocity-differential terms represent the inertial motion in real space due to the electron velocity $\boldsymbol{v}$ and the acceleration motion in velocity space due to $\boldsymbol{E}$ applied as the external force, respectively. Since there is no magnetic field, the acceleration $\boldsymbol{a}$ is here simply a function of the position. As an important characteristics of a flow, the stream lines are continuous and unique for each position in phase space. A locus of an electron during a free flight appears as a smooth continuous curve in six-dimensional phase space.

The uniqueness of a stream line can be easily confirmed by considering the motion of an electron in a Lagrangian description. This motion is represented as Newton's equations of motion as

$$\frac{\mathrm{d}}{\mathrm{d}t}\boldsymbol{v}(t) = \boldsymbol{a}\Big(\boldsymbol{r}(t),t\Big) = \frac{e}{m}\boldsymbol{E}\Big(\boldsymbol{r}(t),t\Big) \tag{2.10}$$

$$\frac{\mathrm{d}}{\mathrm{d}t}\boldsymbol{r}(t) = \boldsymbol{v}(t) \tag{2.11}$$

where e and m are the charge and mass of an electron. The electron position and velocity $\Big(\boldsymbol{r}(t),\boldsymbol{v}(t),t\Big)$ during a free flight is deterministically described as a function of the initial position $(\boldsymbol{r}',\boldsymbol{v}',t')$ in phase space as

$$\boldsymbol{v}(t) = \boldsymbol{v}' + \int_{t'}^{t} \boldsymbol{a}\Big(\boldsymbol{r}(t''),t''\Big)\mathrm{d}t'' \tag{2.12}$$

$$\boldsymbol{r}(t) = \boldsymbol{r}' + \int_{t'}^{t} \boldsymbol{v}(t'')\mathrm{d}t''. \tag{2.13}$$

Translating this fact into Eulerian description again, electron motion is treated as the electron flux. The amount of the electron flow and its direction can be explicitly described at any position in phase space when the electron distribution function is given.

2.3.2 Collision and Scattering

Collision processes considered in analyses of electron swarms are mainly those with gas molecules. They are categorized primarily as two kinds according to whether the kinetic energies of an electron and its collision target particle satisfy the energy conservation or not (*e.g.* Sakamoto and Tagashira 1974); elastic and inelastic collisions.

Let us first consider elastic collisions. It is generally assumed that an electron and a gas molecule undergo a hard sphere collision. Elastic collisions are called momentum transfer collisions since the direction of the electron is changed by the collision and differential momentum is transferred to the target particle. The transferred momentum is a function of the mass ratio between an electron and a gas molecule m/M, which is at most 2×10^{-3} for the lightest species of a hydrogen atom and is usually less than 10^{-4} for most of the other species. Although the momentum transfer is small, it affects the electron swarm behavior when the collisions are frequent.

Typical inelastic collisions include excitation, ionization, dissociation of multi-atomic molecules, and electron attachment.

At an excitation collision, a part of the electron energy is given to a gas molecule as the energy to excite an internal electron from a state to another higher energy state. Other excitation collisions include vibrational and rotational excitations of multi-atomic molecules. These processes produce high potential energy particles such as excimers and radicals, which are utilized for industrial applications. Dissociation would work similarly to excitation for electron swarms in the point of view of the energy loss of electrons, although their physical and chemical results are quite different.

Due to ionization collisions, positive ions and secondary electrons are produced by electron impact. Thus the number of electrons in an electron swarm increases due to ionization collisions. Ionization has two functions both to trigger and to sustain an electric discharge through a chain reaction. Ionization collisions may be stepwise or cumulative ionization of molecules in excited states in addition to direct ionization from those in the ground state.

Electron attachment is the capture of an electron by an electro-negative gas molecule, which produces a negative ion. An electron captured by a molecule does not move freely anymore; therefore, the electron is no longer regarded to be an element of an electron swarm. The number of electrons in an electron swarm decreases due to electron attachment. Electron attachment includes dissociative attachment of multi-atomic molecules. Recombination of an electron and a positive ion is a special case of the electron capture. Recombination may be treated in the same way as attachment, except that a neutral molecule is produced instead of a negative ion.

In addition to the collisions mentioned above, super-elastic collision can be considered as a special case, in which an electron obtains the energy from an excited gas molecule.

Super-elastic collision, recombination and stepwise ionization are often neglected in many cases of electron swarm analyses, since the number densities of ions and excited gas molecules are usually assumed to be much lower than those in the ground state.

Typical values of the threshold energy for excitation and ionization are listed in table 2.1 together with reaction processes.

Table 2.1: Collision processes considered in electron swarm analyses and typical values or orders of the energy associated with the reactions.

elastic collision	A	+	e	$\longrightarrow$	A	+	e			$\epsilon \times 2m/M$
excitation	A	+	e_{fast}	$\longrightarrow$	A^*	+	e_{slow}			$5 \sim 15$ eV
vibrational excitation	A	+	e_{fast}	$\longrightarrow$	A^*	+	e_{slow}			~ 0.1 eV
rotational excitation	A	+	e_{fast}	$\longrightarrow$	A^*	+	e_{slow}			~ 0.01 eV
dissociation	AB	+	e_{fast}	$\longrightarrow$	A^*	+	B^*	+	e_{slow}	$5 \sim 10$ eV
direct ionization	A	+	e_{fast}	$\longrightarrow$	A^+	+	e_{slow}	+	e_{slow}	$10 \sim 20$ eV
stepwise ionization	A^*	+	e_{slow}	$\longrightarrow$	A^+	+	e_{slow}	+	e_{slow}	$5 \sim 10$ eV
electron attachment	A	+	e_{slow}	$\longrightarrow$	A^-					
recombination	A^+	+	e_{slow}	$\longrightarrow$	A					
super-elastic collision	A^*	+	e_{slow}	$\longrightarrow$	A	+	e_{fast}			$5 \sim 15$ eV

Electrons are scattered after collisions. The initial velocity of an electron for restarting free flight, which is the speed and direction, is determined based on the condition assumed for each collision process. The electron speed is determined by the residual energy after subtracting the energy loss for inelastic processes. In case of ionization collision, the residual energy is shared by the primary electron impacting a gas molecule and the secondary electron to be ejected from the molecule. The probability density function for the division ratio of the residual energy could be assumed in various ways.

The scattering angle is a function of the injection direction of the impacting electron and the direction should be defined in the center-of-mass system of colliding two particles. However, isotropic scattering in laboratory system can be adopted as an approximation for simplicity in most cases in fundamental studies on electron swarms, when the momentum transfer between an electron and a gas molecule at a collision is negligibly small.

Since the electron velocity changes instantly at a collision, the locus of an electron in velocity space becomes discontinuous at every collision. When an inelastic collision is observed in velocity space, the electron "jumps" from its original position at the energy ϵ to a destination position at $\epsilon - \epsilon_{\text{loss}}$. Electrons undergoing attachment disappear from phase space, and new electrons are generated by ionization collisions.

2.4 Cells in Phase Space

In a propagator method (PM), phase space is divided into small sections which are called cells, and the electron distribution is treated as the number of electrons in each cell. The electron motion in phase space is treated as a movement of the number of electrons from a cell to another cell.

The volume of a cell is, generally, represented as $\Delta \boldsymbol{r} \Delta \boldsymbol{v} = \Delta x \Delta y \Delta z \Delta v_z \Delta v_y \Delta v_z$. A cell is essentially equivalent to a volume element $\mathrm{d}\boldsymbol{r}\mathrm{d}\boldsymbol{v}$. The size of a cell must be macroscopically small enough to obtain sufficient resolution and microscopically large enough for electrons to be treated as a homogeneous continuum (Tanahashi 1991). The electron distribution within a cell is usually assumed to be uniform with respect to the volume element.

Rewriting equation (2.1) for discrete cells, the number of electrons $n_{\Delta \boldsymbol{r}, \Delta \boldsymbol{v}}(t)$ in a cell $\Delta \boldsymbol{r} \Delta \boldsymbol{v}$ at $(\boldsymbol{r}, \boldsymbol{v})$ is represented as

$$n_{\Delta \boldsymbol{r}, \Delta \boldsymbol{v}}(t) = f(\boldsymbol{r}, \boldsymbol{v}, t) \Delta \boldsymbol{r} \Delta \boldsymbol{v}. \tag{2.14}$$

When the electron distribution is calculated in a computer, the number of electrons in each cell is stored in each corresponding element of an array of computer memory. While phase space has infinite width, the memory storage of a computer is finite. Therefore, only a limited part of phase space can be mapped onto the memory array. In case of velocity space, a physical aspect that $f(\boldsymbol{v})$ decays exponentially with increase of $|\boldsymbol{v}|$ roughly, thus finally $f(\infty) = 0$, tells us that even only a limited region around the origin of velocity space can cover most of electrons under consideration if an observation energy range is appropriately chosen. For real space division, presence of boundary such as electrodes and wall may help us to limit the width of real space under consideration.

The way of division for phase space may be chosen depending on geometrical shape of the simulation model in real space. Symmetry of the simulation model enables us to reduce the dimension of phase space, that helps us to save memory storage and computational load. Some typical cell implementation models are listed in table 2.2. In these models, phase space is divided with appropriate cell widths along the coordinate variables.

Table 2.2: Coordinate systems and cell configurations.

model	real space	velocity space
pulsed Townsend observation	integrated	(v, θ)
infinite parallel plane electrodes	(x)	(v, θ)
spherical symmetry	(r)	(v, θ)
axial symmetry	(x, r)	(v, θ, ϕ)

As typical ways of division for velocity space, Cartesian coordinate system (v_x, v_y, v_z) and polar coordinate system (v, θ, ϕ) can be considered mainly, where θ and ϕ are the

polar and azimuthal angles, and $(v_x, v_y, v_z) = (v\cos\theta, v\sin\theta\cos\phi, v\sin\theta\sin\phi)$. Cartesian coordinate system in a PM (*e.g.* Drallos and Wadehra 1988, 1989) is suitable for treatment of acceleration process of electrons since the acceleration motion of electrons under a uniform $\boldsymbol{E}$ is considered to be a parallel shift in velocity space. Polar coordinate system (*e.g.* Sommerer *et al.* 1989) is, on the other hand, suitable for treatment of electron scattering since it is treated more or less isotropically.

More detailed explanation for the division techniques will be given with practical model of analyses in each of following chapters.

2.5 Propagator

Formally, the temporal variation of $f(\boldsymbol{r}, \boldsymbol{v}, t)$ is described using a propagator P as

$$f(\boldsymbol{r}, \boldsymbol{v}, t + \Delta t) = \int_{\boldsymbol{r}', \boldsymbol{v}'} P(\boldsymbol{r}, \boldsymbol{v}; \boldsymbol{r}', \boldsymbol{v}'; \Delta t) f(\boldsymbol{r}', \boldsymbol{v}', t) \mathrm{d}\boldsymbol{r}' \mathrm{d}\boldsymbol{v}'. \tag{2.15}$$

The propagator represents the transition probability of an electron from $(\boldsymbol{r}', \boldsymbol{v}')$ to $(\boldsymbol{r}, \boldsymbol{v})$ during Δt. The temporal variation of the electron energy distribution is succeedingly derived from that at the preceding time step.

In a practical simulation of a PM, phase space is divided into discrete cells and the number of electrons in a cell is calculated instead of the electron number density. Therefore, the propagator is also modified to represent the movement of the number of electrons from $\Delta\boldsymbol{r}'\Delta\boldsymbol{v}'$ to $\Delta\boldsymbol{r}\Delta\boldsymbol{v}$ as

$$n_{\Delta\boldsymbol{r}, \Delta\boldsymbol{v}}(t + \Delta t) = \sum_{\Delta\boldsymbol{r}', \Delta\boldsymbol{v}'} P(\Delta\boldsymbol{r}, \Delta\boldsymbol{v}; \Delta\boldsymbol{r}', \Delta\boldsymbol{v}') n_{\Delta\boldsymbol{r}', \Delta\boldsymbol{v}'}(t) \Delta t. \tag{2.16}$$

The propagator in equation (2.16) can be rewritten as the sum of those for the two processes as mentioned associated with equation (2.6); the drift and collision processes:

$$P(\Delta\boldsymbol{r}, \Delta\boldsymbol{v}; \Delta\boldsymbol{r}', \Delta\boldsymbol{v}') = P_{\mathrm{drift}}(\Delta\boldsymbol{r}, \Delta\boldsymbol{v}; \Delta\boldsymbol{r}', \Delta\boldsymbol{v}') + P_{\mathrm{coll}}(\Delta\boldsymbol{r}, \Delta\boldsymbol{v}; \Delta\boldsymbol{r}', \Delta\boldsymbol{v}'). \tag{2.17}$$

Explicit forms of these two kinds of propagators are presented in following subsections.

2.5.1 Drift Propagator

An electron flying under $\boldsymbol{E}$ draws a smooth continuous stream line in phase space. This is considered as the electron flux $\boldsymbol{\Gamma}$ when the stream line is weighted by the number density of electrons. The electron flux is defined in each of real space and velocity space:

$$\boldsymbol{\Gamma}_{\mathrm{r}}(\boldsymbol{r}, \boldsymbol{v}, t) = \boldsymbol{v} f(\boldsymbol{r}, \boldsymbol{v}, t) \mathrm{d}\boldsymbol{v} \tag{2.18}$$

$$\boldsymbol{\Gamma}_{\mathrm{v}}(\boldsymbol{r}, \boldsymbol{v}, t) = \boldsymbol{a}(\boldsymbol{r}, t) f(\boldsymbol{r}, \boldsymbol{v}, t) \mathrm{d}\boldsymbol{r}. \tag{2.19}$$

Using the electron flux, temporal variation of $f(\boldsymbol{r}, \boldsymbol{v}, t)$ may be written as

$$\frac{f(\boldsymbol{r}, \boldsymbol{v}, t + \Delta t)\mathrm{d}\boldsymbol{r}\mathrm{d}\boldsymbol{v} - f(\boldsymbol{r}, \boldsymbol{v}, t)\mathrm{d}\boldsymbol{r}\mathrm{d}\boldsymbol{v}}{\Delta t}$$

$$= \int_{s_{\mathrm{r}}} \boldsymbol{\Gamma}_{\mathrm{r}}(\boldsymbol{r}, \boldsymbol{v}, t) \cdot \boldsymbol{n}_{\mathrm{r}} \mathrm{d}s_{\mathrm{r}} + \int_{s_{\mathrm{v}}} \boldsymbol{\Gamma}_{\mathrm{v}}(\boldsymbol{r}, \boldsymbol{v}, t) \cdot \boldsymbol{n}_{\mathrm{v}} \mathrm{d}s_{\mathrm{v}} \tag{2.20}$$

where s_{r} and s_{v} represent the surface elements of a cell $\Delta\boldsymbol{r}'\Delta\boldsymbol{v}'$ defined in real space and velocity space, and $\boldsymbol{n}_{\mathrm{r}}$ and $\boldsymbol{n}_{\mathrm{v}}$ are the element vectors normal to the surface elements

respectively. The total outflow of electrons $n_{\text{out},\Delta\boldsymbol{r}',\Delta\boldsymbol{v}'}\Delta t$ flowing out of a cell $\Delta\boldsymbol{r}'\Delta\boldsymbol{v}'$ through the cell surface during Δt is evaluated based on the electron flux:

$$n_{\text{out},\Delta\boldsymbol{r}',\Delta\boldsymbol{v}'}\Delta t = \int_{s_{\text{r}},\text{out}} \boldsymbol{\Gamma}_{\text{r}}(\boldsymbol{r}',\boldsymbol{v}',t)\cdot\boldsymbol{n}_{\text{r}}\mathrm{d}s_{\text{r}}\Delta t + \int_{s_{\text{v}},\text{out}} \boldsymbol{\Gamma}_{\text{v}}(\boldsymbol{r}',\boldsymbol{v}',t)\cdot\boldsymbol{n}_{\text{v}}\mathrm{d}s_{\text{v}}\Delta t. \tag{2.21}$$

This integration is performed with respect to only the outward flux to avoid double counting, since the inward flux for a cell is evaluated elsewhere as the outward flux from other cells. Here, time step Δt must be short enough so that the total amount of electron flow out of a cell during Δt does not exceed the number of electrons $n_{\Delta\boldsymbol{r}',\Delta\boldsymbol{v}'}(t)$ in the cell:

$$\Delta t < \frac{n_{\Delta\boldsymbol{r}',\Delta\boldsymbol{v}'}(t)}{n_{\text{out},\Delta\boldsymbol{r}',\Delta\boldsymbol{v}}}. \tag{2.22}$$

This limitation must be satisfied for all cells.

A destination cell $\Delta\boldsymbol{r}\Delta\boldsymbol{v}$ of the outflowing electrons must be at the neighboring downstream position of the source cell $\Delta\boldsymbol{r}'\Delta\boldsymbol{v}'$. The drift propagator represents the number of outflowing electrons and the destination cells. The division ratio of the outflowing electrons among the destination cells is determined based on the intersections between $\Delta\boldsymbol{r}'\Delta\boldsymbol{v}'$ and $\Delta\boldsymbol{r}\Delta\boldsymbol{v}$.

Since any $\boldsymbol{E}$ can be regarded to be uniform locally, the electron flux out of a cell can be observed as a parallel flow in phase space. The numbers of electrons flowing out of a cell observed in real space and velocity space are given as

$$n_{\text{out,r},\Delta\boldsymbol{r}',\Delta\boldsymbol{v}'}(t)\Delta t = S_{\text{r}}(\Delta\boldsymbol{r})\boldsymbol{\Gamma}_{\text{r},\Delta\boldsymbol{r},\Delta\boldsymbol{v}}(t)\Delta t \tag{2.23}$$

$$n_{\text{out,v},\Delta\boldsymbol{r}',\Delta\boldsymbol{v}'}(t)\Delta t = S_{\text{v}}(\Delta\boldsymbol{v})\boldsymbol{\Gamma}_{\text{v},\Delta\boldsymbol{r},\Delta\boldsymbol{v}}(t)\Delta t \tag{2.24}$$

where S_{r} and S_{v} are the areas of the orthogonal projections of the cell to planes in real space and velocity space perpendicular to $\boldsymbol{\Gamma}_{\text{r}}$ and $\boldsymbol{\Gamma}_{\text{v}}$ respectively. Distribution of the number of electrons to the destination cells are also calculated based on the area of the orthogonal projection of the intersections between a source cell and the destination cells.

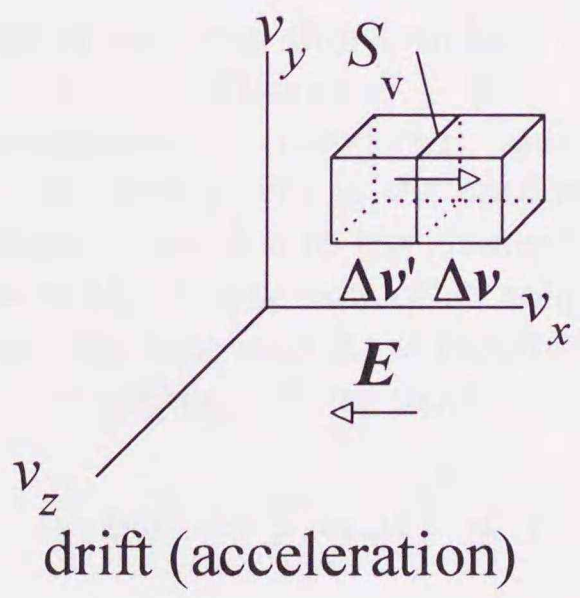

Figure 2.2: Electron acceleration in velocity space. The acceleration due to uniform electric field $\boldsymbol{E}$ appears as parallel shift in velocity space. Electrons in $\Delta\boldsymbol{v}'$ move to the neighboring cell $\Delta\boldsymbol{v}$ through the intersection S_{v}.

The number $n_{\text{out},\Delta\boldsymbol{r}',\Delta\boldsymbol{v}'}$ of electrons flowing out of $\Delta\boldsymbol{r}'\Delta\boldsymbol{v}'$ is subtracted from the cell, and $n_{\text{out},\Delta\boldsymbol{r}',\Delta\boldsymbol{v}'}$ is divided into some fractions for the destination cells $\Delta\boldsymbol{r}\Delta\boldsymbol{v}$. The fractions are displaced and added to the numbers of electrons in the destination cells respectively.

2.5.2 Collision Propagator

Similar to the drift propagator, the collision propagator represents the number of electrons that move from a cell to destination cells. In contrast with that both the position and velocity of an electron vary continuously in the drift process, only the electron velocity changes in the collision process. The position of an electron does not change at a collision. Since the change of the electron velocity occurs instantly, the locus of an electron in phase space becomes discontinuous at every collision. Due to the "jump" in phase space, the collision propagator treats electron transition between cells apart from each other in velocity space.

The number of electrons $\mathrm{d}n_{\mathrm{coll}}$ with velocity $\boldsymbol{v}$ undergoing a collision with an i-th kind of gas molecule during Δt is given by the collision frequency ν_k of process k. It is a function of the cross section q_k, the electron velocity $\boldsymbol{v}$, and the number density N of target molecules:

$$\mathrm{d}n_{\mathrm{coll},i,k}(\boldsymbol{r},\boldsymbol{v})\Delta t = \nu_{i,k}\Delta t f(\boldsymbol{r},\boldsymbol{v})\mathrm{d}\boldsymbol{r}\mathrm{d}\boldsymbol{v} = N_i q_{i,k}(|\boldsymbol{v}|)|\boldsymbol{v}|\Delta t f(\boldsymbol{r},\boldsymbol{v})\mathrm{d}\boldsymbol{r}\mathrm{d}\boldsymbol{v}. \tag{2.25}$$

Hereafter, descriptions for collisions are presented based on the case of a single gas.

In general, the collision term of the BEq can be written as follows (Holstein 1946):

$$\begin{aligned}\left(\frac{\partial}{\partial t}\right)_{\mathrm{coll}} f(\boldsymbol{r},\boldsymbol{v},t)\mathrm{d}\boldsymbol{r}\mathrm{d}\boldsymbol{v}\mathrm{d}t \;=\; & -\sum_k N q_k(|\boldsymbol{v}|)|\boldsymbol{v}| f(\boldsymbol{r},\boldsymbol{v},t)\mathrm{d}\boldsymbol{r}\mathrm{d}\boldsymbol{v}\mathrm{d}t \\ & +\sum_k \int_{\boldsymbol{v}'_k} N q_k(|\boldsymbol{v}'_k|)|\boldsymbol{v}'_k| f(\boldsymbol{r},\boldsymbol{v}'_k,t) Z_k \mathrm{d}\boldsymbol{r}\mathrm{d}\boldsymbol{v}'_k\mathrm{d}t R_{\mathrm{scatt}}(\Delta\omega)\end{aligned} \tag{2.26}$$

where $\boldsymbol{v}'$ is the velocity of a colliding electron, and $\mathrm{d}\omega$ is the solid angle of $\mathrm{d}\boldsymbol{v}$ after the k-th kind of collision viewed relative to the origin of velocity space. R_{scatt} represents the probability of an electron scattering into $\Delta\omega$. When isotropic scattering is assumed, this weight is proportional to the solid angle as

$$R_{\mathrm{scatt}} = \frac{\mathrm{d}\omega}{4\pi}. \tag{2.27}$$

Z_k is the weight of the number of electrons after k-th kind of collisions, which represents the electron generation and loss at a collision; $Z = 2$ for single ionization, $Z = 0$ for electron attachment (or recombination if considered), and $Z = 1$ for the conservative cases. The negative term in equation (2.26) is the outflow term which represents the electrons flowing out of a volume $\mathrm{d}\boldsymbol{r}\mathrm{d}\boldsymbol{v}$ due to the change of velocity at collisions. The positive term represents inflow to the volume from other volumes at higher energies. Here, as well as for the drift process, the time step Δt is required to be short enough so that the probability of an electron to undergo two or more collisions during Δt is negligibly small:

$$(\nu_{\mathrm{T}}\Delta t)^2 = \left(\sum_k \nu_k \Delta t\right)^2 \ll 1 \tag{2.28}$$

where ν_{T} is the total collision frequency.

The relation between $\boldsymbol{v}$ and $\boldsymbol{v}'_k$ for each k is given based on the energy loss at the collision; for example,

$$\frac{1}{2}m|\boldsymbol{v}|^2 \simeq \frac{1}{2}m|\boldsymbol{v}'_{\mathrm{mom}}|^2 \qquad \text{for elastic collision} \tag{2.29}$$

$$\frac{1}{2}m|\boldsymbol{v}|^2 = \frac{1}{2}m|\boldsymbol{v}'_{\mathrm{ex}}|^2 - \epsilon_{\mathrm{ex}} \qquad \text{for excitation} \tag{2.30}$$

$$\frac{1}{2}m|\boldsymbol{v}|^2 = s\left(\frac{1}{2}m|\boldsymbol{v}'_{\mathrm{ion}}|^2 - \epsilon_{\mathrm{ion}}\right) \qquad \text{for ionization} \tag{2.31}$$

where $\boldsymbol{v}'_{\text{mom}}$, $\boldsymbol{v}'_{\text{ex}}$ and $\boldsymbol{v}'_{\text{ion}}$ represent the electron velocity before each collision, and ϵ_{ex} and ϵ_{ion} are the energies for excitation and ionization. The variable s represents the division ratio of the residual energy for a pair of primary and secondary electrons after ionization, where $0 \leq s \leq 1$. The probability density function $P_{\text{div}}(s)$ for s is chosen depending on the given condition.

The collision propagator for discrete cells can be written as

$$P_{\text{coll},k}(\Delta\boldsymbol{r}, \Delta\boldsymbol{v}; \Delta\boldsymbol{r}', \Delta\boldsymbol{v}'_k) = Nq_k(|\boldsymbol{v}'_k|)|\boldsymbol{v}'_k|Z_k R_{\text{coll}} R_{\text{scatt}}(\Delta\omega) \tag{2.32}$$

where the relation between $\Delta\boldsymbol{v}$ and $\Delta\boldsymbol{v}'_k$ is the same as shown in equations (2.29) through (2.31), and $\Delta\omega$ is the solid angle of the destination cell viewed relative to the origin of velocity space. $\Delta\boldsymbol{r} = \Delta\boldsymbol{r}'$ in case of collision. R_{coll} $(0 \leq R_{\text{coll}} \leq 1)$ is a weight determined by a relation of the velocity ranges of $\Delta\boldsymbol{v}'$ and $\Delta\boldsymbol{v}$. When an electron moves from $\Delta\boldsymbol{v}'$ to $\Delta\boldsymbol{v}$ by an inelastic collision with the energy loss ϵ_{loss}, the energy ϵ' of the colliding electron satisfies the following conditions (see figure 2.3):

$$\sqrt{\frac{2\epsilon'}{m}} \in \Delta v', \quad \sqrt{\frac{2(\epsilon' - \epsilon_{\text{loss}})}{m}} \in \Delta v. \tag{2.33}$$

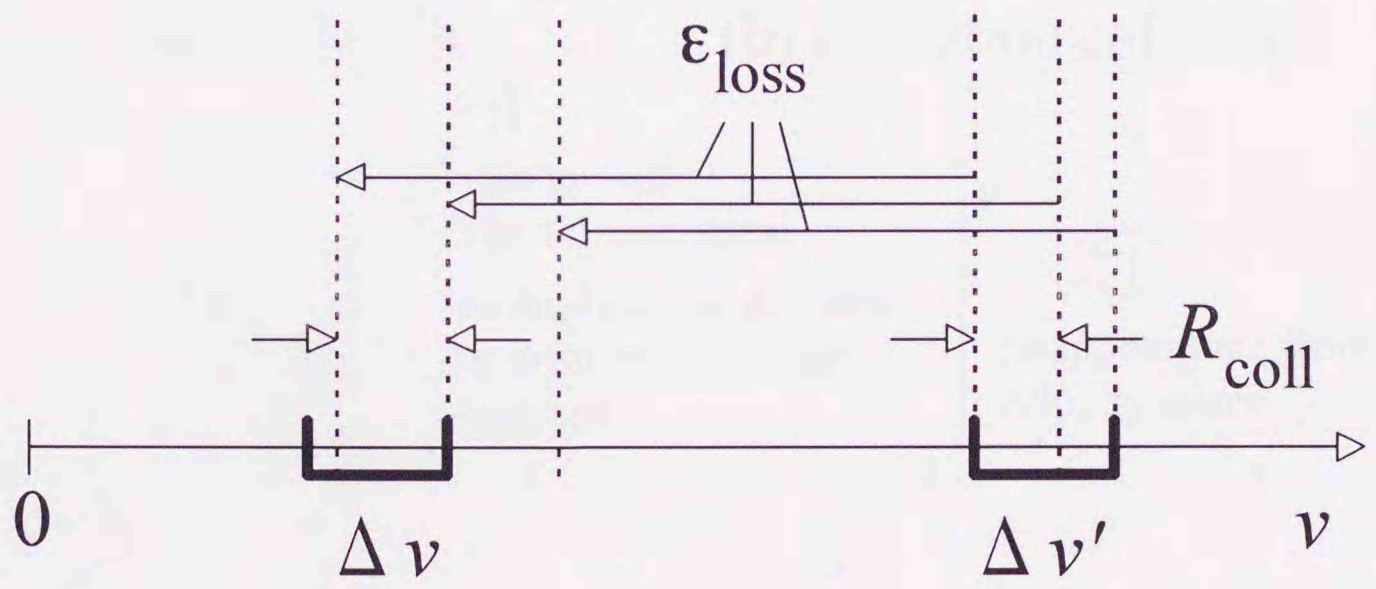

Figure 2.3: The velocity ranges of source and destination cells. A part of electrons in $\Delta v'$ move to Δv.

The number of electrons undergoing collisions is subtracted from a source cell, and distributed to destination cells. The inflow term in equation (2.26) is automatically taken into account as outflow from other cells similarly to the drift process. Visual aspects of the electron displacement in velocity space are shown in figure 2.4.

2.6 Computational Scheme

Basic calculation scheme of a PM is as follows.

Firstly, an appropriate coordinate system for phase space based on the geometrical shape of a simulation model is chosen, and cells are defined by determining the range and the resolution of phase space. In this phase, geometrical symmetry of the model must be considered relevantly to reduce the dimension of phase space, that helps us to save the computational load of memory storage capacity and calculation time.

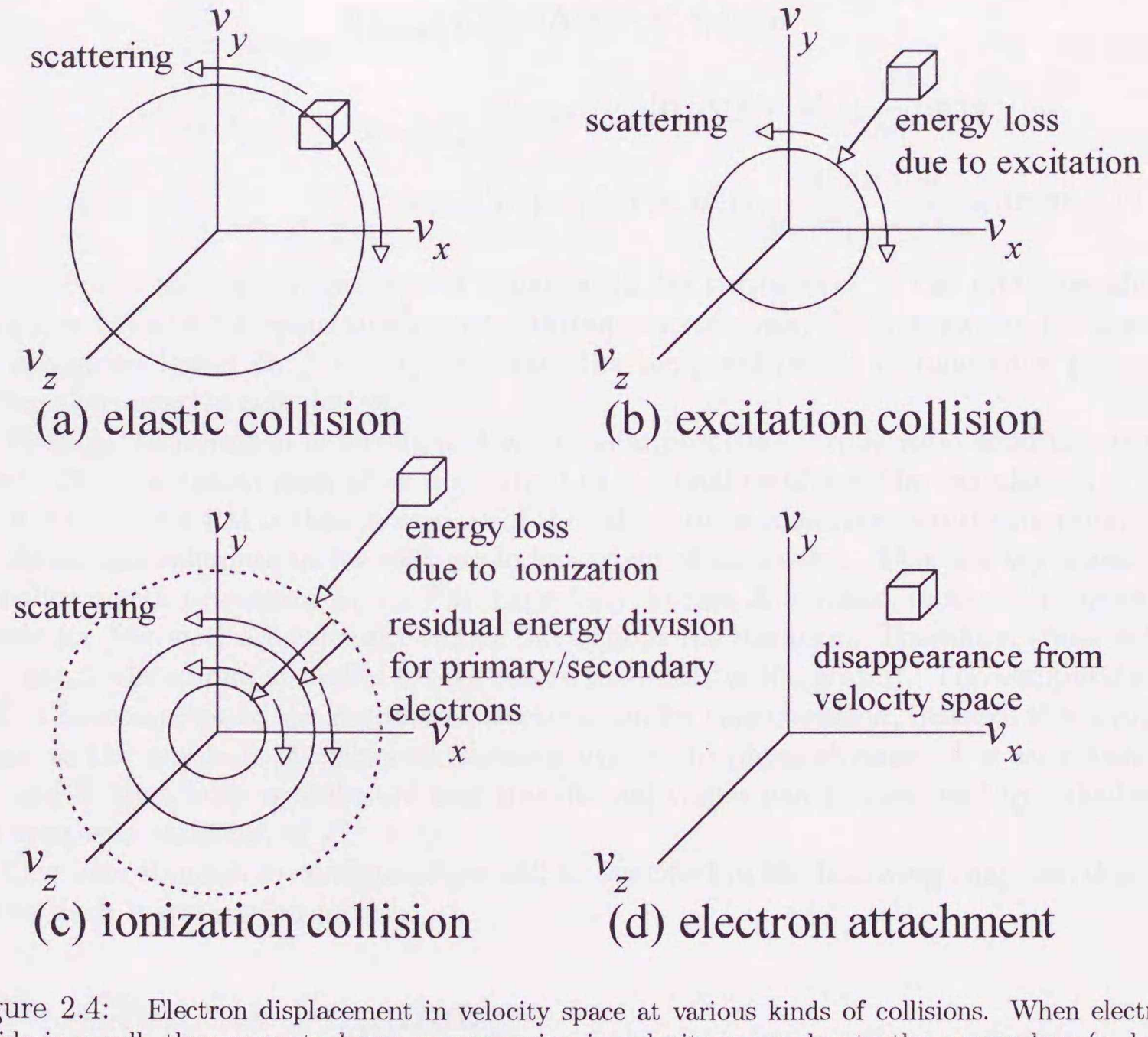

(a) elastic collision (b) excitation collision

(c) ionization collision (d) electron attachment

Figure 2.4: Electron displacement in velocity space at various kinds of collisions. When electrons collide in a cell, they move to lower energy region in velocity space due to the energy loss (a, b, c). However, the energy loss at elastic collisions is negligibly small (a). Scattering after the energy loss is assumed as isotropic. New electrons are generated by ionization (c), and electrons undergoing attachment disappear from velocity space (d).

Secondly, calculation starts with an appropriate initial electron distribution. Two kinds of propagators, for the drift and collision processes, are alternately applied to $f(\boldsymbol{r}, \boldsymbol{v}, t)$ to calculate its temporal variation for every Δt. Here, the physical time passage for a calculation cycle is Δt although two propagators corresponding to a common time step are evaluated sequentially one after the other.

An explicit expression for the processes can be given as

$$\begin{aligned}
&f(\boldsymbol{r}, \boldsymbol{v}, t+\Delta t)\mathrm{d}\boldsymbol{r}\mathrm{d}\boldsymbol{v} \\
&= \left\{1 - \sum_k N q_k(|\boldsymbol{v} - \boldsymbol{a}\Delta t|)|\boldsymbol{v} - \boldsymbol{a}\Delta t|\Delta t\right\} f(\boldsymbol{r} - \boldsymbol{v}\Delta t, \boldsymbol{v} - \boldsymbol{a}\Delta t, t)\mathrm{d}\boldsymbol{r}\mathrm{d}\boldsymbol{v} \\
&\quad + \frac{\mathrm{d}\omega}{4\pi}\int_{|\boldsymbol{v}'|=|\boldsymbol{v}|} N q_{\mathrm{mom}}(|\boldsymbol{v}'|)|\boldsymbol{v}'|\Delta t f(\boldsymbol{r}, \boldsymbol{v}', t)\mathrm{d}\boldsymbol{r}\mathrm{d}\boldsymbol{v}' \\
&\quad + \frac{\mathrm{d}\omega}{4\pi}\sum_k \int_{|\boldsymbol{v}'|^2=|\boldsymbol{v}|^2+\frac{2}{m}\epsilon_{\mathrm{ex},k}} N q_{\mathrm{ex},k}(|\boldsymbol{v}'|)|\boldsymbol{v}'|\Delta t f(\boldsymbol{r}, \boldsymbol{v}', t)\frac{|\boldsymbol{v}'|}{|\boldsymbol{v}|}\mathrm{d}\boldsymbol{r}\mathrm{d}\boldsymbol{v}' \\
&\quad + \frac{\mathrm{d}\omega}{4\pi}\int_{v'^2>v^2+\frac{2}{m}\epsilon_{\mathrm{ion}}} N q_{\mathrm{ion}}(|\boldsymbol{v}'|)|\boldsymbol{v}'|\Delta t f(\boldsymbol{r}, \boldsymbol{v}', t)\frac{4|\boldsymbol{v}'|^2\mathrm{d}|\boldsymbol{v}|}{|\boldsymbol{v}|(|\boldsymbol{v}'|^2 - \frac{2}{m}\epsilon_{\mathrm{ion}})}\mathrm{d}\boldsymbol{r}\mathrm{d}\boldsymbol{v}'. \quad (2.34)
\end{aligned}$$

The terms in the right hand side of equation (2.34) correspond to the processes shown in figures 2.2 and 2.4 respectively. With appropiate intervals, electron swarm parameters are evaluated based on $f(\boldsymbol{r}, \boldsymbol{v}, t)$ to obtain the temporal profile of relaxation processes during the iterative calculation.

Finally, the iteration is terminated when an appropriate termination condition is satisfied. The simulation ends after the output of the final results of the calculation.

A feature of a PM is that most part of the calculations consists of simple summation of products, and calculations for cells are independent of each other. This is a key advantage to utilize vector processing in the PM. Especially, in case $\boldsymbol{E}$ is static, most of the operands except for $f(\boldsymbol{r}, \boldsymbol{v}, t)$ are constant values throughout the iteration. Therefore, those values can be calculated and stored in arrays before the iterative loops start. The computational load is independent of the number of electrons under consideration, instead, it is proportional to the numbers of cells and iteration cycles. In physical sense, it is an advantage of the PM that both equilibrium and transitional values can be obtained by calculating the temporal variation of $f(\boldsymbol{r}, \boldsymbol{v}, t)$.

Concrete simulation configurations will be specified in the following chapters, depending on each investigation model.

2.7 Chapter Summary

Descriptions of the electron energy distribution function in phase space and propagators for the electron processes under consideration were presented in a general form and a basic calculation scheme of the present propagator method was explained.

The electron energy distribution $f(\boldsymbol{r}, \boldsymbol{v}, t)$ is defined in six-dimensional phase space $(\boldsymbol{r}, \boldsymbol{v})$, and phase space is divided into small sections called cells. A cell $\Delta\boldsymbol{r}\Delta\boldsymbol{v}$ at $(\boldsymbol{r}, \boldsymbol{v})$ correspond to an element of an array in computer memory storage. The temporal variation of $f(\boldsymbol{r}, \boldsymbol{v}, t)$ is calculated as that of the number of electrons in each cell.

A propagator is an operator or a function which represents the electron motion in phase space as displacement of electrons from a cell $\Delta\boldsymbol{r}'\Delta\boldsymbol{v}'$ to another cell $\Delta\boldsymbol{r}\Delta\boldsymbol{v}$. The drift and collision processes are considered as the electron motion. Propagators for the drift and collision processes are alternately applied to $f(\boldsymbol{r}, \boldsymbol{v}, t)$ to calculate its temporal variation successively for every time step Δt.

References

Drallos P J and Wadehra J M 1988 *J.Appl.Phys.* **63** 5601-3
Drallos P J and Wadehra J M 1989 *Phys.Rev.A* **40** 1967-75
Hitchon W N G, Koch D J and Adams J B 1989 *J.Comput.Phys.* **83** 79-95
Hitchon W N G, Parker G J and Lawler J E 1993 *IEEE Trans.Plasma Sci.* **21** 228-38
Holstein T 1946 *Phys.Rev.* **70** 367-84
Kang I J 1968 *Phys.Rev.* **179** 101-4
Mankelevich Y A, Rakhimov A T and Suetin N V
1991 *IEEE Trans.Plasma Sci.* **19** 520-4
Parker G J, Hitchon W N G and Lawler J E 1993 *J.Comput.Phys.* **106** 147-54
Sakamoto S and Tagashira H 1974 *"New High Voltage Engineering"*, *Asakura*, Tokyo
Schneider B, Weinberg M, Tully J and Berry R S 1968 *Phys.Rev.* **182** 133-41
Sommerer T J, Hitchon W N G and Lawler J E 1989 *Phys.Rev.A* **39** 6356-66
Sommerer T J, Hitchon W N G, Harvey R E P and Lawler J E
1991 *Phys.Rev.A* **43** 4452-72
Sugawara H, Sakai Y and Tagashira H 1992 *J.Phys.D: Appl.Phys.* **25** 1483-7
Tagashira H (edition)
1982 *"Simulation Techniques for Gas Discharges"*, *IEE Jpn. Technical Report* **II-140**
Tanahashi T 1991 *"GSMAC-FEM;*
Fundamental and Application of Numerical Fluid Dynamics", *IPC*, Tokyo
Yamanashi I, Goto N and Makabe T 1991 *Trans.IEE Jpn.* **111-A** 168-74

Chapter 3

Spatial Relaxation Processes of Electron Swarms under Steady-State Townsend Conditions

3.1 Introduction

A steady-state Townsend (SST) experiment is a fundamental measurement technique for the ionization coefficient of an electron swarm in gases, which is one of the most important quantities for both gas discharges and gas insulation. Initial electrons are supplied continuously from a cathode to the discharge space between parallel plane electrodes under a uniform electric field $\boldsymbol{E}$ by constantly applying UV (ultra violet) light to the cathode. Electron multiplication due to ionization is measured as the discharge current. An exponential spatial growth of the electron population is assumed and the ionization coefficient is obtained from the gradient of a logarithm plotting of the discharge current as a function of the distance between the electrodes.

Perfect exponential spatial growth of the electron swarm is obtained when the electron velocity distribution $f(\boldsymbol{v})$ is in drift equilibrium, where the energy gain and loss of an electron swarm balance with each other and the normalized $f(\boldsymbol{v})$ is position-independent. However, the exponential growth can only be observed in a limited region, because $f(\boldsymbol{v})$ of the initial electrons ejected from the cathode is not in drift equilibrium in general and electron swarms in the vicinity of the electrodes are affected by boundary conditions. It is important to evaluate the effects of boundary conditions and spatial relaxation processes in order to perform appropriate experimental measurements.

An example of analyses for the spatial relaxation processes of an electron swarm between parallel plane electrodes is seen in Sommerer *et al.* (1989). This work was presented to show a technical basis of a propagator method (PM) before applying the PM to analyses of cathode fall region in helium glow discharges. Some electron swarm parameters were shown as functions of the distance from the cathode, and these results agreed fairly well with those obtained by a Monte Carlo simulation (MCS). However, some differences between the results obtained by the PM and the MCS are observable. In particular, the PM results miss the fine structure in the spatially relaxing swarm parameters obtained by the MCS. For example, the threshold position of ionization and overshoots and vibrations of swarm parameters were drawn as smooth curves (see figure 3.8). Generally, it is difficult to distinguish such fine structures from statistical fluctuation if an MCS is performed singly. However, those relaxation processes in the vicinity of the cathode can be explained as follows.

It is experimentally possible that the electron energy distribution $F(\epsilon)$ of initial electrons is concentrated within a narrow energy range when the photon energy of the UV light and the work function of the material of the electrode are appropriately chosen. Typical values of them would be several eV and close to each other. Electrons with such an $F(\epsilon)$ can be called "coherent" electrons. When coherent initial electrons are ejected from the cathode, the electron energy ϵ is represented as a function of the position as $\epsilon = \epsilon_{\text{ini}} + eEx$ until an inelastic collision process starts, since the sum of the kinetic and potential energies of an electron moving under a static electric field is conservative while any energy loss do not occur. The coherence of $F(\epsilon)$ is strictly kept in such a region. Thus, a spatial threshold x_{inel} for an inelastic collision process appears at a position determined by ϵ_{ini}, E, and the threshold energy ϵ_{inal} as $x_{\text{inel}} = (\epsilon_{\text{inel}} - \epsilon_{\text{ini}})/(eE)$. The law of energy conservation is an important criterion to treat the coherence of an electron swarms properly.

In this chapter, the fine structures of spatial relaxation processes of electron swarms in parallel plane electrodes model under an SST condition are investigated using a PM. Initial electrons ejected from a cathode are given with zero energy. In order to avoid the discrepancies that appear in the conventional PM, an appropriate way of PM implementation based on the law of energy conservation is introduced.

3.2 Computational Conditions

3.2.1 Analysis Model

The following conditions are assumed for the present parallel plane electrodes model under SST conditions. The applied electric field $\boldsymbol{E}$ between the electrodes is uniform and static. The electron distribution in real space in the direction parallel to the electrodes is integrated to be one-dimensional, and $f(\boldsymbol{v})$ is azimuthally symmetric. The number density of electrons between the electrodes is low enough so that the electric field distortion due to the space charge can be neglected.

The electron motion in phase space is described by time t and the following three coordinate variables; the distance from cathode x, the electron speed v, and the angle θ between the directions of the acceleration due to $\boldsymbol{E}$ and the motion of an electron. For accurate numerical treatment of the electron energy, polar coordinate system for velocity space is adopted here since the absolute value of the electron velocity directly related to the electron energy. The electron velocity distribution is defined in three-dimensional phase space (x, v, θ) as $f(x, v, \theta)$. Phase space (x, v, θ) is divided into the cells $C_{l,i,j}$ at (x_l, v_i, θ_j) which occupy the volume $\Delta x_l \Delta v_i \Delta \theta_j$, where Δx_l, Δv_i and $\Delta \theta_j$ represent the widths of the cell $C_{l,i,j}$.

The electron number density at each position in phase space is calculated as the number of electrons $n_{l,i,j}$ in $C_{l,i,j}$:

$$n_{l,i,j} = f(x_l, v_i, \theta_j)\Delta x_l \Delta v_i \Delta \theta_j. \tag{3.1}$$

$C_{l,i,j}$ corresponds to the (l, i, j)-th element of an array in the computer memory storage.

3.2.2 The Law of Energy Conservation

In order to satisfy the law of energy conservation, it is required to exactly treat the variation of the electron energy accompanying an electron drift.

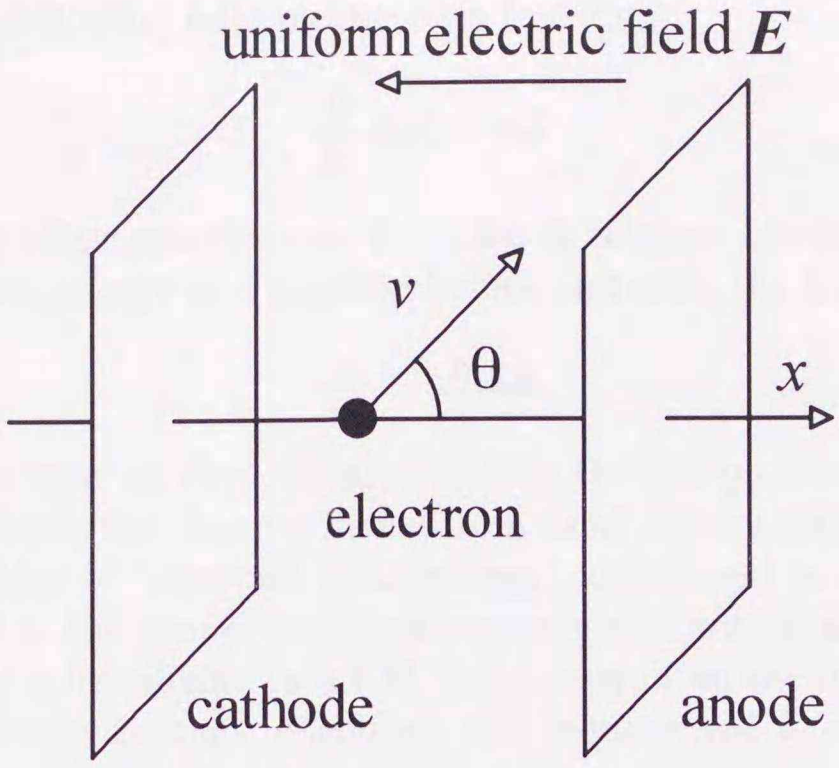

Figure 3.1: Variables to describe the electron motion between parallel plane electrodes; the distance from the cathode x, the electron speed v, and the polar angle θ of the electron motion. The electron distribution in real space in the direction parallel to the electrodes is integrated to be one-dimensional and azimuthal symmetry in velocity space is assumed.

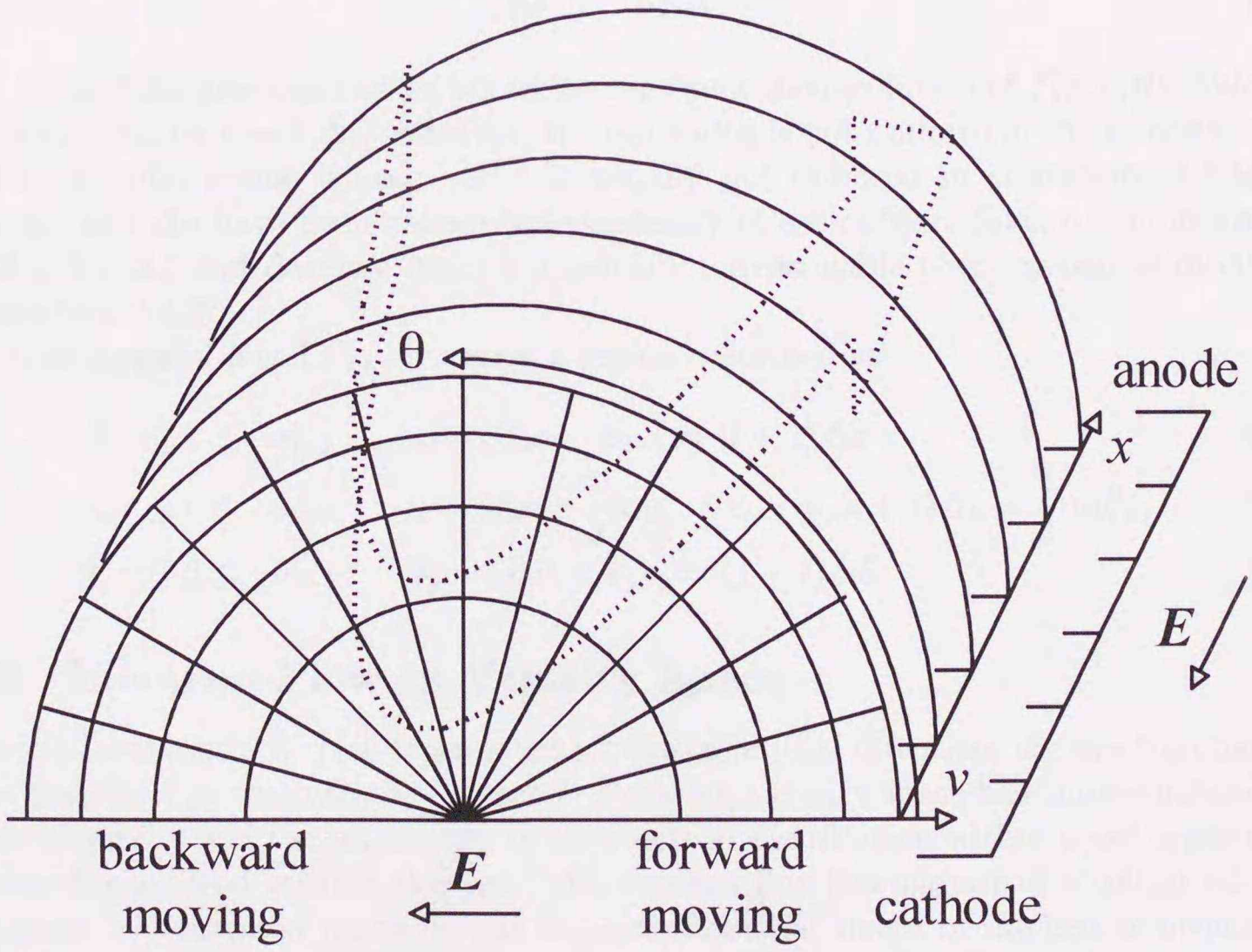

Figure 3.2: Cells defined in three-dimensional phase space (x, v, θ). Each cell has its particular direction for electron flow. An electron draws a parabolic trajectory in this three-dimensional phase space during a free flight. The directions of $\boldsymbol{E}$ in real space and velocity space are originally common.

Under a uniform electric field $\boldsymbol{E}$ in the direction of x, the kinetic energy $\epsilon(x)$ of an electron satisfies the following relation during a free flight:

$$\frac{\mathrm{d}}{\mathrm{d}x}\epsilon(x) = eE \tag{3.2}$$

where e is the charge of an electron and $E = |\boldsymbol{E}|$. A relation binding the differentials $\Delta\epsilon$ and Δx of the electron energy and position before and after the free flight is derived as

$$\Delta\epsilon = eE\Delta x. \tag{3.3}$$

This relation requires that an electron must obtain the energy corresponding to its drift distance Δx exactly when the electron moves from a cell to another cell. This requirement is equivalent to the idea of "constant total energy" introduced to an integral method in Segur *et al.* (1986), *i.e.* the sum of the kinetic energy and potential energy of an electron is conservative during a free flight. In a PM, the energy of an electron is particular to the cell in which the electron belongs, therefore, the requirement is applied to the relation between the source and destination cells of an electron drift.

In order to satisfy this requirement, the cell widths Δx_l and Δv_i in the present PM are chosen as

$$\Delta v_i = v_{i+1} - v_i \tag{3.4}$$

$$\frac{1}{2}mv_i^2 = i\Delta\epsilon \tag{3.5}$$

$$\Delta\epsilon = eE\Delta x \tag{3.6}$$

where $\Delta\epsilon$ and Δx are constant values which represent the resolution of $f(x, v, \theta)$. Velocity space is divided for every $\Delta\epsilon$, therefore, the cell width is not uniform in the velocity scale.

This criterion seems trivial, yet it is usually not imposed in conventional PM, in which Δx and Δv have been chosen independently of each other. Such a computational condition for Δx and Δv may cause a physically unreasonable phenomenon as discussed in subsection 3.4.3.

Formally again, a cell $C_{l,i,j}$ occupies a region described as

$$x_l \le x \le x_{l+1} \qquad x_l = l\Delta x, \quad x_{l+1} = (l+1)\Delta x \tag{3.7}$$

$$\epsilon_i \le \epsilon \le \epsilon_{i+1} \qquad \epsilon_i = i\Delta\epsilon = \frac{1}{2}mv_i^2, \quad \epsilon_{i+1} = (i+1)\Delta\epsilon = \frac{1}{2}mv_{i+1}^2 \tag{3.8}$$

$$\theta_j \le \theta \le \theta_{j+1} \qquad \theta_j = j\Delta\theta, \quad \theta_{j+1} = (j+1)\Delta\theta. \tag{3.9}$$

3.2.3 Electron Flow in Velocity Space

When axial symmetry of $f(\boldsymbol{v})$ is assumed for the azimuthal direction, the electron motion can be described by two variables v and θ. However, velocity space has three-dimensional volume originally and the uniformity of the electron distribution within a cell is assumed for three-dimensional volume element. The electron flux flowing out of a cell in velocity space must be evaluated based on the three-dimensional shape of the cell as mentioned in subsection 2.5.1.

Since $\boldsymbol{E}$ is uniform in the present model, the acceleration of an electron observed in velocity space appears a parallel shift. The electron outflow is evaluated based on the area of the projection of a cell to a plane perpendicular to $\boldsymbol{E}$. In figure 3.4, n_ϵ and n_θ represent the numbers of electrons which flow out of the cell $C_{l,i,j}$ to the neighboring cells with

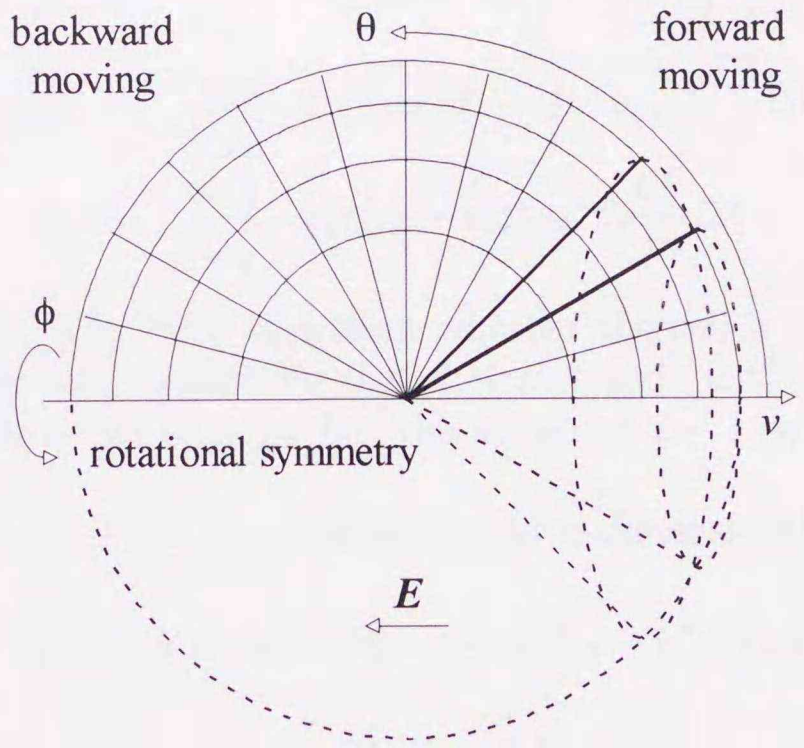

Figure 3.3: Cells defined in velocity space. The concentric contour lines are determined to be uniform in the energy scale, thus they appear non-uniform in the velocity scale. In case rotational symmetry is assumed, electron motion in velocity space is described by two variables v and θ. However, the shape of a cell must be considered three-dimensionally when the electron flow is evaluated, since the uniformity of the electron distribution within a cell is assumed for three-dimensional volume element.

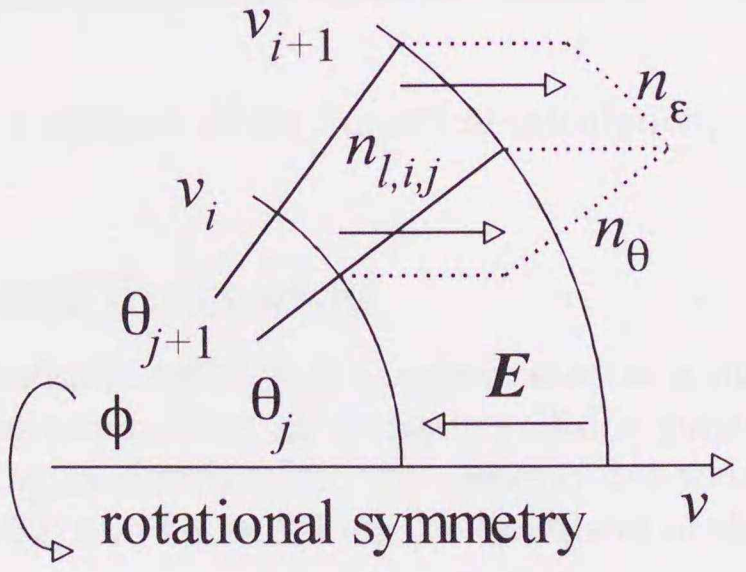

Figure 3.4: The electron flow out of a cell $C_{l,i,j}$. n_ϵ and n_θ represent the numbers of electrons which move to the neighboring cells through the concentric and radial intersections during Δt. $n_\epsilon + n_\theta < n_{l,i,j}$ is required as a condition for Δt.

subscripts $i+1$ and $j-1$ during Δt. Considering the area of the orthogonal projection of the intersections between these cells, n_ϵ and n_θ are given as

$$n_{\epsilon,\text{right}} = \frac{n_{l,i,j}}{V_{l,i,j}} \cdot \pi v_{i+1}^2 (\sin^2\theta_{j+1} - \sin^2\theta_j) \frac{eE}{m} \Delta t \tag{3.10}$$

$$n_{\epsilon,\text{left}} = \frac{n_{l,i,j}}{V_{l,i,j}} \cdot \pi v_i^2 (\sin^2\theta_j - \sin^2\theta_{j+1}) \frac{eE}{m} \Delta t \tag{3.11}$$

$$n_\theta = \frac{n_{l,i,j}}{V_{l,i,j}} \cdot \pi (v_{i+1}^2 - v_i^2) \sin^2\theta_j \frac{eE}{m} \Delta t \tag{3.12}$$

where subscripts "right" and "left" represent whether the cell is in the right hemisphere of velocity space or the left; "right" for $0 \leq \theta \leq \pi/2$ and "left" for $\pi/2 \leq \theta \leq \pi$ here. Note that the destination cell of $n_{\epsilon,\text{left}}$ has the subscript $i-1$, while that of $n_{\epsilon,\text{right}}$ has $i+1$.

$V_{l,i,j}$ is the volume of the cell $C_{l,i,j}$ defined in three-dimensional velocity space:

$$V_{l,i,j} = \int_{v=v_i}^{v_{i+1}} \int_{\theta=\theta_j}^{\theta_{j+1}} \int_{\phi=0}^{2\pi} v \sin\theta \cdot v \mathrm{d}\phi \mathrm{d}\theta \mathrm{d}v = \frac{2}{3}\pi (v_{i+1}^3 - v_i^3)(\cos\theta_j - \cos\theta_{j+1}) \tag{3.13}$$

where ϕ is the azimuthal angle as defined in figure 3.4 (Sugawara *et al.* 1993).

In case source and destination cells of an electron drift are at different energies, the variation of the electron energy is treated as spatial displacement based on the law of energy conservation represented as equation (3.6). Therefore, electrons represented by n_ϵ in the right hemisphere move from $C_{l,i,j}$ to $C_{l+1,i+1,j}$, and those in the left move from $C_{l,i,j}$ to $C_{l-1,i-1,j}$. The subscripts l and i vary together in the present PM (Sugawara *et al.* 1992).

Table 3.1: Electron displacement between source and destination cells.

drift across concentric intersection	left hemisphere	$C_{l,i,j} \longrightarrow C_{l-1,i-1,j}$
	right hemisphere	$C_{l,i,j} \longrightarrow C_{l+1,i+1,j}$
drift across radiative intersection	entire velocity space	$C_{l,i,j} \longrightarrow C_{l,i,j-1}$

As a condition for the stability of the numerical calculation, $n_\epsilon + n_\theta < n_{l,i,j}$ is required when Δt is chosen.

3.2.4 Collision and Scattering

The energy loss at an inelastic collision is approximated as a multiple of $\Delta\epsilon$ so that the coherence of an electron group after an inelastic collision process is kept as well as in the drift process. This approximation and the uniform cell width for every $\Delta\epsilon$ result in $R_{\text{coll}} = 1$ in equation (2.32) and figure 2.3 for the treatment of the energy loss at inelastic collisions.

The probability density function P_{div} for the division ratio $\epsilon_\text{p} : \epsilon_\text{s} = s : 1-s$ of residual energy ϵ_r between a pair of primary and secondary electrons at an ionization collision is assumed to be uniform in the range $0 \leq s \leq 1$:

$$P_{\text{div}}(\epsilon_\text{p})\mathrm{d}\epsilon_\text{p} = \begin{cases} \dfrac{\mathrm{d}\epsilon_\text{p}}{\epsilon_\text{r}} & (0 \leq \epsilon_\text{p} \leq \epsilon_\text{r}) \\ 0 & (\epsilon_\text{p} > \epsilon_\text{r}) \end{cases} \tag{3.14}$$

$$P_{\rm div}(\epsilon_{\rm s})\mathrm{d}\epsilon_{\rm s} = \begin{cases} \dfrac{\mathrm{d}\epsilon_{\rm s}}{\epsilon_{\rm r}} & (0 \le \epsilon_{\rm s} \le \epsilon_{\rm r}) \\ 0 & (\epsilon_{\rm s} > \epsilon_{\rm r}) \end{cases} \tag{3.15}$$

where $|\mathrm{d}s| = |\mathrm{d}\epsilon_{\rm p}/\epsilon_{\rm r}| = |\mathrm{d}\epsilon_{\rm s}/\epsilon_{\rm r}|$. When both of the primary and secondary electrons are treated identically, the energy distribution of the electrons after ionization collision satisfies the following normalization condition:

$$\int_0^{\epsilon_{\rm r}} P_{\rm div}(\epsilon)\mathrm{d}\epsilon = \int_0^{\epsilon_{\rm r}} \frac{2}{\epsilon_{\rm r}}\mathrm{d}\epsilon = 2. \tag{3.16}$$

Electrons after ionization in $\Delta\epsilon_{i'}$ $(\epsilon_{i'} \le \epsilon \le \epsilon_{i'+1})$ are displaced to the cells at $\Delta\epsilon_i$ $(0 \le i \le i' - \epsilon_{\rm ion}/\Delta\epsilon)$ with a distribution shown in figure 3.5. The distribution ratios for the electrons are, approximately, given as

$$\frac{4n_{\rm ion}}{2(i' - \epsilon_{\rm ion}/\Delta\epsilon) + 1} \quad \text{for } \Delta\epsilon_i \quad \left(0 \le i < i' - \frac{\epsilon_{\rm ion}}{\Delta\epsilon}\right) \tag{3.17}$$

$$\frac{2n_{\rm ion}}{2(i' - \epsilon_{\rm ion}/\Delta\epsilon) + 1} \quad \text{for } \Delta\epsilon_i \quad \left(i = i' - \frac{\epsilon_{\rm ion}}{\Delta\epsilon}\right) \tag{3.18}$$

where $n_{\rm ion}$ is the number of electrons undergoing ionization in the source cell. The total number of the distributed electrons is $2n_{\rm ion}$.

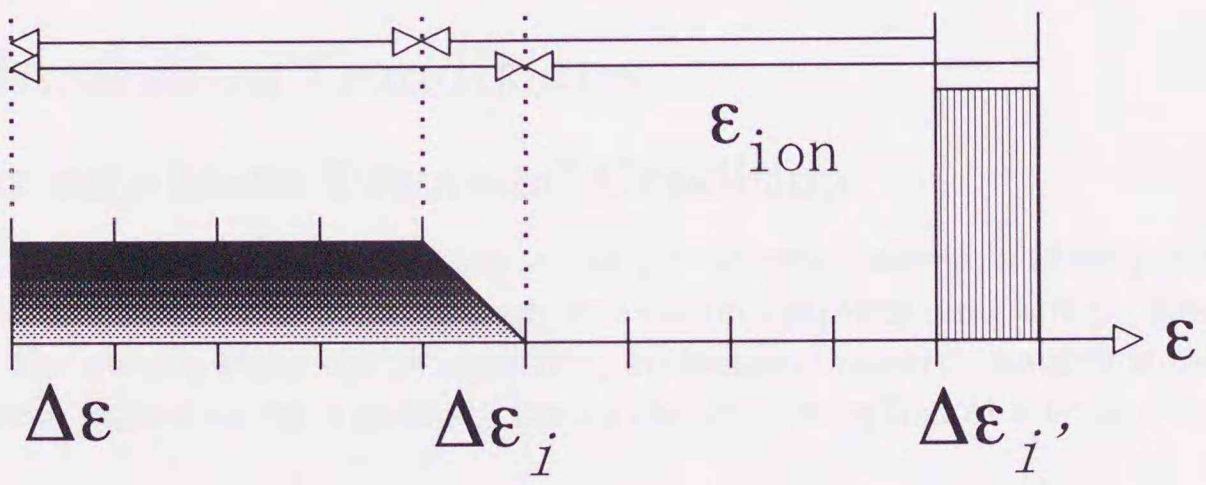

Figure 3.5: Destination cells for the electrons after ionization collision in an energy range $\Delta\epsilon_{i'}$ and their distribution ratios.

Isotropic scattering is assumed for the collisions in the present model. The number of electrons scattered into a cell is proportional to the solid angle of the cell viewed relative to the origin of velocity space. The probability density function $P_{\rm scatt}$ for the scattering angle distribution is derived by integrating the azimuthal distribution:

$$P_{\rm scatt}(\theta) = \int_{\phi=0}^{2\pi} \frac{\mathrm{d}\omega}{4\pi} = \int_{\phi=0}^{2\pi} \frac{\sin\theta \mathrm{d}\phi\mathrm{d}\theta}{4\pi} = \frac{1}{2}\sin\theta. \tag{3.19}$$

Thus, the distribution ratio $R_{{\rm scatt},j}$ for $C_{l,i,j}$ associated with scattering is given as

$$R_{{\rm scatt},j} = \int_{\theta=\theta_j}^{\theta_{j+1}} P_{\rm scatt}(\theta)\mathrm{d}\theta = \frac{1}{2}\{\cos\theta_j - \cos\theta_{j+1}\} = \frac{1}{2}\{\cos j\Delta\theta - \cos(j+1)\Delta\theta\}. \tag{3.20}$$

Totally, the variation of $n_{l,i,j}$ in the collision process may be represented as

$$\frac{n_{l,i,j}(t + \Delta t) - n_{l,i,j}(t)}{\Delta t}$$

$$
\begin{aligned}
= & -Nq_{\mathrm{T}}(\bar{v}_i)\bar{v}_i n_{l,i,j}(t) \\
& + \Bigg[\sum_j Nq_{\mathrm{mom}}(\bar{v}_i)\bar{v}_i n_{l,i,j}(t) + \sum_{j,k} Nq_{\mathrm{ex},k}(\bar{v}_{i+m_{\mathrm{ex},k}})\bar{v}_{i+m_{\mathrm{ex},k}} n_{l,i+m_{\mathrm{ex},k},j}(t) \\
& \quad + \sum_{i'=i+m_{\mathrm{ion}}}^{\infty} \Bigg\{ \frac{2}{2(i'-m_{\mathrm{ion}})+1} \sum_j Nq_{\mathrm{ion}}(\bar{v}_{i'})\bar{v}_{i'} n_{l,i',j}(t) \\
& \qquad + \frac{2}{2(i'+1-m_{\mathrm{ion}})+1} \sum_j Nq_{\mathrm{ion}}(\bar{v}_{i'+1})\bar{v}_{i'+1} n_{l,i'+1,j}(t) \Bigg\} \Bigg] \\
& \times \frac{1}{2}\{\cos j\Delta\theta - \cos(j+1)\Delta\theta\}
\end{aligned} \tag{3.21}
$$

where q_{T} represents the total collision cross section, $m_{\mathrm{ex},k}$ and m_{ion} are the numbers of cells jumped over by the electrons undergoing the energy loss at k-th kind excitation and ionization processes given as

$$m_{\mathrm{ex},k} = \frac{\epsilon_{\mathrm{ex},k}}{\Delta\epsilon} \tag{3.22}$$

$$m_{\mathrm{ion}} = \frac{\epsilon_{\mathrm{ion}}}{\Delta\epsilon} \tag{3.23}$$

and $\bar{v}_i$ is the representative velocity of $C_{l,i,j}$, which is the value at the center of the cell.

3.3 Simulation Conditions

3.3.1 Steady-State Townsend Condition

By continuously supplying initial electrons at an electron source, a steady-state electron flow may be obtained after long enough relaxation distance and time. Here, in order to compose the steady-state electron swarm, an isolated electron swarm is defined as an electron swarm generated by a group of initial electrons supplied at a time τ in an impulse manner.

The isolated electron swarm drifts toward the anode as developing by ionization and diffusion. When the isolated electron swarm is observed at a fixed position between the electrodes, a temporal profile of the electron passage will be obtained. Since isolated electron swarms are continuously supplied from the cathode in an SST experiment, a steady-state electron swarm observed at a fixed position is considered to be the superposition of different parts of all different isolated electron swarms which have been generated and reached the position before the observation moment (Sakai *et al.* 1972):

$$f_{\mathrm{SST}}(x,v,\theta) = \int_{-\infty}^{t} f(x,v,\theta,t-\tau)\mathrm{d}\tau \tag{3.24}$$

$$= \int_{0}^{\infty} f(x,v,\theta,t)\mathrm{d}t \tag{3.25}$$

where $f(x,v,\theta,t-\tau)$ represents the electron velocity distribution of an isolated electron swarm which had been generated at a moment τ. $t-\tau$ represents the passage of time from the moment when an isolated electron swarm had been generated to the moment of observation. Here, it is assumed that the electron swarm behavior is identical for any isolated electron swarm irrespective of the moment of generation. This assumption is valid when the number density of superposed electrons is low enough to neglect the Coulomb interaction between isolated electron swarms.

Two equivalent expressions for observing an electron swarm under an SST condition are obtained here. Equation (3.24) represents the superposition of continuously supplied isolated electron swarms. This way is a simple way of realizing a steady state experimentally. On the other hand, equation (3.25) represents the temporal superposition of an isolated electron swarm. This way would be easier for computational investigation because convergence of the solution can be judged easily by the number of electrons remaining between the electrodes. Equation (3.25) is adopted in the present PM for obtaining $f_{\mathrm{SST}}(x, v, \theta)$.

3.3.2 Gases, Electric Fields, and Other Conditions

In the present analyses, $F(\epsilon)$ and some electron swarm parameters in helium (He) and argon (Ar) are investigated.

The collision cross sections are taken from Frost and Phelps (1964), Montague *et al.* (1984) and Zetner *et al.* (1986) for He, and Sakai *et al.* (1972), Mason and Newell (1987) and Suzuki *et al.* (1990) for Ar. He is chosen for a qualitative comparison with the results of a conventional PM mentioned before. Ar is an example for lower thresholds of excitation and ionization than those of He.

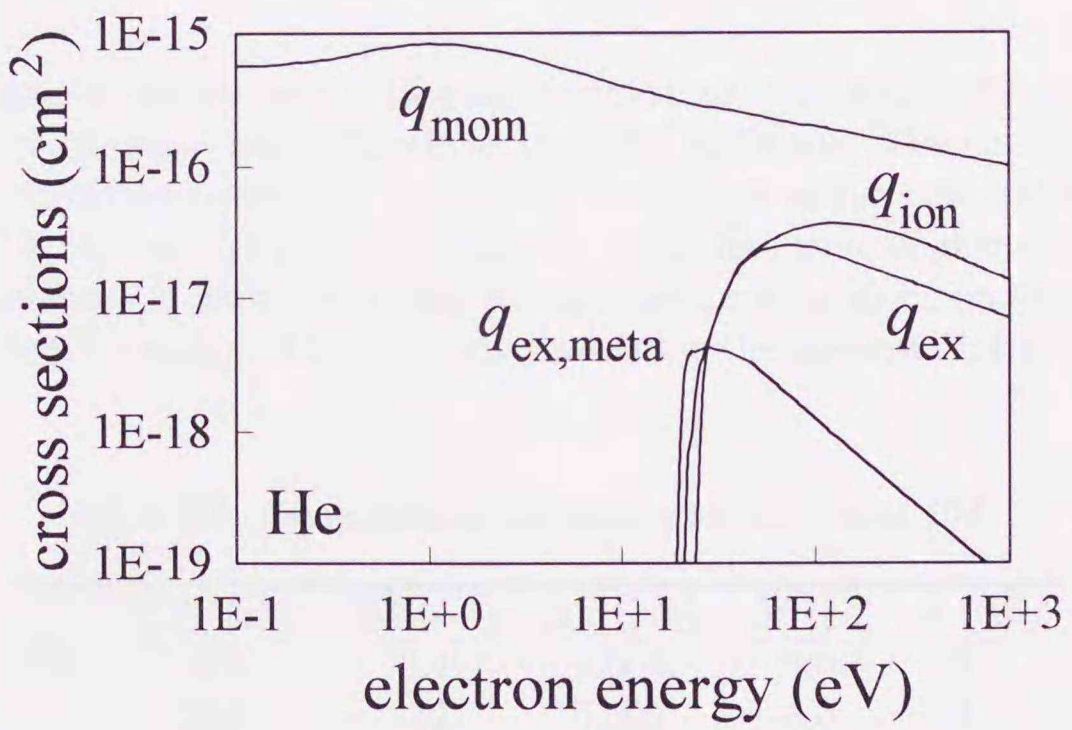

Figure 3.6: Electron collision cross sections of He (Frost and Phelps 1964, Montague *et al.* 1984, Zetner *et al.* 1986); momentum transfer q_{mom}, excitation q_{ex} ($\epsilon_{\mathrm{ex}} = 20.96$ eV), excitation to the metastable state $q_{\mathrm{ex,meta}}$ ($\epsilon_{\mathrm{ex,meta}} = 19.8$ eV), and ionization q_{ion} ($\epsilon_{\mathrm{ion}} = 24.588$ eV).

The reduced electric field E/N applied between the electrodes is chosen to be 283 Td (Townsend; 1 Td $= 10^{-17}$ Vcm^2) for both gases. $E = 100$ Vcm^{-1} and $N = 3.54\times10^{16}$ cm^{-3} (gas pressure $p = 1.0$ Torr at 0 °C) are assumed. The equivalent value of E/p_0 is 100 Vcm^{-1}Torr^{-1}.

Initial electrons are assumed to start from the cathode surface with zero energy, and perfect absorption for the electrons at the electrodes is assumed.

$f_{\mathrm{SST}}(x, v, \theta)$ is obtained based on equation (3.25). Although the time range of the integral is from zero to infinity, the simulation is terminated at the time when the number of electrons remaining between the electrodes becomes less than 1/1000 of the number of the initial electrons ejected from the cathode, since the mathematical probability of the electron presence between the electrodes does never become zero perfectly.

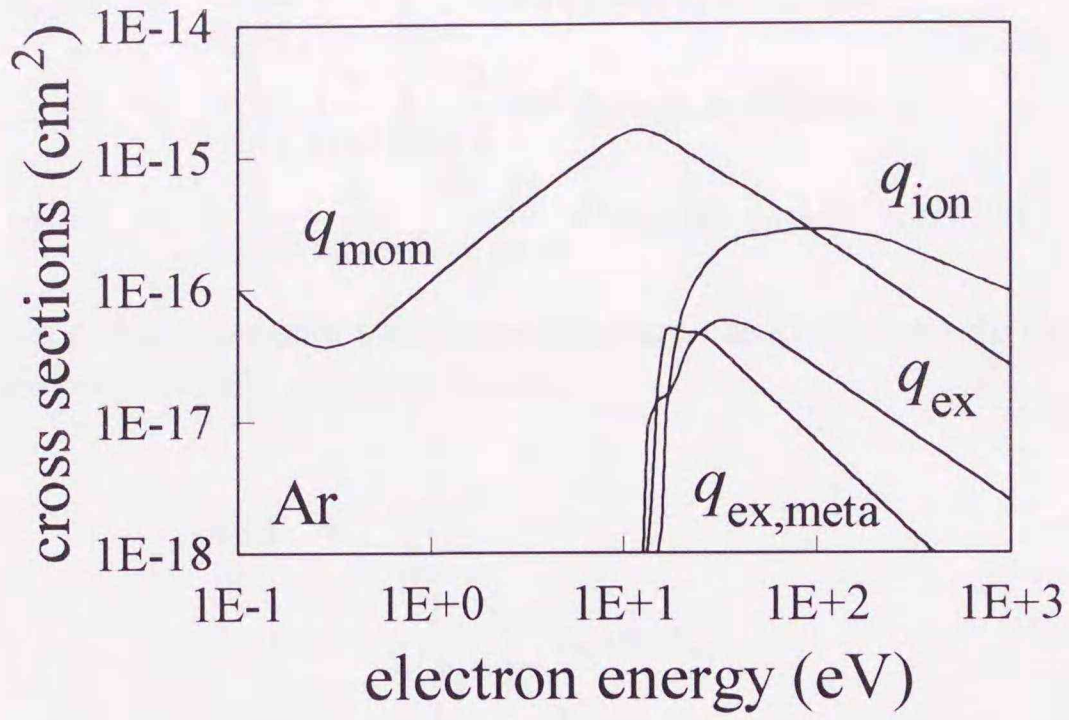

Figure 3.7: Electron collision cross sections of Ar (Sakai *et al.* 1972, Mason and Newell 1987, Suzuki *et al.* 1990); momentum transfer $q_{\rm mom}$, excitation $q_{\rm ex}$ ($\epsilon_{\rm ex} = 12.9$ eV), excitation to the metastable state $q_{\rm ex,meta}$ ($\epsilon_{\rm ex,meta} = 11.55$ eV), and ionization $q_{\rm ion}$ ($\epsilon_{\rm ion} = 15.76$ eV).

The energy loss of the inelastic collisions is truncated to be multiples of the unit energy $\Delta\epsilon$ in order to avoid numerical diffusion at inelastic collisions. The energy resolution $\Delta\epsilon$ represents the real space resolution Δx at the same time using a relation $\Delta x = \Delta\epsilon/eE$. The value of Δt is chosen to be shorter than the mean free time of electrons. The spacing between the electrodes is set to be a long enough distance for electron swarm parameters to reach equilibrium roughly. These values chosen for the present PM are listed in table 3.2

Table 3.2: Computational parameters for the present PM.

	E/N (Td)	$\Delta\epsilon$ (eV)	Δx (cm)	Δt (ps)	d (cm)
He	283	0.4	0.004	3.0	2.0
Ar	283	0.2	0.002	4.0	1.0

3.4 Results and Discussion

3.4.1 Swarm Parameters

Swarm parameters obtained by the present PM are shown in figures 3.8 and 3.9 as functions of distance from the cathode together with the results of an MCS performed under the same conditions; the number of electrons $n(x)$, the electron drift velocity $v_{\rm d}(x)$, the mean electron energy $\bar{\epsilon}(x)$ and the ionization coefficient $\alpha(x)$. They are obtained from $f_{\rm SST}(x, v, \theta)$ as

$$n(x) = \int_{v=0}^{\infty}\int_{\theta=0}^{\pi} f_{\rm SST}(x, v, \theta)\mathrm{d}\theta\mathrm{d}v \tag{3.26}$$

$$v_{\rm d}(x) = \frac{1}{n(x)} \int_{v=0}^{\infty} \int_{\theta=0}^{\pi} v \cos\theta f_{\rm SST}(x, v, \theta) {\rm d}\theta {\rm d}v \tag{3.27}$$

$$\bar{\epsilon}(x) = \frac{1}{n(x)} \int_{v=0}^{\infty} \int_{\theta=0}^{\pi} \frac{1}{2} m v^2 f_{\rm SST}(x, v, \theta) {\rm d}\theta {\rm d}v \tag{3.28}$$

$$\alpha(x) = \frac{1}{v_{\rm d}(x)} \frac{1}{n(x)} \int_{v=0}^{\infty} \int_{\theta=0}^{\pi} N q_{\rm ion}(v) v f_{\rm SST}(x, v, \theta) {\rm d}\theta {\rm d}v. \tag{3.29}$$

The denotations for these electron swarm parameters based on discrete expressions in the MCS and PM are respectively given as follow.

For the MCS,

$$n(x_l) = \sum_m 1 \tag{3.30}$$

$$v_{\rm d}(x_l) = \frac{1}{n(x_l)} \sum_m v_m \cos\theta_m \tag{3.31}$$

$$\bar{\epsilon}(x_l) = \frac{1}{n(x_l)} \sum_m \frac{1}{2} m v_m^2 \tag{3.32}$$

$$\alpha(x_l) = \frac{1}{v_{\rm d}(x_l)} \frac{1}{n(x_l)} \sum_m N q_{\rm ion}(v_m) v_m \tag{3.33}$$

where subscript m represents the m-th sample of electrons in a sampling region Δx_l in the MCS. The weight of the residence time to give the $f_{\rm SST}(v, \theta)$ in Δx_l has been taken into account as the number of samplings.

For the PM,

$$n(x_l) = \sum_{i,j} n_{l,i,j} \tag{3.34}$$

$$v_{\rm d}(x_l) = \frac{1}{n(x_l)} \sum_{i,j} \bar{v}_i \cos\bar{\theta}_j n_{l,i,j} \tag{3.35}$$

$$\bar{\epsilon}(x_l) = \frac{1}{n(x_l)} \sum_{i,j} \frac{1}{2} m \bar{v}_i^2 n_{l,i,j} \tag{3.36}$$

$$\alpha(x_l) = \frac{1}{v_{\rm d}(x_l)} \frac{1}{n(x_l)} \sum_{i,j} N q_{\rm ion}(\bar{v}_i) \bar{v}_i n_{l,i,j} \tag{3.37}$$

where $\bar{v}_i$ and $\bar{\theta}_j$ are the representative velocity and angle of $C_{l,i,j}$.

The values of these parameters obtained by the present PM agree well with the MCS values. In the results of the present PM, the fluctuations near the cathode are clearly shown. In particular the threshold of $\alpha(x)$ appears exactly at $x = \epsilon_{\rm ion}/eE$ for both of He and Ar. These results show that the present PM successfully treats the relation between the energy and position of the electrons. Agreement between the results of the present PM and MCS proves that the fluctuation of electron swarm parameters is not a statistical fluctuation in the MCS but physical processes under relaxation of electron swarms as discussed in Sakai *et al.* (1972).

The swarm parameters obtained as average values in the region in which swarm parameters seem to be constant are listed in table 3.3 together with the values by the MCS and a two-term approximation of Boltzmann equation analysis (BE2). The values calculated by the BE2 are ones under an equilibrium condition in free space, where there are no effects of boundary and relaxation process. Each parameter agrees well in accuracy of $\pm 4\%$, and these results verify the calculation scheme of the present PM.

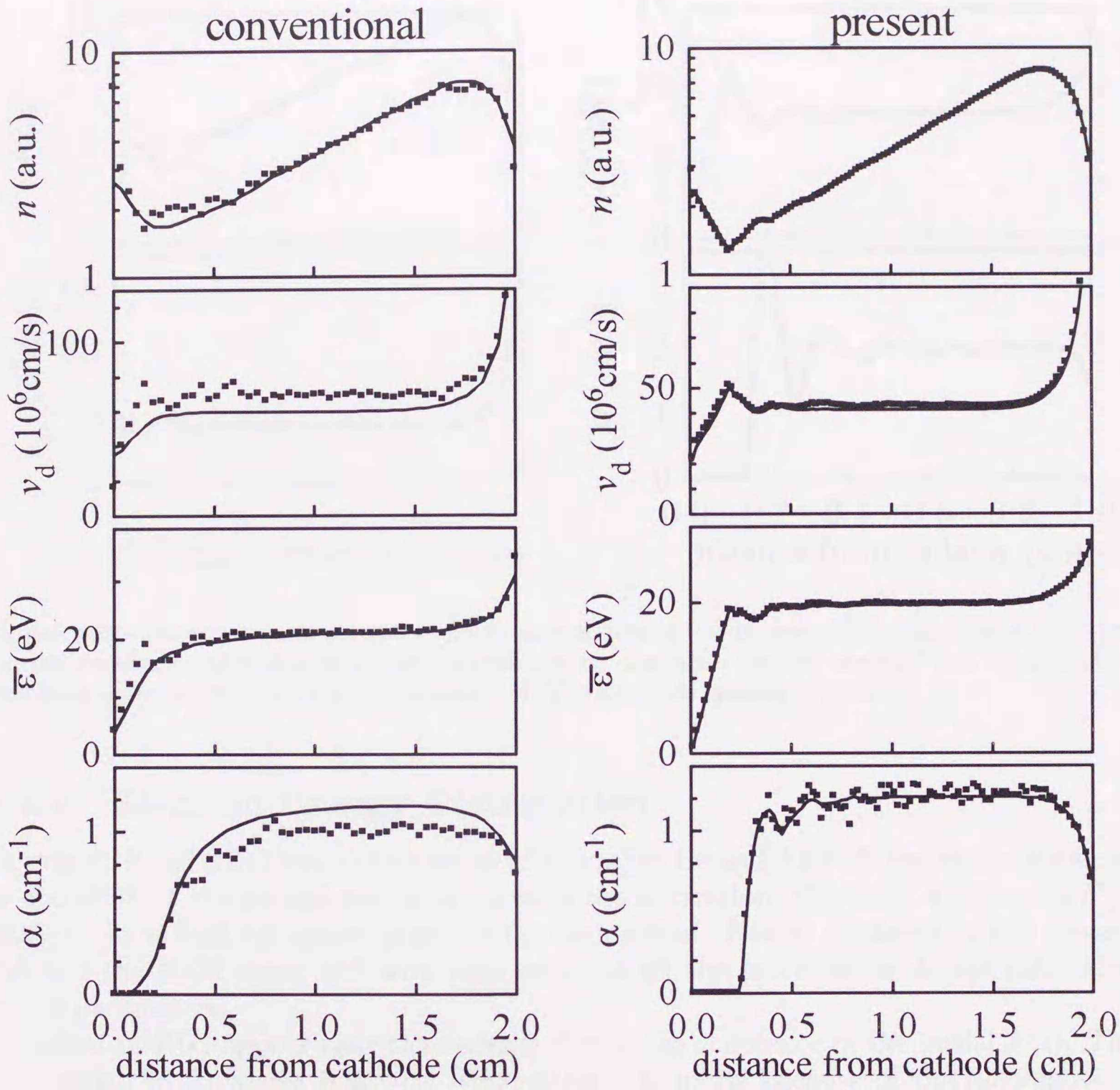

Figure 3.8: Electron swarm parameters in He as functions of the distance from cathode at $E/N = 283$ Td; the electron number density n, the drift velocity v_d, the mean electron energy $\bar{\epsilon}$ and the ionization coefficient α. The electrode spacing is 2 cm. Figures in the left; dots, MCS (reference in Sommerer *et al.* 1989); curves, a conventional PM (Sommerer *et al.* 1989). Figures in the right; dots, the present MCS; curves, the present PM. Only qualitative comparisons are done here since the electron collision cross sections used in the conventional and present cases may be different.

Table 3.3: Comparison of the equilibrium values of swarm parameters in He and Ar at $E/N = 283$ Td. The mean electron energy $\bar{\epsilon}$, the ionization coefficient α, and the drift velocity v_d.

	He			Ar		
	$\bar{\epsilon}$ (eV)	α (cm^{-1})	v_d ($cm\mu s^{-1}$)	$\bar{\epsilon}$ (eV)	α (cm^{-1})	v_d ($cm\mu s^{-1}$)
BE2	19.92	1.23	43.0	8.19	1.96	17.2
MCS	19.66	1.22	42.6	8.16	1.96	17.1
PM	19.69	1.21	41.3	8.16	1.96	16.8

BE2, two-term approximation of Boltzmann equation analysis;
MCS, Monte Carlo simulation; PM, the present propagator method

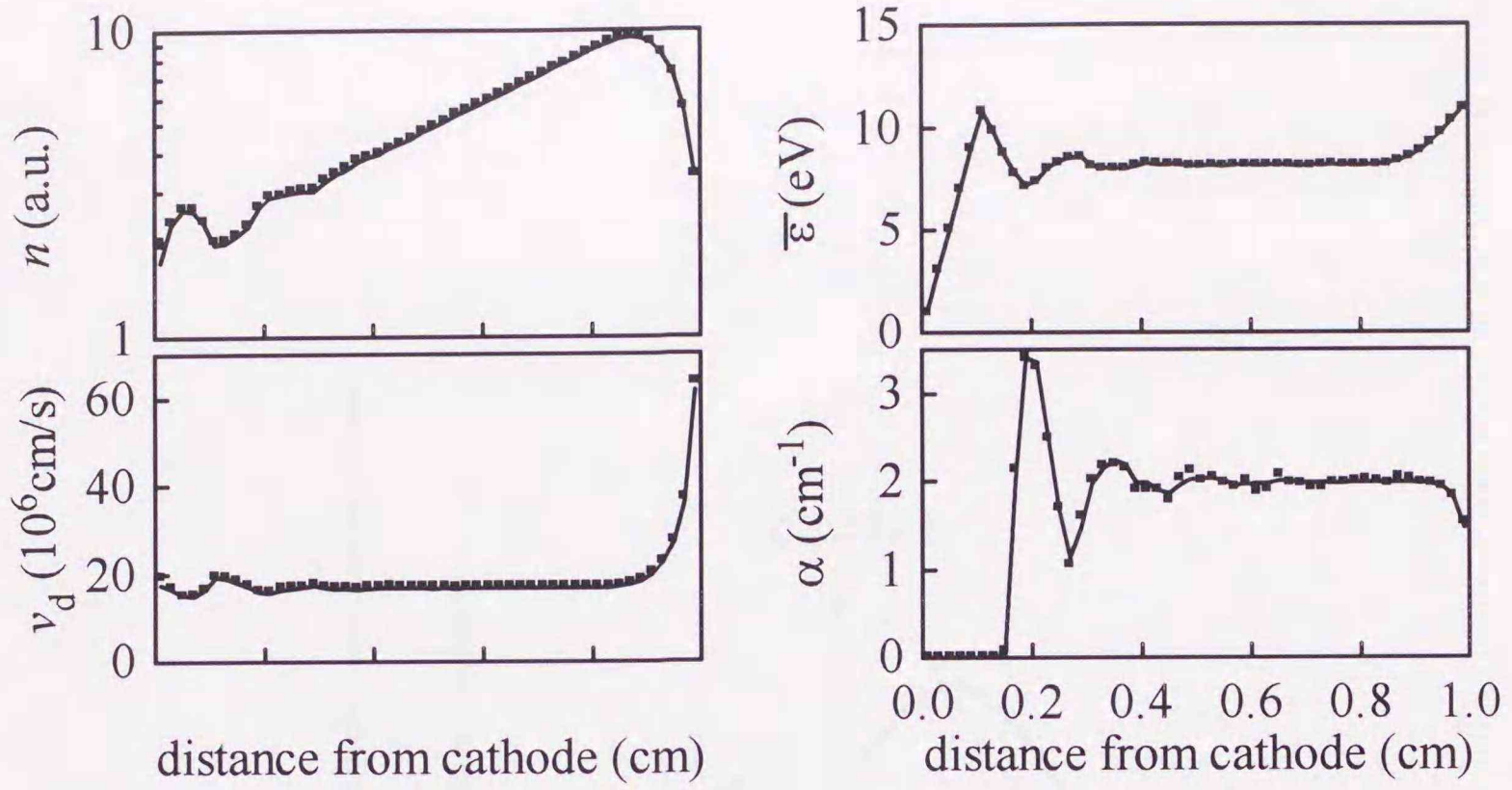

Figure 3.9: Electron swarm parameters in Ar as functions of the distance from cathode at $E/N = 283$ Td; the electron number density n, the drift velocity v_d, the mean electron energy $\bar{\epsilon}$ and the ionization coefficient α. Dots, MCS; curves, the present PM. The electrode spacing is 1 cm.

3.4.2 Electron Energy Distribution

Figures 3.10 and 3.11 show comparisons of $F(x, \epsilon)$ in He and Ar with the values obtained by the MCS at the several positions between the electrodes. The drift equilibrium $F(\epsilon)$ analyzed by a BE2 are shown together for comparison. $F(x, \epsilon)$ obtained by the present PM and the MCS agree well with each other at all the positions as do the calculated swarm parameters.

Spikes in $F(\epsilon)$ appear near the cathode due to the coherence of the initial $F(\epsilon)$. The spike width in Ar seems relatively wider than that in He because of the differences of the thickness of the sampling slabs. Since all initial electrons are given with zero energy, there is no energy loss accompanying inelastic collisions until the coherent electron energy reaches the lowest threshold. The position-dependent $F(\epsilon)$ is kept coherent, and this tendency remains even after excitation collisions. Electrons after ionization collisions are distributed to a wide energy range determined by the residual energy, thus the coherence of $F(\epsilon)$ is lost mainly due to ionization. The broad low energy bands in $F(\epsilon)$ at $x = 0.4$ cm in He and $x = 0.2$ cm in Ar following the rightward-moving spikes represent those spread electrons, where "rightward" means the increase of the electron energy. It can be concluded that ionization collisions contribute to the relaxation process by spreading electrons after ionization over wide energy range.

The spikes become smaller with increasing x. However, $F(x, \epsilon)$ is not in drift equilibrium completely even at a distance where $v_d(x)$, $\bar{\epsilon}(x)$ and $\alpha(x)$ seem to reach their relaxed values. This result shows that the relaxation distance of the swarm parameters seem shorter than that of $F(\epsilon)$, *i.e.* an integral over $F(\epsilon)$ relaxes faster than $F(\epsilon)$.

Nonetheless, $F(\epsilon)$ is close to the drift equilibrium solution at $x = 1.6$ cm in He and $x = 0.8$ cm in Ar. An electron ejected from the cathode with zero energy can obtain at most 160 eV in He and 80 eV in Ar when the electron reaches the distances under the given E. These electron energies permit an electron a few cycles of the energy increase

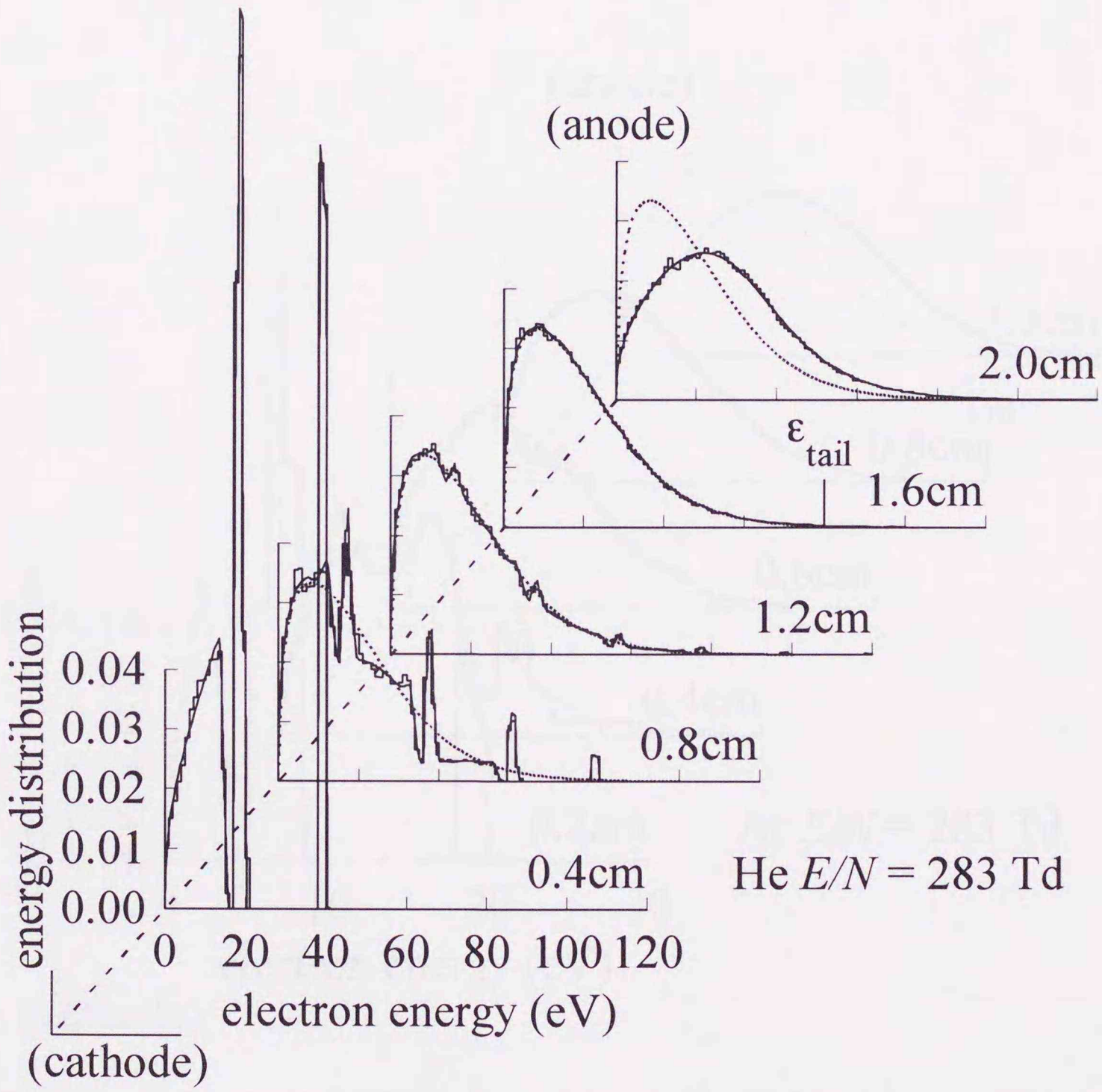

Figure 3.10: Electron energy distribution $F(x, \epsilon)$ in He at $E/N = 283$ Td as a function of the distance from the cathode; histogram, MCS; curves, the present PM; broken curve, BE2. Initial electrons are given at the cathode surface with zero energy. The result of BE2 is for an electron swarm in free space without the effects of boundary and relaxation processes.

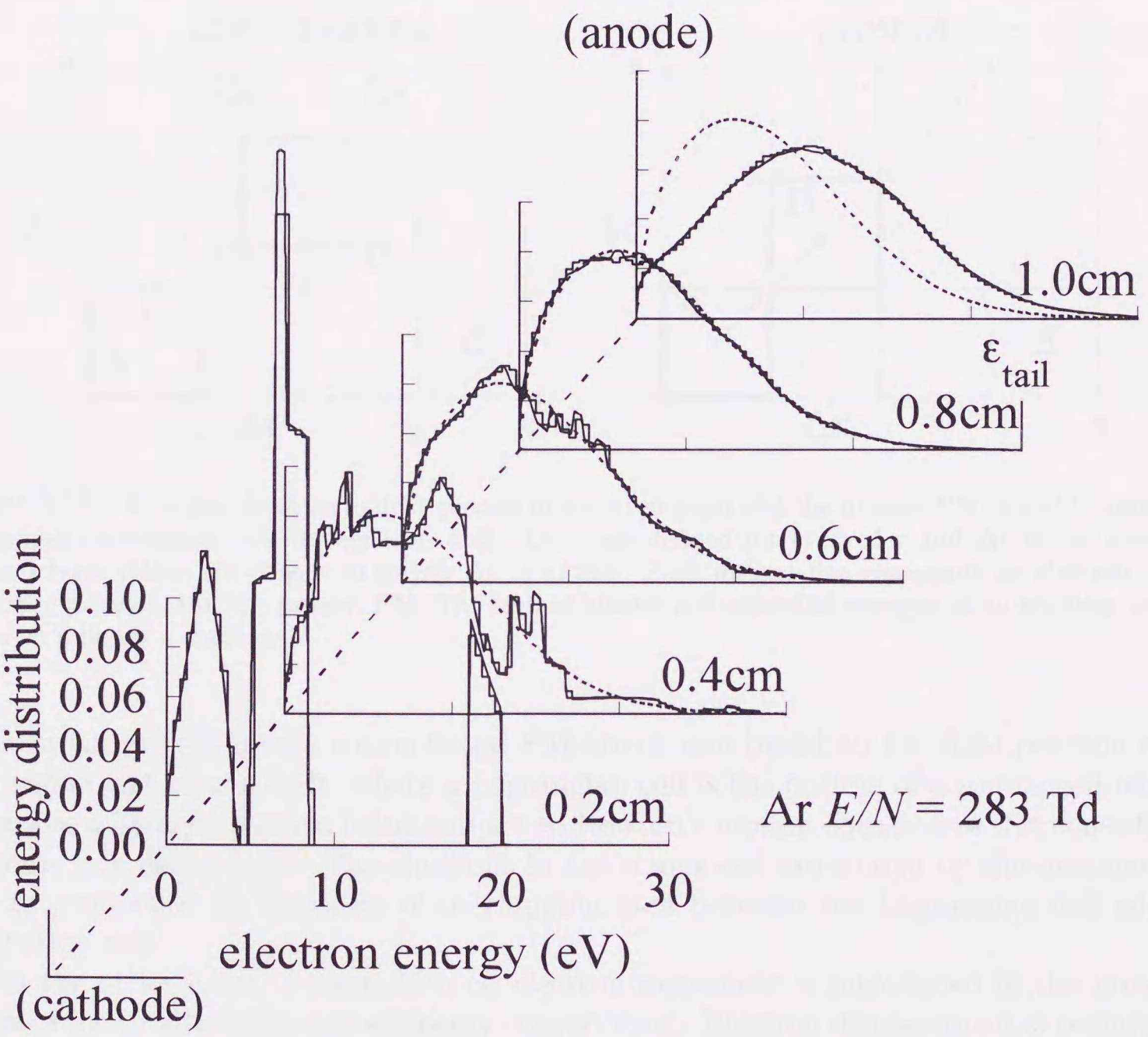

Figure 3.11: Electron energy distribution $F(x, \epsilon)$ in Ar at $E/N = 283$ Td as a function of the distance from the cathode; histogram, MCS; curves, the present PM; broken curve, BE2. Initial electrons are given at the cathode surface with zero energy. The result of BE2 is for an electron swarm in free space without the effects of boundary and relaxation processes.

from $\epsilon = 0$ to $\epsilon = \epsilon_{\text{tail}}$ (see figures 3.10 and 3.11 for ϵ_{tail}). It is suggested that a distance more than a few times as long as $\epsilon_{\text{tail}}/(eE)$ is required as the relaxation distance in the present case.

3.4.3 Numerical Diffusion

In drift process, electrons move from a source cell to a destination cell. The ways of choice of destination cells are compared here between the conventional and the present PM.

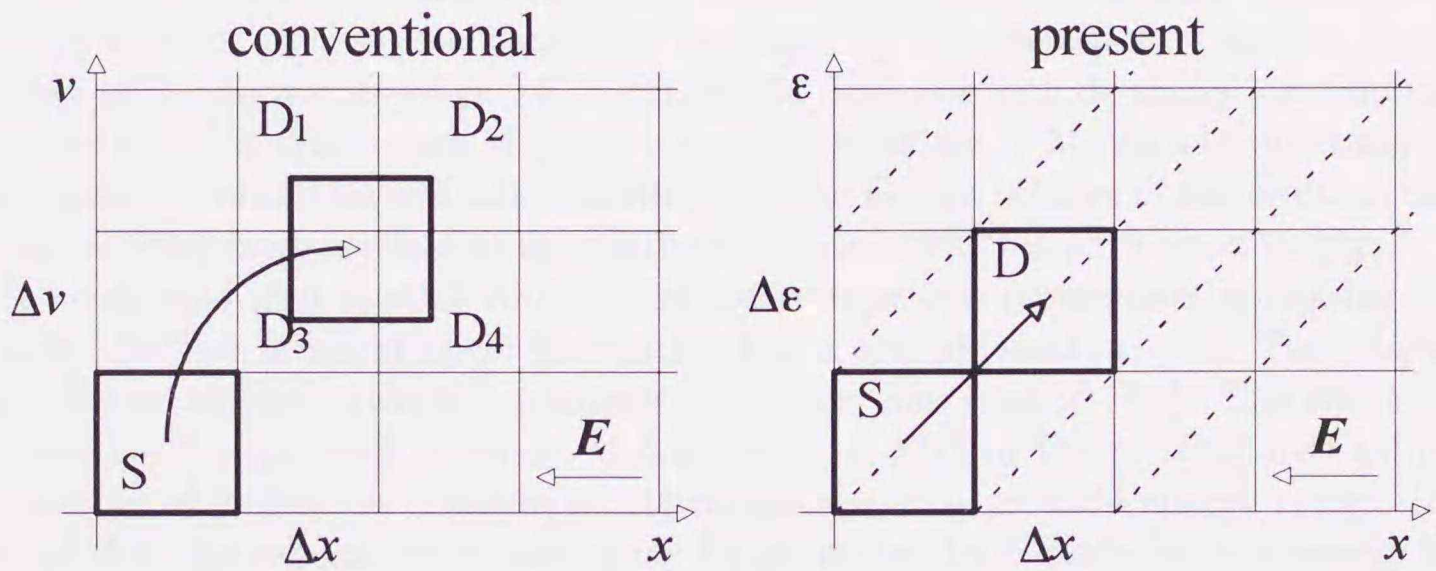

Figure 3.12: Electron motions in drift process in a conventional and the present PM. S and D indicate source and destination cells for electron drift. Cells are defined for every Δx and $\Delta\epsilon$ in the present PM and their values are chosen to satisfy $\Delta\epsilon = eE\Delta x$. Each dashed line represents an electron drift trajectory permitted in the present PM. The sum of kinetic and potential energies of an electron which moves on a line is a constant.

Destination cells in the conventional PM are chosen based on the final position of a Lagrangian cell after a drift, where a Lagrangian cell is the outline of a source cell which undergoes a ballistic motion being subject to Newton's motion equation as if it consists of electrons (see figure 3.12). The electrons in the source cell are shared by the destination cells in proportion to the ratio of overlapping area between the Lagrangian cell and a destination cell.

On the other hand, a restriction on electron movement is introduced in the present PM in order to satisfy the law of energy conservation. Electron displacement is permitted only between those cells which locate on the same "characteristic energy" line, where a characteristic energy represents the sum of kinetic and potential energies.

What may happen in the conventional PM is that the characteristic energy of a destination cell may be higher than that of the source cell. If electrons distributed to such a destination cell fly back to the same position as the initial source cell due to backward scattering at collisions, some of the electrons may have extra energy. This result must be distinguished as a numerical diffusion caused by computational treatment in the conventional PM from physical electron diffusion. The reason why the spatial threshold for ionization and the aspects of spatial vibration of electron swarm parameters did not appear in the conventional PM can be evidently attributed to not imposing energy conservation. The fine structure of the position-dependent electron swarm parameters, which has been explained in terms of coherence of the electron energy, is clearly reproduced by introducing the appropriate way of cell division and treatment of the drift process proposed in the present PM.

3.5 Chapter Summary

Aspects of spatial relaxation of electron swarms between parallel plane electrodes under steady-state Townsend conditions were simulated using a PM. In the present PM, a relation between the cell widths $\Delta\epsilon = eE\Delta x$ was introduced for the law of energy conservation, and an assumption that the electron distribution within a cell is uniform with respect to the volume element of velocity space was adopted for accurate evaluation of the electron flow in velocity space.

Taking into account of these treatments for the present PM, fine structures of spatially relaxing electron swarm parameters, such as threshold, overshoots and vibration, were clearly reproduced. These fine structures obtained by the present PM showed excellent agreement with the results of an MCS. Since PM does not include statistical fluctuation as appears in MCS due to use of pseudo random numbers, PM can obtain statistically stable results. It would be difficult to distinguish the fine structures of the electron energy distribution $F(\epsilon)$ from statistical fluctuations in case a MCS is performed singly.

It is confirmed that spatial vibration of electron swarm parameters appearing in the results of a MCS is not statistical fluctuation but a real physical process. The relaxation distance for an electron swarm parameter is shorter than that of $F(\epsilon)$. The effect of the initial electrons, explained in terms of coherence of $F(\epsilon)$ of them, is diluted primarily by a function of ionization collision to distribute electrons to wide energy range. It was suggested that the relaxation distance may be estimated by considering the energy range of the drift equilibrium solution of $F(\epsilon)$.

References

Drallos P J, and Wadehra J M 1989 *Phys.Rev.A* **40** 1967-75
Frost L S and Phelps A V 1964 *Phys.Rev.A* **136** 1538-45
Hitchon W N G, Koch D J and Adams J B 1989 *J.Comput.Phys.* **83** 79-95
Kitamori K, Tagashira H and Sakai Y 1980 *J.Phys.D: Appl.Phys.* **13** 535-50
Mason N J and Newell W R 1987 *J.Phys.B: At.Mol.Phys.* **5** 1357-77
Montague R G, Harrison M F A and Smith A C H
1984 *J.Phys.B: At.Mol.Phys.* **17** 3295-310
Sakai Y, Tagashira H and Sakamoto S 1972 *J.Phys.B: At.Mol.Phys.* **5** 1010-6
Segur P, Yousfi M, Kadri M H and Bordage M C
1986 *Transp.Theory Stat.Phys.* **15** 705-57
Sommerer T J, Hitchon W N G and Lawler J E 1989 *Phys.Rev.A* **39** 6356-66
Sugawara H, Sakai Y and Tagashira H 1992 *J.Phys.D: Appl.Phys.* **25** 1483-7
Sugawara H, Sakai Y and Tagashira H 1993 *Nat.Conf.IEE Jpn.* 221
Suzuki M, Taniguchi T and Tagashira H 1990 *J.Phys.D: Appl.Phys.* **23** 842-50
Zetner P W, Westerveld W B, King G C and McConkey J W
1986 *J.Phys.B: At.Mol.Phys.* **19** 4205-13

Chapter 4

The Electron Energy Distributions under Steady-State Townsend and Pulsed Townsend Conditions

4.1 Introduction

The electron velocity distribution $f(\boldsymbol{v})$ in gases is generally denoted as a function of the position $\boldsymbol{r}$ and time t as $f(\boldsymbol{r}, \boldsymbol{v}, t)$. As discussed by Tagashira *et al.* (1977), there are three typical observation methods for electron swarms; time-of-flight (TOF), steady-state Townsend (SST) and pulsed Townsend (PT). Values of electron swarm parameters have dependence on these observation methods. Therefore, it is important to strictly define the electron swarm parameters based on each observation method.

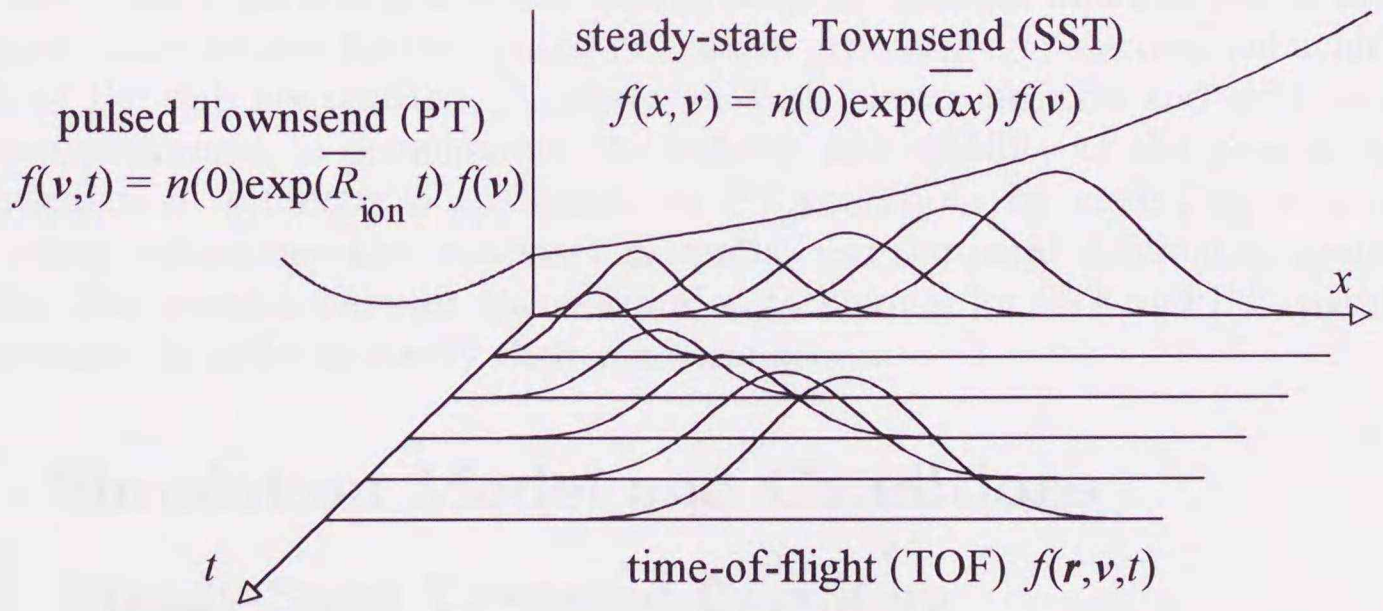

Figure 4.1: Spatio-temporal electron development and observation systems. The electron distributions under steady-state Townsend (SST) and pulsed Townsend (PT) conditions are derived from the time-of-flight (TOF) electron velocity distribution $f_{\mathrm{TOF}}(\boldsymbol{r}, \boldsymbol{v}, t)$ as $f_{\mathrm{SST}}(\boldsymbol{r}, \boldsymbol{v}) = \int_{t=0}^{\infty} f_{\mathrm{TOF}}(\boldsymbol{r}, \boldsymbol{v}, t)\mathrm{d}t$ and $f_{\mathrm{PT}}(\boldsymbol{v}, t) = \int_{\boldsymbol{r}} f_{\mathrm{TOF}}(\boldsymbol{r}, \boldsymbol{v}, t)\mathrm{d}\boldsymbol{r}$. Exponential spatial growth and exponential temporal growth are assumed for electron swarms under SST and PT conditions, respectively.

In TOF experiments, the electron energy distribution is observed as a function of the position and time. $f_{\mathrm{SST}}(\boldsymbol{r}, \boldsymbol{v})$ and $f_{\mathrm{PT}}(\boldsymbol{v}, t)$ are derived from $f_{\mathrm{TOF}}(\boldsymbol{r}, \boldsymbol{v}, t)$ as

$$f_{\mathrm{SST}}(\boldsymbol{r}, \boldsymbol{v}) = \int_{t=0}^{\infty} f_{\mathrm{TOF}}(\boldsymbol{r}, \boldsymbol{v}, t)\mathrm{d}t \tag{4.1}$$

$$f_{\rm PT}(\boldsymbol{v},t) = \int_{\boldsymbol{r}} f_{\rm TOF}(\boldsymbol{r},\boldsymbol{v},t)\mathrm{d}\boldsymbol{r} \tag{4.2}$$

(see figure 4.1). Using the normalized drift equilibrium solutions $f_{\rm SST}(\boldsymbol{v})$ and $f_{\rm PT}(\boldsymbol{v})$, exponential growths of electron swarms under SST and PT conditions with respect to the position and time are respectively represented as

$$f_{\rm SST}(x,\boldsymbol{v}) = n(x=0)f_{\rm SST}(\boldsymbol{v})\exp(\bar{\alpha}x) \tag{4.3}$$

$$f_{\rm PT}(\boldsymbol{v},t) = n(t=0)f_{\rm PT}(\boldsymbol{v})\exp(\bar{R}_{\rm ion}t) \tag{4.4}$$

where $\bar{\alpha}$ and $\bar{R}_{\rm ion}$ are the effective ionization coefficient and frequency, respectively.

$f_{\rm SST}(\boldsymbol{v})$ and $f_{\rm PT}(\boldsymbol{v})$ can be obtained using a multi-term approximation of Boltzmann equation (BEq) analysis assuming the spatial and temporal exponential growths for the SST and PT conditions respectively (*e.g.* Thomas 1969). However, it is necessary to evaluate the influence of neglecting the higher order terms of the Legendre polynomial expansion on the validity of the solutions, especially in case of the calculation at a high E/N where anisotropy may not be negligible.

$f_{\rm PT}(\boldsymbol{v},t)$ can be easily obtained in a Monte Carlo simulation (MCS) by simulating electron behavior in velocity space. The electron behavior in real space can be omitted even in a self-consistent simulation. However, to obtain $f_{\rm SST}(\boldsymbol{v})$, it has been necessary to consider spatial relaxation processes of the swarm as demonstrated in the preceding chapter. One difficulty with an MCS is that the number of electrons decreases due to electron attachment when $\bar{\alpha}$ and $\bar{R}_{\rm ion}$ are negative. In this case, the number of electrons may decay steeply during their relaxation processes before attaining drift equilibrium, and as a result a huge calculation time is required to compensate the decreasing electron population.

In the present chapter, a new calculation technique of a propagator method (PM) is introduced to obtain the drift equilibrium solution of $f_{\rm SST}(\boldsymbol{v})$. The present PM can derive the equilibrium solution by calculating electron behavior in a slab region defined in real space. Calculations for the spatial relaxation processes and electron behavior on the outside of the slab are omitted. Analyses for both electro-positive and electro-negative gases are performed to demonstrate the validity and stability of the present method. This calculation technique is applicable for PT conditions by modifying a calculation factor which determines the treatment of spatial and temporal differential operators in the BEq. The relation between the calculation techniques for SST and PT conditions is also discussed in order to clarify their correspondence.

4.2 Simulation Model and Conditions

4.2.1 Steady-State Townsend Condition

One-dimensional electron flow under a uniform $\boldsymbol{E}$ under an SST condition is considered. In the drift equilibrium region, the number density of electrons $n(x)$ at a position x is denoted as an exponential function (Thomas 1969, Phelps and Pitchford 1985):

$$n(x) = n(0)\exp(\bar{\alpha}x). \tag{4.5}$$

Here, $\bar{\alpha}$ $(=\alpha-\eta)$ is the effective ionization coefficient, which represents the net effect of contributions of the ionization coefficient α and the electron attachment coefficient η. If $f(\boldsymbol{v})$ is assumed to be in drift equilibrium, then its normalized value is identical at any position. $f(x,\boldsymbol{v})$ for the drift equilibrium region is represented as

$$f(x,\boldsymbol{v}) = n(0)\exp(\bar{\alpha}x)f_{\rm SST}(\boldsymbol{v}) \tag{4.6}$$

where $f_{\mathrm{SST}}(\boldsymbol{v})$ is the normalized value of $f(\boldsymbol{v})$ which satisfies

$$\int_{\boldsymbol{v}} f_{\mathrm{SST}}(\boldsymbol{v})\mathrm{d}\boldsymbol{v} = 1. \tag{4.7}$$

Practically, steady-state electron stream may be generated by continuously supplying initial electrons from an electron source. The SST condition defined here is realized after long enough spatio-temporal relaxation processes even if the initial value of $f(\boldsymbol{v})$ is not in drift equilibrium.

4.2.2 Calculation Model

A thin slab of thickness Δx is considered here, which slices the steady-state electron stream perpendicularly to the x axis as shown in figure 4.2.

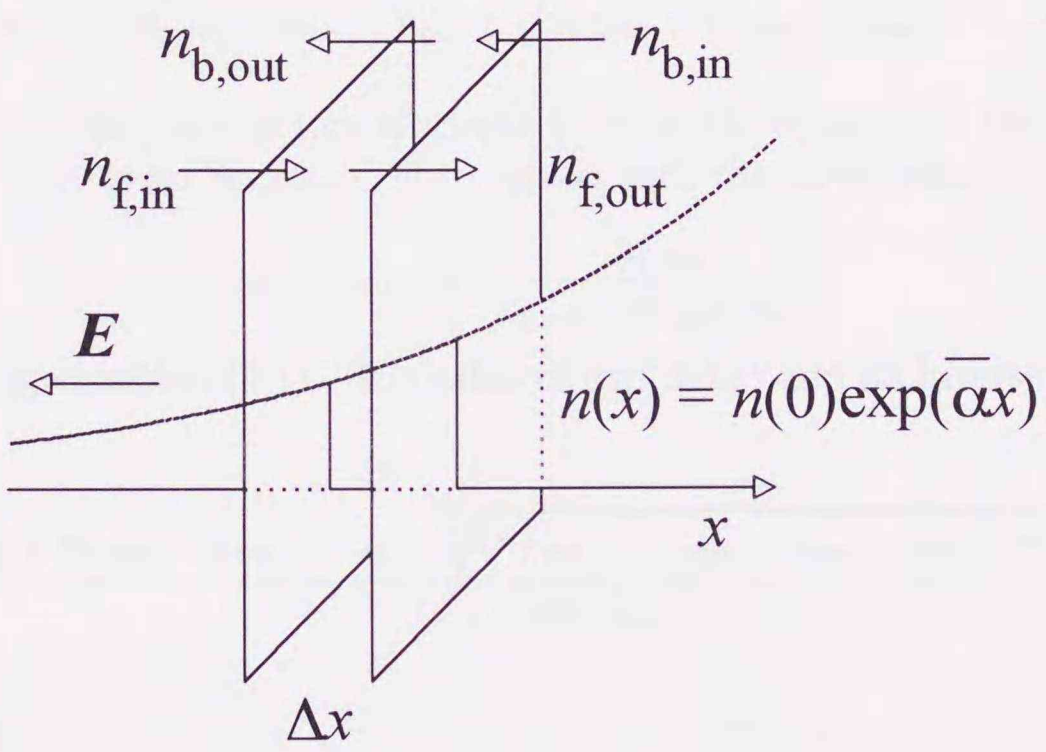

Figure 4.2: Electron stream under an SST condition. Exponential spatial growth of the number of electrons and identity of the normalized electron velocity distribution at any position are assumed. Balance of the electron inflow and outflow for the slab is considered.

The increase and decrease of electrons are observed in the slab Δx. The components of the electron increase are the electron generation due to ionization and the inflow from the outside of the slabs. Similarly, those of the electron decrease are the electron loss due to attachment and the outflow. Here we define the numbers of electrons which represent these increase and decrease as listed in table 4.1.

Table 4.1: The numbers of electrons representing the electron increase and decrease in Δx during Δt.

n_{ion}	generation due to ionization	$n_{\mathrm{f,out}}$, $n_{\mathrm{f,in}}$	forward outflow / inflow
n_{att}	loss due to attachment	$n_{\mathrm{b,out}}$, $n_{\mathrm{b,in}}$	backward outflow / inflow

When $f(\boldsymbol{v})$ in Δx is known, n_{ion} and n_{att} can be derived from $f(\boldsymbol{v})$. $n_{\mathrm{f,out}}$ and $n_{\mathrm{b,out}}$ can be derived from the $f(\boldsymbol{v})$ as well. Furthermore, using $n_{\mathrm{f,out}}$ and $n_{\mathrm{b,out}}$, the numbers

of electrons flowing into Δx, $n_{\mathrm{f,in}}$ and $n_{\mathrm{b,in}}$, are represented as

$$n_{\mathrm{f,in}} = n_{\mathrm{f,out}} \exp(-\bar{\alpha}\Delta x) \tag{4.8}$$
$$n_{\mathrm{b,in}} = n_{\mathrm{b,out}} \exp(\bar{\alpha}\Delta x). \tag{4.9}$$

Note here that the value of $\bar{\alpha}$ is unknown at this moment.

The increase and decrease in the number of electrons must balance under an SST condition. The variation of the number of electrons Δn in the slab is

$$\begin{aligned}\Delta n &= (n_{\mathrm{f,in}} - n_{\mathrm{f,out}}) + (n_{\mathrm{b,in}} - n_{\mathrm{b,out}}) + (n_{\mathrm{ion}} - n_{\mathrm{att}}) \\ &= n_{\mathrm{f,out}}\{\exp(-\bar{\alpha}\Delta x) - 1\} + n_{\mathrm{b,out}}\{\exp(\bar{\alpha}\Delta x) - 1\} + (n_{\mathrm{ion}} - n_{\mathrm{att}}) = 0. \end{aligned} \tag{4.10}$$

The quantity $\exp(\bar{\alpha}\Delta x)$ is obtained from equation (4.10) as

$$\exp(\bar{\alpha}\Delta x) = \frac{2n_{\mathrm{f,out}}}{n_{\mathrm{f,out}} + n_{\mathrm{b,out}} - n_{\mathrm{ion}} + n_{\mathrm{att}} \pm \sqrt{(n_{\mathrm{f,out}} + n_{\mathrm{b,out}} - n_{\mathrm{ion}} + n_{\mathrm{att}})^2 - 4n_{\mathrm{f,out}}n_{\mathrm{b,out}}}}. \tag{4.11}$$

In equation (4.11), the positive sign is adopted so that the equation in the case of $n_{\mathrm{b,out}} = 0$ (that is, when there is no backward flow) agrees with the direct result of equation (4.10), which is

$$\exp(\bar{\alpha}\Delta x) = \frac{n_{\mathrm{f,out}}}{n_{\mathrm{f,out}} - n_{\mathrm{ion}} + n_{\mathrm{att}}}. \tag{4.12}$$

Transforming equation (4.11), the value of $\exp(\bar{\alpha}\Delta x)$ and its inverse are given as

$$\begin{aligned}&\exp(\bar{\alpha}\Delta x) \\ &= \frac{n_{\mathrm{f,out}} + n_{\mathrm{b,out}} - n_{\mathrm{ion}} + n_{\mathrm{att}} - \sqrt{(n_{\mathrm{f,out}} + n_{\mathrm{b,out}} - n_{\mathrm{ion}} + n_{\mathrm{att}})^2 - 4n_{\mathrm{f,out}}n_{\mathrm{b,out}}}}{2n_{\mathrm{b,out}}}\end{aligned} \tag{4.13}$$

$$\begin{aligned}&\exp(-\bar{\alpha}\Delta x) \\ &= \frac{n_{\mathrm{f,out}} + n_{\mathrm{b,out}} - n_{\mathrm{ion}} + n_{\mathrm{att}} + \sqrt{(n_{\mathrm{f,out}} + n_{\mathrm{b,out}} - n_{\mathrm{ion}} + n_{\mathrm{att}})^2 - 4n_{\mathrm{f,out}}n_{\mathrm{b,out}}}}{2n_{\mathrm{f,out}}}.\end{aligned} \tag{4.14}$$

Assuming an exponential spatial growth of an SST electron stream and identity of the normalized $f(\boldsymbol{v})$, not only $n_{\mathrm{f,out}}$ and $n_{\mathrm{b,out}}$ but also $n_{\mathrm{f,in}}$ and $n_{\mathrm{b,in}}$ can be obtained from $f(\boldsymbol{v})$ defined in Δx.

4.2.3 Calculation Scheme

Since one-dimensional model for real space is taken here, the rotational symmetry for the azimuthal component of $f(\boldsymbol{v})$ can be assumed. The electron motion in velocity space can be described as $f(v, \theta)$ where $v = |\boldsymbol{v}|$ and θ is the angle between $\boldsymbol{v}$ and $\boldsymbol{E}$. Cells are defined in the slab for every $\Delta\epsilon$ and $\Delta\theta$ in the same way as done in the preceding chapter. The (i, j)-th cell $C_{i,j}$ occupies a region defined as

$$v_i \le v \le v_{i+1} \qquad \frac{1}{2}mv_i^2 = i\Delta\epsilon, \qquad \frac{1}{2}mv_{i+1}^2 = (i+1)\Delta\epsilon \tag{4.15}$$
$$\theta_j \le \theta \le \theta_{j+1} \qquad \theta_j = j\Delta\theta, \qquad \theta_{j+1} = (j+1)\Delta\theta \tag{4.16}$$

and the number of electrons $n_{i,j}$ in $C_{i,j}$ is represented as

$$n_{i,j} = n(x)\Delta x \int_{v=v_i}^{v_{i+1}} \int_{\theta=\theta_j}^{\theta_{j+1}} f(v,\theta)\frac{1}{2}\sin\theta \mathrm{d}\theta \mathrm{d}v \tag{4.17}$$

where $\frac{1}{2}\sin\theta \mathrm{d}\theta \mathrm{d}v$ is the weight of volume element in v-θ space.

An appropriate set of initial values for $f(v,\theta)$ is necessary to begin iterative relaxation calculation. In the present calculation, $f(v,\theta) = \delta(\boldsymbol{v} = 0)$ is the initial condition. Numerically, only $C_{0,0}$ holds the initial electrons. The electron concentration is assumed to be uniform within a cell with respect to the volume element $\mathrm{d}\boldsymbol{v}$.

The collision and drift processes are calculated as explained below.

In the collision process, the number of electrons undergoing collision k is evaluated as

$$n_k = \sum_{i,j} N q_k(\bar{v}_i)\bar{v}_i \Delta t n_{i,j} \tag{4.18}$$

where N is the number density of gas molecules, q_k is the collision cross section for collision k, and $\bar{v}_i$ is the representative electron velocity of $C_{i,j}$. Equation (4.18) gives n_{ion} and n_{att} in equation (4.10) at the beginning of a calculation cycle, and they are memorized for the subsequent calculation of the drift process. Electrons move to the destination cells depending on their energy loss and scattering angle in the same way as performed in the preceding chapter.

In the drift process, the total number of electrons flowing out of the slab are evaluated based on $n_{i,j}$ for each of forward and backward outflows; $n_{\mathrm{f,out}}$ and $n_{\mathrm{b,out}}$:

$$n_{\mathrm{f,out}} = \sum_{i,j(\mathrm{right})} \frac{n_{i,j}}{V_{i,j}} S_{\epsilon,i+1,j} \frac{eE}{m}\Delta t \tag{4.19}$$

$$n_{\mathrm{b,out}} = \sum_{i,j(\mathrm{left})} \frac{n_{i,j}}{V_{i,j}} S_{\epsilon,i,j} \frac{eE}{m}\Delta t \tag{4.20}$$

where subscripts "right" and "left" represent the right and left hemispheres of velocity space; an electron in the right hemisphere moves forwards in real space, and another in the left does backwards. $V_{i,j}$ is the volume of $C_{i,j}$ defined in velocity space:

$$V_{i,j} = \frac{2}{3}\pi(v_{i+1}^3 - v_i^3)(\cos\theta_j - \cos\theta_{j+1}). \tag{4.21}$$

$S_{\epsilon,i,j}$ is the area of the projection of the intersection between $C_{i,j}$ and $C_{i-1,j}$ to a plane perpendicular to $\boldsymbol{E}$:

$$S_{\epsilon,i,j} = \pi v_i^2(\sin^2\theta_j - \sin^2\theta_{j+1}). \tag{4.22}$$

The quantity $\frac{n_{i,j}}{V_{i,j}} \cdot \frac{eE}{m}$ in equations (4.19) and (4.20) represents the outflowing electron flux, and its product with $S_{\epsilon,i,j}\Delta t$ is the total number of the outflowing electrons through the intersection. Since the electron displacement from $C_{i,j}$ to $C_{i\pm1,j}$ represents the change of the electron energy, those electrons are considered to flow out of the slab spatially. Here, $\Delta\epsilon$ and Δx are chosen to satisfy the relation $\Delta\epsilon = eE\Delta x$ based on the law of energy conservation (Sugawara *et al.* 1992).

Instead of the electrons flowing out of Δx, other electrons flow into Δx from the opposite side (see figure 4.3). The numbers of electrons $n_{\mathrm{f,in},i,j}$ and $n_{\mathrm{b,in},i,j}$ flowing into $C_{i,j}$ forwards and backwards is evaluated based on equations (4.8) and (4.9) as

$$n_{\mathrm{f,in},i,j} = n_{\mathrm{f,out},i-1,j}\exp(-\bar{\alpha}\Delta x) \tag{4.23}$$

$$n_{\mathrm{b,in},i,j} = n_{\mathrm{b,out},i+1,j}\exp(\bar{\alpha}\Delta x). \tag{4.24}$$

Here, the value of $\bar{\alpha}$ is given by equation (4.14). $n_{\mathrm{f,in},i,j}$ and $n_{\mathrm{b,in},i,j}$ are defined for the cells in the right and left hemispheres in velocity space, respectively. $n_{\mathrm{f,out},i,j}$ and $n_{\mathrm{b,out},i,j}$ are subtracted from their source cells. These numbers are divided into fractions corresponding to the destination cells, and the fractions are added to the destination cells.

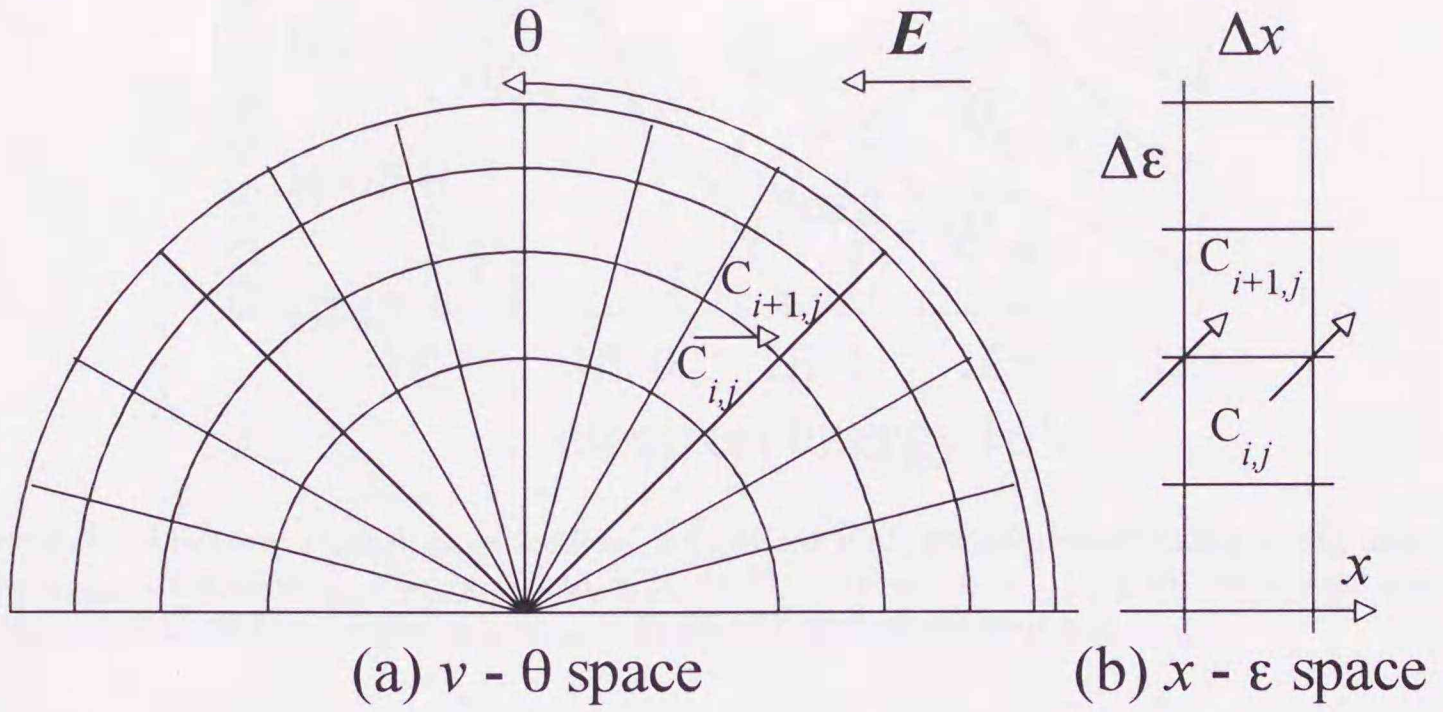

Figure 4.3: Electron motion observed in (a) v-θ space and (b) x-ϵ space. Electrons moving across a concentric intersection between a pair of neighboring cells are accompanied by the change of the electron energy, which corresponds to the change of the position in real space. $\Delta\epsilon = eE\Delta x$ is assumed for the law of energy conservation. Under an assumption of exponential spatial growth, the number of electrons flowing into the cell $C_{i+1,j}$ is evaluated as $n_{\mathrm{f,in},i+1,j} = n_{\mathrm{f,out},i,j} \exp(-\bar{\alpha}\Delta x)$.

Electrons moving across the concentric intersections between a pair of neighboring cells appear as if they multiply, if the observation sight is limited within Δx.

The total number of electrons in Δx, which may vary in the collision process, recovers its initial value after a cycle of iterative calculations. These calculations are repeated until the equilibrium solution of $f(\boldsymbol{v})$ is attained.

4.2.4 Simulation Conditions

The present PM is examined for two kinds of gases; case 1, argon (Ar) at $E/N = 1414$ Td ($\bar{\alpha} > 0$); case 2, an argon (90%) / fluorine (10%) mixture ($\mathrm{Ar/F_2}$) at $E/N = 57$ Td ($\bar{\alpha} < 0$) ~ 141 Td ($\bar{\alpha} > 0$). Case 1 is an example for high E/N condition, under which $\bar{\alpha} \gg 0$. Case 2 includes electron attachment process and its E/N values are chosen so that the sign of $\bar{\alpha}$ changes across zero. Here, the total number density of gas molecules N at 1.0 Torr at 0 °C is 3.54×10^{16} cm^{-3}.

The set of electron collision cross sections for $\mathrm{F_2}$ (figure 4.4) used in the present calculation is taken from Hazi (1981) and Hayashi and Nimura (1983). The cross sections of Ar are the same as in the preceding chapter (Sakai *et al.* 1972, Mason and Newell 1987, Suzuki *et al.* 1990).

4.3 Results and Discussion

$F(\epsilon)$ calculated by the PM are shown in figures 4.5 and 4.6 together with the results of MCS and a two-term approximation of BEq analysis (BE2) for comparison. The Legendre

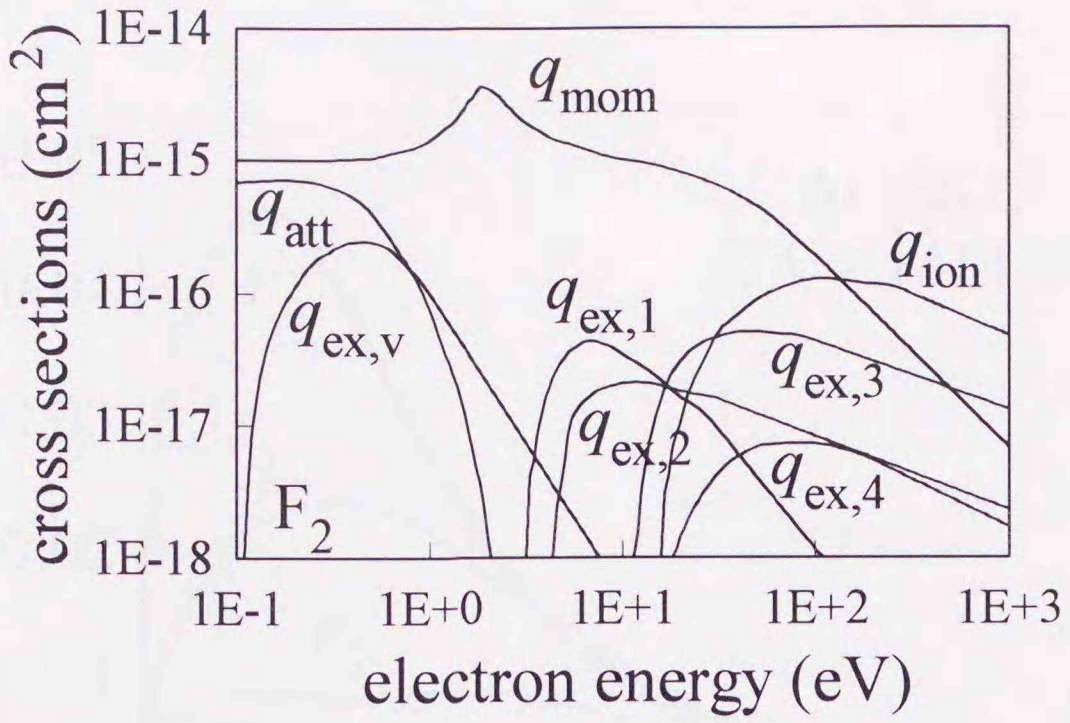

Figure 4.4: Electron collision cross sections of F_2 (Hazi 1981, Hayashi and Nimura 1983); momentum transfer $q_{\rm mom}$, excitation $q_{{\rm ex},k}$ ($\epsilon_{{\rm ex},k} = 3.16$, 4.34, 11.57, 13.08 eV; $k = 1$, 2, 3, 4), vibrational excitation $q_{\rm ex,v}$ ($\epsilon_{\rm ex,v} = 0.11$ eV), ionization $q_{\rm ion}$ ($\epsilon_{\rm ion} = 15.69$ eV), and attachment $q_{\rm att}$.

polynomial expansion terms $F_n(\epsilon)$ ($n = 0, 1, 2, \cdots$) represent the isotropic ($n = 0$) and anisotropic ($n \geq 1$) components of $F(\epsilon)$. $F_n(\epsilon)$ are given using Legendre's polynomials as

$$\begin{aligned} F(\epsilon,\theta) &= F_0(\epsilon)P_0(\cos\theta) + F_1(\epsilon)P_1(\cos\theta) + F_2(\epsilon)P_2(\cos\theta) + \cdots \\ &= \sum_{n=0}^{\infty} F_n(\epsilon)P_n(\cos\theta) \qquad (4.25) \\ F_n(\epsilon) &= \frac{2n+1}{2}\int_{-1}^{1} F(\epsilon,\theta)P_n(\cos\theta)\mathrm{d}(\cos\theta) \qquad (4.26) \end{aligned}$$

where P_n is the n-th order Legendre's polynomial in the series of the spherical harmonic functions:

$$P_0(x) = 1, \quad P_1(x) = x, \quad P_{n+1}(x) = \frac{2n+1}{n+1}xP_n(x) - \frac{n}{n+1}P_{n-1}(x). \qquad (4.27)$$

The swarm parameters, the mean electron energy $\bar{\epsilon}$, the effective ionization coefficient $\bar{\alpha}$, the diffusion coefficient $D_{\rm s}$, the drift velocity $W_{\rm s}$ and the diffusion-modified drift velocity $v_{\rm d}$ ($= W_{\rm s} - \bar{\alpha}D_{\rm s}$), are listed in table 4.2.

The results of MCS except for $\bar{\alpha}$ are sampled in the regions 1.000 cm $\leq x \leq$ 1.002 cm for case 1 and 10.0 cm $\leq x \leq$ 10.1 cm for case 2. Since the values of $\bar{\alpha}$ are sensitive to statistical fluctuation, they are determined as the mean values in regions 0.9 cm $\leq x \leq$ 1.0 cm for case 1 and 2.0 cm $\leq x \leq$ 10.0 cm for case 2. In case 2, a distance longer than that of case 1 is needed to obtain stable results, because electron multiplication in case 2 is small or effectively negative.

4.3.1 Swarm Parameters in Argon

$F(\epsilon)$ obtained by the present PM agrees well with the results of MCS to the higher order terms of Legendre polynomial expansion. The discrepancies of the swarm parameters between the PM and the MCS are less than 1%. These results prove that the present calculation scheme of the PM for the SST condition is properly composed.

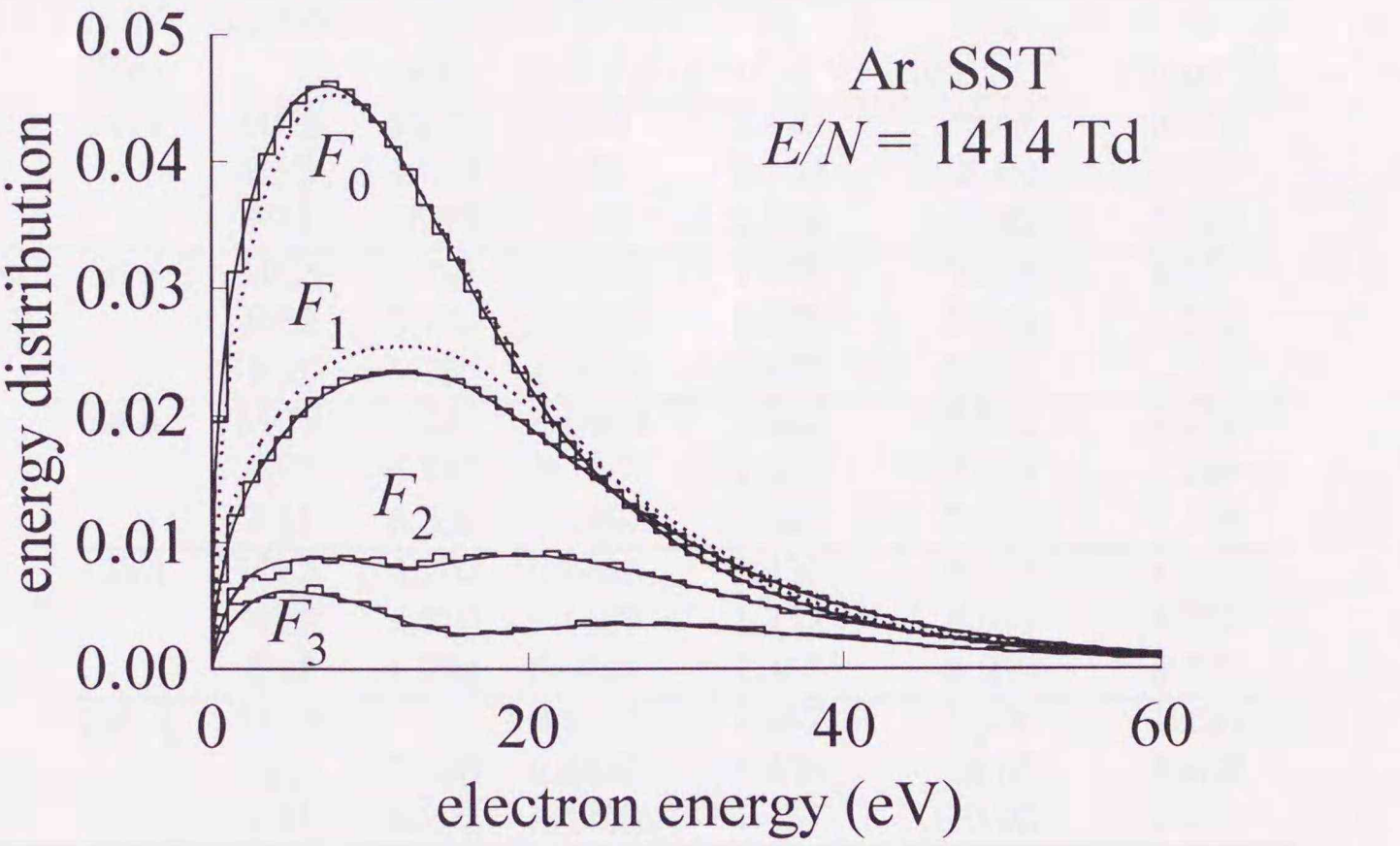

Figure 4.5: The electron energy distribution $F(\epsilon)$ in Ar under the SST condition at E/N = 1414 Td. F_n (n=0,1,2,3) is the n-th term of Legendre polynomial expansion, which represents the isotropic and anisotropic components of the electron velocity distribution. Full curves, the present PM; broken curves, BE2; histograms, MCS.

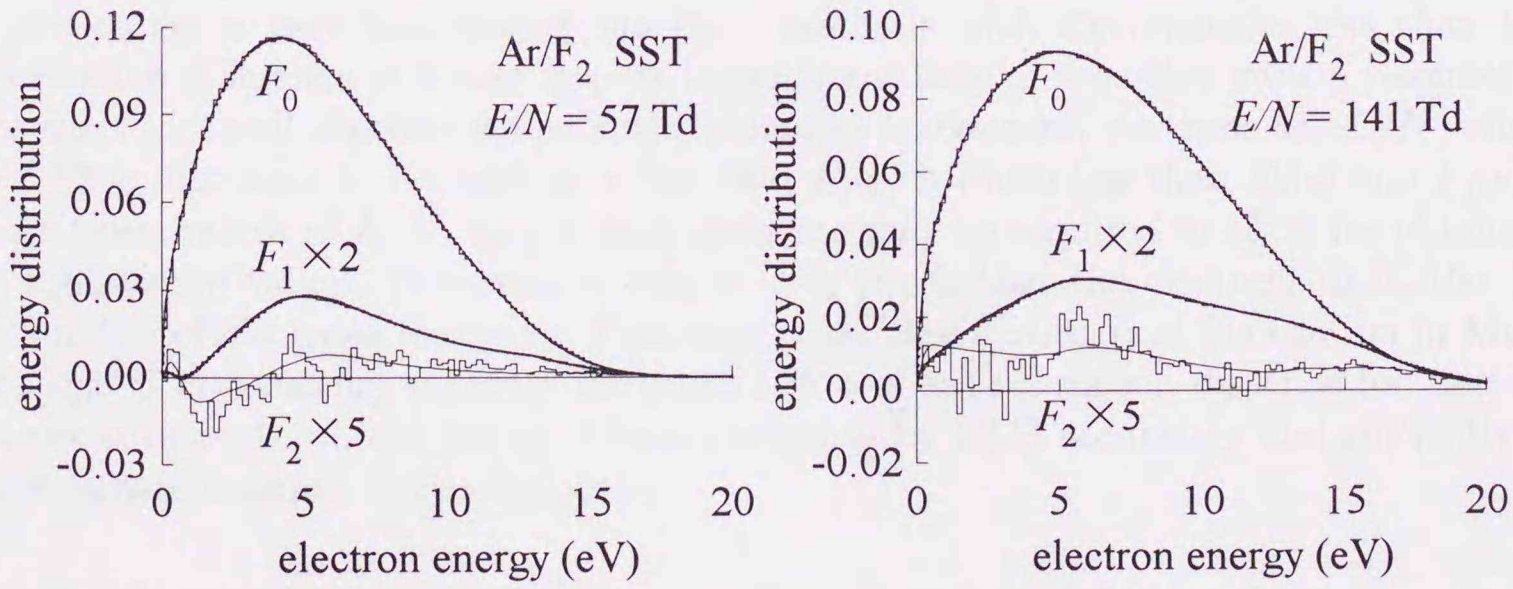

Figure 4.6: The electron energy distribution $F(\epsilon)$ in Ar (90%) / F_2 (10%) mixture under the SST conditions at E/N = 57 Td and 141 Td. Full curves, PM; broken curves, BE2; histograms, MCS. The results of the PM overlap with BE2.

Table 4.2: Comparison of swarm parameters. MCS, Monte Carlo simulation; BE2, Boltzmann equation analysis of 2-term approximation; PM, propagator method.

gas	E/N (Td)	method	$\bar{\epsilon}$ (eV)	$\bar{\alpha}$ (cm^{-1})	D_s ($cm^2 \mu s^{-1}$)	W_s ($cm \mu s^{-1}$)	v_d ($cm \mu s^{-1}$)
Ar	1414	MCS	15.75	10.14	2.120	79.67	58.18
		BE2	16.24	10.56	2.103	81.64	59.43
		PM	15.73	10.12	2.118	79.32	57.89
Ar/F_2 (90:10)	56.6	MCS	5.795	-0.3608	1.475	5.018	5.551
		BE2	5.776	-0.3651	1.475	5.021	5.560
		PM	5.780	-0.3575	1.475	5.024	5.552
	84.8	MCS	6.331	-0.0993	1.462	6.986	7.131
		BE2	6.337	-0.1041	1.461	7.012	7.164
		PM	6.336	-0.0956	1.462	7.016	7.156
	113.1	MCS	6.703	0.1668	1.457	9.017	8.774
		BE2	6.710	0.1609	1.457	8.991	8.757
		PM	6.702	0.1661	1.457	8.989	8.747
	141.4	MCS	7.005	0.4407	1.457	11.00	10.35
		BE2	7.008	0.4339	1.456	10.95	10.32
		PM	6.993	0.4350	1.457	10.93	10.30

The results of the BE2 slightly deviate from those of the PM and MCS. The large values of $F_2(\epsilon)$ and $F_3(\epsilon)$ obtained by the PM and MCS, which are neglected in BE2, suggest that the two-term approximation in BE2 is no longer valid at such a high E/N value.

4.3.2 Swarm Parameters in Argon / Fluorine Mixture

In case 2, $F(\epsilon)$ given by the MCS, BE2 and PM agree well with each other for both positive and negative $\bar{\alpha}$ around zero as shown in figure 4.6. The swarm parameters except for $\bar{\alpha}$ also agree very well among the three methods with discrepancies less than 1%. The relative difference of $\bar{\alpha}$ may appear larger than those of the other swarm parameters because of its small absolute values since $\bar{\alpha}$ changes across zero. At these low E/N values, the BE2 is indicated to be valid by a fact that $F_2(\epsilon)$ is much less than $F_0(\epsilon)$ and $F_1(\epsilon)$.

At lower values of E/N, longer drift distances may be required in MCS for obtaining the equilibrium values. However, in case $\bar{\alpha} < 0$, the farther the electrons drift, the less the number of electrons becomes. That may cause larger statistical fluctuation in MCS. Although it is necessary to know the exact value of the relaxation distance for electron swarms in order to obtain the equilibrium solution by MCS accurately and efficiently, it is not easy to evaluate it quantitatively.

4.3.3 Features of the Present Propagator Method

The calculation in the present PM is performed within only one slab. The cells are defined only in the slab and calculation for the spatial relaxation processes can be omitted. Behavior of electrons outside of the slab is considered in terms of $\bar{\alpha}$ and identity of the normalized f($\boldsymbol{v}$). The present PM skillfully utilizes the definition of the SST condition, exponential spatial growth of the electron swarm.

For the same resolution of $\Delta\epsilon$ and $\Delta\theta$, the number of cells required in the present calculation for obtaining the drift equilibrium solution is 1/500 of the number required in the preceding chapter. This feature directly leads to saving the computational load such as the capacity of memory storage and calculation time, that is an advantage for efficient analyses of $F_{\mathrm{SST}}(\epsilon)$.

The present PM for $F_{\mathrm{SST}}(\epsilon)$ is based on an integral calculation manner. Therefore, the PM is free from numerical instability, which may be caused by differential calculations such as in BEq analyses. For every case examined in this chapter, $f(\boldsymbol{v})$ converged steadily even though the calculations started with one of the most special initial conditions, δ function at $\boldsymbol{v} = 0$.

Throughout the calculation scheme of the present PM, the number of electrons in the slab is kept constant for any values of $\bar{\alpha}$. That may represent the possibility of the present PM to stably calculate $F_{\mathrm{SST}}(\epsilon)$ under extremely large or small $\bar{\alpha}$.

4.4 Observation-System-Dependent Configurations

As shown in the beginning of this chapter, $f_{\mathrm{SST}}(\boldsymbol{r}, \boldsymbol{v})$ and $f_{\mathrm{PT}}(\boldsymbol{v}, t)$ are given by integrating $f_{\mathrm{TOF}}(\boldsymbol{r}, \boldsymbol{v}, t)$ with respect to time and position respectively. In a multi-term approximation of BEq analysis performed in velocity space, $f_{\mathrm{SST}}(\boldsymbol{v})$ and $f_{\mathrm{PT}}(\boldsymbol{v})$ are derived assuming exponential spatial growth and exponential temporal growth of electron swarms under SST and PT conditions respectively. In mathematical descriptions of the BEq analysis, the spatial and temporal effects are represented as differential operators $\partial/\partial x$ and $\partial/\partial t$ (Thomas 1969, Tagashira 1982). The condition of the exponential growths allows us replacing the operators $\partial/\partial x$ and $\partial/\partial t$ appropriately with $\bar{\alpha}$ and $\bar{R}_{\mathrm{ion}}$, or zero, when a drift equilibrium solution is assumed.

Table 4.3: Replacement rule for differential operators in Boltzmann equation analyses in velocity space.

observation condition	spatial aspect	temporal aspect
SST	$\partial/\partial x = \bar{\alpha}$	$\partial/\partial t = 0$
	(exponential spatial growth)	(steady state)
PT	$\partial/\partial x = 0$	$\partial/\partial t = \bar{R}_{\mathrm{ion}}$
	(spatial integration)	(exponential temporal growth)

$\partial/\partial x = \bar{\alpha}$ and $\partial/\partial t = 0$ are assumed for an SST condition. These conditions directly represent the exponential spatial growth quantified by the effective ionization coefficient $\bar{\alpha}$ and a steady state of an electron swarm. On the other hand, $\partial/\partial x = 0$ and $\partial/\partial t = \bar{R}_{\mathrm{ion}}$ are assumed for a PT condition. $\partial/\partial t = \bar{R}_{\mathrm{ion}}$ represents the exponential temporal growth of an electron swarm. $\partial/\partial x = 0$ may represent that $f(x, \boldsymbol{v}, t)$ is integrated spatially to give $f(\boldsymbol{v}, t)$ of the whole electron swarm, because the integral of the differential term $(\partial/\partial x) f(x, \boldsymbol{v}, t)$ throughout x becomes zero when $f(x = \pm\infty, \boldsymbol{v}, t) = 0$ can be assumed as a boundary condition. This condition is equivalent to a model that $f(\boldsymbol{r}, \boldsymbol{v}, t)$ is spatially uniform.

Similarly to the case of BEq analyses, the calculation scheme of the present PM introduced in this chapter gives the drift equilibrium solution under a PT condition when $\bar{\alpha} = 0$ is forcedly assumed in the calculation scheme. In this case, the number of electrons in the slab varies every calculation cycle, and its tendency is described as $\exp(\bar{R}_{\mathrm{ion}} t)$.

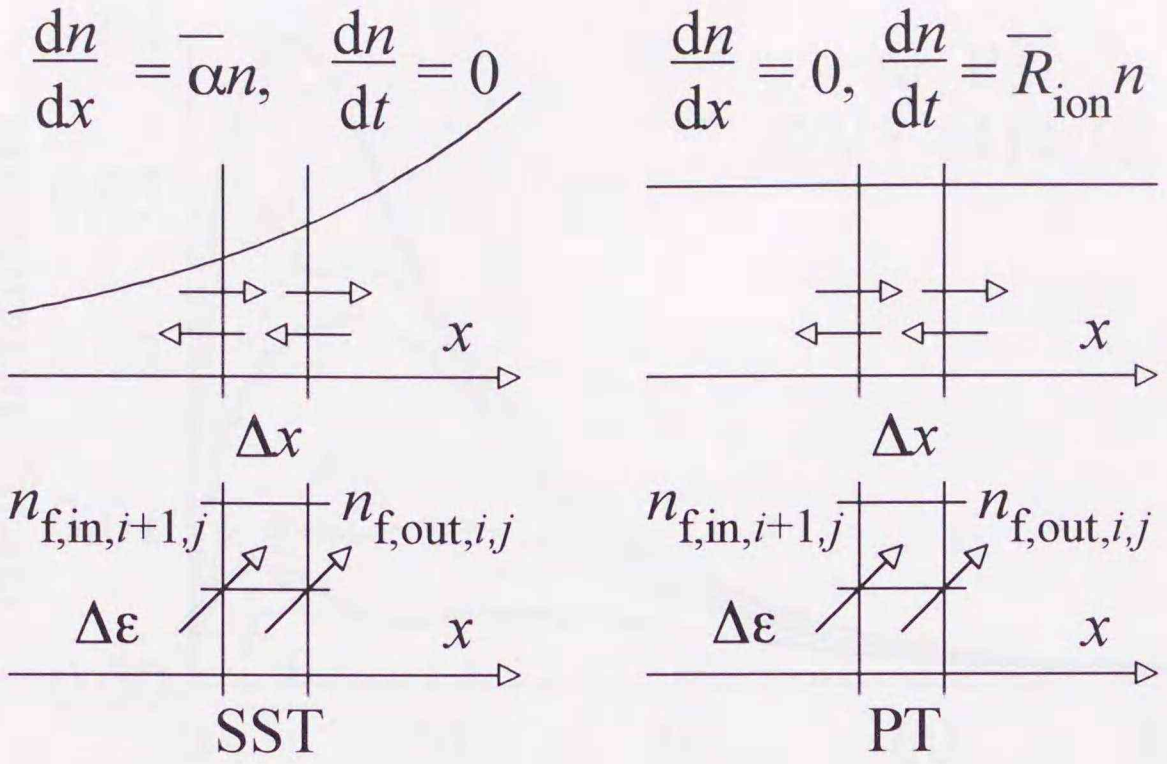

Figure 4.7: Correspondence between the evaluation factors for the electron flow around a slab and the spatial density gradient of electrons under steady-state Townsend (SST) and pulsed Townsend (PT) conditions. The relations between $n_{\mathrm{f,in},i+1,j}$ and $n_{\mathrm{f,out},i,j}$ are given as $n_{\mathrm{f,in},i+1,j} = n_{\mathrm{f,out},i,j} \exp(-\bar{\alpha}\Delta x)$ for SST conditions and $n_{\mathrm{f,in},i+1,j} = n_{\mathrm{f,out},i,j}$ for PT conditions.

As an example of a PT solution, $F(\epsilon)$ in Ar is shown in figure 4.8, which is calculated at the same E/N value as examined for case 1 of the SST conditions. The results of the present PM agree well with that of an MCS as well. Stability of the calculation scheme of the PT-PM, especially in cases of $\bar{R}_{\mathrm{ion}} < 0$, is expected similarly to the cases under SST conditions.

The only difference between the PT and SST calculation schemes based on the PM is the following point. The relaxation processes observed in a PT simulation is real physical processes corresponding to the temporal development of an electron swarm. On the other hand, the iterative calculation performed in an SST simulation is simply a numerical relaxation.

4.5 Chapter Summary

A new calculation technique for obtaining $F(\epsilon)$ of electron swarms in gases under SST condition was introduced based on a PM. The present PM can give the drift equilibrium solution from calculations performed in only one slab in real space. In contrast, MCS and conventional PM require calculations for the spatial relaxation processes of electron swarms.

The results of the present PM agreed well with those obtained by MCS and BE2. For both electro-positive and electro-negative gases, the present PM gave accurate solutions stably.

The calculation scheme for SST conditions can be modified for PT conditions with a minor change of evaluation factor for the electron flow. The calculation results under a PT condition obtained by the modified PM also showed excellent agreement with the results of an MCS. Correspondence between the computational treatments for SST and PT conditions was discussed.

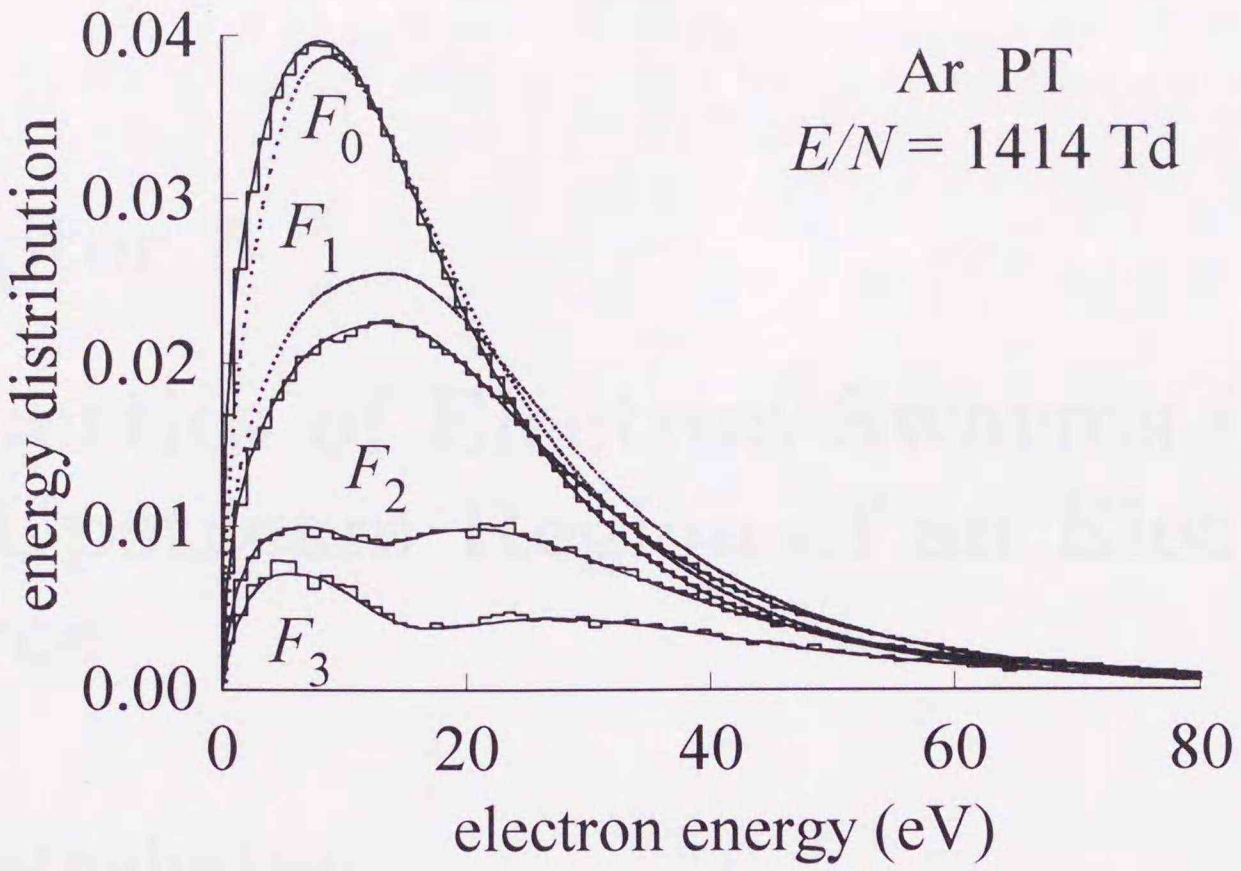

Figure 4.8: The electron energy distribution $F(\epsilon)$ in Ar under the PT condition at E/N = 1414 Td. F_n (n=0,1,2,3) is the n-th term of Legendre polynomial expansion. Full curves, PM; broken curves, BE2; histograms, MCS. The distributions have longer tails at high energies than that under the SST condition shown in figure 4.5.

References

Hayashi M and Nimura T 1983 *J.Appl.Phys.* **54** 4879-82
Hazi A U 1981 *Phys.Rev.Lett.* **46** 918-22
Mason N J and Newell W R 1987 *J.Phys.B: At.Mol.Phys.* **5** 1357-77
Phelps A V and Pitchford L C 1985 *Phys.Rev.A* **31** 2932-49
Sakai Y, Tagashira H and Sakamoto S 1972 *J.Phys.B: At.Mol.Phys.* **5** 1010-6
Sugawara H, Sakai Y and Tagashira H 1992 *J.Phys.D: Appl.Phys.* **25** 1483-7
Suzuki M, Taniguchi T and Tagashira H 1990 *J.Phys.D: Appl.Phys.* **23** 842-50
Tagashira H, Sakai Y and Sakamoto S 1977 *J.Phys.D: Appl.Phys.* **10** 1051-63
Tagashira H (edition)
1982 *"Simulation Techniques for Gas Discharges"*, *IEE Jpn. Technical Report* **II-140**
Thomas W R L 1969 *J.Phys.B: At.Mol.Phys.* **2** 551-61

Chapter 5

Properties of Electron Swarms in the Upstream Region of an Electron Source

5.1 Introduction

A steady-state electron swarm is formed by continuously supplying initial electrons from a point source in gases in the presence of an electric field $\boldsymbol{E}$. These electrons drift toward $-\boldsymbol{E}$ direction from the electron source. Here, this direction, usually considered to be forward direction, is defined as the downstream direction. Under a steady-state Townsend (SST) condition, exponential spatial growth of the number of electrons is assumed.

Because of scattering at collisions with gas molecules, electrons may move backward against $\boldsymbol{E}$. When initial electrons have high enough energies, electrons may be observed not only in the downstream region (DSR) but also in the upstream region (USR) relative to the electron source due to backward diffusion of electrons as has been demonstrated by a Monte Carlo simulation (Braglia and Lowke 1979), for example. Here, backward diffusion is defined as being the mechanism by which electrons penetrate the USR. Such an aspect would be realized by adopting a mesh cathode as the electron source in an experimental observation.

Although most of the literature on electron swarms has dealt with those in the DSR, a number of investigators have addressed electron behavior in the USR. Exponential spatial growth of electron swarms under SST conditions has been predicted not only in the DSR but also in the USR due to backward diffusion. Tagashira (1985, 1991) obtained two solutions of the ionization coefficient α by solving the continuity equation assuming exponentially varying electron population in real space, and suggested that these two solutions correspond to the coefficients of the relative density gradient in the USR and DSR. Standish (1989) solved a kinetic equation for the steady-state spatial distributions of charged particles using eigenfunctions for particle transport. This analysis showed the exponential spatial dependence of the charged particle number density in both the USR and DSR. Standish (1989), Kondo and Tagashira (1990) and Robson (1991) concluded that the two solutions of α are the real roots of the 0-th order dispersion relation for electron transport and they correspond to the USR and DSR.

It is known that effects of the backward-diffusing electrons on the spatial electron distribution are implicitly included in phenomena related to boundary conditions. An example of such phenomena is the decay in the electron number density in front of an absorbing anode, which can be found in the results of analyses for electron swarms between

parallel plane electrodes investigated in chapter 3. Chantry (1982) investigated the decay in the electron number density in front of an absorbing anode in terms of complementarity theorem. The principal idea of the theorem is that the decay is considered to be vacancies missing backward-diffusing electrons which have been absorbed at the anode. The vacancy might be filled up if the absorbed electrons could continue their flight even after the absorption in the same way as in discharge space.

A simulation technique of a propagator method (PM) was introduced in the preceding chapter for obtaining the drift equilibrium solution of the electron velocity distribution $f_{\rm SST}(\boldsymbol{v})$ under an SST condition. In the present chapter, this technique is modified for the USR and applied to investigations of electron swarm properties in the USR. Relations among swarm parameters in the USR are deduced, and the electron energy distribution $F(\epsilon)$ in some gases are calculated by the PM. Particular features of the relations among swarm parameters and $F(\epsilon)$ in the USR are presented.

5.2 Analysis Model

As shown in figure 5.1, three regions can be defined relative to the electron source position; the near-source region, the downstream region (USR) and the upstream region (DSR). The near-source region is a region of non-equilibrium relaxation. The DSR and USR are regions in drift equilibrium. Here, the DSR is defined as being the direction of the acceleration for an electron due to $\boldsymbol{E}$. The USR is simply the opposite direction.

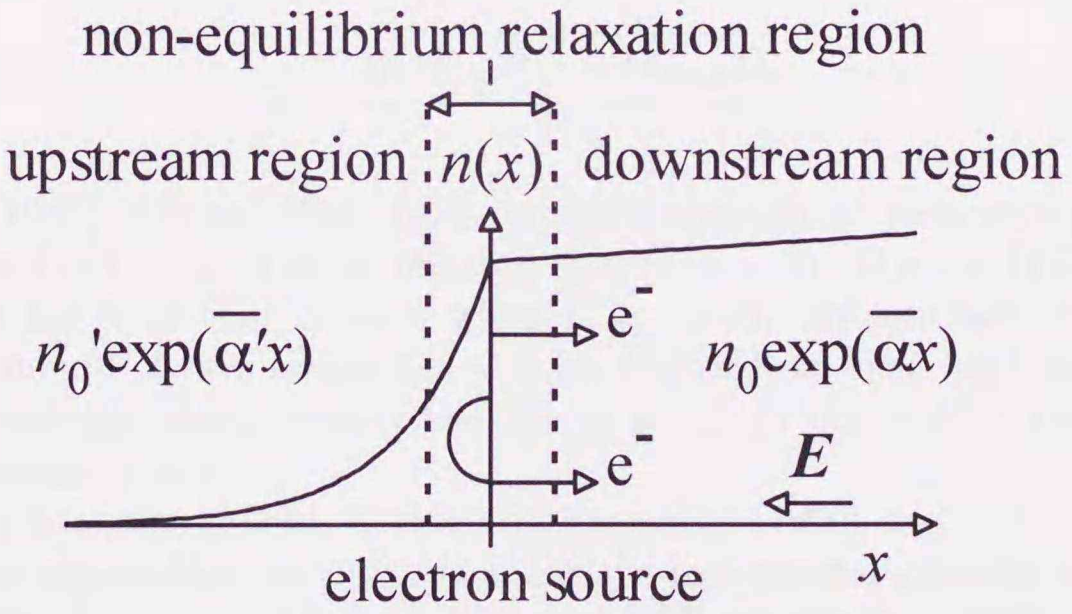

Figure 5.1: The regions around an electron source. The "downstream" and "upstream" directions are defined based on the direction of the acceleration for an electron due to $\boldsymbol{E}$ along x axis. Exponential spatial distribution of electrons is assumed for the steady-state electron stream in both upstream region (USR) and downstream region (DSR).

In an SST condition, it is assumed that the number of electrons exponentially increases due to ionization or decreases due to attachment in the DSR with the increase in the distance from the source, and $f_{\rm SST}(\boldsymbol{v})$ in drift equilibrium in each of the USR and DSR is particular to each region.

The electron number density $n(x)$ and $f_{\rm SST}(x, \boldsymbol{v})$ at position x are described using the effective ionization coefficient $\bar{\alpha}$ as follow (Thomas 1969, Phelps and Pitchford 1985):

$$n(x) = n_0 \exp(\bar{\alpha} x) \tag{5.1}$$

$$f(x, \boldsymbol{v}) = f_{\rm SST}(\boldsymbol{v}) n(x) \tag{5.2}$$

where $f_{\mathrm{SST}}(\boldsymbol{v})$ is the normalized electron velocity distribution in drift equilibrium. In addition to the exponential spatial growth of electron swarms, identity of the electron velocity distribution is assumed here.

5.3 Relations among Swarm Parameters

5.3.1 Relative Density Gradient Coefficient

The continuity equation for electrons under SST conditions may be described using SST swarm parameters as follows (Thomas 1969, Tagashira *et al.* 1977, Blevin and Fletcher 1984):

$$R_{\mathrm{ion,s}} n(x) - W_{\mathrm{s}} \frac{\partial}{\partial x} n(x) + D_{\mathrm{s}} \frac{\partial^2}{\partial x^2} n(x) = 0 \tag{5.3}$$

where $R_{\mathrm{ion,s}}$, W_{s} and D_{s} are the effective ionization frequency, the electron drift velocity and the electron diffusion coefficient for SST conditions, respectively. The SST parameters were defined by rearranging all the higher order parameters for the time-of-flight experiment.

When an exponential solution $n(x) = n_0 \exp(\bar{\alpha} x)$ is assumed, the operator $\partial/\partial x$ may be replaced by $\bar{\alpha}$ to give

$$R_{\mathrm{ion,s}} n_0 - \bar{\alpha} W_{\mathrm{s}} n_0 + \bar{\alpha}^2 D_{\mathrm{s}} n_0 = 0. \tag{5.4}$$

Two solutions for $\bar{\alpha}$ are obtained as

$$\bar{\alpha} = \frac{W_{\mathrm{s}} \pm \sqrt{W_{\mathrm{s}}^2 - 4 R_{\mathrm{ion,s}} D_{\mathrm{s}}}}{2 D_{\mathrm{s}}}. \tag{5.5}$$

Tagashira (1985) inferred that these solutions correspond respectively to the USR ($x < 0$) and the DSR ($x > 0$) of an electron source ($x = 0$). For the DSR, the negative sign is adopted for $\bar{\alpha}$ so that $\bar{\alpha} \to 0$ when $R_{\mathrm{ion,s}} \to 0$. In contrast, the exponent in equation (5.1) should always satisfy $\bar{\alpha} x < 0$ for the USR so that $n(x)$ always decays in the upstream direction irrespective of the sign of $R_{\mathrm{ion,s}}$. In this case, $\bar{\alpha}$ simply represents the relative gradient of $n(x)$.

As shown by Standish (1989), Kondo and Tagashira (1990) and Robson (1991), there are two different eigenvalues for $\bar{\alpha}$ representing the exponential growths in the USR and DSR. Two solutions of $f_{\mathrm{SST}}(\boldsymbol{v})$ for the USR and DSR are determined by different eigenvalues, *i.e.* $\bar{\alpha}$, thus they must be different from each other. Therefore, electron swarm parameters such as W_{s}, D_{s} and $R_{\mathrm{ion,s}}$ will have different values for the USR and DSR, although the formulations to deduce them are identical for both USR and DSR (Tagashira *et al.* 1977, section 3.3; Blevin and Fletcher 1984, section 3(b)).

Hereafter, the primed swarm parameters indicate those obtained from $f_{\mathrm{SST}}(\boldsymbol{v})$ in the USR while the unprimed ones indicate those in the DSR as follow:

$$\bar{\alpha} = \frac{W_{\mathrm{s}} - \sqrt{W_{\mathrm{s}}^2 - 4 R_{\mathrm{ion,s}} D_{\mathrm{s}}}}{2 D_{\mathrm{s}}} \qquad \text{(DSR; downstream region)} \tag{5.6}$$

$$\bar{\alpha}' = \frac{W_{\mathrm{s}}' + \sqrt{W_{\mathrm{s}}'^2 - 4 R_{\mathrm{ion,s}}' D_{\mathrm{s}}'}}{2 D_{\mathrm{s}}'} \qquad \text{(USR; upstream region).} \tag{5.7}$$

5.3.2 Drift Velocity

When an exponential distribution for the electrons, $n_0 \exp(\bar{\alpha}' x)$, is assumed in the USR (Standish, 1989), the total number of electrons $N_e(x')$ on the upstream side of a position $x'(< 0)$ has a finite value and can be written as

$$N_e(x') = \int_{-\infty}^{x'} n_0 \exp(\bar{\alpha}' x) \mathrm{d}x = \frac{n_0}{\bar{\alpha}'} \exp(\bar{\alpha}' x'). \tag{5.8}$$

Since $N_e(x')$ is constant under a steady state, the electron generation per unit time $R'_{ion,s} \times N_e(x')$ in this region must be equal to the electron outflow across the position $x = x'$ towards the DSR per unit time. Equating the generation rate to the outflow, which is the flux denoted as $n_0 \exp(\bar{\alpha}' x') \times v'_d$, the following relation is obtained.

$$R'_{ion,s} \cdot \frac{n_0}{\bar{\alpha}'} \exp(\bar{\alpha}' x') = n_0 \exp(\bar{\alpha}' x') \cdot v'_d. \tag{5.9}$$

Here, v'_d is the average electron velocity ($\equiv$ flux / density, Robson 1991), which is identical with the diffusion-modified drift velocity ($\equiv W'_s - \bar{\alpha}' D'_s$, Tagashira *et al.* 1977) under SST conditions. This velocity represents the average of the velocity component parallel to $\boldsymbol{E}$ throughout the electrons at a position. Equation (5.9) can be simplified to

$$R'_{ion,s} = v'_d \bar{\alpha}' \tag{5.10}$$

which is similar to a relation among swarm parameters in the DSR:

$$R_{ion,s} = v_d \bar{\alpha}. \tag{5.11}$$

An equivalent discussion may be presented by using a differential form of the continuity equation of electrons for one-dimensional SST conditions:

$$\frac{\partial}{\partial t} n(x) = -v_d(x) \mathrm{div}\, n(x) - a(x) \mathrm{div}\, v_d(x) + R_{ion,s}(x) n(x) \tag{5.12}$$

where a is the acceleration due to $\boldsymbol{E}$. Putting $\frac{\partial}{\partial t} n(x)$ and $\mathrm{div}\, v_d(x)$ to be zero based on the assumption of steady state, and substituting $\bar{\alpha}$ for $\mathrm{div}\, n(x)$, the same result as equation (5.10) is obtained.

Since $v_d > 0$ is always satisfied in the DSR, the same sign is shared by $\bar{R}_{ion,s}$ and $\bar{\alpha}$. The relative electron density gradient $\bar{\alpha}$ of $n(x) = n_0 \exp(\bar{\alpha} x)$ directly represents electron multiplication due to ionization ($\bar{R}_{ion,s}, \bar{\alpha} > 0$) or decay due to electron attachment ($\bar{R}_{ion,s}, \bar{\alpha} < 0$). On the other hand, $\bar{\alpha}' > 0$ in the USR is always satisfied, $\bar{R}'_{ion,s}$ and v'_d must share the same sign. Therefore, the sign of average velocity v'_d as well as that of $\bar{R}'_{ion,s}$ indicates whether the gas is effectively electro-positive ($\bar{R}'_{ion,s}, v'_d > 0$) or electro-negative ($\bar{R}'_{ion,s}, v'_d < 0$).

In the special case that the number of electrons is conservative, *i.e.* the gain of electrons due to ionization exactly balances the loss due to attachment, v'_d becomes zero since $R'_{ion,s} = 0$. Under this condition, the following relation is deduced by giving $R_{ion,s} = 0$ to equation (5.4) as

$$W'_s = \bar{\alpha}' D'_s. \tag{5.13}$$

This relation represents a balance between drift due to $\boldsymbol{E}$ and backward diffusion caused by the density gradient, in contrast that equation (5.4) becomes trivial when $\bar{R}_{ion,s} = 0$ and $\bar{\alpha} = 0$ in the DSR.

5.4 Calculation for the Electron Velocity Distribution

In the preceding section, it was shown that equation (5.10) in the USR is exactly analogous to that in the DSR. The validity of equation (5.10) is demonstrated in this section by a simulation based on a PM. The PM for $f_{\mathrm{SST}}(\boldsymbol{v})$ introduced in the preceding chapter is modified here for analyses in the USR.

5.4.1 Computational Configuration for the Upstream Region

$f_{\mathrm{SST}}(\boldsymbol{v})$ is calculated in a thin slab Δx normal to the electron stream in the same manner as in the preceding chapter. Most part of the computational scheme for the USR is analogous to that for the DSR. Rotational symmetry for $f_{\mathrm{SST}}(\boldsymbol{v})$ is assumed under a uniform $\boldsymbol{E}$. Electron motion in velocity space is described by the electron speed v and the angle θ between $\boldsymbol{v}$ and $\boldsymbol{E}$. Velocity space is divided into cells for every $\Delta\epsilon$ and $\Delta\theta$. $f_{\mathrm{SST}}(\boldsymbol{v})$ is calculated as the numbers of electrons in the cells. The acceleration due to $\boldsymbol{E}$ and scattering at collisions with gas molecules are calculated based on the propagators for the drift and collision processes alternately.

The only difference of the present computational scheme for USR from that for DSR is the treatment for the sign in the roots of the quadratic equation to determine the quantities $\exp(\bar{\alpha}'\Delta x)$.

The value $\exp(\bar{\alpha}'\Delta x)$ was determined based on the following conservation equation for the number of electrons in Δx:

$$n_{\mathrm{b,out}}\{\exp(\bar{\alpha}'\Delta x) - 1\} + n_{\mathrm{f,out}}\{\exp(-\bar{\alpha}'\Delta x) - 1\} + (n_{\mathrm{ion}} - n_{\mathrm{att}}) = 0. \tag{5.14}$$

Here, $n_{\mathrm{f,out}}$, $n_{\mathrm{b,out}}$, n_{ion} and n_{att} are the changes of the number of electrons in a time step due to forward and backward outflows, ionization, and attachment, respectively. Equation (5.14) has two solutions:

$$\exp(\bar{\alpha}'\Delta x) = \frac{n_{\mathrm{f,out}} + n_{\mathrm{b,out}} - n_{\mathrm{ion}} + n_{\mathrm{att}} \pm \sqrt{(n_{\mathrm{f,out}} + n_{\mathrm{b,out}} - n_{\mathrm{ion}} + n_{\mathrm{att}})^2 - 4n_{\mathrm{f,out}}n_{\mathrm{b,out}}}}{2n_{\mathrm{b,out}}}. \tag{5.15}$$

The sign of the solution is chosen in the same way as discussed in the preceding section; the positive sign is adopted for $\bar{\alpha}'$ so that it always has a positive value in the USR. Note that the choice of the negative sign was shown to be valid for determining the electron velocity distributions and electron swarm parameters in the DSR in the preceding chapter:

$$\exp(\bar{\alpha}'\Delta x) = \frac{n_{\mathrm{f,out}} + n_{\mathrm{b,out}} - n_{\mathrm{ion}} + n_{\mathrm{att}} + \sqrt{(n_{\mathrm{f,out}} + n_{\mathrm{b,out}} - n_{\mathrm{ion}} + n_{\mathrm{att}})^2 - 4n_{\mathrm{f,out}}n_{\mathrm{b,out}}}}{2n_{\mathrm{b,out}}} \tag{5.16}$$

$$\exp(\bar{\alpha}\Delta x) = \frac{n_{\mathrm{f,out}} + n_{\mathrm{b,out}} - n_{\mathrm{ion}} + n_{\mathrm{att}} - \sqrt{(n_{\mathrm{f,out}} + n_{\mathrm{b,out}} - n_{\mathrm{ion}} + n_{\mathrm{att}})^2 - 4n_{\mathrm{f,out}}n_{\mathrm{b,out}}}}{2n_{\mathrm{b,out}}}. \tag{5.17}$$

The calculation starts with an appropriate initial $f(\boldsymbol{v})$ in Δx and iterative relaxation process is repeated until $f_{\mathrm{SST}}(\boldsymbol{v})$ is attained. In the USR, some of the electrons must have high enough energies so that they can diffuse backwards against $\boldsymbol{E}$. Therefore, a high enough maximum velocity v_{max} and appropriate values for $f(v_{\mathrm{max}})$ were chosen for the present calculation as boundary conditions.

Table 5.1: Conditions for USR analyses.

case 1	Ar	$E/N = 1414$ Td	$R'_{\mathrm{ion,s}} > 0$
case 2	ramp model gas	$E/N = 283$ Td	$R'_{\mathrm{ion,s}} = 0$
case 3	SF_6	$E/N = 141$ Td	$R'_{\mathrm{ion,s}} < 0$

5.4.2 Gases and Electric Fields

Three kinds of gases listed in table 5.1 are chosen to confirm equation (5.10); argon (Ar), a ramp model gas and sulphur-hexafluoride (SF_6). The sets of cross sections used in the present calculations are taken from Reid (1979) for the ramp model gas, and Itoh *et al.* (1988, 1993) for SF_6. The cross sections of argon (Mason and Newell 1987, Sakai *et al.* 1972, Suzuki *et al.* 1990) is the same as used in preceding chapters.

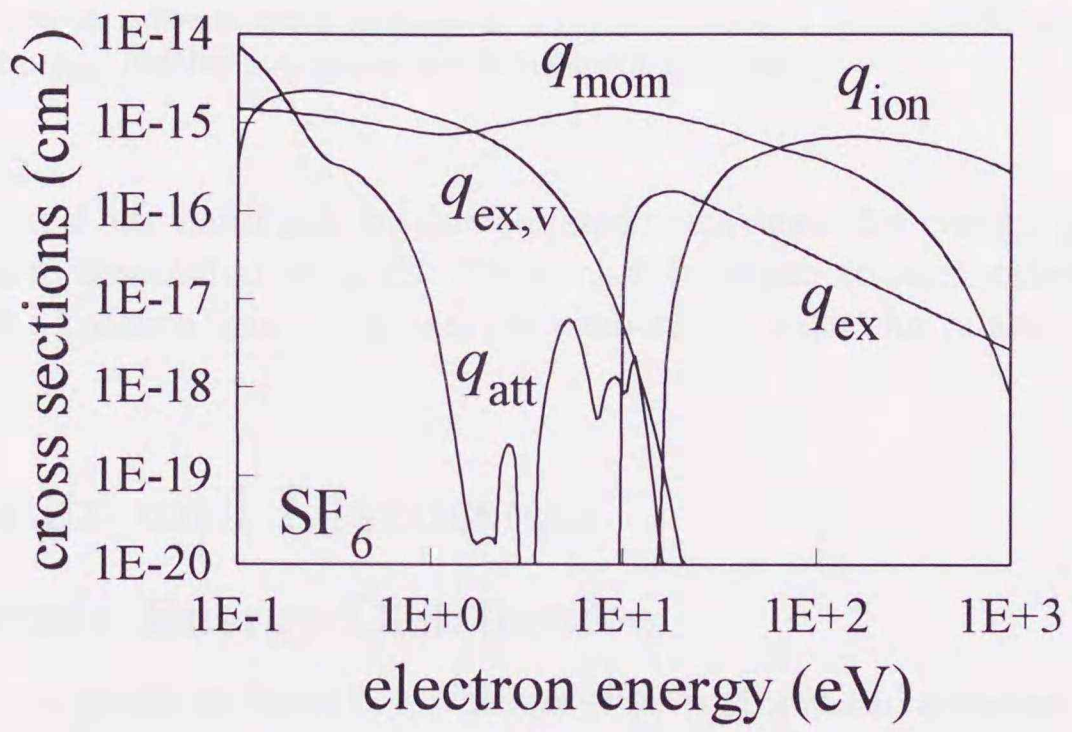

Figure 5.2: Electron collision cross sections of sulphur-hexafluoride (Itoh *et al.* 1988); momentum transfer q_{mom}, excitation q_{ex} ($\epsilon_{\mathrm{ex}} = 9.8$ eV), vibrational excitation $q_{\mathrm{ex,v}}$ ($\epsilon_{\mathrm{ex,v}} = 0.095$ eV), ionization q_{ion} ($\epsilon_{\mathrm{ion}} = 15.8$ eV), and electron attachment q_{att}. q_{att} is the total attachment cross section to form SF_6^-, SF_5^-, SF_4^-, F^- and F_2^-.

For case 1, a high E/N is chosen so that $R'_{\mathrm{ion,s}}$ is large enough to give a significant value of v'_{d}. On the other hand, a low E/N is chosen for case 3 so that $R'_{\mathrm{ion,s}}$ becomes a large negative value. They are chosen to emphasize the ionization in case 1 and attachment in case 3. The number density of gas molecules N is assumed to be 3.53×10^{16} cm^{-3}, which is the value at 1.0 Torr at 0 °C.

The following energy balance equation (Thomas 1969) has been examined for all the drift equilibrium solutions obtained by the present PM for the USR in order to confirm their validity:

$$\sum_k R'_{\mathrm{ex},k}\epsilon_{\mathrm{ex},k} + R'_{\mathrm{ion,s}}\epsilon_{\mathrm{ion}} + \tilde{R}'_{\mathrm{att}} + \bar{\alpha}'(\tilde{W}'_{\mathrm{s}} - \bar{\alpha}'\tilde{D}'_{\mathrm{s}}) = (W'_{\mathrm{s}} - \bar{\alpha}' D'_{\mathrm{s}})E \qquad (5.18)$$

where R' and ϵ are the collision frequency and the inelastic energy loss for each kind of collision. The tildes represent the energy-weighted electron swarm parameters. The

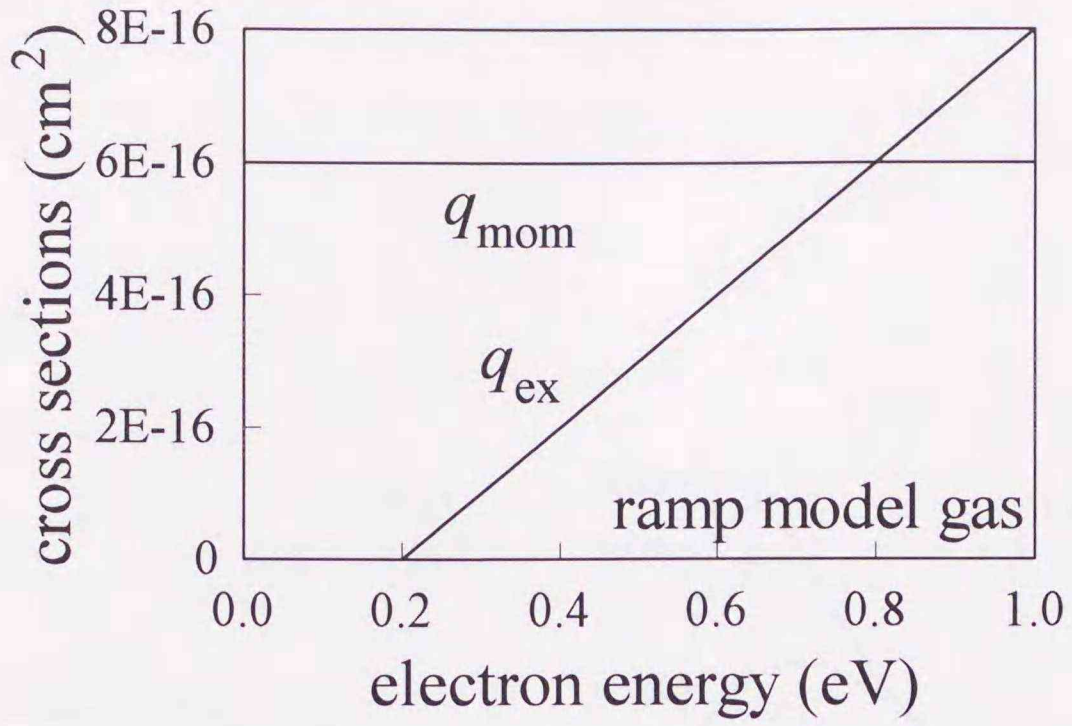

Figure 5.3: Electron collision cross sections of a ramp model gas (Reid 1979); momentum transfer q_{mom} and excitation q_{ex}. Neither ionization nor attachment is present.

right hand side and left hand side of this equation represent the energy gain and loss of an electron swarm associated with $\boldsymbol{E}$. They must be equal to each other when in drift equilibrium. The balance was confirmed for each result with the relative difference less than 1%.

5.5 Results and Discussion

5.5.1 Electron Energy Distribution

$F_0(\epsilon)$ and $F_1(\epsilon)$ are shown in figure 5.4, which are the isotropic and anisotropic components of the Legendre polynomial expansion terms of the electron energy distribution $F(\epsilon)$.

There are two important differences between $F(\epsilon)$ in the USR and DSR. In contrast to the DSR, the electron energies in the USR are in general lower and the high energy electrons move backwards on the average.

Electrons diffuse backwards into the USR because of large $\bar{\alpha}'$. In this case, only high energy electrons can diffuse backwards since diffusion against $\boldsymbol{E}$ results in rapid energy decay.

Some electrons lose part of their energies by inelastic collisions during their stay in a region $x < x'$, where x' is a position in the USR. After the energy loss, they drift towards the DSR. All of them pass the position $x = x'$ again towards the DSR eventually unless they disappear in the USR by attachment. At that time, electrons that have undergone backward diffusion will necessarily have a lower energies than their previous energies before undergoing backward diffusion. Therefore, $F_1(\epsilon) > 0$ for low energy electrons as shown in figure 5.4 for Ar and the model gas in the USR. In the electro-negative gas, the number of electrons decreases due to attachment while they diffuse backwards. As a result, $F_1(\epsilon) < 0$ for all ϵ for the conditions in case of SF_6 in the USR.

As expected, shift in $F_0(\epsilon)$ towards higher energies with increasing E/N was observed even in the USR. This is similar to what occurs in the DSR. At a high E/N, low energy electrons are prevented from diffusing backwards. The total number of electrons pene-

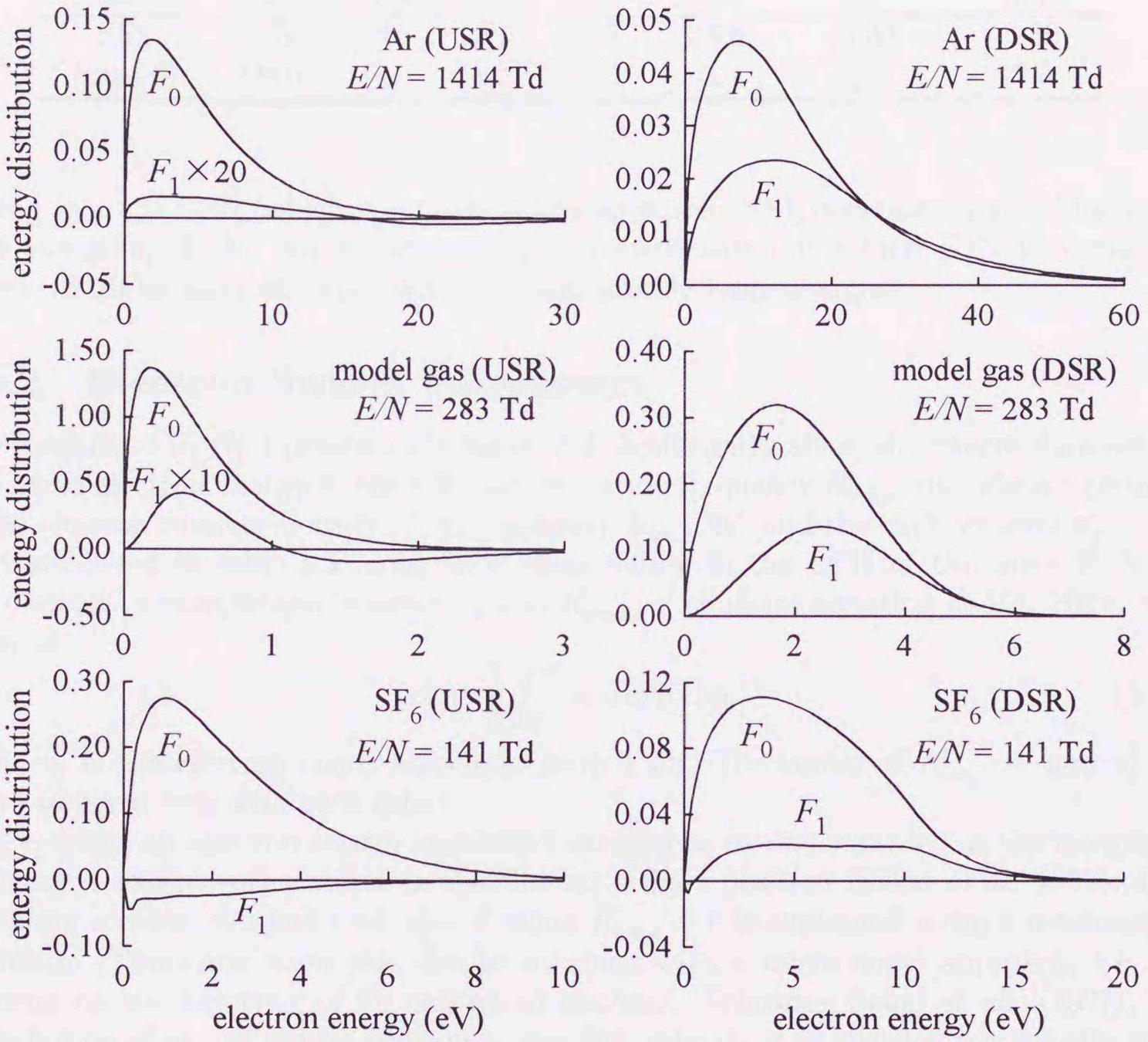

Figure 5.4: Comparisons of electron energy distributions in the upstream region (USR) and downstream region (DSR) in argon (Ar) at $E/N = 1414$ Td, the ramp model gas at $E/N = 283$ Td, and sulphur-hexafluoride (SF_6) at $E/N = 141$ Td.

Table 5.2: List of swarm parameters in the upstream region (USR) and the downstream region (DSR). — indicates that $R_{\mathrm{ion,s}}/\bar{\alpha}$ is undefined since $\bar{\alpha} = 0$.

gas	region	E/N (Td)	$\bar{\epsilon}'$ $\bar{\epsilon}$ (eV)	$R'_{\mathrm{ion,s}}$ $R_{\mathrm{ion,s}}$ ($\mu\mathrm{s}^{-1}$)	$\bar{\alpha}'$ $\bar{\alpha}$ (cm^{-1})	$R'_{\mathrm{ion,s}}/\bar{\alpha}'$ $R_{\mathrm{ion,s}}/\bar{\alpha}$ ($\mathrm{cm}\mu\mathrm{s}^{-1}$)	v'_{d} v_{d} ($\mathrm{cm}\mu\mathrm{s}^{-1}$)
Ar	USR	1414	5.37	17.3	138	0.126	0.125
(case 1)	DSR	1414	15.7	590	10.1	58.2	57.9
model gas	USR	283	0.54	0.0	270	0.0	-0.004
(case 2)	DSR	283	2.13	0.0	0.0	—	13.3
SF_6	USR	141	2.71	-112	33.6	-3.33	-3.30
(case 3)	DSR	141	5.62	-30.1	-2.4	12.3	12.3

trating into the USR, which is represented in equation (5.8), decreases since $\bar{\alpha}'$ increases with increasing E/N. An exponential spatial distribution at a high E/N is formed by backward diffusion of electrons with commensurately large energies.

5.5.2 Electron Swarm Parameters

The tendencies in $F(\epsilon)$ presented in figure 5.4 significantly affect the swarm parameters. The mean electron energy $\bar{\epsilon}'$, the effective ionization frequency $R'_{\mathrm{ion,s}}$, the relative gradient of the electron number density $\bar{\alpha}'$, the quantity $R'_{\mathrm{ion,s}}/\bar{\alpha}'$, and the drift velocity v'_{d} in the USR are listed in table 5.2 along with those values in the DSR at the same E/N for comparison. A comparison between v'_{d} and $R'_{\mathrm{ion,s}}/\bar{\alpha}'$ confirms equation (5.10). Here, v'_{d} is given as

$$v'_{\mathrm{d}} = \frac{1}{3}\int_0^\infty v_1\sqrt{\epsilon} f_1(\epsilon) d\epsilon \tag{5.19}$$

where v_1 is the electron speed associated with 1 eV. The values of $R'_{\mathrm{ion,s}}/\bar{\alpha}'$ and v'_{d} are found to agree well with each other.

Typically, an electron swarm under SST conditions can be regarded as the integral of an isolated swarm with respect to the time at a fixed position (Sakai *et al.* 1977). In a preceding section, the fact that $v'_{\mathrm{d}} = 0$ when $R'_{\mathrm{ion,s}} = 0$ is explained using a macroscopic approach. This conclusion can also be attained with a microscopic approach, *i.e.* by focusing on the behavior of an individual electron. Following Sakai *et al.* (1977), the contribution of an individual electron to the drift velocity v'_{d} is the electron velocity component parallel to the electric filed weighted by its residence time in a small interval in space with a thickness Δx. If there is no production and loss of electrons, an electron that passes across Δx at a position in the USR toward the upstream direction must eventually return across Δx towards the DSR, *i.e.* the number of crossings by an individual electron across Δx is necessarily even (see figure 5.5). Since the residence time is inversely proportional to the velocity component parallel to the electric field and the velocity changes sign with each crossing, the net contribution to the drift velocity is zero. In contrast, the number of crossings is odd in the DSR. The difference in the parity of the number of crossings in the two regions is the key difference between the drift velocities for the USR and DSR.

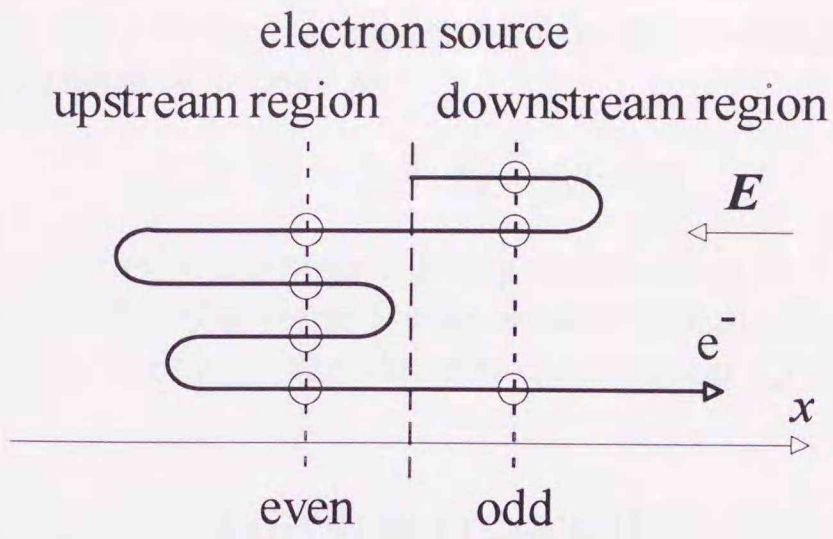

Figure 5.5: The parity of the number of crossings. When the number of electrons is conservative, the positive and negative contributions of an electron crossing a position in the upstream region cancel each other, while the positive contribution exceeds the negative in the downstream region.

5.6 A Practical Example of Backward Diffusion

5.6.1 Effect of Absorbing Anode

A practical example of backward diffusion in the USR, as previously discussed, is seen in an SST experiment between parallel plane electrodes. The decay in the electron number density in front of an absorbing anode may be regarded as the appearance of vacancies due to the absorption of electrons at the anode. Here, the vacancies can be defined as being missing electrons.

Chantry (1982) discussed the effect of an absorbing anode on the SST electron swarm using a concept of complementarity. The complementarity theorem of Chantry (1982) is as follows. As shown in figure 5.6, if a plane which is perpendicular to the electric field is placed in the region where the electron swarm is in equilibrium, electrons near the plane are a mixture of those electrons which are diffusing forwards and backwards across the plane. When we regard the plane as an absorbing anode, electron swarm parameters on the upstream side near the plane would vary spatially corresponding to the contribution of backward-diffusing electrons to the electron distribution, since these electrons would be lost by absorption.

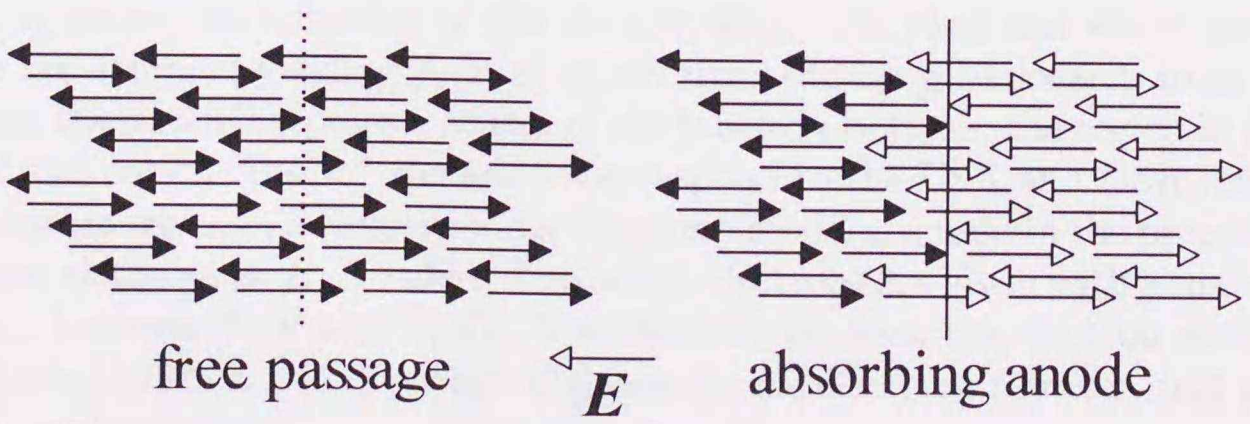

Figure 5.6: Concept of complementarity theorem (Chantry 1982). Arrows represent random motion of electrons. The absorbed electrons represented by white arrows appear as vacancies in front of the anode.

If those electrons absorbed at the anode could move freely as if they were in free

space under the electric field even after absorption, they could diffuse backwards and fill the vacancies. Here, the velocity distribution of backward-diffusing electrons $f_{\mathrm{v}}(x, \boldsymbol{v})$ necessary to fill the vacancies is defined as

$$f_{\mathrm{v}}(x, \boldsymbol{v}) = f_{\mathrm{d}}(x, \boldsymbol{v}) - f_{\mathrm{a}}(x, \boldsymbol{v}) \tag{5.20}$$

where $f_{\mathrm{d}}(\boldsymbol{v})$ and $f_{\mathrm{a}}(x, \boldsymbol{v})$ are the electron velocity distribution in drift equilibrium in the DSR and that affected by the absorbing anode as shown in figure 5.7. Here, $f_{\mathrm{v}}(x, \boldsymbol{v})$ is expected to show a similar profile to the electron distribution $f_{\mathrm{u}}(x, \boldsymbol{v})$ in the USR.

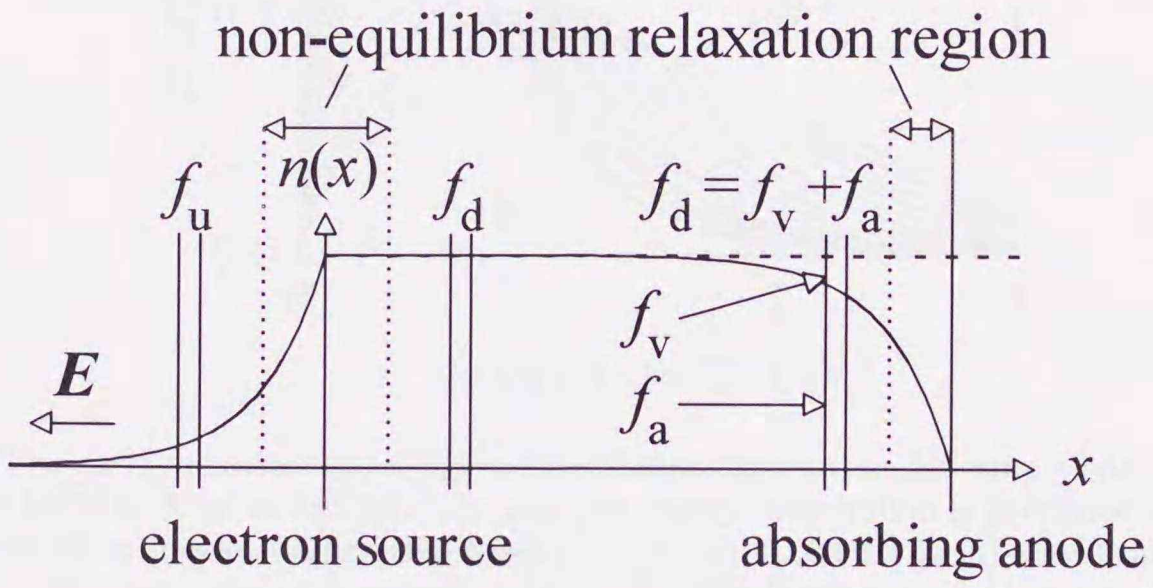

Figure 5.7: Model of steady-state electron swarm in front of the anode. The electron distribution $f_{\mathrm{a}}(x, \boldsymbol{v})$ in front of the anode may be described as $f_{\mathrm{a}}(x, \boldsymbol{v}) = f_{\mathrm{d}}(x, \boldsymbol{v}) - f_{\mathrm{v}}(x, \boldsymbol{v})$ where $f_{\mathrm{d}}(x, \boldsymbol{v})$ and $f_{\mathrm{v}}(x, \boldsymbol{v})$ are the electron distribution in the upstream region (USR) and the downstream region (DSR), respectively. $f_{\mathrm{v}}(x, \boldsymbol{v})$ is expected to be similar to $f_{\mathrm{u}}(x, \boldsymbol{v})$.

5.6.2 Monte Carlo Simulation

To examine the concept of backward diffusion of vacancies as defined by equation (5.20), a Monte Carlo simulation (MCS) was performed to obtain $f_{\mathrm{v}}(x, \boldsymbol{v})$. It is assumed that the initial electrons are supplied at a plane source and they drift and diffuse downstream. Those electrons which arrive at the position of an imaginary anode are labeled to indicate that they have been absorbed at least once. Then they are permitted to continue their propagation under the influence of the electric field. The electrons which return across the anode are sampled yielding $f_{\mathrm{v}}(x, \boldsymbol{v})$ of electrons diffusing backwards from the anode. In this case, the anode becomes a source of the labeled electrons; the region in front of the anode and the region "inside" the anode correspond to the USR and DSR respectively.

As a benchmark case, a simulation for the ramp model gas used in the preceding section is performed at the same E/N value. The initial electrons are given with a uniform energy distribution between 0 eV and 10 eV. The distance between the electron source and the anode is 5 mm, which is a long enough distance for the electrons to reach drift equilibrium under the condition.

The results of the MCS are shown in figures 5.8 and 5.9.

In figure 5.8, the energy distributions of the vacancies, $F_{\mathrm{v}}(x, \epsilon)$, are presented as a function of the distance from the anode. An important profile is that the shape of $F_{\mathrm{v}}(x, \epsilon)$ converges to the drift equilibrium solution $F_{\mathrm{u}}(\epsilon)$ in the USR when x varies from (a) -0.002 cm to (b) -0.030 cm. In the region where the gradient of the electron population in a

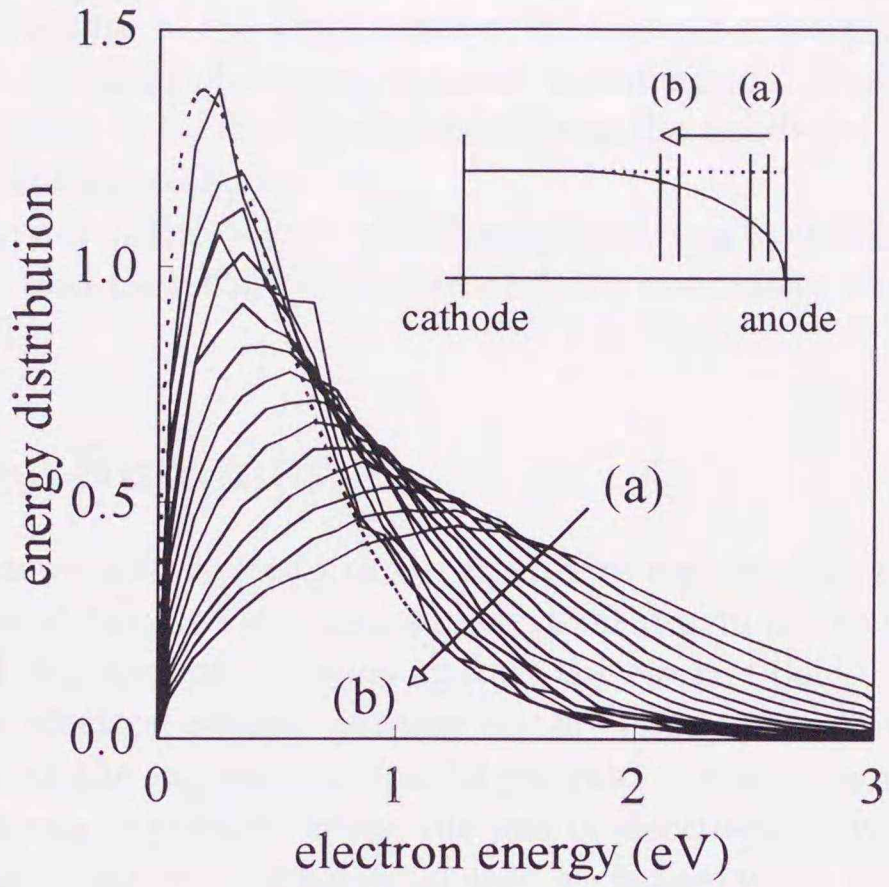

Figure 5.8: The energy distribution of backward-diffusing electrons in the ramp model gas (Reid 1979) obtained by an MCS at $E/N = 283$ Td. The electron energy distribution is presented as a function of distance from the absorbing anode for every 0.004 cm from (a) -0.002 cm to (b) -0.030 cm. The electrons are permitted to move even after their arrival at the anode. The distribution tends to the drift equilibrium solution indicated by the broken curve, which was obtained by the PM in the upstream region.

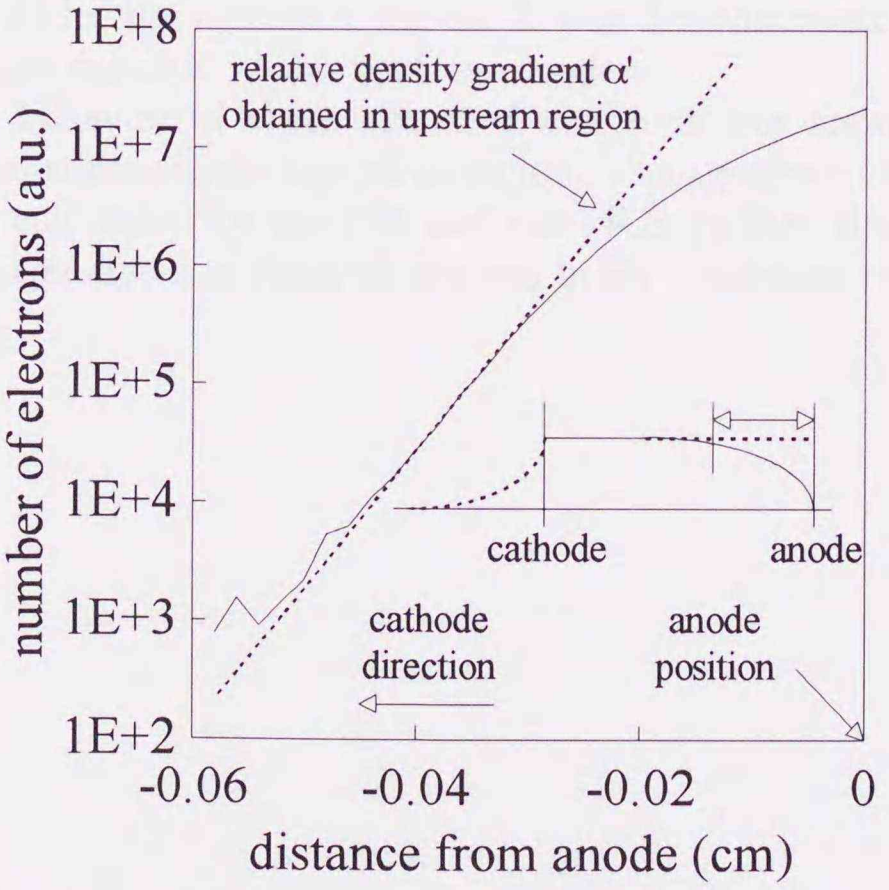

Figure 5.9: The population of backward-diffusing electrons in the ramp model gas (Reid 1979) as a function of the distance from the absorbing anode under an SST condition obtained by an MCS at $E/N = 283$ Td. Each electron is sampled only after its arrival at the anode. The broken line represents the relative density gradient $\bar{\alpha}'$ taken from table 5.2, which was obtained by the PM in the upstream region. The deviation from linearity towards the cathode direction is a statistical fluctuation due to the low electron number density.

logarithm plot agrees with $\bar{\alpha}'$ in table 5.2, the shape of $F_{\mathrm{v}}(x, \epsilon)$ in figure 5.8 is essentially the same as $F_{\mathrm{u}}(\epsilon)$. Because of the large value of $\bar{\alpha}'$, there is a steep decay in the number density of backward-diffusing electrons adjacent to the anode. Due to the low number density of these electrons at increasing distances from the anode (< -0.05 cm), statistical fluctuation appears in figure 5.9.

These results prove that the backward-diffusing electrons from the anode also undergo relaxation processes, and they show exponential decay essentially identical to that of the electrons in the USR.

5.7 Chapter Summary

Properties of electron swarms in gases in the upstream region of an electron source, were studied under SST conditions. A steady-state electron swarm in the upstream region was formed by backward diffusion of electrons against the electric field.

Relations among electron swarm parameters in the upstream region were deduced under an assumption of the exponential spatial growth. It was shown that the sign of the electron drift velocity v_{d} is positive when the gas is electro-positive, and v_{d} is negative when the gas is electro-negative. As a special case, v_{d} is zero when the effective ionization frequency is zero. These characteristics were confirmed quantitatively by calculating the electron energy distribution $F(\epsilon)$ using a PM modified for analyses in the upstream region.

A steady-state electron swarm between parallel plane electrodes was simulated using an MCS to demonstrate that the decay in the electron number density in front of an absorbing anode is due to vacancies missing electrons absorbed at the anode. The exponential decay in the number density of the vacancies with the increase in distance from the anode was also confirmed by the MCS. The density gradient in front of the anode agreed with that obtained in an analysis for the upstream region. It was demonstrated that $F(\epsilon)$ converges to the drift equilibrium solution in the upstream region.

The equilibrium behavior of these absorbed electrons was shown to be essentially equivalent to that of electrons in the upstream region. The agreement between the electron energy distributions calculated by the PM and the MCS verified the calculation scheme of the present PM for analyses of electron swarms in the upstream region.

References

Blevin H A and Fletcher J 1984 *Aust.J.Phys.* **37** 593-600
Braglia G L and Lowke J J 1979 *J.Phys.D: Appl.Phys.* **12** 1831-8
Chantry P J 1982 *Phys.Rev.A* **25** 1209-13
Itoh H, Miura Y, Ikuta N, Nakao Y and Tagashira H
1988 *J.Phys.D: Appl.Phys.* **21** 922-30
Itoh H, Matsumura T, Satoh K, Date H, Nakao Y and Tagashira H
1993 *J.Phys.D: Appl.Phys.* **26** 1975-9
Kondo K and Tagashira H 1990 *J.Phys.D: Appl.Phys.* **23** 1175-83
Mason N J and Newell W R 1987 *J.Phys.B: At.Mol.Phys.* **5** 1357-77
Phelps A V and Pitchford L C 1985 *Phys.Rev.A* **31** 2932-49
Reid I D 1979 *Aust.J.Phys.* **32** 231-54
Robson R E 1991 *Aust.J.Phys.* **44** 685-92
Robson R E 1991 *"Gaseous Electronics and Its Applications"*,
KTK Scientific Publishers Tokyo 89-101
Sakai Y, Tagashira H and Sakamoto S 1972 *J.Phys.B: At.Mol.Phys.* **5** 1010-6
Sakai Y, Tagashira H and Sakamoto S 1977 *J.Phys.D: Appl.Phys.* **10** 1035-49
Standish R K 1989 *Aust.J.Phys.* **42** 223-32
Sugawara H, Sakai Y and Tagashira H 1994 *J.Phys.D: Appl.Phys.* **27** 90-4
Suzuki M, Taniguchi T and Tagashira H 1990 *J.Phys.D: Appl.Phys.* **23** 842-50
Tagashira H, Sakai Y and Sakamoto S 1977 *J.Phys.D: Appl.Phys.* **10** 1051-63
Tagashira H
1985 *Papars of Technical Committee for Electrical Discharges, IEE Jpn.* ED-85-115
Tagashira H 1991 *Trans.IEE Jpn.* **111-A** 147-51
Thomas W R L 1969 *J.Phys.B: At.Mol.Phys.* **2** 551-61

Chapter 6

Evaluation of the Centroid Drift Velocity of an Electron Swarm using Moment Equations

6.1 Introduction

The electron drift velocity in gases is one of the most important plasma properties which are essential for development of plasma technologies. Several kinds of definitions for the electron drift velocities have been introduced corresponding to observation conditions (Tagashira *et al.* 1977). Their relations were studied from the point of view of correspondence between theoretical and experimental definitions of the electron drift velocities (Robson 1991; Satoh *et al.* 1991, 1994). Among these drift velocities, the centroid drift velocity W_{r} and the mean electron velocity W_{v} are typical quantities, which are defined under time-of-flight (TOF) and pulsed Townsend (PT) conditions and are most frequently referred to in fluid model simulations.

W_{r} is the particular drift velocity which appears as the coefficient of the first order concentration gradient of the usual continuity equation of electron flow, and is derived from spatial motion of an isolated electron swarm in real space. W_{r} can be measured by TOF experiments using double-shutter drift tubes (*e.g.* Nakamura 1988). On the other hand, W_{v} is theoretically defined for an isolated electron swarm under PT conditions as the average velocity of electrons in velocity space, and determines the external current as $en(t)W_{\mathrm{v}}$, where n is the number of electrons at time t and e is the charge of an electron.

It is known that W_{r} and W_{v} have different values even in the same gas under the same reduced electric field E/N when ionization and / or electron attachment processes are present (Tagashira *et al.* 1977). Experimental results compared in Nakamura (1988) also suggested the difference between the drift velocities measured under TOF and PT conditions. However, W_{r} and W_{v} are likely to be confused in fluid-model simulations of electric discharges. In order to deal with a set of the drift velocity data appropriately, it would be important to recognize the quantitative differences between W_{r} and W_{v}.

In the present chapter, a new evaluation technique for W_{r} is developed based on a propagator method (PM). In the present technique, W_{r} is calculated in velocity space using moment equations (Kumar 1981, Skullerud and Kuhn 1983, Skullerud 1984, Penetrante *et al.* 1985), despite the W_{r} is originally defined based on spatial motion of an electron swarm in real space. The moment equations quantitatively describe the effects of ionization and electron attachment on W_{r}. Those effects can be categorized as four cases according to the combinations of the signs of the first order moment of the electron position and the

effective ionization frequency. The four cases of the effects are demonstrated through analyses of the electron drift velocities in some gases. The mechanism to cause the difference between W_{r} and W_{v} is illustrated.

The present numerical technique is fundamentally based on a PM under PT conditions discussed in chapter 4. Its calculation scheme is modified by adopting simultaneous moment equations. A possibility of the computational scheme of the PM for further efficient parallelization is also discussed.

6.2 Effects of Ionization and Electron Attachment

An electron swarm under a uniform electric field $\boldsymbol{E}$ in the direction x is considered in boundary-less free space.

W_{r} and W_{v} of the electron swarm are defined as

$$W_{\mathrm{r}}(t) \equiv \frac{\mathrm{d}}{\mathrm{d}t}G(t) = \frac{\mathrm{d}}{\mathrm{d}t}\frac{\int_{\boldsymbol{r},\boldsymbol{v}} x f(\boldsymbol{r},\boldsymbol{v},t)\mathrm{d}\boldsymbol{r}\mathrm{d}\boldsymbol{v}}{\int_{\boldsymbol{r},\boldsymbol{v}} f(\boldsymbol{r},\boldsymbol{v},t)\mathrm{d}\boldsymbol{r}\mathrm{d}\boldsymbol{v}} \tag{6.1}$$

$$W_{\mathrm{v}}(t) \equiv \bar{v}_x(t) = \frac{\int_{\boldsymbol{r},\boldsymbol{v}} v_x f(\boldsymbol{r},\boldsymbol{v},t)\mathrm{d}\boldsymbol{r}\mathrm{d}\boldsymbol{v}}{\int_{\boldsymbol{r},\boldsymbol{v}} f(\boldsymbol{r},\boldsymbol{v},t)\mathrm{d}\boldsymbol{r}\mathrm{d}\boldsymbol{v}} \tag{6.2}$$

where $f(\boldsymbol{r},\boldsymbol{v},t)$ represents the electron distribution function, $\boldsymbol{r}$ and $\boldsymbol{v}$ are the position (x,y,z) and the velocity (v_x,v_y,v_z) respectively, and t is time. $G(t)$ is the centroid position in the direction of x and $\bar{v}_x$ is the mean value of v_x throughout the electrons in an electron swarm.

A relation between W_{r} and W_{v} is derived from the definition of W_{r} by transforming it using a relation of $(v/u)' = (uv' - vu')/u^2$ and the following Boltzmann equation (see Appendix A for detailed transformation processes):

$$\frac{\partial}{\partial t}f(\boldsymbol{r},\boldsymbol{v},t) = \left\{-\boldsymbol{v}\cdot\frac{\partial}{\partial \boldsymbol{r}} - \boldsymbol{a}\cdot\frac{\partial}{\partial \boldsymbol{v}} + \left(\frac{\partial}{\partial t}\right)_{\mathrm{coll}}\right\} f(\boldsymbol{r},\boldsymbol{v},t). \tag{6.3}$$

Here, the acceleration $\boldsymbol{a}$ due to $\boldsymbol{E}$ is assumed to be $\boldsymbol{a} = (a_x,a_y,a_z) = (eE/m,0,0)$ in the present model, where e and m are the charge and mass of an electron. The result of the transformation is

$$W_{\mathrm{r}}(t) = \frac{\int_{\boldsymbol{r},\boldsymbol{v}} x(\partial/\partial t)f(\boldsymbol{r},\boldsymbol{v},t)\mathrm{d}\boldsymbol{r}\mathrm{d}\boldsymbol{v}}{\int_{\boldsymbol{r},\boldsymbol{v}} f(\boldsymbol{r},\boldsymbol{v},t)\mathrm{d}\boldsymbol{r}\mathrm{d}\boldsymbol{v}} - \frac{G(t)\cdot\int_{\boldsymbol{r},\boldsymbol{v}}(\partial/\partial t)f(\boldsymbol{r},\boldsymbol{v},t)\mathrm{d}\boldsymbol{r}\mathrm{d}\boldsymbol{v}}{\int_{\boldsymbol{r},\boldsymbol{v}} f(\boldsymbol{r},\boldsymbol{v},t)\mathrm{d}\boldsymbol{r}\mathrm{d}\boldsymbol{v}} \tag{6.4}$$

$$= \frac{\int_{\boldsymbol{r},\boldsymbol{v}}\{x-G(t)\}\{(\partial/\partial t)_{\mathrm{coll}} - \boldsymbol{v}\cdot(\partial/\partial \boldsymbol{r}) - \boldsymbol{a}\cdot(\partial/\partial \boldsymbol{v})\}f(\boldsymbol{r},\boldsymbol{v},t)\mathrm{d}\boldsymbol{r}\mathrm{d}\boldsymbol{v}}{\int_{\boldsymbol{r},\boldsymbol{v}} f(\boldsymbol{r},\boldsymbol{v},t)\mathrm{d}\boldsymbol{r}\mathrm{d}\boldsymbol{v}} \tag{6.5}$$

$$= W_{\mathrm{v}}(t) + \int_{-\infty}^{\infty}\{x-G(t)\}\bar{R}_{\mathrm{ion}}(x,t)p(x,t)\mathrm{d}x \tag{6.6}$$

where $\bar{R}_{\mathrm{ion}}(x,t)$ is the position-dependent effective ionization frequency and $p(x,t)$ is the normalized electron distribution. Equation (6.6) agrees with a result of Tagashira *et al.* (1977) which was theoretically deduced from a comparison between the drift terms in continuity equations for the electron number densities in TOF and PT systems.

This relation indicates that in addition to W_{v}, which is the average velocity of the individual electrons, the whole electron swarm has a different kind of velocity component. As shown in Blevin and Fletcher (1984) and Phelps and Pitchford (1985) as well, the second term derives from electron production and loss by ionization and electron attachment. These two collision processes have a function to shift the centroid as illustrated

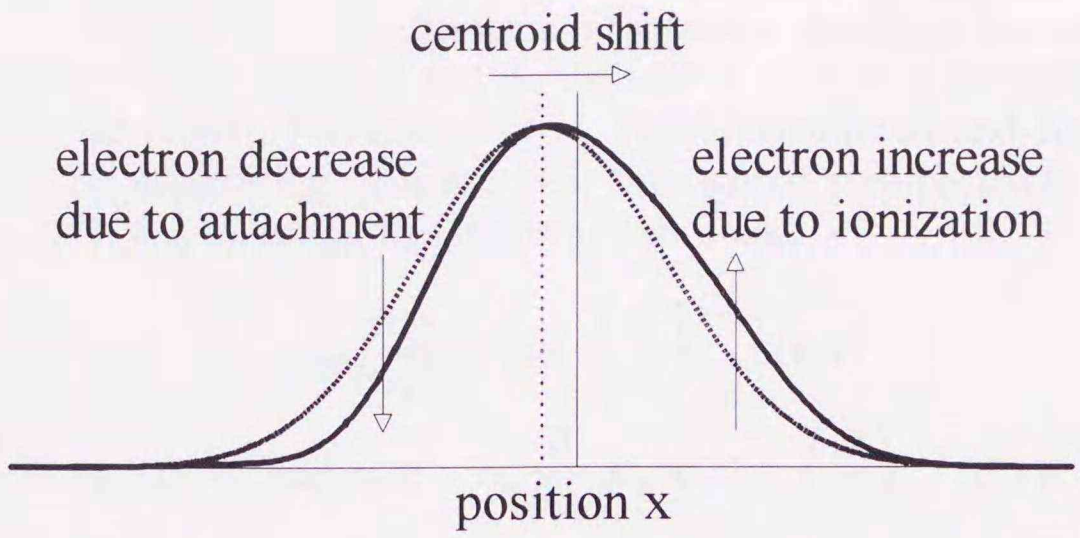

Figure 6.1: Shift of the centroid of an electron swarm. The centroid drift velocity of an electron swarm has a velocity component due to ionization and electron attachment in addition to the average velocity throughout the individual electrons in the swarm.

in figure 6.1. For example, ionization in the leading part of the electron swarm would result in shifting the centroid forward since the increasing electron population attracts the centroid ahead, and electron attachment affects in the opposite manner. A tendency $W_\mathrm{r} > W_\mathrm{v}$ can be found in some real gases (*e.g.* Kitamori *et al.* 1980; Satoh *et al.* 1988, 1991, 1994). This fact would imply that ionization tends to occur in the region ahead of the centroid, and electron attachment does behind.

This tendency agrees with a qualitative expectation that the leading electrons would have higher energies than those of electrons behind since high electron energies are necessary to cause ionization and low energy electrons will be easily captured by electro-negative gas molecules.

Evaluation of the second term $\int_{-\infty}^{\infty}\{x - G(t)\}\bar{R}_\mathrm{ion}(x,t)p(x,t)\mathrm{d}x$ in equation (6.6) will give the quantitative difference between W_r and W_v. However, if the calculation for the term is performed in the given form, it is required to deal with the electron energy distribution as a function of x.

In the present investigation, an alternative simpler approach to the term based on moment equations is introduced, in which the term is denoted as a function defined in velocity space. This approach enables us to avoid special treatments for the calculation of the position-dependent electron energy distribution such as series expansion and spatial resolution.

6.3 Calculation Method

6.3.1 Moment Equations

The centroid $G(t)$ of an electron swarm is obtained using the first order moment $M_x(t)$ with respect to the position x and the number of electrons $n(t)$ in an electron swarm:

$$G(t) = \frac{M_x(t)}{n(t)} \tag{6.7}$$

$$n(t) = \int_{\boldsymbol{r},\boldsymbol{v}} f(\boldsymbol{r},\boldsymbol{v},t)\mathrm{d}\boldsymbol{r}\mathrm{d}\boldsymbol{v} = \int_{\boldsymbol{v}} f(\boldsymbol{v},t)\mathrm{d}\boldsymbol{v} \tag{6.8}$$

$$M_x(t) = \int_{\boldsymbol{r},\boldsymbol{v}} xf(\boldsymbol{r},\boldsymbol{v},t)\mathrm{d}\boldsymbol{r}\mathrm{d}\boldsymbol{v} = \int_{\boldsymbol{v}} M_x(\boldsymbol{v},t)\mathrm{d}\boldsymbol{v}. \tag{6.9}$$

The temporal variations of $n(t)$ and $M_x(t)$ are described by the 0-th and first order moment equations derived from the Boltzmann equation shown as equation (6.3) previously. The definition of the moment and its deduction have been presented in Kitamori *et al.* (1980), Kumar (1981), Penetrante *et al.* (1985), Skullerud and Kuhn (1983) and Skullerud (1984). By integrating equation (6.3) throughout $\boldsymbol{r}$ respectively with weights 1 ($= x^0$) and x ($= x^1$), the following equations are obtained:

$$\frac{\partial}{\partial t}f(\boldsymbol{v},t) = -\alpha_x\frac{\partial}{\partial v_x}f(\boldsymbol{v},t) + \left(\frac{\partial}{\partial t}\right)_{\text{coll}} f(\boldsymbol{v},t) \tag{6.10}$$

$$\frac{\partial}{\partial t}M_x(\boldsymbol{v},t) = v_x f(\boldsymbol{v},t) - \alpha_x\frac{\partial}{\partial v_x}M_x(\boldsymbol{v},t) + \left(\frac{\partial}{\partial t}\right)_{\text{coll}} M_x(\boldsymbol{v},t). \tag{6.11}$$

The collision operators in equations (6.10) and (6.11) are commonly described as

$$\left(\frac{\partial}{\partial t}\right)_{\text{coll}} = \sum_k \left\{-Nq_k(\boldsymbol{v})|\boldsymbol{v}| + \int_{\boldsymbol{v}'} Nq_k(\boldsymbol{v}')|\boldsymbol{v}'|P_k(\boldsymbol{v}',\boldsymbol{v})\mathrm{d}\boldsymbol{v}'\right\} \tag{6.12}$$

where N is the number density of gas molecules and q_k is the cross section for k-th kind of collision. $P_k(\boldsymbol{v}',\boldsymbol{v})$ is a propagator which represents the transition probability of electrons from a velocity $\boldsymbol{v}'$ to another velocity $\boldsymbol{v}$ by the collision of k-th kind. Further integration for equations (6.10) and (6.11) throughout $\boldsymbol{v}$ give

$$\frac{\mathrm{d}}{\mathrm{d}t}n(t) = \int_{\boldsymbol{v}} \bar{R}_{\text{ion}}(\boldsymbol{v})f(\boldsymbol{v},t)\mathrm{d}\boldsymbol{v} \tag{6.13}$$

$$\frac{\mathrm{d}}{\mathrm{d}t}M_x(t) = \int_{\boldsymbol{v}} v_x f(\boldsymbol{v},t)\mathrm{d}\boldsymbol{v} + \int_{\boldsymbol{v}} \bar{R}_{\text{ion}}(\boldsymbol{v})M_x(\boldsymbol{v},t)\mathrm{d}\boldsymbol{v} \tag{6.14}$$

where $\bar{R}_{\text{ion}}(\boldsymbol{v})$ is the effective ionization frequency defined as $\bar{R}_{\text{ion}}(\boldsymbol{v}) = R_{\text{ion}}(\boldsymbol{v}) - R_{\text{att}}(\boldsymbol{v})$. It is found here that the temporal variations of $n(t)$ and $M_x(t)$, which consist of collision and drift terms can be calculated in velocity space irrespective of the position $\boldsymbol{r}$. Temporal variation of $M_x(t)$ is independent of $\boldsymbol{r}$ as well as $n(t)$.

Here, in order to explain this fact, an electron swarm subset $S(\boldsymbol{v})$ is defined as the electrons in a volume $\mathrm{d}\boldsymbol{v}$ at $\boldsymbol{v}$ in velocity space.

Firstly, the probabilities of ionization and electron attachment are functions of $\boldsymbol{v}$ independent of $\boldsymbol{r}$. Therefore, they are uniform for every electron in $S(\boldsymbol{v})$. When we define further subsets $S_{\text{ion}}(\boldsymbol{v})$ and $S_{\text{att}}(\boldsymbol{v})$ in $S(\boldsymbol{v})$ for the electrons undergoing ionization and attachment respectively, both of the centroids of $S_{\text{ion}}(\boldsymbol{v})$ and $S_{\text{att}}(\boldsymbol{v})$ are at the same position as that of $S(\boldsymbol{v})$ due to the uniformity of the collision probabilities. As a result, the total amount of the increase or decrease of $M_x(\boldsymbol{v},t)$ due to the collisions can be simply represented as the products of the centroid position $M_x(\boldsymbol{v},t)/f(\boldsymbol{v},t)$ and the numbers of electrons in $S_{\text{ion}}(\boldsymbol{v})$ and $S_{\text{att}}(\boldsymbol{v})$. Here, the numbers of electrons in $S_{\text{ion}}(\boldsymbol{v})$ and $S_{\text{att}}(\boldsymbol{v})$ are represented as $R_{\text{ion}}(\boldsymbol{v})f(\boldsymbol{v},t)\mathrm{d}\boldsymbol{v}\mathrm{d}t$ and $R_{\text{att}}(\boldsymbol{v})f(\boldsymbol{v},t)\mathrm{d}\boldsymbol{v}\mathrm{d}t$ respectively.

Secondly, drift of the electrons in $S(\boldsymbol{v})$ during a free flight time $\mathrm{d}t$ is considered to be a parallel shift in real space since electron motion is unique in each $S(\boldsymbol{v})$. Therefore, the increase or decrease of $M_x(t)$ due to drift is simply the product of the drift distance $\mathrm{d}x = v_x\mathrm{d}t$ and the number of electrons in $S(\boldsymbol{v})$. The drift term is also independent of the position.

The 0-th and first order moment equations can be calculated even though the electron distribution in real space is unknown. Information of the spatial distribution of electrons itself is not necessary for obtaining $G(t)$ since the essential quantity is involved in $M_x(\boldsymbol{v},t)$ as integrated values.

6.3.2 Propagator Method

The PM for PT conditions discussed in chapter 4 is modified for the present calculation. Electron motion is described in two-dimensional velocity space (v, θ) here due to the rotational symmetry of the present model. Velocity space (v, θ) is divided into cells for every $\Delta\epsilon$ and $\Delta\theta$ in the same way as the preceding investigations. Division for real space can be omitted as explained before, that may be an advantage in computational efficiency. Note that two sets of cells are defined in common velocity space, with which $f(\boldsymbol{v}, t)$ and $M_x(\boldsymbol{v}, t)$ are dealt with numerically (see figure 6.2).

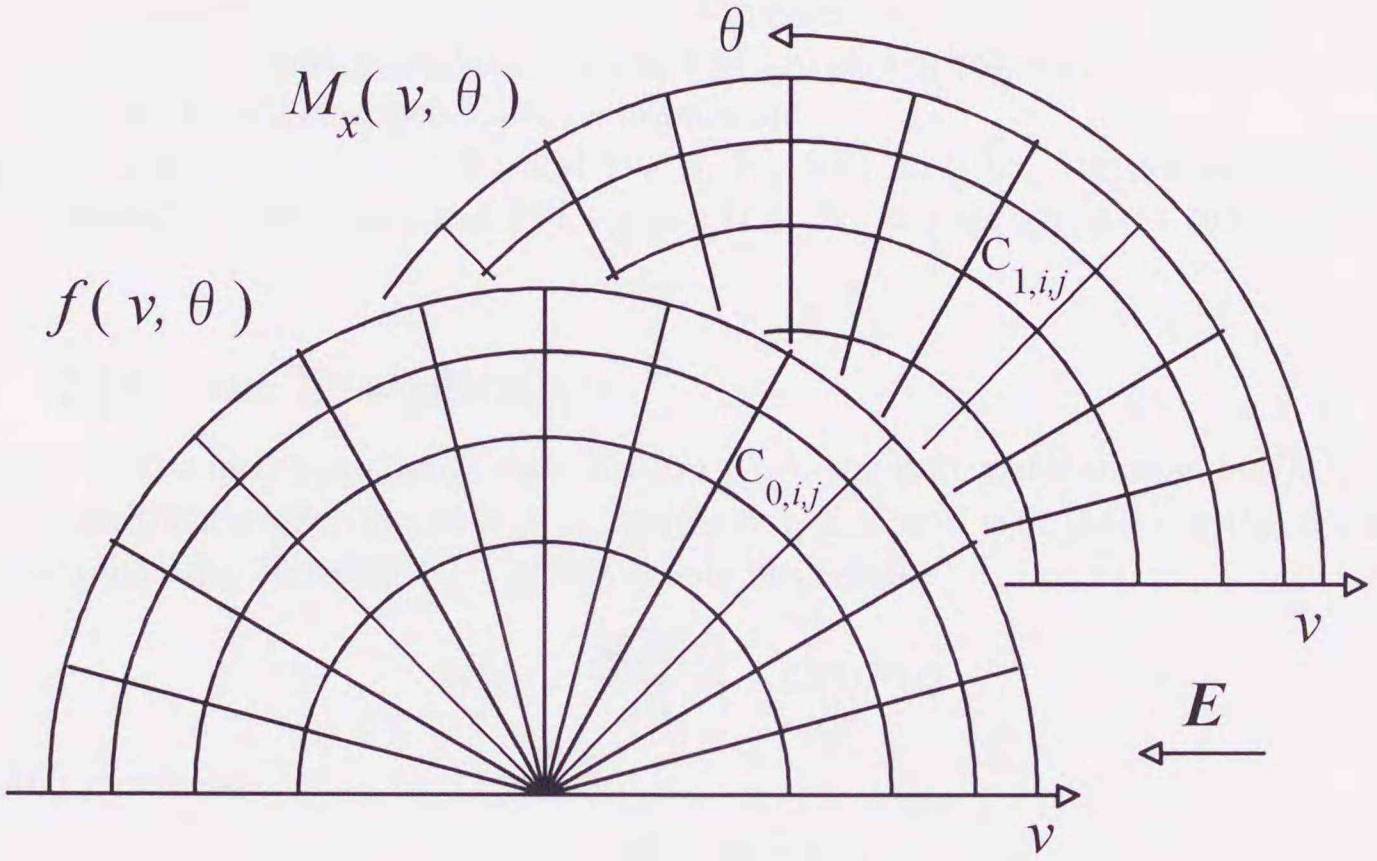

Figure 6.2: Computational configuration for 0-th and first order moments distribution $f(\boldsymbol{v}, t)$ and $M_x(\boldsymbol{v}, t)$. Two sets of cells $\mathrm{C}_{0,i,j}$ and $\mathrm{C}_{1,i,j}$ are defined for simultaneous calculations.

Appropriate initial distributions for $M_x(\boldsymbol{v}, t)$ and $f(\boldsymbol{v}, t)$ are given, and calculations for the drift and collision terms in equations (6.10) and (6.11) are performed simultaneously until equilibrium solutions are attained. The drift distance Δx for each electron during Δt is evaluated based on the variation of the electron energy $\Delta\epsilon$ using the relation $\Delta x = \Delta\epsilon/(eE)$ which was introduced to satisfy the law of energy conservation. Other details of the present technique are fundamentally same as the preceding calculations.

6.4 Simulation Conditions

W_r and W_v are calculated in fluorine ($\mathrm{F_2}$), sulphur-hexafluoride ($\mathrm{SF_6}$) and argon (Ar). $\mathrm{F_2}$ and $\mathrm{SF_6}$ are chosen as typical examples which have both ionization and electron attachment processes, and Ar is an example of electro-positive gas without attachment. Their cross sections are taken from literature referred to in preceding chapters. In addition to these gases, a model gas (Satoh *et al.* 1994) is adopted as another example to demonstrate the theoretical possibility of a certain effect of ionization on the electron drift velocities.

The E/N values are chosen from a range around 283 Td to 1414 Td. This range includes the limiting E/N, $(E/N)_\mathrm{lim}$, of $\mathrm{F_2}$ and $\mathrm{SF_6}$ so that both of the electro-positive

($\bar{R}_{\rm ion} > 0$) and electro-negative ($\bar{R}_{\rm ion} < 0$) cases can be investigated. The gas pressure is assumed to be 1.0 Torr at 0 °C ($N = 3.54 \times 10^{16}$ cm^{-3}). The initial electrons are given at $x = 0$ with a Maxwell-Boltzmann distribution determined by a mean energy close to the equilibrium value under given E/N in order to save calculation time for temporal relaxation processes of the electron swarm.

6.5 Results and Discussion

6.5.1 The Energy and Centroid Distributions

The drift equilibrium values of the electron drift velocities, the electron energy distribution and some other quantities calculated by the PM are shown together with results obtained by Monte Carlo simulation (MCS) for comparison.

Figure 6.3 shows values of $W_{\rm r}$ and $W_{\rm v}$ in F_2, SF_6 and Ar. Agreement between the results obtained by MCS and the PM verifies that $W_{\rm r}$ is appropriately calculated by the PM.

6.5.2 Moment Distribution

The results of the electron energy distribution $F(\epsilon)$, the first order moment $M(\epsilon)$, and the centroid distribution $g(\epsilon)$ are shown in figures 6.4, 6.5, and 6.6. $M(\epsilon)$ is the normalized moment around the centroid $G(t)$ of the whole electrons:

$$M(\epsilon) = \frac{M_x(\epsilon, t)}{n(t)} - G(t)F(\epsilon) \tag{6.15}$$

where $M(\epsilon)$ satisfies

$$\int_0^\infty M(\epsilon)\mathrm{d}\epsilon = 0. \tag{6.16}$$

$g(\epsilon)$ represents the centroid of an electron swarm subset $S(\epsilon)$, which is defined as

$$g(\epsilon) = \frac{M(\epsilon)}{F(\epsilon)}. \tag{6.17}$$

This value is the average position of the electrons in $S(\epsilon)$ relative to $G(t)$. A positive value of $g(\epsilon)$ represents that the average position of the electrons in $S(\epsilon)$ is ahead of $G(t)$, and a negative value implies behind.

Results of $g(\epsilon)$ confirm the qualitative explanation discussed in section 6.2, *i.e.* electrons with higher energy lead the electron swarm.

6.5.3 The Moment Generation Rate

$W_{\rm r}$ can be represented as follows using the moments shown as equations (6.8) through (6.11):

$$W_{\rm r} = \frac{\mathrm{d}}{\mathrm{d}t}G(t) = \frac{\mathrm{d}}{\mathrm{d}t}\frac{\int_{\boldsymbol{r}} M_x(\boldsymbol{v}, t)\mathrm{d}\boldsymbol{v}}{\int_{\boldsymbol{r}} f(\boldsymbol{v}, t)\mathrm{d}\boldsymbol{v}}. \tag{6.18}$$

A transformation using a relation of $(v/u)' = (uv' - vu')/u^2$, which is similar to that performed for equation (6.3), gives the following relation (see Appendix A for detailed transformation processes):

$$W_{\rm r} - W_{\rm v} = \int_0^\infty \bar{R}_{\rm ion}(\epsilon)M(\epsilon)\mathrm{d}\epsilon = \int_0^\infty N\{q_{\rm ion}(\epsilon) - q_{\rm att}(\epsilon)\}v_1\sqrt{\epsilon}M(\epsilon)\mathrm{d}\epsilon \tag{6.19}$$

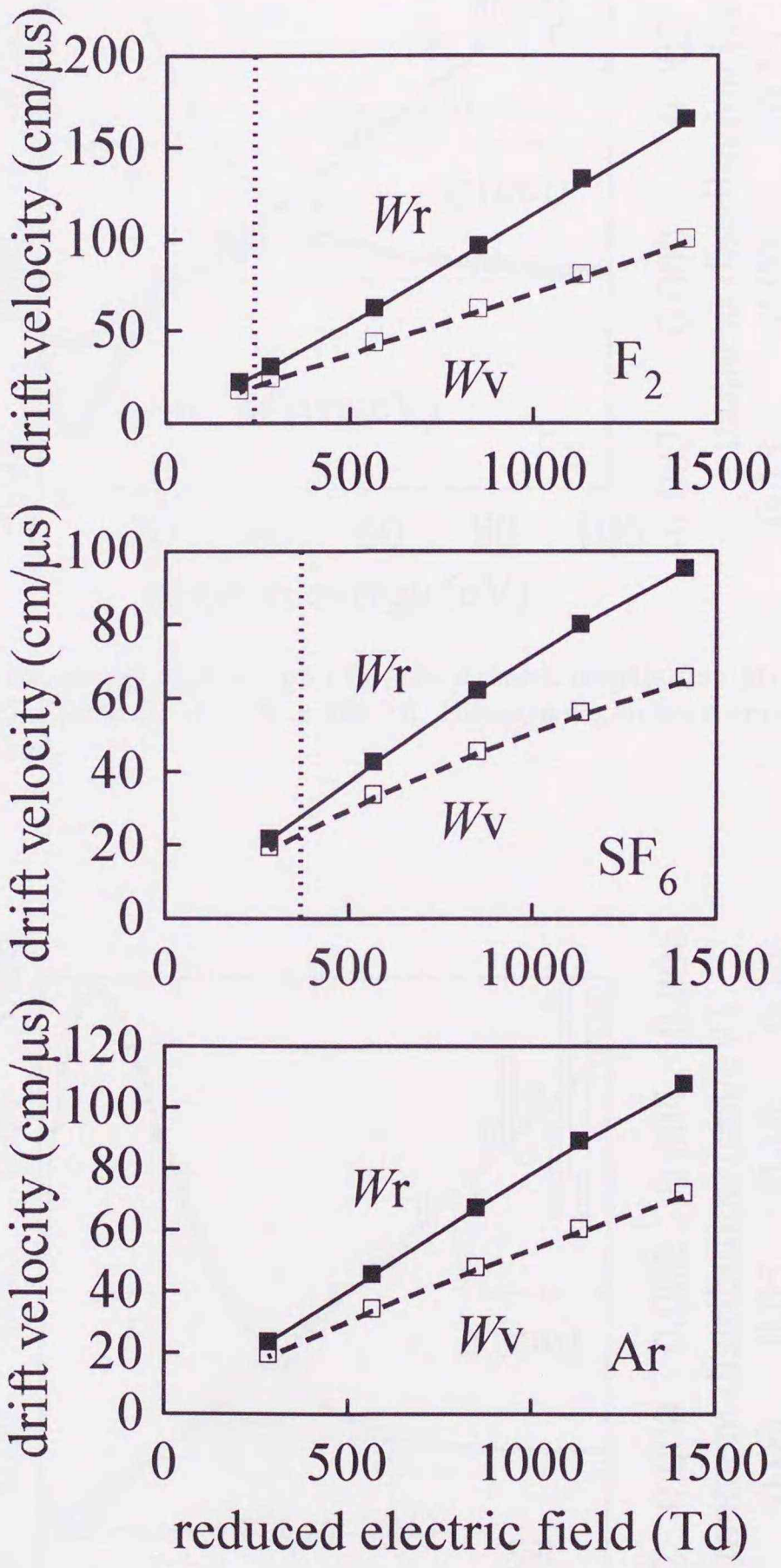

Figure 6.3: The centroid drift velocities W_r and the mean velocity W_v in F_2, SF_6 and Ar. Full and open squares, MCS; full and broken curves, PM. The vertical dotted lines indicate $(E/N)_{lim}$ at which $\bar{R}_{ion} = 0$; each gas is electro-negative in the left region of the line and electro-positive in the right.

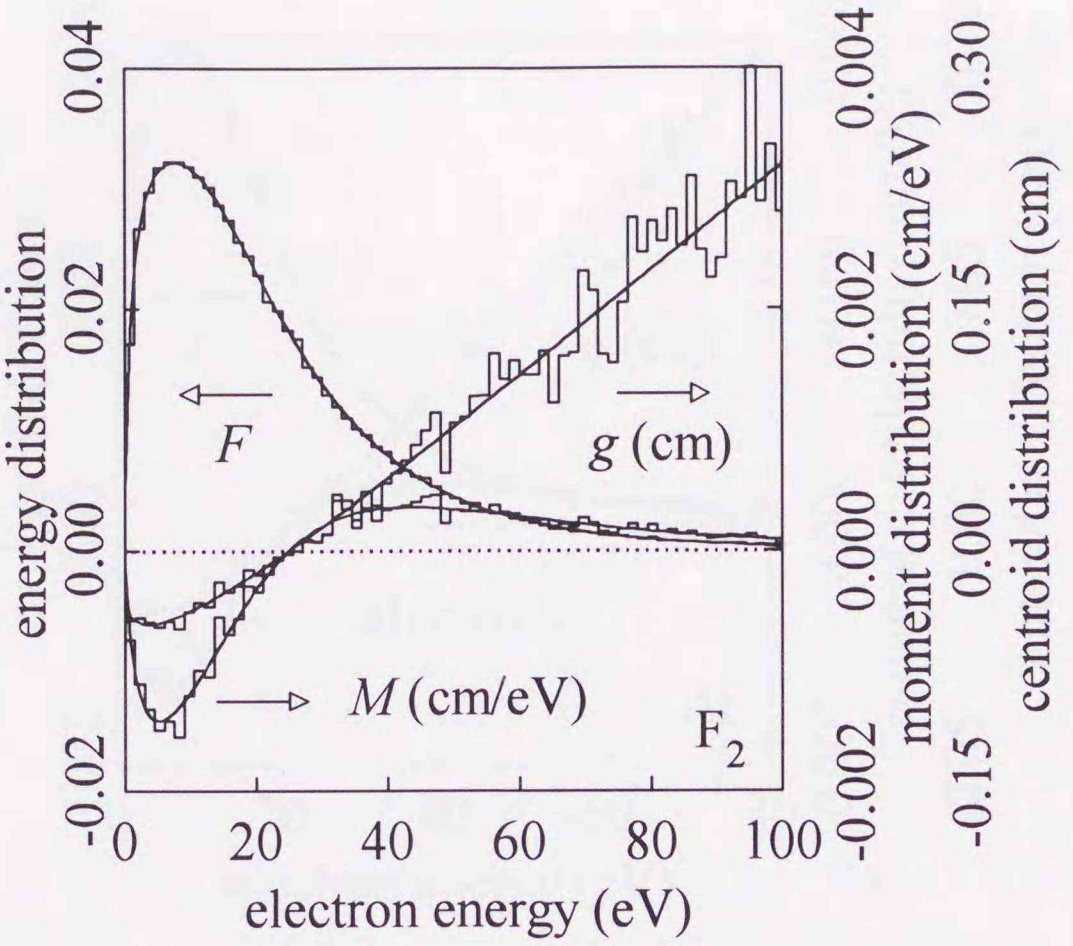

Figure 6.4: The electron energy distribution $F(\epsilon)$, the moment distribution $M(\epsilon)$ and relative centroid distribution $g(\epsilon) = M(\epsilon)/F(\epsilon)$ in F_2 at $E/N = 848$ Td. Histograms, Monte Carlo simulation; curves, the present propagator method.

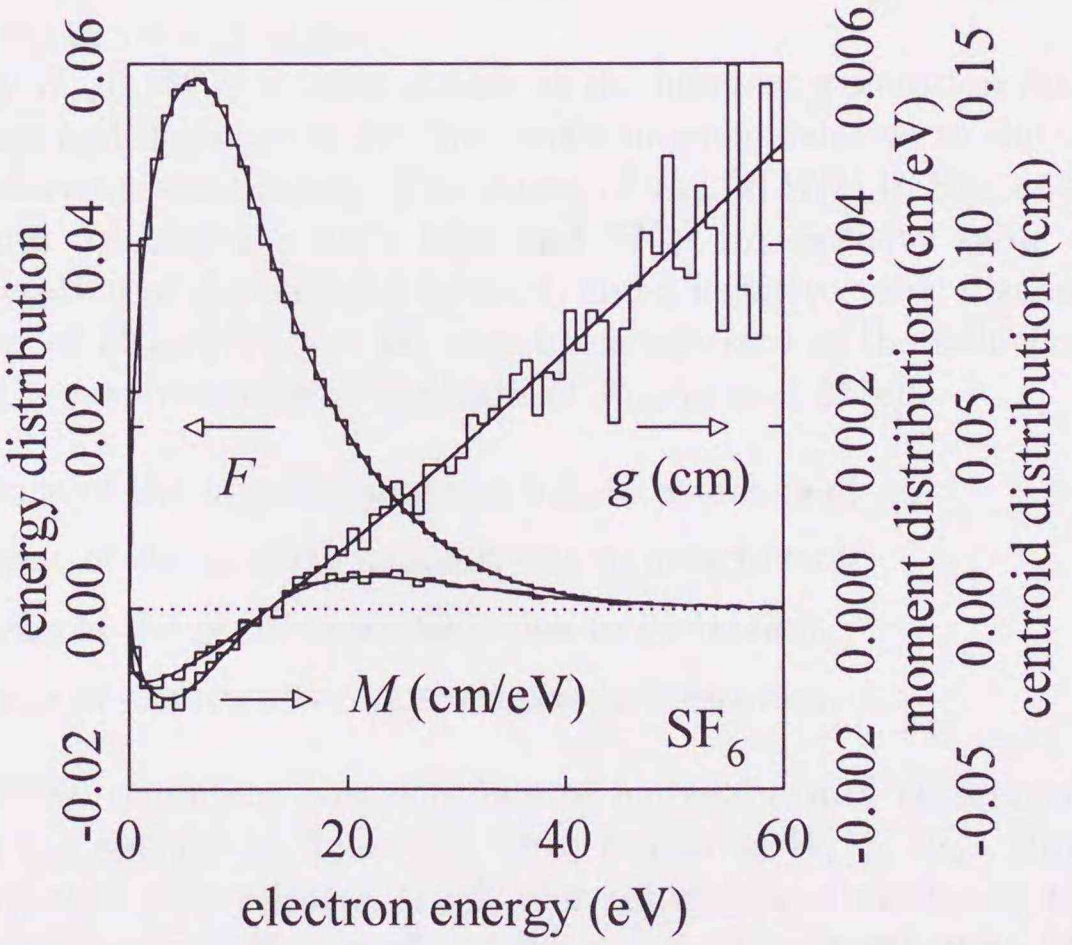

Figure 6.5: The electron energy distribution $F(\epsilon)$, the moment distribution $M(\epsilon)$ and relative centroid distribution $g(\epsilon) = M(\epsilon)/F(\epsilon)$ in SF_6 at $E/N = 848$ Td. Histograms, Monte Carlo simulation; curves, the present propagator method.

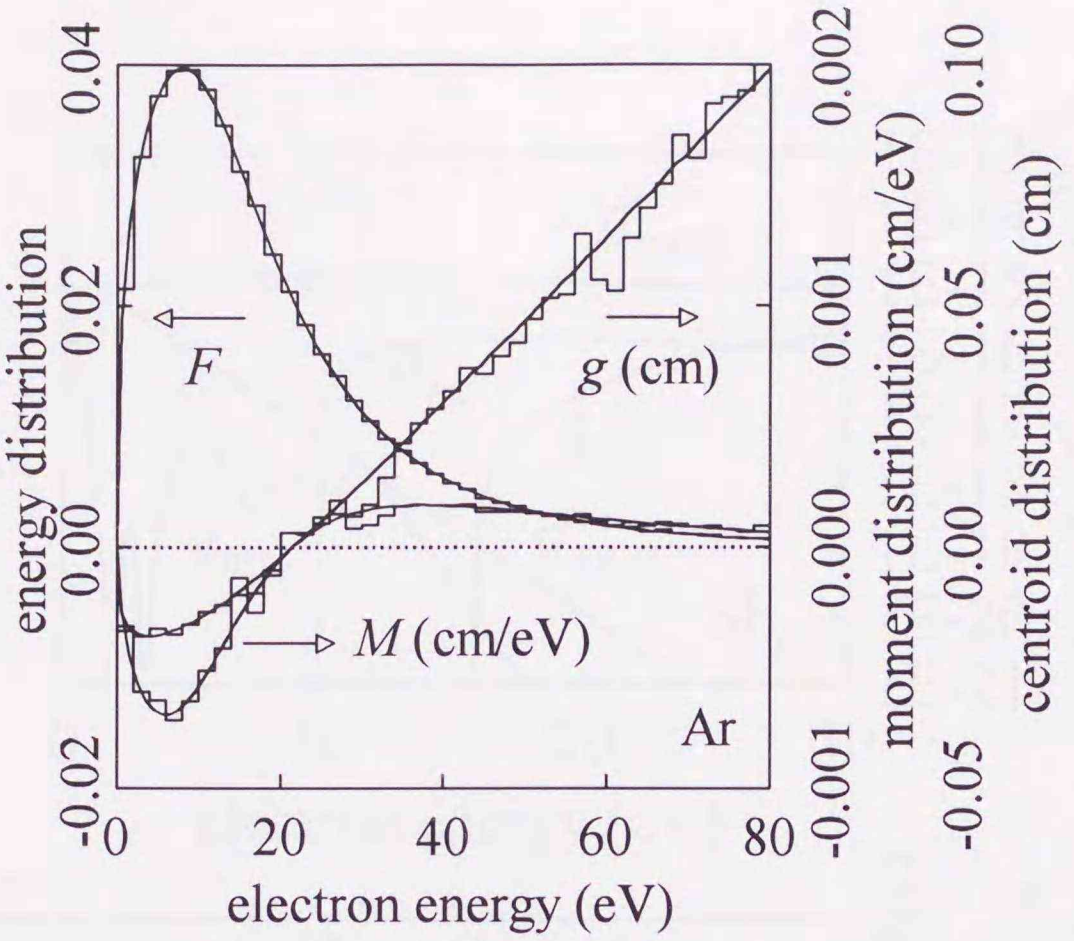

Figure 6.6: The electron energy distribution $F(\epsilon)$, the moment distribution $M(\epsilon)$ and relative centroid distribution $g(\epsilon) = M(\epsilon)/F(\epsilon)$ in Ar at $E/N = 1414$ Td. Histograms, Monte Carlo simulation; curves, the present propagator method.

where $q_{\rm ion}$ and $q_{\rm att}$ are the ionization and attachment cross sections, and v_1 is the electron speed associated with 1 eV. Equation (6.19) is an alternative expression of equation (6.6), which is described in velocity space.

The quantity $\bar{R}_{\rm ion}(\epsilon)M(\epsilon)$ is defined here as the moment generation rate, which represents the increase and decrease of the first order moment relative to the centroid due to ionization and electron attachment. The values of $\bar{R}_{\rm ion}(\epsilon)M(\epsilon)$ in SF_6 and Ar are shown in figures 6.7 and 6.8 together with $F(\epsilon)$ and $M(\epsilon)$. A positive value of $\bar{R}_{\rm ion}(\epsilon)M(\epsilon)$ represents acceleration of the centroid forward, and a negative value means slowing down.

Contributions of $\bar{R}_{\rm ion}(\epsilon)M(\epsilon)$ to $W_{\rm r}$ may be categorized as the following four types of cases based on the combinations of the signs of $\bar{R}_{\rm ion}(\epsilon)$ and $M(\epsilon)$;

(a) decrease of the negative moment due to attachment

(b) decrease of the positive moment due to attachment

(c) increase of the positive moment due to ionization

(d) increase of the negative moment due to ionization.

As expected before, dominant contributions of ionization and attachment are positive as indicated by (a) and (c) in figure 6.7, that results in $W_{\rm r} > W_{\rm v}$. However, electron attachment associated with relatively high energies such as dissociative attachment may affect as a negative contribution as (b) in figure 6.7. The fourth type (d) is caused by ionization associated with relatively low energies at which $M(\epsilon) < 0$. Yachi and Tagashira (1991) and Satoh *et al.* (1994) demonstrated case (d) using model gases, where $W_{\rm r} < W_{\rm v}$.

A calculation result using a model gas taken from Satoh *et al.* (1994) is presented in figure 6.9 as an additional example to show case (d) for comparison with figure 6.7. The

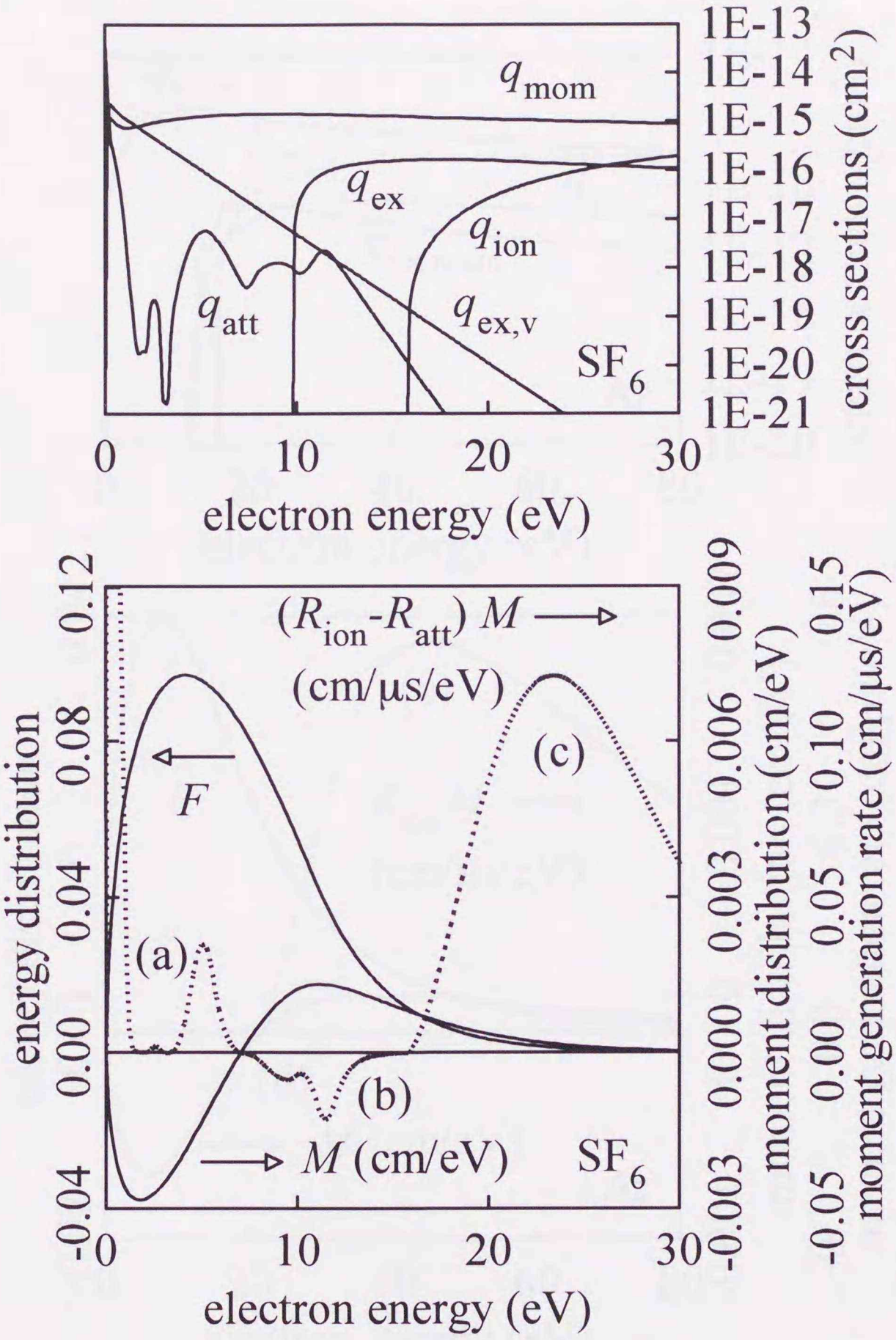

Figure 6.7: Upper figure; the collision cross sections of SF_6 (Itoh *et al.* 1988); momentum transfer q_{mom}, excitation q_{ex}, vibrational excitation $q_{ex,v}$, ionization q_{ion} and electron attachment q_{att}. q_{att} is the total attachment cross section to form SF_6^-, SF_5^-, SF_4^-, F^- and F_2^-. Lower figure; the electron energy distribution $F(\epsilon)$, the moment distribution $M(\epsilon)$ and the moment generation rate $\bar{R}_{ion}(\epsilon)M(\epsilon)$ in SF_6 calculated by the present propagator method at $E/N = 283$ Td. Contribution of $\bar{R}_{ion}(\epsilon)M(\epsilon)$ to W_r consists of (a) decrease of the negative moment due to attachment, (b) decrease of the positive moment due to attachment, and (c) increase of the positive moment due to ionization. $W_r = 21.2$ cmμs^{-1}, $W_v = 18.9$ cmμs^{-1}; $W_r > W_v$.

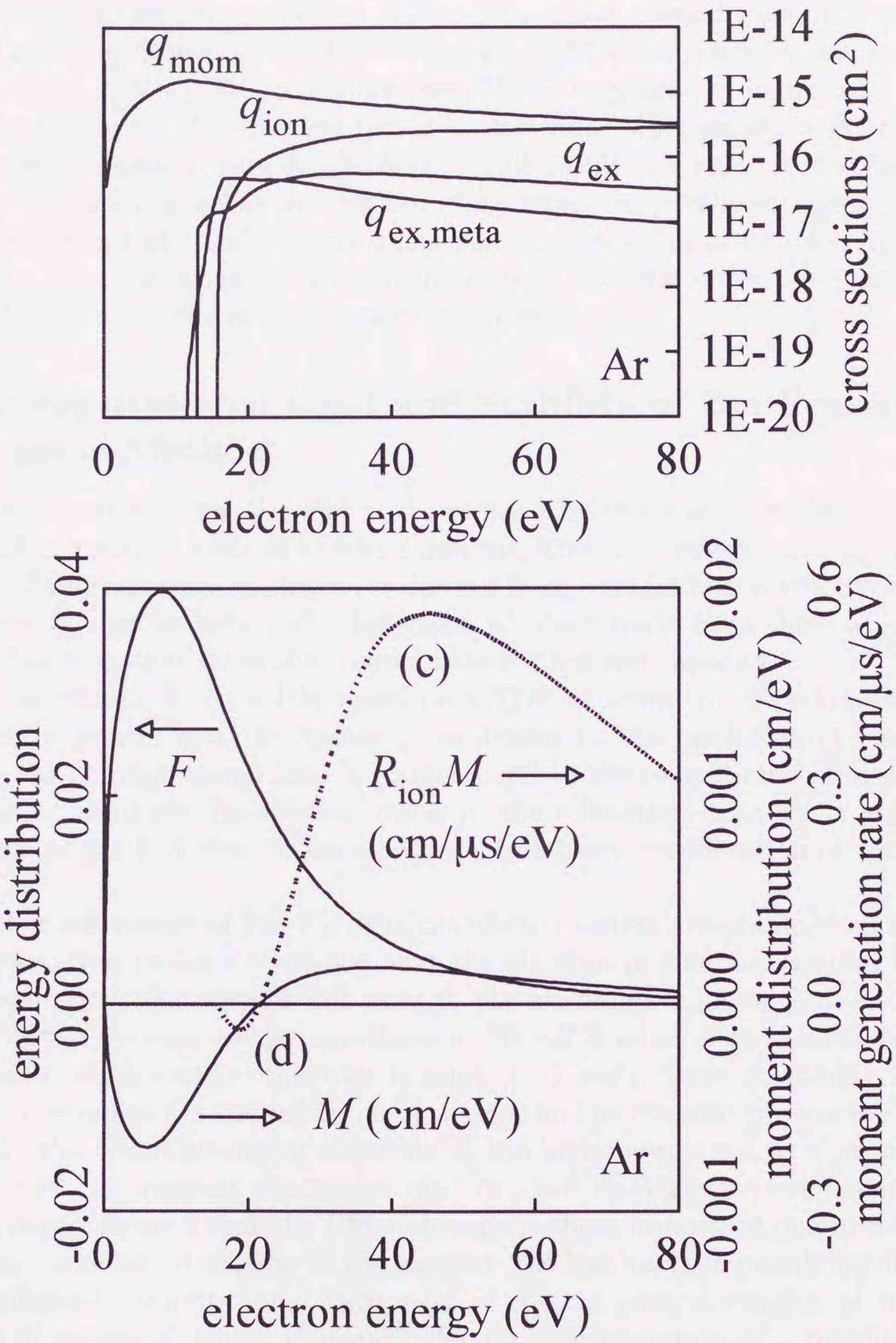

Figure 6.8: Upper figure; the collision cross sections of Ar (Suzuki *et al.* 1990); momentum transfer $q_{\rm mom}$, excitation $q_{\rm ex}$, excitation to the metastable state $q_{\rm ex,meta}$, ionization $q_{\rm ion}$. Lower figure; the electron energy distribution $F(\epsilon)$, the moment distribution $M(\epsilon)$ and the moment generation rate $\bar{R}_{\rm ion}(\epsilon)M(\epsilon)$ in Ar calculated by the present propagator method at $E/N = 1414$ Td. Contribution of $\bar{R}_{\rm ion}(\epsilon)M(\epsilon)$ to $W_{\rm r}$ consists of (c) increase of the positive moment due to ionization and (d) increase of the negative moment due to ionization. $W_{\rm r} = 106.7$ cmμs^{-1}, $W_{\rm v} = 71.3$ cmμs^{-1}; $W_{\rm r} > W_{\rm v}$.

set of the cross sections of the model gas is rather unreal since $q_{\rm ion}$ is on the lower-energy side of $q_{\rm ex}$. However, this situation could appear in gas mixtures.

The condition required to realize $W_{\rm r} = W_{\rm v}$ is balance of the positive and negative contributions of $\bar{R}_{\rm ion}(\epsilon)M(\epsilon)$, therefore, single $\bar{R}_{\rm ion}(\epsilon)$ without the weight of $M(\epsilon)$ does not determine whether $W_{\rm r} > W_{\rm v}$ or $W_{\rm r} < W_{\rm v}$. As a special case, $W_{\rm r} = W_{\rm v}$ when $\bar{R}_{\rm ion}(\epsilon) = 0$ at any ϵ. However, $\bar{R}_{\rm ion}(\epsilon) = 0$ and $W_{\rm r} = W_{\rm v}$ are essentially events of different orders. Even at $(E/N)_{\rm lim}$, $W_{\rm r}$ may differ from $W_{\rm v}$ as suggested in figure 6.3.

It can be concluded that the key factor to determine whether $W_{\rm r} > W_{\rm v}$ or $W_{\rm r} < W_{\rm v}$ is the moment generation rate $\bar{R}_{\rm ion}(\epsilon)M(\epsilon)$. This result is similar to the fact that the quantity to determine whether the number of electrons temporally increases or decreases is $\bar{R}_{\rm ion}(\epsilon)F(\epsilon)$, from which the effective ionization frequency $\bar{R}_{\rm ion}$ is obtained by integration throughout ϵ. The correspondence between the 0-th and first order relations above may suggest a kind of hierarchy of the moment equations.

6.5.4 Computational Load and Stability of the Present Propagator Method

The computational load for the PM is determined by the resolution for velocity space and physical relaxation time of electron swarms, and it is irrespective of the electron population. Using equation (6.19), $W_{\rm r}$ is derived from calculations in velocity space. This expression enables us to reduce the dimension of phase space from three as investigated in chapter 3 to two, that saves the computational time and capacity.

In order to obtain $W_{\rm r}$ by a PM based on a TOF experiment, the relaxation distance for the electron swarm must be evaluated to determine the resolution of real space. In this model, the computational load is proportional to the relaxation distance. However, it is difficult to evaluate the accurate value of the relaxation distance in general. It is an advantage of the PM that its calculation is free from consideration of the relaxation distance.

As another advantage of the PM, the calculation results are obtained as numerically smooth curves even under a condition that the electron population is quite low. A low electron population may appear not only in electro-negative gases, but also at a high energy tail of the electron energy distribution. An MCS under such conditions may tend to be unstable statistically, otherwise it tends to become time-consuming since much more electron samples are needed to compensate the low electron population. As shown in figure 6.7, the contributions of electrons at the high energy tail to a certain physical properties, *e.g.* the moment generation rate, can not be neglected even though $F(\epsilon)$ is small. It is demonstrated that the PM stably gives those important quantities.

The basic calculation scheme of the present PM has another possibility for more efficient parallelized computation. Most part of the calculation consists of independent summation of products, which is suitable for pipeline operation of a parallel computation technique as mentioned before. In addition, the present calculation scheme based on simultaneous moment equations is considered to be applicable to multi-processor system expected as a near-future computer architecture. When the present PM is extended based on the hierarchy of moment equations for electron swarms, higher efficiency of parallelization may be expected.

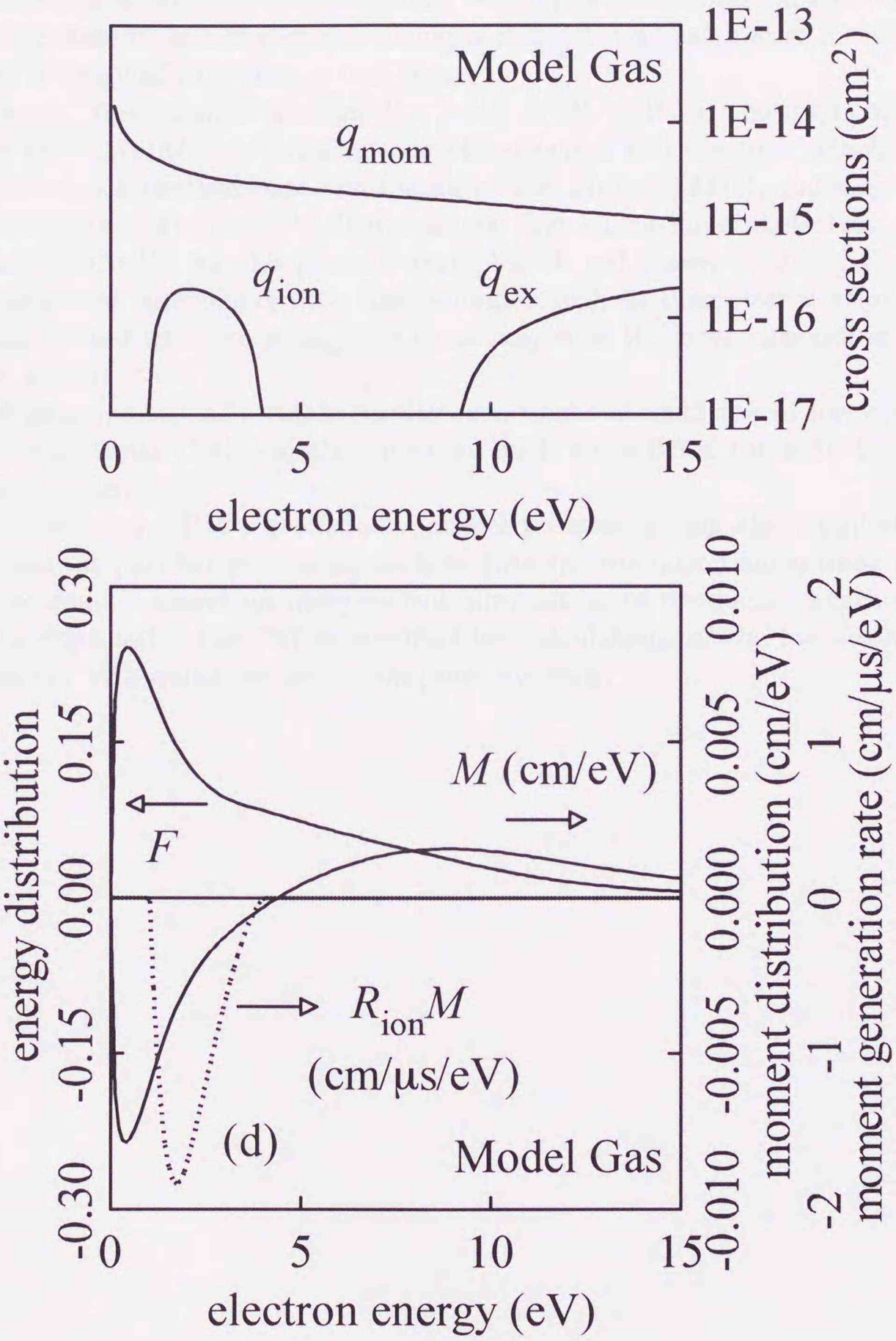

Figure 6.9: Upper figure; the collision cross sections of a model gas (Satoh *et al.* 1994, case 3); momentum transfer $q_{\rm mom}$, excitation $q_{\rm ex}$ ($\epsilon_{\rm ex} = 9.0$ eV), and ionization $q_{\rm ion}$ ($\epsilon_{\rm ion} = 1.0$ eV). Lower figure; the electron energy distribution $F(\epsilon)$, the moment distribution $M(\epsilon)$ and the moment generation rate $\bar{R}_{\rm ion}(\epsilon)M(\epsilon)$ in the model gas calculated by the present propagator method at $E/N = 283$ Td. The fourth type of the contribution of $\bar{R}_{\rm ion}(\epsilon)M(\epsilon)$ to $W_{\rm r}$ appears as (d) increase of the negative moment due to ionization. $W_{\rm r} = 14.4$ cmμs^{-1}, $W_{\rm v} = 17.3$ cmμs^{-1}; $W_{\rm r} < W_{\rm v}$.

6.6 Chapter Summary

A new evaluation method to obtain the centroid drift velocity W_r of an electron swarm in gases was introduced based on a PM. In the present investigation, the quantitative difference between W_r and the mean electron velocity W_v was obtained based on moment equations described in velocity space. Using a PM, W_r was calculated in velocity space although W_r is originally defined in real space.

A key factor to determine whether $W_r > W_v$ or $W_r < W_v$ is the moment generation rate defined as $\bar{R}_{ion}(\epsilon)M(\epsilon)$. Contributions of ionization and electron attachment to W_r were categorized as four cases based on the signs of $\bar{R}_{ion}(\epsilon)$ and $M(\epsilon)$, and they were quantitatively demonstrated by the PM. It was shown that ionization and electron attachment primarily accelerate W_r for the present examples of real gases; F_2 and SF_6. However, electron attachment associated with high energies such as dissociative attachment and ionization associated with low energy electrons may slow W_r down depending on $M(\epsilon)$ of the electron swarm.

The PM gave numerically stable results even under a condition of low electron population, while a Monte Carlo simulation under such a condition tends to be affected by statistical fluctuation.

A possibility of the PM for efficient parallel processing was also pointed out. The PM is suitable for parallel processing such as pipeline operation since most part of the calculation scheme is based on independent summation of products. Further efficiency of the PM is expected if the PM is modified for calculations of the hierarchy system of electron swarms with multi-processor computer systems.

References

Blevin H A and Fletcher J 1984 *Aust.J.Phys.* **37** 593-600
Hayashi M and Nimura T 1983 *J.Appl.Phys.* **54** 4879-82
Hazi A U 1981 *Phys.Rev.A* **46** 918-22
Itoh H, Matsumura T, Satoh K, Date H, Nakao Y and Tagashira H
1993 *J.Phys.D: Appl.Phys.* **26** 1975-9
Kitamori K, Tagashira H and Sakai Y 1980 *J.Phys.D: Appl.Phys.* **13** 535-50
Kumar K 1981 *J.Phys.D: Appl.Phys.* **16** 2199-208
Nakamura Y 1988 *J.Phys.D: Appl.Phys.* **21** 67-72
Penetrante B M, Bardsley J N and Pitchford L C
1985 *J.Phys.D: Appl.Phys.* **18** 1087-100
Phelps A V and Pitchford L C 1985 *Phys.Rev.A* **31** 2932-49
Robson R E 1991 *Aust.J.Phys.* **44** 685-92
Satoh K, Itoh H, Nakao Y and Tagashira H 1988 *J.Phys.D: Appl.Phys.* **21** 931-6
Satoh K, Ohmori Y, Sakai Y and Tagashira H 1991 *J.Phys.D: Appl.Phys.* **24** 1354-9
Satoh K, Hamaguchi M, Itoh H, Sakai Y and Tagashira H
1994 *J.Phys.D: Appl.Phys.* **27** 1480-6
Skullerud H R and Kuhn S 1983 *J.Phys.D: Appl.Phys.* **16** 1225-34
Skullerud H R 1984 *J.Phys.B: At.Mol.Phys.* **17** 913-29
Sugawara H, SakaiY and Tagashira H 1994 *J.Phys.D: Appl.Phys.* **27** 90-4
Suzuki M, Taniguchi T and Tagashira H 1990 *J.Phys.D: Appl.Phys.* **23** 842-50
Tagashira H, Sakai Y and Sakamoto S 1977 *J.Phys.D: Appl.Phys.* **10** 1051-63
Yachi S and Tagashira H 1991 *Trans.IEE Jpn.* **111-A** 152-8

Chapter 7

Conclusions

7.1 Summary of the Present Work

In the present thesis, a simulation method for analyzing electron swarms, propagator method (PM), has been developed based on continuum model as an advanced computational technique.

The background of the present work and the principles of the PM were presented in chapters 1 and 2. Based on the PM, the following subjects of electron swarm analyses have been investigated in each chapter;

1. the spatial relaxation processes of an electron swarm between parallel plane electrodes under steady-state Townsend (SST) conditions (chapter 3),

2. drift equilibrium solutions of the electron velocity distribution under SST and pulsed Townsend (PT) conditions (chapter 4),

3. electron swarm properties in the upstream region of an electron source (chapter 5),

4. relation between the centroid drift velocity W_{r} and the mean electron velocity W_{v} of an electron swarm (chapter 6).

In chapter 3, the spatial relaxation processes of an electron swarm between parallel plane electrodes under SST conditions were investigated. The PM for this subject was composed concerning the law of energy conservation. Some rules for dividing phase space and electron motion were newly introduced to the PM. Fine aspects of the relaxation processes of electron swarm parameters and the electron energy distribution were clearly reproduced by the PM, which agreed with the results obtained by a Monte Carlo simulation. The importance of the rules for the PM was demonstrated. The conclusions of chapter 3 can be summarized as follows.

- A relation $\Delta\epsilon = eE\Delta x$ for the cell width $\Delta\epsilon$ and Δx and a rule for electron motion were introduced to satisfy the law of energy conservation.

- Fine structures of the relaxation processes of electron swarms were successfully obtained due to this treatment.

- The relaxation distance of the electron energy distribution is longer than that of electron swarm parameters.

- Relaxation distance of an electron swarm to attain a drift equilibrium may be evaluated based on the energy range of the drift equilibrium electron energy distribution.

In chapter 4, a calculation technique of PM for obtaining the drift equilibrium solutions of the electron velocity distributions under SST conditions were developed. The electron velocity distribution is calculated in velocity space, and calculations for the spatial relaxation processes as performed in the preceding chapter were omitted by utilizing an assumption of the exponential spatial growth of electron swarms. This SST calculation was applicable to PT conditions by modifying the treatment of the electron number density gradient. Treatments of the two typical observation systems of electron swarm development, SST and PT conditions, were discussed comparing Boltzmann equation analyses and the PM. The conclusions of chapter 4 are as follows.

- In a new calculation technique of PM for obtaining drift equilibrium solutions under SST conditions, treatment for the spatial relaxation processes can be omitted by considering exponential spatial growth of electron swarms.

- Calculation of the PM is stable even at high E/N values and electro-negative ($\bar{R}_{\rm ion} < 0$) conditions which would be difficult conditions for conventional simulation methods.

- The calculation scheme of the PM for SST conditions can be modified for PT conditions by putting $\bar{\alpha} = 0$.

- This treatment corresponds to that for the differential operators $\partial/\partial x$ and $\partial/\partial t$ depending on the observation conditions in Boltzmann equation analyses.

Modifying the PM developed in chapter 4 for a special condition, properties of electron swarms in the upstream region of an electron source were investigated in chapter 5. When initial electrons are given with high energies, some of them may diffuse toward the upstream direction from the electron source due to backward scattering by collision with gas molecules. Assuming an exponential spatial decay of electron number density toward the upstream direction, characteristics of electron swarm parameters and the electron energy distribution particular to the upstream region were derived. Behavior of electron swarms in front of an absorbing anode was simulated as a practical example of the appearance of the effect of the backward diffusion. The decay of the electron number density in front of the absorbing anode was explained as behavior of vacancies which might be filled up by missing electrons absorbed at the anode. It was confirmed that the behavior of the vacancies are similar to the electrons in the upstream region. The vacancies have relaxation processes before attaining drift equilibrium solution as well. The following conclusions were obtained in chapter 4.

- Relations among swarm parameters in the upstream region of an electron source were derived assuming exponential spatial growth of electron swarms under SST conditions:

$$\bar{\alpha}' = \frac{W'_{\rm s} + \sqrt{W'^2_{\rm s} - 4R'_{\rm ion,s}D'_{\rm s}}}{2D'_{\rm s}}, \qquad R'_{\rm ion,s} = v'_{\rm d}\bar{\alpha}'.$$

- The sign of the electron drift velocity $v'_{\rm d}$ represents whether the gas medium is effectively electro-positive or electro-negative in the upstream region as well as the sign of the effective ionization frequency $\bar{R}'_{\rm ion,s}$.

- The decay of the electron number density in front of an absorbing anode is vacancies missing electrons absorbed at the anode.

- Behavior of the vacancies is identical to that of backward-diffusing electrons observed in the upstream region.
- The backward-diffusing electrons also have relaxation processes and equilibrium solutions.
- A key difference between contributions of electrons in the upstream and downstream regions to electron swarm parameters is the parity of the electron passages across an observation position.

In chapter 6, W_{r} of an electron swarm was derived from moment equations based on the Boltzmann equation. The effects of ionization and electron attachment were categorized as four types according to the combination of the signs of $\bar{R}_{\mathrm{ion}}(\epsilon)$ and the first order moment $M(\epsilon)$ with respect to the electron position. These effects were quantified as the moment generation rates $\bar{R}_{\mathrm{ion}}(\epsilon)M(\epsilon)$. $M(\epsilon)$ and $\bar{R}_{\mathrm{ion}}(\epsilon)M(\epsilon)$ of electron swarms were calculated by the PM, and the four types of the effects were quantitatively demonstrated. It was shown that the quantitative difference between W_{r} and W_{v} is represented as the total amount of $\bar{R}_{\mathrm{ion}}(\epsilon)M(\epsilon)$. Related to the simultaneous calculation scheme of the propagator method, a possibility of the PM was discussed for more efficient electron swarm analyses by another form of parallelization technique of computer architecture using a multi-processor system. The conclusions of chapter 6 are as follows.

- Calculation for obtaining W_{r} can be performed in velocity space based on moment equations while W_{r} is originally defined in real space.
- A relation between W_{r} and W_{v} was derived as

$$W_{\mathrm{r}} - W_{\mathrm{v}} = \int_0^\infty \bar{R}_{\mathrm{ion}}(\epsilon)M(\epsilon)\mathrm{d}\epsilon$$

  where $\bar{R}_{\mathrm{ion}}(\epsilon)$ and $M(\epsilon)\mathrm{d}\epsilon$ are the effective ionization frequency and the first order moment with respect to the position of an electron swarm.
- The quantity $\bar{R}_{\mathrm{ion}}(\epsilon)M(\epsilon)$ was defined as the moment generation rate, which is a key quantity to determine whether $W_{\mathrm{r}} > W_{\mathrm{v}}$ or $W_{\mathrm{r}} < W_{\mathrm{v}}$.
- The contributions of $\bar{R}_{\mathrm{ion}}(\epsilon)M(\epsilon)$ can be categorized as four cases based on the combinations of the signs of $\bar{R}_{\mathrm{ion}}(\epsilon)$ and $M(\epsilon)$.
- Primary effects of ionization and attachment are represented by positive value of $\bar{R}_{\mathrm{ion}}(\epsilon)M(\epsilon)$, however, ionization at low energies and attachment of high energy electrons may result in negative $\bar{R}_{\mathrm{ion}}(\epsilon)M(\epsilon)$.
- A possibility for parallelized calculation scheme based on hierarchy system of moment equations was suggested.

7.2 Future Orientation of the Study

The present study have been initiated with the following objectives primarily:

- to establish a PM as an accurate and general simulation method for weakly ionized non-equilibrium plasma analyses,

- to realize analyses under severe conditions for conventional simulation techniques for obtaining new knowledge of the plasma properties,
- to utilize recent and near-future parallel processing technique for realizing efficient computation of the plasma analyses.

Although some results obtained in the present thesis owe to particular conditions which enabled us to reduce the computational load, it can be said that some part of these objectives has been attained as demonstrated in each investigation in this thesis.

For further development of the PM for weakly ionized plasma investigations, there still remain many physical phenomena to be introduced; effects of space charge field, magnetic field, photo reactions, and behavior of ions. Since the computational scheme of PM is one of the most fundamental forms of numerical calculation, most of these physical conditions could be taken into account immediately in principle. For example, the effect of the space charge field will be considered as position-dependent electric field derived from Poisson's equation. Although the computational resource is now still limited in both of memory storage size and calculation speed, it is doubtless that the resource will be extended quite soon by introducing a huge capacity of memories and new parallelization techniques. PM will be established as a simple and general calculation method for weakly ionized non-equilibrium plasma investigations which can fully utilize such a new computational environment.

Author's Publications Related to the Present Work

Papers

Sugawara H, Sakai Y and Tagashira H
1992 *J.Phys.D: Appl.Phys.* **25** 1483-7
"Position-dependent electron swarm behaviour in steady-state Townsend discharges"
Sugawara H, Sakai Y and Tagashira H
1994 *J.Phys.D: Appl.Phys.* **27** 90-4
"Analyses of electron swarms in gases under steady-state Townsend conditions"
Sugawara H, Sakai Y and Tagashira H
1995 *J.Phys.D: Appl.Phys.* **28** 61-7
"Properties of electron swarms in gases in the upstream region of an electron source"
Sugawara H, Tagashira H and Sakai Y
1996 *J.Phys.D: Appl.Phys.* **29** 1168-74
"The velocity distribution of ions in warm gas under a constant-collision-frequency symmetric charge exchange model"
Sugawara H, Tagashira H and Sakai Y
1997 *J.Phys.D: Appl.Phys.* **30** 368-73
"Evaluation of real space electron drift velocity in gases using moment equations performed in velocity space"

Technical Papers

Sugawara H, Sakai Y and Tagashira H
1991 *IEE Jpn., Papers of Technical Committee on Electric Discharges* ED-91-69
"Electron swarm simulations in Ar using a direct solution of the Boltzmann equation"
Sugawara H, Sakai Y and Tagashira H
1993 *IEE Jpn., Papers of Technical Committee on Electric Discharges* ED-93-198
"Electron swarm analyses using a propagator method under SST conditions"
Uchida S, Sugawara H, Ventzek P L G, Sakai Y and Tagashira H
1995 *IEE Jpn., Papers of Technical Committee on Electric Discharges* ED-95-128
"Simulations of plasma diagnostics by optogalvanic spectroscopy"
Sugawara H, Tagashira H and Sakai Y
1996 *IEE Jpn., Papers of Technical Committee on Electric Discharges* ED-96-218
"The centroid drift velocity of electron swarms in gases
— derivation using moment equations described in velocity space —"

International Conference Papers

Sakai Y, Sugawara H and Tagashira H
1991 *The Am.Phys.Soc., 44th Ann.Gaseous Electronics Conf.* HA-7
"An analysis of position-dependent electron swarm behavior
in steady-state Townsend discharges by convective-scheme technique"
Sugawara H, Sakai Y and Tagashira H
1994 *Int.Assoc.Comput.Mechanics, The 3rd World Cong.on Comput.Mechanics* D7-2
"Parallel computing of electric discharges — electron flow in phase space"
Tagashira H, Sugawara H and Sakai Y
1994 *Jpn-Aust.Workshop on Electron Swarms*
"Properties of electron swarms in gases in the upstream region of the electron source"
Sugawara H, Sakai Y and Tagashira H
1994 *The Am.Phys.Soc., 47th Ann.Gaseous Electronics Conf.* EB-4
"Electron swarms in the upstream region of an electron source"
Uchida S, Sugawara H, Ventzek P L G, Sakai Y and Tagashira H
1995 *The Am.Phys.Soc., 48th Ann.Gaseous Electronics Conf.* CA-5
"A computer simulation of optogalvanic signals in neon gas discharges"

Oral Presentation Proceedings

Sugawara H, Sakai Y and Tagashira H
1990 *Jpn.Soc.Appl.Phys., 25th Conf.of Hokkaido Chapt.* B13
"simulation of electron swarms in velocity space"
Sugawara H, Sakai Y and Tagashira H
1990 *IEE Jpn., Nat.Conf.* No.155
"Swarm parameters in gases (CLXXXVIII)
direct solution of the Boltzmann equation"
Sugawara H, Sakai Y and Tagashira H
1990 *IEE Jpn.and Rel.Inst., Joint Conv.of Hokkaido Chapts.* No.156
"Swarm parameters in gases (CXCV)
direct solution of the Boltzmann equation: real space model"
Sugawara H, Sakai Y and Tagashira H
1991 *Jpn.Soc.Appl.Phys., 26th Conf.of Hokkaido Chapt.* A32
"simulation of gas discharges using direct solution of the Boltzmann equation (1):
SST simulation"
Sugawara H, Sakai Y and Tagashira H
1991 *IEE Jpn., Nat.Conf.* No.221
"Swarm parameters in gases (CCIX)
direct solution of the Boltzmann equation: SST simulation"
Sugawara H, Sakai Y and Tagashira H
1991 *IEE Jpn.and Rel.Inst., Joint Conv.of Hokkaido Chapts.* No.191
"Swarm parameters in gases (CCXV)
direct solution of the Boltzmann equation: spatial variation of SST parameters"
Sugawara H, Sakai Y and Tagashira H
1992 *Jpn.Soc.Appl.Phys., 27th Conf.of Hokkaido Chapt.* C7
"simulation of gas discharges using direct solution of the Boltzmann equation (2):
introduction of electric field distortion"
Sugawara H, Sakai Y and Tagashira H

1992 *IEE Jpn., Nat.Conf.* No.89
"Swarm parameters in gases (CCXVIII)
simulation of electric field distortion by propagator method"
Sugawara H, Sakai Y and Tagashira H
1993 *IEE Jpn., Nat.Conf.* No.221
"Swarm parameters in gases (CCXXIV)
evaluation for the electron flow in propagator method"
Sugawara H, Sakai Y and Tagashira H
1993 *IEE Jpn.and Rel.Inst., Joint Conv.of Hokkaido Chapts.* No.49
"Swarm parameters in gases (CCXXV)
SST electron swarm analysis using propagator method"
Sugawara H, Sakai Y and Tagashira H
1994 *IEE Jpn., Nat.Conf.* No.231
"Swarm parameters in gases (CCXXIX)
electron swarm analyses in the upstream region of an electron source"
Sugawara H, Sakai Y and Tagashira H
1994 *IEE Jpn.and Rel.Inst., Joint Conv.of Hokkaido Chapts.* No.50
"Swarm parameters in gases (CCXXXV)
an effect by backward diffusion of electrons in the vicinity of absorbing anode"
Uchida S, Sugawara H, Ventzek P L G, Sakai Y and Tagashira H
1995 *IEE Jpn., Nat.Conf.* No.59
"Diagnostics of non-equilibrium plasmas by optogalvanic spectroscopy (III)
variation of the electron number density due to laser irradiation in positive column"
Sugawara H, Uchida S, Sakai Y and Tagashira H
1995 *IEE Jpn., Nat.Conf.* No.180
"Swarm parameters in gases (CCXXXVII)
modeling of positive column by a propagator method"
Uchida S, Sugawara H, Ventzek P L G, Sakai Y and Tagashira H
1995 *IEE Jpn.and Rel.Inst., Joint Conv.of Hokkaido Chapts.* No.90
"Diagnostics of non-equilibrium plasmas by optogalvanic spectroscopy (IV)
analyses of optogalvanic signals by a propagator method"
Uchida S, Sugawara H, Ventzek P L G, Sakai Y and Tagashira H
1995 *Jpn.Soc.Appl.Phys., 30th Conf.of Hokkaido Chapt.* C38
"Diagnostics of non-equilibrium plasmas by optogalvanic spectroscopy (V)
simulations of optogalvanic effect at low E/N values
Uchida S, Sugawara H, Ventzek P L G, Sakai Y and Tagashira H
1996 *IEE Jpn., Nat.Conf.* No.71
"Diagnostics of non-equilibrium plasmas by optogalvanic spectroscopy (VI)
analyses of optogalvanic signals from Ne plasmas using a propagator method"

Appendix A

Derivation of Relations between Drift Velocities

Relations between the centroid drift velocity W_{r} observed under a time-of-flight condition and the mean velocity W_{v} of an electron swarm under a pulsed Townsend condition are derived by transforming the definition of W_{r} using the Boltzmann equation. Two ways of expressions of the relation are presented here, which have been shown as equations (6.6) and (6.19). These equations represent relations between W_{r} and W_{v} described in real and velocity space, respectively. A uniform electric field $\boldsymbol{E}$ in the x direction is assumed and real space is treated to be one-dimensional here.

A.1 Relation Described in Real Space

The centroid drift velocity W_{r} and the mean electron velocity W_{v} of an electron swarm are defined as

$$W_{\mathrm{r}}(t) \equiv \frac{\mathrm{d}}{\mathrm{d}t}G(t) = \frac{\mathrm{d}}{\mathrm{d}t}\frac{\int_{\boldsymbol{r},\boldsymbol{v}} x f(\boldsymbol{r},\boldsymbol{v},t)\mathrm{d}\boldsymbol{r}\mathrm{d}\boldsymbol{v}}{\int_{\boldsymbol{r},\boldsymbol{v}} f(\boldsymbol{r},\boldsymbol{v},t)\mathrm{d}\boldsymbol{r}\mathrm{d}\boldsymbol{v}} \tag{A.1}$$

$$W_{\mathrm{v}}(t) \equiv \bar{v}_x(t) = \frac{\int_{\boldsymbol{r},\boldsymbol{v}} v_x f(\boldsymbol{r},\boldsymbol{v},t)\mathrm{d}\boldsymbol{r}\mathrm{d}\boldsymbol{v}}{\int_{\boldsymbol{r},\boldsymbol{v}} f(\boldsymbol{r},\boldsymbol{v},t)\mathrm{d}\boldsymbol{r}\mathrm{d}\boldsymbol{v}} \tag{A.2}$$

where $G(t)$ represents the centroid of the electron swarm, and $\bar{v}_x$ is the average velocity of the electrons in the electron swarm.

The definition of W_{r} is transformed using the following relation for the differential of the quotient of functions:

$$\left(\frac{v}{u}\right)' = \frac{uv' - u'v}{u^2} = \frac{v'}{u} - \frac{v}{u}\cdot\frac{u'}{u} \tag{A.3}$$

$$W_{\mathrm{r}}(t) = \frac{\frac{\mathrm{d}}{\mathrm{d}t}\int_{\boldsymbol{r},\boldsymbol{v}} x f(\boldsymbol{r},\boldsymbol{v},t)\mathrm{d}\boldsymbol{r}\mathrm{d}\boldsymbol{v}}{\int_{\boldsymbol{r},\boldsymbol{v}} f(\boldsymbol{r},\boldsymbol{v},t)\mathrm{d}\boldsymbol{r}\mathrm{d}\boldsymbol{v}}$$

$$- \frac{\int_{\boldsymbol{r},\boldsymbol{v}} x f(\boldsymbol{r},\boldsymbol{v},t)\mathrm{d}\boldsymbol{r}\mathrm{d}\boldsymbol{v}}{\int_{\boldsymbol{r},\boldsymbol{v}} f(\boldsymbol{r},\boldsymbol{v},t)\mathrm{d}\boldsymbol{r}\mathrm{d}\boldsymbol{v}} \cdot \frac{\frac{\mathrm{d}}{\mathrm{d}t}\int_{\boldsymbol{r},\boldsymbol{v}} f(\boldsymbol{r},\boldsymbol{v},t)\mathrm{d}\boldsymbol{r}\mathrm{d}\boldsymbol{v}}{\int_{\boldsymbol{r},\boldsymbol{v}} f(\boldsymbol{r},\boldsymbol{v},t)\mathrm{d}\boldsymbol{r}\mathrm{d}\boldsymbol{v}} \tag{A.4}$$

$$= \frac{\int_{\boldsymbol{r},\boldsymbol{v}} x\frac{\partial}{\partial t} f(\boldsymbol{r},\boldsymbol{v},t)\mathrm{d}\boldsymbol{r}\mathrm{d}\boldsymbol{v}}{\int_{\boldsymbol{r},\boldsymbol{v}} f(\boldsymbol{r},\boldsymbol{v},t)\mathrm{d}\boldsymbol{r}\mathrm{d}\boldsymbol{v}} - \frac{G(t)\cdot\int_{\boldsymbol{r},\boldsymbol{v}} \frac{\partial}{\partial t} f(\boldsymbol{r},\boldsymbol{v},t)\mathrm{d}\boldsymbol{r}\mathrm{d}\boldsymbol{v}}{\int_{\boldsymbol{r},\boldsymbol{v}} f(\boldsymbol{r},\boldsymbol{v},t)\mathrm{d}\boldsymbol{r}\mathrm{d}\boldsymbol{v}}. \tag{A.5}$$

The temporal differential terms in both of the first and second terms in equation (A.5) are replaced by the drift and collision terms in the Boltzmann equation:

$$\frac{\partial}{\partial t}f(\boldsymbol{r},\boldsymbol{v},t) = \left\{-\boldsymbol{v}\cdot\frac{\partial}{\partial \boldsymbol{r}} - \boldsymbol{a}\cdot\frac{\partial}{\partial \boldsymbol{v}} + \left(\frac{\partial}{\partial t}\right)_{\text{coll}}\right\} f(\boldsymbol{r},\boldsymbol{v},t) \tag{A.6}$$

$$\boldsymbol{v}\cdot\frac{\partial}{\partial \boldsymbol{r}} = v_x\frac{\partial}{\partial x} + v_y\frac{\partial}{\partial y} + v_z\frac{\partial}{\partial z} \tag{A.7}$$

$$\boldsymbol{a}\cdot\frac{\partial}{\partial \boldsymbol{v}} = a_x\frac{\partial}{\partial v_x} + a_y\frac{\partial}{\partial v_y} + a_z\frac{\partial}{\partial v_z} \tag{A.8}$$

where the acceleration $\boldsymbol{a}$ due to $\boldsymbol{E}$ is assumed as follows in the present model:

$$\boldsymbol{a} = (a_x, a_y, a_z) = (eE/m, 0, 0) \tag{A.9}$$

where e and m are the charge and mass of an electron.

The numerator of the first term in equation (A.5) can be transformed as

$$\begin{aligned}
&\int_{\boldsymbol{r},\boldsymbol{v}} x\frac{\partial}{\partial t}f(\boldsymbol{r},\boldsymbol{v},t)\mathrm{d}\boldsymbol{r}\mathrm{d}\boldsymbol{v} \\
&= \int_{\boldsymbol{r},\boldsymbol{v}} x\left\{\left(\frac{\partial}{\partial t}\right)_{\text{coll}} - \boldsymbol{v}\cdot\frac{\partial}{\partial \boldsymbol{r}} - \boldsymbol{a}\cdot\frac{\partial}{\partial \boldsymbol{v}}\right\} f(\boldsymbol{r},\boldsymbol{v},t)\mathrm{d}\boldsymbol{r}\mathrm{d}\boldsymbol{v} && \text{(A.10)} \\
&= \int_{\boldsymbol{r},\boldsymbol{v}} x\left\{\left(\frac{\partial}{\partial t}\right)_{\text{coll}} - v_x\frac{\partial}{\partial x}\right\} f(\boldsymbol{r},\boldsymbol{v},t)\mathrm{d}\boldsymbol{r}\mathrm{d}\boldsymbol{v} && \text{(A.11)} \\
&= \int_{\boldsymbol{r},\boldsymbol{v}} x\left(\frac{\partial}{\partial t}\right)_{\text{coll}} f(\boldsymbol{r},\boldsymbol{v},t)\mathrm{d}\boldsymbol{r}\mathrm{d}\boldsymbol{v} - \int_{\boldsymbol{r},\boldsymbol{v}} v_x x\frac{\partial}{\partial x}f(\boldsymbol{r},\boldsymbol{v},t)\mathrm{d}\boldsymbol{r}\mathrm{d}\boldsymbol{v} && \text{(A.12)} \\
&= \int_{\boldsymbol{r},\boldsymbol{v}} x\left(\frac{\partial}{\partial t}\right)_{\text{coll}} f(\boldsymbol{r},\boldsymbol{v},t)\mathrm{d}\boldsymbol{r}\mathrm{d}\boldsymbol{v} \\
&\quad - \int_{y,z,\boldsymbol{v}} v_x\left\{\int_{-\infty}^{\infty} x\frac{\partial}{\partial x}f(\boldsymbol{r},\boldsymbol{v},t)\mathrm{d}x\right\}\mathrm{d}y\mathrm{d}z\mathrm{d}\boldsymbol{v} && \text{(A.13)} \\
&= \int_{\boldsymbol{r},\boldsymbol{v}} x\left(\frac{\partial}{\partial t}\right)_{\text{coll}} f(\boldsymbol{r},\boldsymbol{v},t)\mathrm{d}\boldsymbol{r}\mathrm{d}\boldsymbol{v} \\
&\quad - \int_{y,z,\boldsymbol{v}} v_x\left\{[xf(\boldsymbol{r},\boldsymbol{v},t)]_{-\infty}^{\infty} - \int_{-\infty}^{\infty} f(\boldsymbol{r},\boldsymbol{v},t)\mathrm{d}x\right\}\mathrm{d}y\mathrm{d}z\mathrm{d}\boldsymbol{v} && \text{(A.14)} \\
&= \int_{\boldsymbol{r},\boldsymbol{v}} x\left(\frac{\partial}{\partial t}\right)_{\text{coll}} f(\boldsymbol{r},\boldsymbol{v},t)\mathrm{d}\boldsymbol{r}\mathrm{d}\boldsymbol{v} + \int_{\boldsymbol{r},\boldsymbol{v}} v_x f(\boldsymbol{r},\boldsymbol{v},t)\mathrm{d}\boldsymbol{r}\mathrm{d}\boldsymbol{v}. && \text{(A.15)}
\end{aligned}$$

Here, physical aspects $f(\boldsymbol{r},\boldsymbol{v},t) = 0$ at $|\boldsymbol{v}| = \infty$ and at $|\boldsymbol{r}| = \infty$ have been referred to as boundary conditions for the above integrals, therefore

$$\int_{y=-\infty}^{\infty}\frac{\partial}{\partial y}f(\boldsymbol{r},\boldsymbol{v},t)\mathrm{d}y = [f(\boldsymbol{r},\boldsymbol{v},t)]_{y=-\infty}^{\infty} = 0 \tag{A.16}$$

$$\int_{z=-\infty}^{\infty}\frac{\partial}{\partial z}f(\boldsymbol{r},\boldsymbol{v},t)\mathrm{d}z = [f(\boldsymbol{r},\boldsymbol{v},t)]_{z=-\infty}^{\infty} = 0 \tag{A.17}$$

$$\int_{v_x=-\infty}^{\infty}\frac{\partial}{\partial v_x}f(\boldsymbol{r},\boldsymbol{v},t)\mathrm{d}v_x = [f(\boldsymbol{r},\boldsymbol{v},t)]_{v_x=-\infty}^{\infty} = 0. \tag{A.18}$$

The numerator of the second term in equation (A.5) is transformed in a similar way as

$$G(t)\cdot\int_{\boldsymbol{r},\boldsymbol{v}}\frac{\partial}{\partial t}f(\boldsymbol{r},\boldsymbol{v},t)\mathrm{d}\boldsymbol{r}\mathrm{d}\boldsymbol{v}$$

$$= \int_{\boldsymbol{r},\boldsymbol{v}} G(t) \left\{ \left(\frac{\partial}{\partial t} \right)_{\text{coll}} - \boldsymbol{v} \cdot \frac{\partial}{\partial \boldsymbol{r}} - \boldsymbol{a} \cdot \frac{\partial}{\partial \boldsymbol{v}} \right\} f(\boldsymbol{r}, \boldsymbol{v}, t) \mathrm{d}\boldsymbol{r}\mathrm{d}\boldsymbol{v} \tag{A.19}$$

$$= \int_{\boldsymbol{r},\boldsymbol{v}} G(t) \left(\frac{\partial}{\partial t} \right)_{\text{coll}} f(\boldsymbol{r}, \boldsymbol{v}, t) \mathrm{d}\boldsymbol{r}\mathrm{d}\boldsymbol{v}. \tag{A.20}$$

Using equations (A.15) and (A.20), equation (A.5) becomes as

$$W_{\mathrm{r}}(t) = \frac{\int_{\boldsymbol{r},\boldsymbol{v}} v_x f(\boldsymbol{r}, \boldsymbol{v}, t) \mathrm{d}\boldsymbol{r}\mathrm{d}\boldsymbol{v}}{\int_{\boldsymbol{r},\boldsymbol{v}} f(\boldsymbol{r}, \boldsymbol{v}, t) \mathrm{d}\boldsymbol{r}\mathrm{d}\boldsymbol{v}} + \frac{\int_{\boldsymbol{r},\boldsymbol{v}} \{x - G(t)\} \left(\frac{\partial}{\partial t} \right)_{\text{coll}} f(\boldsymbol{r}, \boldsymbol{v}, t) \mathrm{d}\boldsymbol{r}\mathrm{d}\boldsymbol{v}}{\int_{\boldsymbol{r},\boldsymbol{v}} f(\boldsymbol{r}, \boldsymbol{v}, t) \mathrm{d}\boldsymbol{r}\mathrm{d}\boldsymbol{v}} \tag{A.21}$$

$$= W_{\mathrm{v}}(t) + \int_{-\infty}^{\infty} \{x - G(t)\} \frac{\bar{R}_{\text{ion}}(x, t) n(x, t)}{n(t)} \mathrm{d}x \tag{A.22}$$

$$= W_{\mathrm{v}}(t) + \int_{-\infty}^{\infty} \{x - G(t)\} \bar{R}_{\text{ion}}(x, t) p(x, t) \mathrm{d}x \tag{A.23}$$

where $\bar{R}_{\text{ion}}(x, t)$ is the position-dependent effective ionization frequency, and $p(x, t)$ is the normalized electron distribution. $p(x, t)$ is represented by the electron distribution $n(x, t)$ and its total $n(t)$ as

$$n(t) = \int_{-\infty}^{\infty} n(x, t) \mathrm{d}x \tag{A.24}$$

$$p(x, t) = \frac{n(x, t)}{n(t)}. \tag{A.25}$$

A.2 Relation Described in Velocity Space

Another definition of W_{r} using the first order moment M_x is

$$W_{\mathrm{r}}(t) = \frac{\mathrm{d}}{\mathrm{d}t} G(t) = \frac{\mathrm{d}}{\mathrm{d}t} \frac{M_x(t)}{n(t)}. \tag{A.26}$$

Using the same relation as equation (A.3), the following equations are derived:

$$W_{\mathrm{r}}(t) = \frac{\frac{\mathrm{d}}{\mathrm{d}t} M_x(t)}{n(t)} - \frac{M_x(t)}{n(t)} \frac{\frac{\mathrm{d}}{\mathrm{d}t} n(t)}{n(t)} \tag{A.27}$$

$$= \frac{\frac{\mathrm{d}}{\mathrm{d}t} M_x(t)}{n(t)} - G(t) \frac{\frac{\mathrm{d}}{\mathrm{d}t} n(t)}{n(t)}. \tag{A.28}$$

The temporal variation terms of $\frac{\mathrm{d}}{\mathrm{d}t} n(t)$ and $\frac{\mathrm{d}}{\mathrm{d}t} M_x(t)$ are described by the moment equations below:

$$\frac{\mathrm{d}}{\mathrm{d}t} n(t) = \int_{\boldsymbol{v}} \bar{R}_{\text{ion}}(\boldsymbol{v}) f(\boldsymbol{v}, t) \mathrm{d}\boldsymbol{v} \tag{A.29}$$

$$\frac{\mathrm{d}}{\mathrm{d}t} M_x(t) = \int_{\boldsymbol{v}} v_x f(\boldsymbol{v}, t) \mathrm{d}\boldsymbol{v} + \int_{\boldsymbol{v}} \bar{R}_{\text{ion}}(\boldsymbol{v}) M_x(\boldsymbol{v}, t) \mathrm{d}\boldsymbol{v}. \tag{A.30}$$

Substituting these equations into $\frac{\mathrm{d}}{\mathrm{d}t} n(t)$ and $\frac{\mathrm{d}}{\mathrm{d}t} M_x(t)$, equation (A.28) becomes as

$$W_{\mathrm{r}}(t) = \frac{\int_{\boldsymbol{v}} v_x f(\boldsymbol{v}, t) \mathrm{d}\boldsymbol{v}}{n(t)} + \frac{\int_{\boldsymbol{v}} \bar{R}_{\text{ion}}(\boldsymbol{v}) M_x(\boldsymbol{v}, t) \mathrm{d}\boldsymbol{v}}{n(t)} - \frac{G(t) \int_{\boldsymbol{v}} \bar{R}_{\text{ion}}(\boldsymbol{v}) f(\boldsymbol{v}, t) \mathrm{d}\boldsymbol{v}}{n(t)} \tag{A.31}$$

$$= W_{\mathrm{v}}(t) + \int_{\boldsymbol{v}} \bar{R}_{\text{ion}}(\boldsymbol{v}) \frac{f(\boldsymbol{v}, t)}{n(t)} \left\{ \frac{M_x(\boldsymbol{v}, t)}{f(\boldsymbol{v}, t)} - G(t) \right\} \mathrm{d}\boldsymbol{v}. \tag{A.32}$$

A factor $M_x(\boldsymbol{v},t)/f(\boldsymbol{v},t)-G(t)$ in the above equation can be defined as the centroid $g(\boldsymbol{v},t)$ of an electron swarm subset consisting of the electrons with velocity $\boldsymbol{v}$, where $g(\boldsymbol{v},t)$ is relative to the centroid $G(t)$ of the whole electron swarm:

$$g(\boldsymbol{v},t) = \frac{M_x(\boldsymbol{v},t)}{f(\boldsymbol{v},t)} - G(t). \tag{A.33}$$

Another factor $f(\boldsymbol{v},t)/n(t)$ represents the normalized electron velocity distribution, which is denoted as $f_{\rm n}(\boldsymbol{v},t)$ here:

$$f_{\rm n}(\boldsymbol{v},t) = \frac{f(\boldsymbol{v},t)}{n(t)}. \tag{A.34}$$

When the normalized first order moment distribution $M(\boldsymbol{v},t)$ relative to $G(t)$ is defined as well to satisfy

$$g(\boldsymbol{v},t) = \frac{M(\boldsymbol{v},t)}{f_{\rm n}(\boldsymbol{v},t)} \tag{A.35}$$

equation (A.32) becomes as

$$W_{\rm r}(t) = W_{\rm v}(t) + \int_{\boldsymbol{v}} \bar{R}_{\rm ion}(\boldsymbol{v}) M(\boldsymbol{v},t) {\rm d}\boldsymbol{v} = W_{\rm v}(t) + \int_{\epsilon=0}^{\infty} \bar{R}_{\rm ion}(\epsilon) M(\epsilon,t) {\rm d}\epsilon. \tag{A.36}$$

Appendix B

FORTRAN 77 Programs of Propagator Method

B.1 Spatial Relaxation Processes in He

```
* ========================================================================
*  "Propagator Method" for Steady-State Townsend conditions
*                      derived from time-of-flight observation
*
*  Hirotake Sugawara 1991.03.02.-1993.12.23.
*  Applied Electricity Laboratory,
*  Dept.of Electrical Eng., Hokkaido Univ., N13 W8 Sapporo 060 Japan
*  TEL 011-706-6482, FAX 011-706-7890, sgwr@e5.hines.hokudai.ac.jp
* ========================================================================
* ---------- initial setting ---------------------------------------------
      PARAMETER ( EBYP=100.0       , GPRS=1.0          , EFLD=EBYP*GPRS   ,
     >            XLEN=2.0         , NXXX=500          , NXDV=5           ,
     >            DXXX=XLEN/(NXXX*1.0)                 , DTIM=0.0030E-09  ,
     >            EMAX=160.0       , DENG=EFLD*DXXX    ,
     >            NENG=EMAX/DENG+0.5                   ,
     >            NANG=18          , NAHF=NANG/2       ,
     >            EEXM=19.800      , KEXM=EEXM/DENG+0.5                   ,
     >            EEXC=20.960      , KEXC=EEXC/DENG+0.5                   ,
     >            EION=24.588      , KION=EION/DENG+0.5                   ,
     >            NSUP=NENG+KION+1                     ,
     >            ECHG=1.602E-19   , EMAS=9.109E-28    )
      REAL FXV0(-1:NXXX,-1:NENG,0:NANG),FXE0(0:NXXX-1,0:NSUP),
     >     FXV1(-1:NXXX,-1:NENG,0:NANG),FXE1(0:NXXX-1,0:NSUP),
     >     FXV2(-1:NXXX,-1:NENG,0:NANG),FXE2(0:NXXX-1,0:NSUP),
     >     RDR0(-1:NENG,0:NANG),
     >     RDR1(-1:NENG,0:NANG),
     >     RDR2(-1:NENG,0:NANG)
      REAL BENG(0:NSUP),CENG(0:NSUP),
     >     BVLC(0:NSUP),CVLC(0:NSUP),
     >     BANG(0:NANG),CANG(0:NANG),
     >     BSIN(0:NANG),
     >     BCOS(0:NANG),CCOS(0:NANG)
      REAL FISM(0:NSUP),RSCT(0:NANG),
     >     QMOM(0:NSUP),FMOM(0:NSUP),
     >     QEXC(0:NSUP),FEXC(0:NSUP),
     >     QEXM(0:NSUP),FEXM(0:NSUP),
     >     QION(0:NSUP),FION(0:NSUP),GION(0:NSUP),
     >     QTTL(0:NSUP),FNUL(0:NSUP)
      REAL XNEL(0:NXXX-1),XENG(0:NXXX-1),XVDS(0:NXXX-1),
     >     XMOM(0:NXXX-1),XION(0:NXXX-1),
     >     XEXC(0:NXXX-1),XEXM(0:NXXX-1),
     >     XFE0(0:NXXX-1,0:NENG),
     >     XFE1(0:NXXX-1,0:NENG)
      PI00=ATAN(1.0)*4.0
      FCEV=2.00*ECHG/EMAS*1.0E+07
      FCVE=0.50*EMAS/ECHG*1.0E-07
      DACC=ECHG*EFLD/EMAS*1.0E+07  *DTIM
      DANG=PI00/REAL(NANG)
```

Constants and Variables

EBYP	E/p ($\mathrm{Vcm^{-1}Torr^{-1}}$)
GPRS	the gas pressure p (Torr)
EFLD	the electric field E ($\mathrm{Vcm^{-1}}$)
XLEN	the gap length d (cm) between parallel plane electrodes
NXXX	the number of divisions for x
DXXX	the cell width Δx (cm)
DTIM	the time step Δt (s)
EMAX	ϵ_{max} (eV)
DENG	the cell width $\Delta\epsilon$ (eV)
NENG	the number of division for ϵ
NANG	the number of division for θ
EEXC	ϵ_{ex} (eV)
EEXM	$\epsilon_{ex,meta}$ (eV)
EION	ϵ_{ion} (eV)
KEXC	$\epsilon_{ex}/\Delta\epsilon$
KEXM	$\epsilon_{ex,meta}/\Delta\epsilon$
KION	$\epsilon_{ion}/\Delta\epsilon$
NSUP	the number of divisions for ϵ with margin
ECHG	$e = 1.602 \times 10^{-19}$ C
EMAS	$m = 9.109 \times 10^{-28}$ g
PI00	$\pi = 3.14159265\cdots$
DANG	the cell width $\Delta\theta$ (rad)
FCEV	$v_1 = 5.79 \times 10^7$ $\mathrm{cms^{-1}}$
FCVE	$1/v_1$
DACC	the acceleration $a\Delta t$ ($\mathrm{cms^{-1}}$)

```
* ---------- arrays of collisions & scattering -------------------------
      DO 0010 IENG=0,NENG
        BENG(IENG)=DENG*REAL(IENG)
        BVLC(IENG)=SQRT(BENG(IENG)*FCEV)
 0010 CONTINUE
      DO 0020 IENG=0,NENG-1
        CVLC(IENG)=(BVLC(IENG)+BVLC(IENG+1))*0.5
        CENG(IENG)=CVLC(IENG)**2*FCVE
 0020 CONTINUE
      QDMY=SHEMOM(0.0)+SHEEXM(0.0)+SHEEXC(0.0)+SHEION(0.0)+QDMY
      DO 0030 IENG=0,NENG-1
        QMOM(IENG)=QHEMOM(CENG(IENG))*GPRS
        QEXC(IENG)=QHEEXC(CENG(IENG))*GPRS
        QEXM(IENG)=QHEEXM(CENG(IENG))*GPRS
        QION(IENG)=QHEION(CENG(IENG))*GPRS
 0030 CONTINUE
      DO 0040 IENG=0,NENG-1
        QTTL(IENG)=QMOM(IENG)+QEXC(IENG)+QEXM(IENG)+QION(IENG)
        FNUL(IENG)=EXP(-QTTL(IENG)*CVLC(IENG)*DTIM)
        FCOL      =(1.0-FNUL(IENG))/QTTL(IENG)
        FMOM(IENG)=FCOL*QMOM(IENG)
        FEXC(IENG)=FCOL*QEXC(IENG)
        FEXM(IENG)=FCOL*QEXM(IENG)
        FION(IENG)=FCOL*QION(IENG)
        GION(IENG)=FION(IENG)/REAL(DIM(IENG,KION)*2+1)*2.0
 0040 CONTINUE
      DO 0050 IANG=0,NANG
        BANG(IANG)=DANG*REAL(IANG)
        BSIN(IANG)=SIN(BANG(IANG))
        BCOS(IANG)=COS(BANG(IANG))
        CANG(IANG)=DANG*(REAL(IANG)+0.5)
        CCOS(IANG)=COS(CANG(IANG))
 0050 CONTINUE
      DO 0060 IANG=0,NANG-1
        RSCT(IANG)=(BCOS(IANG)-BCOS(IANG+1))*0.5
 0060 CONTINUE
* ---------- arrays of drift -------------------------------------------
      PI23=PI00*2.0/3.0
      DO 0070 IANG=0,NAHF-1
      DO 0070 IENG=0,NENG-1
        RCEL           =PI23 *(BVLC(IENG+1)**3-BVLC(IENG)**3)
     >                       *(BCOS(IANG)-BCOS(IANG+1))
        RDR1(IENG,IANG)=PI00 *(BVLC(IENG+1)**2-BVLC(IENG)**2)
     >                       *BSIN(IANG)**2                    *DACC/RCEL
        RDR2(IENG,IANG)=PI00 *BVLC(IENG+1)**2
     >                       *(BSIN(IANG+1)**2-BSIN(IANG)**2) *DACC/RCEL
        RDR0(IENG,IANG)=1.0-RDR1(IENG,IANG)-RDR2(IENG,IANG)
 0070 CONTINUE
      DO 0080 IANG=NAHF,NANG-1
      DO 0080 IENG=   0,NENG-1
        RCEL           =PI23 *(BVLC(IENG+1)**3-BVLC(IENG)**3)
     >                       *(BCOS(IANG)-BCOS(IANG+1))
        RDR1(IENG,IANG)=PI00 *(BVLC(IENG+1)**2-BVLC(IENG)**2)
     >                       *BSIN(IANG)**2                    *DACC/RCEL
        RDR2(IENG,IANG)=PI00 *BVLC(IENG)**2
     >                       *(BSIN(IANG)**2-BSIN(IANG+1)**2) *DACC/RCEL
        RDR0(IENG,IANG)=1.0-RDR1(IENG,IANG)-RDR2(IENG,IANG)
 0080 CONTINUE
      DO 0090 IANG=0,NANG-1
      DO 0090 IENG=0,NENG-1
        IF (RDR0(IENG,IANG) .LE. 0.0) THEN
          WRITE(6,*) 'rate negative : cell No. (E,A) ',IENG,IANG
          WRITE(6,*) RDR0(IENG,IANG),RDR1(IENG,IANG),RDR2(IENG,IANG)
          STOP
        END IF
 0090 CONTINUE
* ---------- initial condition -----------------------------------------
      ENEL=40000.0
      ETRM=ENEL*1.0E-03
      FXV0(0,0,0)=ENEL
* ---------- collision & scattering ------------------------------------
 0100 CONTINUE
      DO 0110 IENG=0,NENG-1
      DO 0110 IXXX=0,NXXX-1
        FXE0(IXXX,IENG)=0.0
 0110 CONTINUE
      DO 0120 IANG=0,NANG-1
      DO 0120 IENG=0,NENG-1
      DO 0120 IXXX=0,NXXX-1
        FXE0(IXXX,IENG)=FXE0(IXXX,IENG)+FXV0(IXXX,IENG,IANG)
 0120 CONTINUE
```

Constants and Variables

IENG	subscript i of ϵ_i and v_i
BENG	$\epsilon_i = i\Delta\epsilon$ (eV)
BVLC	$v_i = \sqrt{2\epsilon_i/m}$ (cms^{-1})
CVLC	$\bar{v}_i$ (cms^{-1})
CENG	$\bar{\epsilon}_i$ (eV)
QDMY	a dummy variable for initialization of function subprograms
QMOM	$Nq_{\rm mom}(\epsilon)$ (cm^{-1})
QEXC	$Nq_{\rm ex}(\epsilon)$ (cm^{-1})
QEXM	$Nq_{\rm ex,meta}(\epsilon)$ (cm^{-1})
QION	$Nq_{\rm ion}(\epsilon)$ (cm^{-1})
QTTL	$Nq_{\rm T}(\epsilon)$ (cm^{-1})
FNUL	the probability of no collision
FMOM,FEXM,FEXC,FION	the ratios of colliding electrons
GION	the distribution ratio of electrons after ionization
IANG	subscript j of θ_j
BANG	$\theta_j = j\Delta\theta$ (rad)
BSIN	$\sin\theta_j$
BCOS	$\cos\theta_j$
CANG	$\bar{\theta}_j$ (rad)
CCOS	$\cos\bar{\theta}_j$
RSCT	the scattering ratio $(1/2)\sin\theta\Delta\theta$
RCEL	the volume of a cell (cms^{-1})^3
RDR0	the ratio of electrons remaining in $C_{l,i,j}$
RDR1	the ratio of electrons flowing out of $C_{l,i,j}$ to $C_{l,i,j+1}$
RDR2	the ratio of electrons flowing out of $C_{l,i,j}$ to $C_{l\pm1,i\pm1,j}$
ENEL	the number of initial electrons
ETRM	termination factor
IXXX	subscript l of x_l
FXV0	$F(x,\epsilon,\theta)$ before collision
FXE0	$F(x,\epsilon)$ before collision

```
      DO 0130 IXXX=0,NXXX-1
      FISM(NENG)=0.0
      DO 0130 IENG=NENG-1,0,-1
        FISM(IENG)     =FISM(IENG+1)
     >                 +FXE0(IXXX,IENG+KION  )*GION(IENG+KION  )
     >                 +FXE0(IXXX,IENG+KION+1)*GION(IENG+KION+1)
        FXE1(IXXX,IENG)=FXE0(IXXX,IENG       )*FMOM(IENG       )
     >                 +FXE0(IXXX,IENG+KEXM  )*FEXM(IENG+KEXM  )
     >                 +FXE0(IXXX,IENG+KEXC  )*FEXC(IENG+KEXC  )
     >                 +FISM(IENG)
 0130 CONTINUE
      DO 0140 IANG=0,NANG-1
      DO 0140 IENG=0,NENG-1
      DO 0140 IXXX=0,NXXX-1
        FXV1(IXXX,IENG,IANG)=FXV0(IXXX,IENG,IANG)*FNUL(IENG)
     >                      +FXE1(IXXX,IENG)*RSCT(IANG)
 0140 CONTINUE
* ---------- drift ------------------------------------------------------
      DO 0150 IANG=0,NAHF-1
      DO 0150 IENG=0,NENG-1
      DO 0150 IXXX=0,NXXX-1
        FXV0(IXXX,IENG,IANG)
     >    =FXV1(IXXX  ,IENG  ,IANG  )*RDR0(IENG  ,IANG  )
     >    +FXV1(IXXX  ,IENG  ,IANG+1)*RDR1(IENG  ,IANG+1)
     >    +FXV1(IXXX-1,IENG-1,IANG  )*RDR2(IENG-1,IANG  )
 0150 CONTINUE
      DO 0160 IANG=NAHF,NANG-1
      DO 0160 IENG=   0,NENG-1
      DO 0160 IXXX=   0,NXXX-1
        FXV0(IXXX,IENG,IANG)
     >    =FXV1(IXXX  ,IENG  ,IANG  )*RDR0(IENG  ,IANG  )
     >    +FXV1(IXXX  ,IENG  ,IANG+1)*RDR1(IENG  ,IANG+1)
     >    +FXV1(IXXX+1,IENG+1,IANG  )*RDR2(IENG+1,IANG  )
 0160 CONTINUE
* ---------- integration with respect to time ---------------------------
      DO 0170 IENG=0,NENG-1
      DO 0170 IXXX=0,NXXX-1
        FXE2(IXXX,IENG)=FXE2(IXXX,IENG)+FXE0(IXXX,IENG)
 0170 CONTINUE
      SPNE=0.0
      DO 0180 IANG=0,NANG-1
      DO 0180 IENG=0,NENG-1
      DO 0180 IXXX=0,NXXX-1
        FXV2(IXXX,IENG,IANG)=FXV2(IXXX,IENG,IANG)
     >                      +FXV0(IXXX,IENG,IANG)
     >                      +FXV1(IXXX,IENG,IANG)
        SPNE=SPNE+FXV0(IXXX,IENG,IANG)
 0180 CONTINUE
      KLOP=KLOP+1
      IF (SPNE .GT. ETRM) GOTO 0100
* ---------- SST parameters (collision frequency) ----------------------
      DO 0190 IXDV=0,NXXX-NXDV,NXDV
      DO 0190 IXXX=IXDV+1,IXDV+NXDV-1
      DO 0190 IENG=0,NENG-1
        FXE2(IXDV,IENG)=FXE2(IXDV,IENG)+FXE2(IXXX,IENG)
 0190 CONTINUE
      DO 0200 IXDV=0,NXXX-NXDV,NXDV
      DO 0200 IENG=0,NENG-1
        XION(IXDV)=XION(IXDV)+FXE2(IXDV,IENG)*FION(IENG)
        XEXC(IXDV)=XEXC(IXDV)+FXE2(IXDV,IENG)*FEXC(IENG)
        XEXM(IXDV)=XEXM(IXDV)+FXE2(IXDV,IENG)*FEXM(IENG)
        XMOM(IXDV)=XMOM(IXDV)+FXE2(IXDV,IENG)*FMOM(IENG)
 0200 CONTINUE
* ---------- SST parameters ---------------------------------------------
      DO 0210 IXDV=0,NXXX-NXDV,NXDV
      DO 0210 IXXX=IXDV+1,IXDV+NXDV-1
      DO 0210 IANG=0,NANG-1
      DO 0210 IENG=0,NENG-1
        FXV2(IXDV,IENG,IANG)=FXV2(IXDV,IENG,IANG)+FXV2(IXXX,IENG,IANG)
 0210 CONTINUE
      DO 0220 IANG=0,NANG-1
      DO 0220 IXDV=0,NXXX-NXDV,NXDV
      DO 0220 IENG=0,NENG-1
        FXV2(IXDV,IENG,IANG)=FXV2(IXDV,IENG,IANG)*0.5
 0220 CONTINUE
      DO 0230 IANG=0,NANG-1
      DO 0230 IXDV=0,NXXX-NXDV,NXDV
      DO 0230 IENG=0,NENG-1
        XFE0(IXDV,IENG)=XFE0(IXDV,IENG)+FXV2(IXDV,IENG,IANG)
        XFE1(IXDV,IENG)=XFE1(IXDV,IENG)+FXV2(IXDV,IENG,IANG)*CCOS(IANG)
 0230 CONTINUE
      DO 0240 IXDV=0,NXXX-NXDV,NXDV
      DO 0240 IENG=0,NENG-1
        XNEL(IXDV)=XNEL(IXDV)+XFE0(IXDV,IENG)
        XENG(IXDV)=XENG(IXDV)+XFE0(IXDV,IENG)*CENG(IENG)
        XVDS(IXDV)=XVDS(IXDV)+XFE1(IXDV,IENG)*CVLC(IENG)
 0240 CONTINUE
```

Constants and Variables

FISM	the number of electrons after ionization
FXV1	$F(x,\epsilon,\theta)$ after collision
FXE1	$F(x,\epsilon)$ after collision
FXE2	$F_{\mathrm{SST}}(x,\epsilon)$
FXV2	$F_{\mathrm{SST}}(x,\epsilon,\theta)$
SPNE	the number of remaining electrons
XMOM	$R_{\mathrm{mom}}(x)$ (s^{-1})
XEXM	$R_{\mathrm{ex}}(x)$ (s^{-1})
XEXC	$R_{\mathrm{ex,meta}}(x)$ (s^{-1})
XION	$R_{\mathrm{ion}}(x)$ (s^{-1})
XFE0	$F_{0,\mathrm{SST}}(x,\epsilon)$
XFE1	$F_{1,\mathrm{SST}}(x,\epsilon)$
XNEL	$n(x)$
XENG	$\bar{\epsilon}(x)$ (eV)
XVDS	$v_{\mathrm{d}}(x)$ (cms^{-1})

```
* ---------- output -------------------------------------------------
      WRITE(40,'(I5,X,I5                                  )') 14,NXXX/NXDV
      WRITE(40,'(''position (cm)''                        )')
      WRITE(40,'(''total electron energy (eV)''           )')
      WRITE(40,'(''number of electrons (pass)'',I10       )') KLOP
      WRITE(40,'(''number of electrons (a.u.)''           )')
      WRITE(40,'(''mean energy (eV)''                     )')
      WRITE(40,'(''drift velocity V_d (cm/~ms)''          )')
      WRITE(40,'(''ionization coefficient (cm^-^1)''      )')
      WRITE(40,'(''collision count (ion)''                )')
      WRITE(40,'(''collision frequency (ion) (~ms^-^1)'')')
      WRITE(40,'(''collision count (exc)''                )')
      WRITE(40,'(''collision frequency (exc) (~ms^-^1)'')')
      WRITE(40,'(''collision count (exm)''                )')
      WRITE(40,'(''collision frequency (exm) (~ms^-^1)'')')
      WRITE(40,'(''collision count (mom)''                )')
      WRITE(40,'(''collision frequency (mom) (~ms^-^1)'')')
      DO 0250 IXDV=0,NXXX-NXDV,NXDV
        WRITE(40,'(F9.5,7(X,E9.4))')
     >       (IXDV+0.5*NXDV)*DXXX ,
     >       XENG(IXDV) , ENEL , XNEL(IXDV) ,
     >       XENG(IXDV)/XNEL(IXDV) ,
     >       XVDS(IXDV)/XNEL(IXDV)*1.0E-06 ,
     >       LOG(1.0+XION(IXDV)/ENEL)/(DXXX*NXDV)
        WRITE(40,'(E9.4,7(X,E9.4))')
     >       XION(IXDV) , XION(IXDV)/(XNEL(IXDV)*DTIM)*1.0E-06 ,
     >       XEXC(IXDV) , XEXC(IXDV)/(XNEL(IXDV)*DTIM)*1.0E-06 ,
     >       XEXM(IXDV) , XEXM(IXDV)/(XNEL(IXDV)*DTIM)*1.0E-06 ,
     >       XMOM(IXDV) , XMOM(IXDV)/(XNEL(IXDV)*DTIM)*1.0E-06
        ENEL=ENEL+XION(IXDV)
 0250 CONTINUE
      WRITE(41,'(I5,X,I5)') NXXX/NXDV,NENG+1
      WRITE(41,'(''electron energy (eV)''                 )')
      WRITE(41,'(''energy distribution (x='',F12.6,'')'')')
     >     ( (IXDV+0.5*NXDV)*DXXX , IXDV=0,NXXX-NXDV,NXDV )
      WRITE(41,'(F12.6)') 0.0
      WRITE(41,'(5(E12.6,X))') ( 0.0 , IXDV=0,NXXX-NXDV,NXDV )
      WRITE(42,'(I5,X,I5)') NXXX/NXDV,NENG+1
      WRITE(42,'(''electron energy (eV)''                   )')
      WRITE(42,'(''energy distribution F_1 (x='',F12.6,'')'')')
     >     ( (IXDV+0.5*NXDV)*DXXX , IXDV=0,NXXX-NXDV,NXDV )
      WRITE(42,'(F12.6)') 0.0
      WRITE(42,'(5(E12.6,X))') ( 0.0 , IXDV=0,NXXX-NXDV,NXDV )
      DO 0260 IENG=0,NENG-1
        WRITE(41,'(F12.6)') (REAL(IENG)+0.5)*DENG
        WRITE(42,'(F12.6)') (REAL(IENG)+0.5)*DENG
        WRITE(41,'(5(E12.6,X))')
     >       ( XFE0(IXDV,IENG)/XNEL(IXDV)/DENG , IXDV=0,NXXX-NXDV,NXDV )
        WRITE(42,'(5(E12.6,X))')
     >       ( XFE1(IXDV,IENG)/XNEL(IXDV)/DENG , IXDV=0,NXXX-NXDV,NXDV )
 0260 CONTINUE
      STOP
      END
* ========== momentum transfer cross section of He ====================
* Frost L S and Phelps A V 1964 Phys.Rev.A 136 1538-45
      FUNCTION SHEMOM(EV)
      REAL X(50),Y(50),A(50),B(50),C(50)
      DATA (X(I),Y(I),I=1,17) /
     >  0.1,5.7  ,   0.15,5.8 ,  0.2,6.0 ,  0.3,6.4 ,  0.5,7.5  ,
     >  0.8,8.2  ,   1.0 ,8.4 ,  1.5,8.1 ,  2.0,7.6 ,  3.0,6.7  ,
     >  5.0,5.4  ,   7.0 ,4.7 , 10.0,4.0 , 20.0,3.1 , 30.0,2.75 ,
     > 70.0,2.15 , 100.0 ,2.0 /
      DO 0010 I=3,17,2
        A(I)=(Y(I)-Y(I-1))/(X(I)-X(I-1))-(Y(I-1)-Y(I-2))/(X(I-1)-X(I-2))
        A(I)=A(I)/(X(I)-X(I-2))
        B(I)=(Y(I-2)-Y(I-1))/(X(I-2)-X(I-1))-A(I)*(X(I-2)+X(I-1))
        C(I)=Y(I)-X(I)*(A(I)*X(I)+B(I))
 0010 CONTINUE
      ENTRY QHEMOM(EV)
      IF (EV .LT. X(1)) THEN
        QHEMOM=6.21143*(EV**0.03732)  *3.5355
        RETURN
      END IF
      DO 0020 I=3,17,2
        IF (EV .LT. X(I)) THEN
          QHEMOM=(EV*(A(I)*EV+B(I))+C(I))  *3.5355
          RETURN
        END IF
 0020 CONTINUE
      QHEMOM=8.0/(EV**0.30103)  *3.5355
      RETURN
      END
```

```
* ========== excitation cross section of He (metastable) ===============
* Zetner P W, Westerveld W B, King G C and McConkey J W,
* 1986 J.Phys.B: At.Mol.Phys. 19 4205-13
      FUNCTION SHEEXM(EV)
      REAL X(50),Y(50),A(50),B(50),C(50)
      DATA (X(I),Y(I),I=1,15) /
     >  19.8,0.0 , 19.9,0.5  , 20.0,1.0  , 20.5,2.0 , 21.0,2.8 ,
     >  22.0,3.6 , 24.0,3.9  , 26.0,4.1  , 28.0,4.2 , 30.0,4.1 ,
     >  32.0,4.0 , 34.0,3.95 , 36.0,3.85 , 40.0,3.6 , 45.0,3.4 /
      DO 0010 I=3,15,2
        A(I)=(Y(I)-Y(I-1))/(X(I)-X(I-1))-(Y(I-1)-Y(I-2))/(X(I-1)-X(I-2))
        A(I)=A(I)/(X(I)-X(I-2))
        B(I)=(Y(I-2)-Y(I-1))/(X(I-2)-X(I-1))-A(I)*(X(I-2)+X(I-1))
        C(I)=Y(I)-X(I)*(A(I)*X(I)+B(I))
 0010 CONTINUE
      ENTRY QHEEXM(EV)
      IF (EV .LT. X(1)) THEN
        QHEEXM=0.0
        RETURN
      END IF
      DO 0020 I=3,15,2
        IF (EV .LT. X(I)) THEN
          QHEEXM=(EV*(A(I)*EV+B(I))+C(I))  *3.5355E-02
          RETURN
        END IF
 0020 CONTINUE
      QHEEXM=4.0102E2/(EV**1.25313)  *3.5355E-02
      RETURN
      END
* ========== excitation cross section of He (excitation) ===============
* Zetner P W, Westerveld W B, King G C and McConkey J W,
* 1986 J.Phys.B: At.Mol.Phys. 19 4205-13
      FUNCTION SHEEXC(EV)
      REAL X(50),Y(50),A(50),B(50),C(50)
      DATA (X(I),Y(I),I=1,15) /
     >  20.96,0.0 , 21.0,0.01 , 22.0,0.05 , 23.0,0.1  ,  25.0,0.3 ,
     >  27.0 ,0.4 , 30.0,0.65 , 35.0,1.1  , 40.0,1.7  ,  50.0,2.2 ,
     >  60.0 ,2.4 , 70.0,2.5  , 80.0,2.5  , 90.0,2.45 , 100.0,2.4 /
      DO 0010 I=3,15,2
        A(I)=(Y(I)-Y(I-1))/(X(I)-X(I-1))-(Y(I-1)-Y(I-2))/(X(I-1)-X(I-2))
        A(I)=A(I)/(X(I)-X(I-2))
        B(I)=(Y(I-2)-Y(I-1))/(X(I-2)-X(I-1))-A(I)*(X(I-2)+X(I-1))
        C(I)=Y(I)-X(I)*(A(I)*X(I)+B(I))
 0010 CONTINUE
      ENTRY QHEEXC(EV)
      IF (EV .LT. X(1)) THEN
        QHEEXC=0.0
        RETURN
      END IF
      DO 0020 I=3,15,2
        IF (EV .LT. X(I)) THEN
          QHEEXC=(EV*(A(I)*EV+B(I))+C(I))  *3.5355E-01
          RETURN
        END IF
 0020 CONTINUE
      QHEEXC=28.21224/(EV**0.53511)  *3.5355E-01
      RETURN
      END
* ========== ionization cross section of He ============================
* Montague R G, Harrison M F A and Smith A C H
* 1984 J.Phys.B: At.Mol.Phys. 17 3295-310
      FUNCTION SHEION(EV)
      REAL X(50),Y(50),A(50),B(50),C(50)
      DATA (X(I),Y(I),I=1,17) /
     >  24.588,0.0  , 25.0,0.052 , 26.0,0.19 , 28.0,0.43 , 30.0,0.66 ,
     >  35.0  ,1.14 , 40.0,1.64  , 50.0,2.3  , 60.0,2.75 , 70.0,3.08 ,
     >  80.0  ,3.31 ,100.0,3.58  ,130.0,3.66 ,150.0,3.62 ,200.0,3.39 ,
     > 300.0  ,2.88 ,400.0,2.45  /
      DO 0010 I=3,17,2
        A(I)=(Y(I)-Y(I-1))/(X(I)-X(I-1))-(Y(I-1)-Y(I-2))/(X(I-1)-X(I-2))
        A(I)=A(I)/(X(I)-X(I-2))
        B(I)=(Y(I-2)-Y(I-1))/(X(I-2)-X(I-1))-A(I)*(X(I-2)+X(I-1))
        C(I)=Y(I)-X(I)*(A(I)*X(I)+B(I))
 0010 CONTINUE
      ENTRY QHEION(EV)
      IF (EV .LT. X(1)) THEN
        QHEION=0.0
        RETURN
      END IF
      DO 0020 I=3,17,2
        IF (EV .LT. X(I)) THEN
          QHEION=(EV*(A(I)*EV+B(I))+C(I))  *3.5355E-01
          RETURN
        END IF
 0020 CONTINUE
      QHEION=1.2068E2/(EV**0.65)  *3.5355E-01
      RETURN
      END
```

B.2 Drift Equilibrium $F(\epsilon)$ in Ar/F_2 (steady-state Townsend condition)

```
* ========================================================================
*  "Propagator Method" for steady-state Townsend condition in free space
*
*  Hirotake Sugawara 1993.04.03.-1993.11.11.
*  Applied Electricity Laboratory,
*  Dept.of Electrical Eng., Hokkaido Univ., N13 W8 Sapporo 060 Japan
*  TEL 011-706-6482, FAX 011-706-7890, sgwr@e5.hines.hokudai.ac.jp
* ========================================================================
* ---------- initial setting ---------------------------------------------
      PARAMETER ( NENG=1500        , NANG=100         , NAHF=NANG/2      ,
     >            EBYP=020.0       , EMAX=020.0       ,
     >            TLIM=100.00E-09  , TSM0=100.00E-09  ,
     >            TSM1=01.000E-09  , TUNT=0.0010E-09  ,
*    >            EBYP=030.0       , EMAX=030.0       ,
*    >            TLIM=080.00E-09  , TSM0=080.00E-09  ,
*    >            TSM1=00.800E-09  , TUNT=0.0008E-09  ,
*    >            EBYP=040.0       , EMAX=030.0       ,
*    >            TLIM=060.00E-09  , TSM0=060.00E-09  ,
*    >            TSM1=00.600E-09  , TUNT=0.0006E-09  ,
*    >            EBYP=050.0       , EMAX=030.0       ,
*    >            TLIM=050.00E-09  , TSM0=050.00E-09  ,
*    >            TSM1=00.500E-09  , TUNT=0.0005E-09  ,
     >            GPRS=1.0         , RTF2=0.10*GPRS   , RTAR=0.90*GPRS   )
      PARAMETER ( DENG=EMAX/(NENG*1.0)                                    ,
     >            EEXM=11.55       , KEXM=EEXM/DENG+0.5                  ,
     >            EEXC=12.9        , KEXC=EEXC/DENG+0.5                  ,
     >            EION=15.76       , KION=EION/DENG+0.5                  ,
     >            EFEV= 0.11       , KFEV=EFEV/DENG+0.5                  ,
     >            EFE1= 3.16       , KFE1=EFE1/DENG+0.5                  ,
     >            EFE2= 4.34       , KFE2=EFE2/DENG+0.5                  ,
     >            EFE3=11.57       , KFE3=EFE3/DENG+0.5                  ,
     >            EFE4=13.08       , KFE4=EFE4/DENG+0.5                  ,
     >            EFIO=15.69       , KFIO=EFIO/DENG+0.5                  ,
     >            NSUP=NENG+KION+1                                       ,
     >            ECHG=1.602E-19   , EMAS=9.109E-28   )
      REAL*8 FETO(-1:NENG,0:NANG),FET1(-1:NENG,0:NANG),
     >       RDR0(-1:NENG,0:NANG),RDR1(-1:NENG,0:NANG),
     >       RDR2(-1:NENG,0:NANG)
      REAL*8 FEI0(0:NSUP),FEI1(0:NSUP),FISM(0:NSUP),RSCT(0:NANG),
     >       QMOM(0:NSUP),FMOM(0:NSUP),RMOM,
     >       QEXM(0:NSUP),FEXM(0:NSUP),REXM,
     >       QEXC(0:NSUP),FEXC(0:NSUP),REXC,
     >       QION(0:NSUP),FION(0:NSUP),RION,GION(0:NSUP),
     >       QFEV(0:NSUP),FFEV(0:NSUP),RFEV,
     >       QFE1(0:NSUP),FFE1(0:NSUP),RFE1,
     >       QFE2(0:NSUP),FFE2(0:NSUP),RFE2,
     >       QFE3(0:NSUP),FFE3(0:NSUP),RFE3,
     >       QFE4(0:NSUP),FFE4(0:NSUP),RFE4,
     >       QFIO(0:NSUP),FFIO(0:NSUP),RFIO,GFIO(0:NSUP),
     >       QATT(0:NSUP),FATT(0:NSUP),RATT,
     >       QTTL(0:NSUP),FNUL(0:NSUP),FCOL
      REAL   BENG(0:NSUP),CENG(0:NSUP),
     >       BVLC(0:NSUP),CVLC(0:NSUP),
     >       BANG(0:NANG),CANG(0:NANG),
     >       BSIN(0:NANG),
     >       BCOS(0:NANG),CCOS(0:NANG),
     >       CP00(0:NANG),CP01(0:NANG),CP02(0:NANG),
     >       CP03(0:NANG),CP04(0:NANG),CP05(0:NANG)
      REAL*8 FE00(0:NENG),FE01(0:NENG),FE02(0:NENG),
     >       FE03(0:NENG),FE04(0:NENG),FE05(0:NENG)
      REAL*8 REFF,RNEL,RFWD,RBWD,EAXP,EAXN,
     >       SPNE,SPME,SPVD,SPDS,SPWS
* ---------- constants ---------------------------------------------------
      PI00=ATAN(1.0)*4.0
      DANG=PI00/REAL(NANG)
      FCEV=2.0*ECHG/EMAS*1.0E+07
      FCVE=0.5*EMAS/ECHG*1.0E-07
      EFLD=EBYP*GPRS
      DDRF=ECHG*EFLD/EMAS*1.0E+07  *TUNT
      DXIN=EFLD/DENG
      NIT0=NINT(TLIM/TSM0)
      NIT1=NINT(TSM0/TSM1)
      NIT2=NINT(TSM1/TUNT)
      DO 0010 IENG=0,NENG
        BENG(IENG)=DENG*REAL(IENG)
        BVLC(IENG)=SQRT(BENG(IENG)*FCEV)
 0010 CONTINUE
      DO 0020 IENG=0,NENG-1
        CVLC(IENG)=(BVLC(IENG)+BVLC(IENG+1))*0.5
        CENG(IENG)=CVLC(IENG)**2*FCVE
 0020 CONTINUE
```

Constants and Variables

NENG	the number of divisions for ϵ
NANG	the number of divisions for θ
EBYP	E/p ($\mathrm{Vcm^{-1}Torr^{-1}}$)
EMAX	ϵ_{max} (eV)
TLIM	the simulation time (s)
TSM0	the sampling interval (s) for $F(\epsilon)$
TSM1	the sampling interval (s) for electron swarm parameters
TUNT	the time step Δt (s)
GPRS	the gas pressure p (Torr)
RTF2	the mixture ratio of F_2
RTAR	the mixture ratio of Ar
DENG	the cell width $\Delta\epsilon$ (eV)
EEXC	$\epsilon_{Ar,ex}$ (eV)
EEXM	$\epsilon_{Ar,ex,meta}$ (eV)
EION	$\epsilon_{Ar,ion}$ (eV)
EFEV	$\epsilon_{F2,ex,v}$ (eV)
EFE1,EFE2,EFE3,EFE4	$\epsilon_{F2,ex,k}$ (eV) ($k = 1, \cdots, 4$)
EFIO	$\epsilon_{F2,ion}$ (eV)
KEXC	$\epsilon_{Ar,ex}/\Delta\epsilon$
KEXM	$\epsilon_{Ar,ex,meta}/\Delta\epsilon$
KION	$\epsilon_{Ar,ion}/\Delta\epsilon$
KFEV	$\epsilon_{F2,ex,v}/\Delta\epsilon$
KFE1,KFE2,KFE3,KFE4	$\epsilon_{F2,ex,k}/\Delta\epsilon$ ($k = 1, \cdots, 4$)
KFIO	$\epsilon_{F2,ion}/\Delta\epsilon$
NSUP	the number of divisions for ϵ with margin
ECHG	$e = 1.602 \times 10^{-19}$ C
EMAS	$m = 9.109 \times 10^{-28}$ g
PI00	$\pi = 3.14159265\cdots$
DANG	the cell width $\Delta\theta$ (rad)
FCEV	$v_1 = 5.79 \times 10^7$ $\mathrm{cms^{-1}}$
FCVE	$1/v_1$
EFLD	the electric field E ($\mathrm{Vcm^{-1}}$)
DDRF	the acceleration $a\Delta t$ ($\mathrm{cms^{-1}}$)
DXIN	$1/\Delta x$ ($\mathrm{cm^{-1}}$)
NIT0,NIT1,NIT2	iteration cycles
IENG	subscript i of ϵ_i and v_i
BENG	$\epsilon_i = i\Delta\epsilon$ (eV)
BVLC	$v_i = \sqrt{2\epsilon_i/m}$ ($\mathrm{cms^{-1}}$)
CVLC	$\bar{v}_i$ ($\mathrm{cms^{-1}}$)
CENG	$\bar{\epsilon}_i$ (eV)

```
      DO 0030 IANG=0,NANG
        BANG(IANG)=DANG*REAL(IANG)
        BSIN(IANG)=SIN(BANG(IANG))
        BCOS(IANG)=COS(BANG(IANG))
        CANG(IANG)=DANG*(REAL(IANG)+0.5)
        CCOS(IANG)=COS(CANG(IANG))
        CP00(IANG)=1.0
        CP01(IANG)=CCOS(IANG)
        CP02(IANG)=(CCOS(IANG)*CP01(IANG)* 3.0-CP00(IANG)* 1.0)/ 2.0
        CP03(IANG)=(CCOS(IANG)*CP02(IANG)* 5.0-CP01(IANG)* 2.0)/ 3.0
        CP04(IANG)=(CCOS(IANG)*CP03(IANG)* 7.0-CP02(IANG)* 3.0)/ 4.0
        CP05(IANG)=(CCOS(IANG)*CP04(IANG)* 9.0-CP03(IANG)* 4.0)/ 5.0
 0030 CONTINUE
* ---------- arrays for collisions -----------------------------------
      QDMY=SARMOM(0.0)+SAREXC(0.0)+SAREXM(0.0)+SARION(0.0)
     >    +SF2MOM(0.0)+SF2EXV(0.0)+SF2EX1(0.0)+SF2EX2(0.0)
     >    +SF2EX3(0.0)+SF2EX4(0.0)+SF2ION(0.0)+SF2ATT(0.0)+QDMY
      DO 0040 IENG=0,NENG-1
        QMOM(IENG)=QARMOM(CENG(IENG))*RTAR
     >            +QF2MOM(CENG(IENG))*RTF2
        QEXM(IENG)=QAREXM(CENG(IENG))*RTAR
        QEXC(IENG)=QAREXC(CENG(IENG))*RTAR
        QION(IENG)=QARION(CENG(IENG))*RTAR
        QFEV(IENG)=QF2EXV(CENG(IENG))*RTF2
        QFE1(IENG)=QF2EX1(CENG(IENG))*RTF2
        QFE2(IENG)=QF2EX2(CENG(IENG))*RTF2
        QFE3(IENG)=QF2EX3(CENG(IENG))*RTF2
        QFE4(IENG)=QF2EX4(CENG(IENG))*RTF2
        QFIO(IENG)=QF2ION(CENG(IENG))*RTF2
        QATT(IENG)=QF2ATT(CENG(IENG))*RTF2
 0040 CONTINUE
      DO 0050 IENG=0,NENG-1
        QTTL(IENG)=QMOM(IENG)+QEXM(IENG)+QEXC(IENG)+QION(IENG)
     >            +QFEV(IENG)+QFE1(IENG)+QFE2(IENG)+QFE3(IENG)
     >            +QFE4(IENG)+QFIO(IENG)+QATT(IENG)
        FNUL(IENG)=EXP(-QTTL(IENG)*CVLC(IENG)*TUNT)
        FCOL      =(1.0-FNUL(IENG))/QTTL(IENG)
        FMOM(IENG)=FCOL*QMOM(IENG)
        FEXM(IENG)=FCOL*QEXM(IENG)
        FEXC(IENG)=FCOL*QEXC(IENG)
        FION(IENG)=FCOL*QION(IENG)
        FFEV(IENG)=FCOL*QFEV(IENG)
        FFE1(IENG)=FCOL*QFE1(IENG)
        FFE2(IENG)=FCOL*QFE2(IENG)
        FFE3(IENG)=FCOL*QFE3(IENG)
        FFE4(IENG)=FCOL*QFE4(IENG)
        FFIO(IENG)=FCOL*QFIO(IENG)
        FATT(IENG)=FCOL*QATT(IENG)
        GION(IENG)=FION(IENG)/REAL(DIM(IENG,KION)*2+1)*2.0
        GFIO(IENG)=FFIO(IENG)/REAL(DIM(IENG,KFIO)*2+1)*2.0
 0050 CONTINUE
      DO 0060 IANG=0,NANG-1
        RSCT(IANG)=(BCOS(IANG)-BCOS(IANG+1))*0.5
 0060 CONTINUE
* ---------- arrays for acceleration ---------------------------------
      PI23=PI00*2.0/3.0
      DO 0070 IANG=0,NAHF-1
      DO 0070 IENG=0,NENG-1
        RCEL           =PI23 *(BVLC(IENG+1)**3-BVLC(IENG)**3)
     >                       *(BCOS(IANG)-BCOS(IANG+1))
        RDR1(IENG,IANG)=PI00 *(BVLC(IENG+1)**2-BVLC(IENG)**2)
     >                       *BSIN(IANG)**2                      *DDRF/RCEL
        RDR2(IENG,IANG)=PI00 *BVLC(IENG+1)**2
     >                       *(BSIN(IANG+1)**2-BSIN(IANG)**2) *DDRF/RCEL
        RDR0(IENG,IANG)=1.0-RDR1(IENG,IANG)-RDR2(IENG,IANG)
 0070 CONTINUE
      DO 0080 IANG=NAHF,NANG-1
      DO 0080 IENG=   0,NENG-1
        RCEL           =PI23 *(BVLC(IENG+1)**3-BVLC(IENG)**3)
     >                       *(BCOS(IANG)-BCOS(IANG+1))
        RDR1(IENG,IANG)=PI00 *(BVLC(IENG+1)**2-BVLC(IENG)**2)
     >                       *BSIN(IANG)**2                      *DDRF/RCEL
        RDR2(IENG,IANG)=PI00 *BVLC(IENG)**2
     >                       *(BSIN(IANG)**2-BSIN(IANG+1)**2) *DDRF/RCEL
        RDR0(IENG,IANG)=1.0-RDR1(IENG,IANG)-RDR2(IENG,IANG)
 0080 CONTINUE
      DO 0090 IANG=0,NANG-1
      DO 0090 IENG=0,NENG-1
        IF (RDR0(IENG,IANG) .LT. 0.0) THEN
          WRITE(6,*) 'ratio negative : cell No.',IENG*NANG+IANG
          WRITE(6,*) RDR0(IENG,IANG),RDR1(IENG,IANG),RDR2(IENG,IANG)
          STOP
        END IF
 0090 CONTINUE
```

Constants and Variables

`IANG` subscript j of θ_j

`BANG` $\theta_j = j\Delta\theta$ (rad)
`BSIN` $\sin\theta_j$
`BCOS` $\cos\theta_j$
`CANG` $\bar{\theta}_j$ (rad)
`CCOS` $\cos\bar{\theta}_j$

`CP00,CP01,CP02,CP03,CP04,CP05`
Legendre's polynomials
$P_n(\cos\bar{\theta}_j)$ $(n = 0, \cdots, 5)$

`QDMY` a dummy variable for initialization of function subprograms

`QMOM` $N_{\mathrm{Ar}} q_{\mathrm{Ar,mom}}(\epsilon)$ $+N_{\mathrm{F2}} q_{\mathrm{F2,mom}}(\epsilon)$ (cm^{-1})
`QEXC` $N_{\mathrm{Ar}} q_{\mathrm{Ar,ex}}(\epsilon)$ (cm^{-1})
`QEXM` $N_{\mathrm{Ar}} q_{\mathrm{Ar,ex,meta}}(\epsilon)$ (cm^{-1})
`QION` $N_{\mathrm{Ar}} q_{\mathrm{Ar,ion}}(\epsilon)$ (cm^{-1})
`QFEV` $N_{\mathrm{F2}} q_{\mathrm{F2,ex,v}}(\epsilon)$ (cm^{-1})
`QFE1,QFE2,QFE3,QFE4`
$N_{\mathrm{F2}} q_{\mathrm{F2,ex},i}(\epsilon)$ (cm^{-1})
$(i = 1, \cdots, 4)$
`QFIO` $N_{\mathrm{F2}} q_{\mathrm{F2,ion}}(\epsilon)$ (cm^{-1})
`QATT` $N_{\mathrm{F2}} q_{\mathrm{F2,att}}(\epsilon)$ (cm^{-1})

`QTTL` $N_{\mathrm{Ar}} q_{\mathrm{Ar,T}}(\epsilon)$ $+N_{\mathrm{F2}} q_{\mathrm{F2,T}}(\epsilon)$ (cm^{-1})

`FNUL` the probability of no collision
`FMOM,FEXM,FEXC,FION,FFEV,`
`FFE1,FFE2,FFE3,FFE4,FFIO,FATT`
the ratios of colliding electrons
`GION,GFIO`
the distribution ratio of electrons after ionization

`RSCT` the scattering ratio $(1/2)\sin\theta\Delta\theta$

`RCEL` the volume of a cell $(\mathrm{cms}^{-1})^3$
`RDR0` the ratio of electrons remaining in $C_{l,i,j}$
`RDR1` the ratio of electrons flowing out of $C_{l,i,j}$ to $C_{l,i,j+1}$
`RDR2` the ratio of electrons flowing out of $C_{l,i,j}$ to $C_{l\pm1,i\pm1,j}$

```
* ---------- initial condition ----------------------------------------
      SPN0=1.0
      FET0(0,0)=SPN0*0.5
      WRITE(40,'(I5,X,I5)') 21,NIT0*NIT1+1
      WRITE(40,'(''time (ns)''                                  )')
      WRITE(40,'(''number of electrons''                        )')
      WRITE(40,'(''mean energy (eV)''                           )')
      WRITE(40,'(''ionization coefficient (cm^-^1)''            )')
      WRITE(40,'(''ionization frequency Ri (~ms^-^1)''          )')
      WRITE(40,'(''attachment frequency Ra (~ms^-^1)''          )')
      WRITE(40,'(''effective ionization frequency (~ms^-^1)'')')
      WRITE(40,'(''drift velocity Vd (cm/~ms)''                 )')
      WRITE(40,'(''drift velocity Ws (cm/~ms)''                 )')
      WRITE(40,'(''diffusion coefficient Ds (cm^2/~ms)''        )')
      WRITE(40,'(''ionization coefficient Ri/Vd (cm^-^1)''      )')
      WRITE(40,'(''collision frequency Rmom (~ms^-^1)''         )')
      WRITE(40,'(''collision frequency Rex0 (~ms^-^1)''         )')
      WRITE(40,'(''collision frequency Rex1 (~ms^-^1)''         )')
      WRITE(40,'(''collision frequency Rion (~ms^-^1)''         )')
      WRITE(40,'(''collision frequency Rf2i (~ms^-^1)''         )')
      WRITE(40,'(''collision frequency Ratt (~ms^-^1)''         )')
      WRITE(40,'(''collision frequency Rfev (~ms^-^1)''         )')
      WRITE(40,'(''collision frequency Rfe1 (~ms^-^1)''         )')
      WRITE(40,'(''collision frequency Rfe2 (~ms^-^1)''         )')
      WRITE(40,'(''collision frequency Rfe3 (~ms^-^1)''         )')
      WRITE(40,'(''collision frequency Rfe4 (~ms^-^1)''         )')
      WRITE(40,'(  E12.6,X )') 0.0
      WRITE(40,'(6(E12.6,X))') SPN0, 0.0 , 0.0 , 0.0 , 0.0 , 0.0
      WRITE(40,'(4(E12.6,X))') 0.0 , 0.0 , 0.0 , 0.0
      WRITE(40,'(6(E12.6,X))') 0.0 , 0.0 , 0.0 , 0.0 , 0.0 , 0.0
      WRITE(40,'(5(E12.6,X))') 0.0 , 0.0 , 0.0 , 0.0 , 0.0
* ---------- passage of time ------------------------------------------
      DO 0300 IIT0=0,NIT0-1
      DO 0250 IIT1=0,NIT1-1
      DO 0180 IIT2=0,NIT2-1
* ---------- collision & scattering -----------------------------------
      DO 0100 IENG=0,NENG-1
        FEI0(IENG)=0.0
 0100 CONTINUE
      DO 0110 IANG=0,NANG-1
      DO 0110 IENG=0,NENG-1
        FEI0(IENG)=FEI0(IENG)+FET0(IENG,IANG)
 0110 CONTINUE
      FISM(NENG)=0.0
      REFF=0.0
      DO 0120 IENG=NENG-1,0,-1
        FISM(IENG)=FISM(IENG+1)
     >            +FEI0(IENG+KION  )*GION(IENG+KION  )
     >            +FEI0(IENG+KION+1)*GION(IENG+KION+1)
     >            +FEI0(IENG+KFI0  )*GFI0(IENG+KFI0  )
     >            +FEI0(IENG+KFI0+1)*GFI0(IENG+KFI0+1)
        FEI1(IENG)=FEI0(IENG       )*FMOM(IENG       )
     >            +FEI0(IENG+KEXM  )*FEXM(IENG+KEXM  )
     >            +FEI0(IENG+KEXC  )*FEXC(IENG+KEXC  )
     >            +FEI0(IENG+KFEV  )*FFEV(IENG+KFEV  )
     >            +FEI0(IENG+KFE1  )*FFE1(IENG+KFE1  )
     >            +FEI0(IENG+KFE2  )*FFE2(IENG+KFE2  )
     >            +FEI0(IENG+KFE3  )*FFE3(IENG+KFE3  )
     >            +FEI0(IENG+KFE4  )*FFE4(IENG+KFE4  )
     >            +FISM(IENG)
        REFF=REFF+FEI0(IENG)*(FION(IENG)+FFI0(IENG)-FATT(IENG))
 0120 CONTINUE
      DO 0130 IANG=0,NANG-1
      DO 0130 IENG=0,NENG-1
        FET1(IENG,IANG)=FET0(IENG,IANG)*FNUL(IENG)+FEI1(IENG)*RSCT(IANG)
 0130 CONTINUE
* ---------- drift ----------------------------------------------------
      RFWD=0.0
      DO 0140 IANG=0,NAHF-1
      DO 0140 IENG=0,NENG-1
        RFWD=RFWD+FET1(IENG,IANG)*RDR2(IENG,IANG)
 0140 CONTINUE
      RBWD=0.0
      DO 0150 IANG=NAHF,NANG-1
      DO 0150 IENG=   0,NENG-1
        RBWD=RBWD+FET1(IENG,IANG)*RDR2(IENG,IANG)
 0150 CONTINUE
      RNEL=RFWD+RBWD-REFF
      EAXN=ABS(RNEL+SQRT(RNEL**2-4.0*RFWD*RBWD))/RFWD*0.5
      EAXP=1.0/EAXN
```

Constants and Variables

SPN0	the number of initial electrons
FET0	$F(\epsilon,\theta)$ before collision
FEI0	$F(\epsilon)$ before collision
FISM	the number of electrons after ionization
FEI1	$F(\epsilon)$ after collision
FET1	$F(\epsilon,\theta)$ after collision
REFF	$n_{\rm ion}-n_{\rm att}$
RBWD	$n_{\rm b,out}$
RFWD	$n_{\rm f,out}$
EAXN	$\exp(-\bar{\alpha}\Delta x)$
EAXP	$\exp(+\bar{\alpha}\Delta x)$

```
      DO 0160 IANG=0,NAHF-1
      DO 0160 IENG=0,NENG-1
        FET0(IENG,IANG)=FET1(IENG  ,IANG  )*RDR0(IENG  ,IANG  )
     >                 +FET1(IENG  ,IANG+1)*RDR1(IENG  ,IANG+1)
     >                 +FET1(IENG-1,IANG  )*RDR2(IENG-1,IANG  )*EAXN
 0160 CONTINUE
      DO 0170 IANG=NAHF,NANG-1
      DO 0170 IENG=   0,NENG-1
        FET0(IENG,IANG)=FET1(IENG  ,IANG  )*RDR0(IENG  ,IANG  )
     >                 +FET1(IENG  ,IANG+1)*RDR1(IENG  ,IANG+1)
     >                 +FET1(IENG+1,IANG  )*RDR2(IENG+1,IANG  )*EAXP
 0170 CONTINUE
 0180 CONTINUE
* ---------- sampling (interval TSM1) ---------------------------------
      RION=0.0
      RFIO=0.0
      RMOM=0.0
      REXM=0.0
      REXC=0.0
      RFEV=0.0
      RFE1=0.0
      RFE2=0.0
      RFE3=0.0
      RFE4=0.0
      RATT=0.0
      DO 0190 IENG=0,NENG-1
        RION=RION+FEIO(IENG)*FION(IENG)
        RFIO=RFIO+FEIO(IENG)*FFIO(IENG)
        RMOM=RMOM+FEIO(IENG)*FMOM(IENG)
        REXM=REXM+FEIO(IENG)*FEXM(IENG)
        REXC=REXC+FEIO(IENG)*FEXC(IENG)
        RFEV=RFEV+FEIO(IENG)*FFEV(IENG)
        RFE1=RFE1+FEIO(IENG)*FFE1(IENG)
        RFE2=RFE2+FEIO(IENG)*FFE2(IENG)
        RFE3=RFE3+FEIO(IENG)*FFE3(IENG)
        RFE4=RFE4+FEIO(IENG)*FFE4(IENG)
        RATT=RATT+FEIO(IENG)*FATT(IENG)
 0190 CONTINUE
      DO 0200 IANG=0,NANG-1
      DO 0200 IENG=0,NENG-1
        FET1(IENG,IANG)=FET1(IENG,IANG)+FET0(IENG,IANG)
 0200 CONTINUE
      DO 0210 IENG=0,NENG-1
        FE00(IENG)=0.0
        FE01(IENG)=0.0
 0210 CONTINUE
      DO 0220 IANG=0,NANG-1
      DO 0220 IENG=0,NENG-1
        FE00(IENG)=FE00(IENG)+FET1(IENG,IANG)*CP00(IANG)
        FE01(IENG)=FE01(IENG)+FET1(IENG,IANG)*CP01(IANG)
 0220 CONTINUE
      SPNE=0.0
      DO 0230 IENG=0,NENG-1
        SPNE=SPNE+FE00(IENG)
 0230 CONTINUE
      FNRM=1.0/(SPNE*0.5)/TUNT
      SPRI=LOG((SPNE*0.5+RION+RFIO     )*FNRM)
      SPRA=LOG((SPNE*0.5          -RATT)*FNRM)
      SPRS=LOG((SPNE*0.5+RION+RFIO-RATT)*FNRM)
      RION=RION*FNRM  *1.0E-06
      RFIO=RFIO*FNRM  *1.0E-06
      RMOM=RMOM*FNRM  *1.0E-06
      REXM=REXM*FNRM  *1.0E-06
      REXC=REXC*FNRM  *1.0E-06
      RFEV=RFEV*FNRM  *1.0E-06
      RFE1=RFE1*FNRM  *1.0E-06
      RFE2=RFE2*FNRM  *1.0E-06
      RFE3=RFE3*FNRM  *1.0E-06
      RFE4=RFE4*FNRM  *1.0E-06
      RATT=RATT*FNRM  *1.0E-06
      SPME=0.0
      SPVD=0.0
      SPDS=0.0
      DO 0240 IENG=0,NENG-1
        SPME=SPME+FE00(IENG)*CENG(IENG)
        SPVD=SPVD+FE01(IENG)*CVLC(IENG)
        SPDS=SPDS+FE00(IENG)*CVLC(IENG)/QTTL(IENG)
 0240 CONTINUE
      SPAL=-LOG(EAXN)*DXIN
      SPRI=SPRI           *1.0E-06
      SPRA=SPRA           *1.0E-06
      SPRS=SPRS           *1.0E-06
      SPME=SPME/SPNE
      SPVD=SPVD/SPNE      *1.0E-06
      SPDS=SPDS/SPNE/3.0  *1.0E-06
      SPAV=SPRS/SPVD
      SPWS=SPVD+SPAL*SPDS
      WRITE(40,'(  E12.6,X )') (IIT0*TSM0+(IIT1+1)*TSM1)*1.0E+09
      WRITE(40,'(6(E12.6,X))') SPNE,SPME,SPAL,SPRI,SPRA,SPRS
      WRITE(40,'(4(E12.6,X))') SPVD,SPWS,SPDS,SPAV
      WRITE(40,'(6(E12.6,X))') RMOM,REXM,REXC,RION,RFIO,RATT
      WRITE(40,'(5(E12.6,X))') RFEV,RFE1,RFE2,RFE3,RFE4
 0250 CONTINUE
```

Constants and Variables

RION	$R_{\mathrm{Ar,ion}}$ (μs^{-1})
RFIO	$R_{\mathrm{F2,ion}}$ (μs^{-1})
RMOM	$R_{\mathrm{Ar,mom}}$ $+R_{\mathrm{F2,mom}}$ (μs^{-1})
REXC	$R_{\mathrm{Ar,ex}}$ (μs^{-1})
REXM	$R_{\mathrm{Ar,ex,meta}}$ (μs^{-1})
RFEV	$R_{\mathrm{F2,ex,v}}$ (μs^{-1})
RFE1	$R_{\mathrm{F2,ex,1}}$ (μs^{-1})
RFE2	$R_{\mathrm{F2,ex,2}}$ (μs^{-1})
RFE3	$R_{\mathrm{F2,ex,3}}$ (μs^{-1})
RFE4	$R_{\mathrm{F2,ex,4}}$ (μs^{-1})
RATT	$R_{\mathrm{F2,att}}$ (μs^{-1})
SPNE	the number of electrons n
SPME	the mean electron energy $\bar{\epsilon}$ (eV)
SPVD	the drift velocity v_{d} ($\mathrm{cm}\mu s^{-1}$)
SPWS	the drift velocity W_{s} ($\mathrm{cm}\mu s^{-1}$)
SPDS	the diffusion coefficient D_{s} ($\mathrm{cm}^2\mu s^{-1}$)
SPRI	the ionization frequency R_{ion} (μs^{-1})
SPRA	the attachment frequency R_{att} (μs^{-1})
SPRS	the effective ionization frequency $\bar{R}_{\mathrm{ion}}$ (μs^{-1})
SPAL	the effective ionization coefficient $\bar{\alpha}$ (cm^{-1})
SPAV	$\bar{R}_{\mathrm{ion}}/v_{\mathrm{d}}$

```
* ---------- sampling (interval TSM0) ---------------------------------
      DO 0260 IENG=0,NENG-1
        FE00(IENG)=0.0
        FE01(IENG)=0.0
        FE02(IENG)=0.0
        FE03(IENG)=0.0
        FE04(IENG)=0.0
        FE05(IENG)=0.0
 0260 CONTINUE
      DO 0270 IANG=0,NANG-1
      DO 0270 IENG=0,NENG-1
        FE00(IENG)=FE00(IENG)+FET1(IENG,IANG)*CP00(IANG)
        FE01(IENG)=FE01(IENG)+FET1(IENG,IANG)*CP01(IANG)
        FE02(IENG)=FE02(IENG)+FET1(IENG,IANG)*CP02(IANG)
        FE03(IENG)=FE03(IENG)+FET1(IENG,IANG)*CP03(IANG)
        FE04(IENG)=FE04(IENG)+FET1(IENG,IANG)*CP04(IANG)
        FE05(IENG)=FE05(IENG)+FET1(IENG,IANG)*CP05(IANG)
 0270 CONTINUE
      WRITE(41,'(I5,X,I5)') 6,NENG/2+1
      WRITE(41,'(''electron energy (eV) (t='',F8.3,''ns)'')')
     >     (IIT0+1)*TSM0*1.0E+09
      WRITE(41,'(''energy distribution F_0'')')
      WRITE(41,'(''energy distribution F_1'')')
      WRITE(41,'(''energy distribution F_2'')')
      WRITE(41,'(''energy distribution F_3'')')
      WRITE(41,'(''energy distribution F_4'')')
      WRITE(41,'(''energy distribution F_5'')')
      FNRM=1.0/(SPNE*DENG)
      DO 0280 IENG=0,NENG-1
        FE00(IENG)=FE00(IENG)*FNRM* 1.0
        FE01(IENG)=FE01(IENG)*FNRM* 3.0
        FE02(IENG)=FE02(IENG)*FNRM* 5.0
        FE03(IENG)=FE03(IENG)*FNRM* 7.0
        FE04(IENG)=FE04(IENG)*FNRM* 9.0
        FE05(IENG)=FE05(IENG)*FNRM*11.0
 0280 CONTINUE
      WRITE(41,'(  F12.6,X )') 0.0
      WRITE(41,'(6(E12.6,X))') 0.0 , 0.0 , 0.0 , 0.0 , 0.0 , 0.0
      DO 0290 IENG=0,NENG-2,2
        WRITE(41,'(  F12.6,X )') (REAL(IENG)+0.5)*DENG
        WRITE(41,'(6(E12.6,X))') FE00(IENG),FE01(IENG),FE02(IENG),
     >                           FE03(IENG),FE04(IENG),FE05(IENG)
 0290 CONTINUE
 0300 CONTINUE
      STOP
      END
* ========== momentum transfer cross section of Ar ====================
* Suzuki M, Taniguchi T and Tagashira H
* 1990 J.Phys.D: Appl.Phys. 23 842-50
      FUNCTION SARMOM(EV)
      REAL X(50),Y(50),A(50),B(50),C(50)
      DATA (X(I),Y(I),I=1,17) /
     >  0.3, 0.37 ,  0.4, 0.42 , 0.5, 0.49 ,  1.0,1.16 ,  2.0, 2.69 ,
     >  5.0, 7.52 ,  9.0,13.6  ,10.0,14.7  , 12.0,15.8 , 14.0,15.0  ,
     > 16.0,14.0  , 20.0,11.48 ,25.0, 9.33 , 30.0,7.92 , 40.0, 6.22 ,
     > 50.0, 5.09 , 62.5, 4.18 /
      DO 0010 I=3,17,2
        A(I)=(Y(I)-Y(I-1))/(X(I)-X(I-1))-(Y(I-1)-Y(I-2))/(X(I-1)-X(I-2))
        A(I)=A(I)/(X(I)-X(I-2))
        B(I)=(Y(I-2)-Y(I-1))/(X(I-2)-X(I-1))-A(I)*(X(I-2)+X(I-1))
        C(I)=Y(I)-X(I)*(A(I)*X(I)+B(I))
 0010 CONTINUE
      ENTRY QARMOM(EV)
      IF (EV .LT. X(1)) THEN
        QARMOM=(0.141/(EV+0.001)+(1.55*EV)-0.566)  *3.5355
        RETURN
      END IF
      DO 0020 I=3,17,2
        IF (EV .LT. X(I)) THEN
          QARMOM=(EV*(A(I)*EV+B(I))+C(I))  *3.5355
          RETURN
        END IF
 0020 CONTINUE
      QARMOM=261.25/EV  *3.5355
      RETURN
      END
```

Constants and Variables

FE00,FE01,FE02,FE03,FE04,FE05
: Legendre's polynomial expansion terms of $F(\epsilon)$; $F_n(\epsilon)$ $(n = 0, \cdots, 5)$

```
* ========== excitation cross section of Ar (excitation) ===============
* Zetner P W, Westerveld W B, King G C and McConkey J W,
* 1986 J.Phys.B: At.Mol.Phys. 19 4205-13
      FUNCTION SAREXC(EV)
      REAL X(50),Y(50),A(50),B(50),C(50)
      DATA (X(I),Y(I),I=1,21) /
     >  12.9,0.0  , 13.0,0.8 , 13.1,0.84 , 13.2,0.88 , 13.5,1.0 ,
     >  14.0,1.15 , 14.5,1.3 , 15.0,1.4  , 16.0,1.5  , 18.0,1.8 ,
     >  20.0,2.7  , 23.0,4.1 , 25.0,4.65 , 27.0,5.1  , 30.0,5.6 ,
     >  32.0,5.7  , 36.0,5.7 , 40.0,5.5  , 50.0,4.8  , 60.0,4.2 ,
     >  70.0,3.6  /
      DO 0010 I=3,21,2
        A(I)=(Y(I)-Y(I-1))/(X(I)-X(I-1))-(Y(I-1)-Y(I-2))/(X(I-1)-X(I-2))
        A(I)=A(I)/(X(I)-X(I-2))
        B(I)=(Y(I-2)-Y(I-1))/(X(I-2)-X(I-1))-A(I)*(X(I-2)+X(I-1))
        C(I)=Y(I)-X(I)*(A(I)*X(I)+B(I))
 0010 CONTINUE
      ENTRY QAREXC(EV)
      IF (EV .LT. X(1)) THEN
        QAREXC=0.0
        RETURN
      END IF
      DO 0020 I=3,21,2
        IF (EV .LT. X(I)) THEN
          QAREXC=(EV*(A(I)*EV+B(I))+C(I))  *3.5355E-01
          RETURN
        END IF
 0020 CONTINUE
      QAREXC=256.376/(EV**1.004)  *3.5355E-01
      RETURN
      END
* ========== excitation cross section of Ar (metastable) ===============
* Sakai Y, Tagashira H and Sakamoto S,
* 1972 J.Phys.B: At.Mol.Phys. 20 1010-6
      FUNCTION SAREXM(EV)
      REAL X(50),Y(50),A(50),B(50),C(50)
      DATA (X(I),Y(I),I=1,23) /
     > 11.55,0.0   , 11.8,0.008 , 12.0,0.01 , 12.3,0.02 , 12.6,0.04 ,
     > 13.0 ,0.075 , 13.5,0.15  , 14.0,0.3  , 14.5,0.75 , 15.0,1.5  ,
     > 16.0 ,3.5   , 16.5,4.7   , 17.0,4.9  , 17.2,5.0  , 17.3,5.0  ,
     > 17.4 ,5.0   , 18.0,4.95  , 18.5,4.9  , 19.0,4.85 , 20.0,4.75 ,
     > 23.0 ,4.7   , 25.0,4.5   , 30.0,3.75 /
      DO 0010 I=3,23,2
        A(I)=(Y(I)-Y(I-1))/(X(I)-X(I-1))-(Y(I-1)-Y(I-2))/(X(I-1)-X(I-2))
        A(I)=A(I)/(X(I)-X(I-2))
        B(I)=(Y(I-2)-Y(I-1))/(X(I-2)-X(I-1))-A(I)*(X(I-2)+X(I-1))
        C(I)=Y(I)-X(I)*(A(I)*X(I)+B(I))
 0010 CONTINUE
      ENTRY QAREXM(EV)
      IF (EV .LT. X(1)) THEN
        QAREXM=0.0
        RETURN
      END IF
      DO 0020 I=3,23,2
        IF (EV .LT. X(I)) THEN
          QAREXM=(EV*(A(I)*EV+B(I))+C(I))  *3.5355E-01
          RETURN
        END IF
 0020 CONTINUE
      QAREXM=429.78/(EV**1.394)  *3.5355E-01
      RETURN
      END
```

```
* ========== ionization cross section of Ar ============================
* Montague R G, Harrison M F A and Smith A C H
* 1984 J.Phys.B: At.Mol.Phys. 17 3295-310
      FUNCTION SARION(EV)
      REAL X(50),Y(50),A(50),B(50),C(50)
      DATA (X(I),Y(I),I=1,23) /
     >  15.76,0.0 , 16.0,0.04 , 16.7,0.125 , 18.0,0.29 , 20.0,0.63 ,
     >  22.0 ,0.93, 24.0,1.18 , 26.0,1.41  , 28.0,1.6  , 30.0,1.8  ,
     >  34.0 ,2.11, 36.0,2.24 , 40.0,2.39  , 45.0,2.49 , 50.0,2.54 ,
     >  60.0 ,2.66, 70.0,2.77 , 80.0,2.84  , 90.0,2.86 ,100.0,2.85 ,
     > 120.0 ,2.8 ,150.0,2.68 ,300.0,1.98  /
      DO 0010 I=3,23,2
        A(I)=(Y(I)-Y(I-1))/(X(I)-X(I-1))-(Y(I-1)-Y(I-2))/(X(I-1)-X(I-2))
        A(I)=A(I)/(X(I)-X(I-2))
        B(I)=(Y(I-2)-Y(I-1))/(X(I-2)-X(I-1))-A(I)*(X(I-2)+X(I-1))
        C(I)=Y(I)-X(I)*(A(I)*X(I)+B(I))
 0010 CONTINUE
      ENTRY QARION(EV)
      IF (EV .LT. X(1)) THEN
        QARION=0.0
        RETURN
      END IF
      DO 0020 I=3,23,2
        IF (EV .LT. X(I)) THEN
          QARION=(EV*(A(I)*EV+B(I))+C(I))  *3.5355
          RETURN
        END IF
 0020 CONTINUE
      QARION=64.226/(EV**0.61)  *3.5355
      RETURN
      END
* ========== momentum transfer cross section of F2 ====================
* Hayashi M and Nimura T 1983 J.Appl.Phys. 54 4879-82
      FUNCTION SF2MOM(EV)
      REAL X(50),Y(50),A(50),B(50),C(50)
      DATA (X(I),Y(I),I=1,27) /
     >  0.1,10.0 ,   0.3,10.0 ,  0.5,10.3 ,  0.6,11.0 ,  0.8,12.0 ,
     >  1.0,14.0 ,   1.2,17.5 ,  1.4,21.0 ,  1.6,28.0 ,  1.7,31.0 ,
     >  1.8,36.0 ,   1.9,36.0 ,  2.0,35.0 ,  2.2,32.0 ,  2.4,28.0 ,
     >  2.6,25.0 ,   3.0,20.0 ,  4.0,15.5 ,  5.0,13.5 ,  7.0,11.5 ,
     > 10.0,10.0 ,  15.0, 9.0 , 20.0, 8.0 , 30.0, 6.5 , 50.0, 4.4 ,
     > 70.0, 3.0 , 100.0, 1.9 /
      DO 0010 I=3,27,2
        A(I)=(Y(I)-Y(I-1))/(X(I)-X(I-1))-(Y(I-1)-Y(I-2))/(X(I-1)-X(I-2))
        A(I)=A(I)/(X(I)-X(I-2))
        B(I)=(Y(I-2)-Y(I-1))/(X(I-2)-X(I-1))-A(I)*(X(I-2)+X(I-1))
        C(I)=Y(I)-X(I)*(A(I)*X(I)+B(I))
 0010 CONTINUE
      ENTRY QF2MOM(EV)
      IF (EV .LT. X(1)) THEN
        QF2MOM=10.0  *3.5355
        RETURN
      END IF
      DO 0020 I=3,27,2
        IF (EV .LT. X(I)) THEN
          QF2MOM=(EV*(A(I)*EV+B(I))+C(I))  *3.5355
          RETURN
        END IF
 0020 CONTINUE
      QF2MOM=1521.7/(EV**1.4518)  *3.5355
      RETURN
      END
* ========== vibrational excitation cross section of F2 ===============
* Hayashi M and Nimura T 1983 J.Appl.Phys. 54 4879-82
      FUNCTION SF2EXV(EV)
      REAL X(50),Y(50),A(50),B(50),C(50)
      DATA (X(I),Y(I),I=1,21) /
     > 0.11,0.0  , 0.12,0.09 , 0.13,0.2  , 0.14,0.34 , 0.16,0.6  ,
     > 0.18,0.86 , 0.2 ,1.1  , 0.25,1.7  , 0.3 ,2.0  , 0.35,2.3  ,
     > 0.4 ,2.4  , 0.45,2.45 , 0.5 ,2.4  , 0.6 ,2.2  , 0.7 ,1.8  ,
     > 0.8 ,1.5  , 1.0 ,1.0  , 1.5 ,0.38 , 2.0 ,0.18 , 3.0 ,0.06 ,
     > 4.0 ,0.03 /
      DO 0010 I=3,21,2
        A(I)=(Y(I)-Y(I-1))/(X(I)-X(I-1))-(Y(I-1)-Y(I-2))/(X(I-1)-X(I-2))
        A(I)=A(I)/(X(I)-X(I-2))
        B(I)=(Y(I-2)-Y(I-1))/(X(I-2)-X(I-1))-A(I)*(X(I-2)+X(I-1))
        C(I)=Y(I)-X(I)*(A(I)*X(I)+B(I))
0010 CONTINUE
      ENTRY QF2EXV(EV)
      IF (EV .LT. X(1)) THEN
        QF2EXV=0.0
        RETURN
      END IF
      DO 0020 I=3,21,2
        IF (EV .LT. X(I)) THEN
          QF2EXV=(EV*(A(I)*EV+B(I))+C(I))  *3.5355
          RETURN
        END IF
0020 CONTINUE
      QF2EXV=0.32419/(EV**1.7169)  *3.5355
      RETURN
      END
```

```
* ========== excitation cross section of F2 (A3 pi U) =================
* Hayashi M and Nimura T 1983 J.Appl.Phys. 54 4879-82
      FUNCTION SF2EX1(EV)
      REAL X(50),Y(50),A(50),B(50),C(50)
      DATA (X(I),Y(I),I=1,17) /
     >  3.16,0.0 ,  3.2,0.16 ,  3.4,0.4 ,  3.6,0.8 ,  4.0,1.6 ,
     >  4.5 ,2.5 ,  5.0,3.2  ,  6.0,4.1 ,  6.5,4.3 ,  7.0,4.3 ,
     >  8.0 ,4.1 ,  9.0,3.8  , 10.0,3.4 , 15.0,2.3 , 20.0,1.6 ,
     > 25.0 ,1.3 , 30.0,1.0  /
      DO 0010 I=3,17,2
        A(I)=(Y(I)-Y(I-1))/(X(I)-X(I-1))-(Y(I-1)-Y(I-2))/(X(I-1)-X(I-2))
        A(I)=A(I)/(X(I)-X(I-2))
        B(I)=(Y(I-2)-Y(I-1))/(X(I-2)-X(I-1))-A(I)*(X(I-2)+X(I-1))
        C(I)=Y(I)-X(I)*(A(I)*X(I)+B(I))
 0010 CONTINUE
      ENTRY QF2EX1(EV)
      IF (EV .LT. X(1)) THEN
        QF2EX1=0.0
        RETURN
      END IF
      DO 0020 I=3,17,2
        IF (EV .LT. X(I)) THEN
          QF2EX1=(EV*(A(I)*EV+B(I))+C(I))  *3.5355E-01
          RETURN
        END IF
 0020 CONTINUE
      QF2EX1=450.3/(EV**1.7964)  *3.5355E-01
      RETURN
      END
* ========== excitation cross section of F2 (A1 pi U) =================
* Hayashi M and Nimura T 1983 J.Appl.Phys. 54 4879-82
      FUNCTION SF2EX2(EV)
      REAL X(50),Y(50),A(50),B(50),C(50)
      DATA (X(I),Y(I),I=1,19) /
     >  4.34,0.0  ,  4.4,0.13 ,  4.6,0.23 ,  4.8,0.34 ,  5.0,0.5 ,
     >  5.2 ,0.8  ,  5.4,1.1  ,  5.6,1.2  ,  5.8,1.3  ,  6.0,1.4 ,
     >  6.5 ,1.55 ,  7.0,1.7  ,  8.0,1.9  , 10.0,2.05 , 12.0,2.1 ,
     > 14.0 ,2.05 , 16.0,1.95 , 20.0,1.8  , 30.0,1.6  /
      DO 0010 I=3,19,2
        A(I)=(Y(I)-Y(I-1))/(X(I)-X(I-1))-(Y(I-1)-Y(I-2))/(X(I-1)-X(I-2))
        A(I)=A(I)/(X(I)-X(I-2))
        B(I)=(Y(I-2)-Y(I-1))/(X(I-2)-X(I-1))-A(I)*(X(I-2)+X(I-1))
        C(I)=Y(I)-X(I)*(A(I)*X(I)+B(I))
 0010 CONTINUE
      ENTRY QF2EX2(EV)
      IF (EV .LT. X(1)) THEN
        QF2EX2=0.0
        RETURN
      END IF
      DO 0020 I=3,19,2
        IF (EV .LT. X(I)) THEN
          QF2EX2=(EV*(A(I)*EV+B(I))+C(I))  *3.5355E-01
          RETURN
        END IF
 0020 CONTINUE
      QF2EX2=10.5/(EV**0.55316)  *3.5355E-01
      RETURN
      END
* ========== excitation cross section of F2 (C1 sigma U+) =============
* Hayashi M and Nimura T 1983 J.Appl.Phys. 54 4879-82
* Hazi A U 1981 Phys.Rev.Lett. 46 918-22
      FUNCTION SF2EX3(EV)
      REAL X(50),Y(50),A(50),B(50),C(50)
      DATA (X(I),Y(I),I=1,15) /
     >  11.57,0.0 , 12.0,0.15 , 13.0,0.44 , 14.0,0.8 ,  16.0,1.6 ,
     >  18.0 ,2.4 , 20.0,3.0  , 25.0,4.0  , 30.0,4.5 ,  40.0,5.0 ,
     >  50.0 ,5.0 , 60.0,4.9  , 70.0,4.8  , 80.0,4.7 , 100.0,4.3 /
      DO 0010 I=3,15,2
        A(I)=(Y(I)-Y(I-1))/(X(I)-X(I-1))-(Y(I-1)-Y(I-2))/(X(I-1)-X(I-2))
        A(I)=A(I)/(X(I)-X(I-2))
        B(I)=(Y(I-2)-Y(I-1))/(X(I-2)-X(I-1))-A(I)*(X(I-2)+X(I-1))
        C(I)=Y(I)-X(I)*(A(I)*X(I)+B(I))
 0010 CONTINUE
      ENTRY QF2EX3(EV)
      IF (EV .LT. X(1)) THEN
        QF2EX3=0.0
        RETURN
      END IF
      DO 0020 I=3,15,2
        IF (EV .LT. X(I)) THEN
          QF2EX3=(EV*(A(I)*EV+B(I))+C(I))  *3.5355E-01
          RETURN
        END IF
 0020 CONTINUE
      QF2EX3=47.045/(EV**0.51952)  *3.5355E-01
      RETURN
      END
```

```
* ========== excitation cross section of F2 (H1 pi U) =================
* Hayashi M and Nimura T 1983 J.Appl.Phys. 54 4879-82
* Hazi A U 1981 Phys.Rev.Lett. 46 918-22
      FUNCTION SF2EX4(EV)
      REAL X(50),Y(50),A(50),B(50),C(50)
      DATA (X(I),Y(I),I=1,17) /
     >  13.08,0.0 ,  13.5,0.25 , 14.0,0.31 ,  16.0,0.52 ,  18.0,0.85 ,
     >  20.0 ,1.4 ,  25.0,2.7  , 30.0,4.0  ,  40.0,5.8  ,  50.0,6.8  ,
     >  60.0 ,7.1 ,  70.0,7.2  , 80.0,7.2  , 100.0,7.2  , 120.0,6.9  ,
     > 150.0 ,6.3 , 200.0,5.4  /
      DO 0010 I=3,17,2
        A(I)=(Y(I)-Y(I-1))/(X(I)-X(I-1))-(Y(I-1)-Y(I-2))/(X(I-1)-X(I-2))
        A(I)=A(I)/(X(I)-X(I-2))
        B(I)=(Y(I-2)-Y(I-1))/(X(I-2)-X(I-1))-A(I)*(X(I-2)+X(I-1))
        C(I)=Y(I)-X(I)*(A(I)*X(I)+B(I))
 0010 CONTINUE
      ENTRY QF2EX4(EV)
      IF (EV .LT. X(1)) THEN
        QF2EX4=0.0
        RETURN
      END IF
      DO 0020 I=3,17,2
        IF (EV .LT. X(I)) THEN
          QF2EX4=(EV*(A(I)*EV+B(I))+C(I))  *3.5355E-02
          RETURN
        END IF
 0020 CONTINUE
      QF2EX4=242.56/(EV**0.71812)  *3.5355E-02
      RETURN
      END
* ========== ionization cross section of F2 ============================
* Hayashi M and Nimura T 1983 J.Appl.Phys. 54 4879-82
      FUNCTION SF2ION(EV)
      REAL X(50),Y(50),A(50),B(50),C(50)
      DATA (X(I),Y(I),I=1,23) /
     >  15.69,0.0 ,  16.0,0.015,  17.0,0.03,  18.0,0.06,  20.0,0.1 ,
     >  22.0 ,0.17,  24.0,0.23 ,  26.0,0.29,  28.0,0.36,  30.0,0.45,
     >  35.0 ,0.58,  40.0,0.68 ,  50.0,0.88,  60.0,1.01,  70.0,1.1 ,
     >  80.0 ,1.18,  90.0,1.22 , 100.0,1.25, 120.0,1.25, 150.0,1.2 ,
     > 200.0 ,1.15, 250.0,1.1  , 300.0,1.0 /
      DO 0010 I=3,23,2
        A(I)=(Y(I)-Y(I-1))/(X(I)-X(I-1))-(Y(I-1)-Y(I-2))/(X(I-1)-X(I-2))
        A(I)=A(I)/(X(I)-X(I-2))
        B(I)=(Y(I-2)-Y(I-1))/(X(I-2)-X(I-1))-A(I)*(X(I-2)+X(I-1))
        C(I)=Y(I)-X(I)*(A(I)*X(I)+B(I))
 0010 CONTINUE
      ENTRY QF2ION(EV)
      IF (EV .LT. X(1)) THEN
        QF2ION=0.0
        RETURN
      END IF
      DO 0020 I=3,23,2
        IF (EV .LT. X(I)) THEN
          QF2ION=(EV*(A(I)*EV+B(I))+C(I))  *3.5355
          RETURN
        END IF
 0020 CONTINUE
      QF2ION=35.762/(EV**0.62711)  *3.5355
      RETURN
      END
* ========== attachment cross section of F2 ============================
* Hazi A U 1981 Phys.Rev.Lett. 46 918-22
      FUNCTION SF2ATT(EV)
      REAL X(50),Y(50),A(50),B(50),C(50)
      DATA ( X(I),Y(I),I=1,21 ) /
     > 0.0001,3.0 , 0.0003,3.0  , 0.001,3.0  , 0.002,4.4    ,
     > 0.004 ,5.2 , 0.01  ,5.6  , 0.03 ,6.15 , 0.1  ,6.8    ,
     > 0.15  ,7.0 , 0.2   ,7.0  , 0.25 ,6.8  , 0.35 ,5.8    ,
     > 0.5   ,4.0 , 0.6   ,2.8  , 0.75 ,1.75 , 1.0  ,0.75   ,
     > 1.25  ,0.3 , 1.5   ,0.13 , 1.8  ,0.04 , 1.801,0.03987,
     > 2.101 ,0.0 /
      DO 0010 I=3,21,2
        A(I)=(Y(I)-Y(I-1))/(X(I)-X(I-1))-(Y(I-1)-Y(I-2))/(X(I-1)-X(I-2))
        A(I)=A(I)/(X(I)-X(I-2))
        B(I)=(Y(I-2)-Y(I-1))/(X(I-2)-X(I-1))-A(I)*(X(I-2)+X(I-1))
        C(I)=Y(I)-X(I)*(A(I)*X(I)+B(I))
 0010 CONTINUE
      ENTRY QF2ATT(EV)
      IF ((EV .LT. X(1)) .OR. (EV.GE.X(21))) THEN
        QF2ATT=0.0
        RETURN
      END IF
      DO 0020 I=3,21,2
        IF (EV .LT. X(I)) THEN
          QF2ATT=(EV*(A(I)*EV+B(I))+C(I))  *3.5355
          RETURN
        END IF
 0020 CONTINUE
      QF2ATT=0.0
      RETURN
      END
```

B.3 Drift Equilibrium $F(\epsilon)$ in Ar (pulsed Townsend condition)

```
* ======================================================================
*  "Propagator Method" for pulsed Townsend conditions
*
*  Hirotake Sugawara 1993.11.12.
*  Applied Electricity Laboratory,
*  Dept.of Electrical Eng., Hokkaido Univ., N13 W8 Sapporo 060 Japan
*  TEL 011-706-6482, FAX 011-706-7890, sgwr@e5.hines.hokudai.ac.jp
* ======================================================================
* ---------- initial setting ------------------------------------------
      PARAMETER ( NENG=1000        , NANG=100         , NAHF=NANG/2      ,
     >            EBYP=500.0       , GPRS=1.0         , EMAX=150.0       ,
     >            TLIM=04.000E-09  , TSM0=04.000E-09  ,
     >            TSM1=00.040E-09  , TUNT=000.05E-12  ,
     >            DENG=EMAX/(NENG*1.0)                ,
     >            EEXM=11.55       , KEXM=EEXM/DENG+0.5                ,
     >            EEXC=12.9        , KEXC=EEXC/DENG+0.5                ,
     >            EION=15.76       , KION=EION/DENG+0.5                ,
     >            NSUP=NENG+KION+1                     ,
     >            ECHG=1.602E-19   , EMAS=9.109E-28   )
      REAL FET0(-1:NENG,0:NANG),FET1(-1:NENG,0:NANG),
     >     RAC0(-1:NENG,0:NANG),RAC1(-1:NENG,0:NANG),
     >     RAC2(-1:NENG,0:NANG)
      REAL FEI0(0:NSUP),FEI1(0:NSUP),FISM(0:NSUP),RSCT(0:NANG),
     >     QMOM(0:NSUP),FMOM(0:NSUP),
     >     QEXM(0:NSUP),FEXM(0:NSUP),
     >     QEXC(0:NSUP),FEXC(0:NSUP),
     >     QION(0:NSUP),FION(0:NSUP),GION(0:NSUP),
     >     QTTL(0:NSUP),FNUL(0:NSUP)
      REAL BENG(0:NSUP),CENG(0:NSUP),
     >     BVLC(0:NSUP),CVLC(0:NSUP),
     >     BANG(0:NANG),CANG(0:NANG),
     >     BSIN(0:NANG),CSIN(0:NANG),
     >     BCOS(0:NANG),CCOS(0:NANG),
     >     CP00(0:NANG),CP01(0:NANG),CP02(0:NANG),
     >     CP03(0:NANG),CP04(0:NANG),CP05(0:NANG)
      REAL FE00(0:NENG),FE01(0:NENG),FE02(0:NENG),
     >     FE03(0:NENG),FE04(0:NENG),FE05(0:NENG)
* ---------- constants -----------------------------------------------
      PI00=ATAN(1.0)*4.0
      DANG=PI00/REAL(NANG)
      FCEV=2.0*ECHG/EMAS*1.0E+07
      FCVE=0.5*EMAS/ECHG*1.0E-07
      EFLD=EBYP*GPRS
      DACC=ECHG*EFLD/EMAS*1.0E+07  *TUNT
      NIT0=NINT(TLIM/TSM0)
      NIT1=NINT(TSM0/TSM1)
      NIT2=NINT(TSM1/TUNT)
      DO 0010 IENG=0,NENG
        BENG(IENG)=DENG*REAL(IENG)
        BVLC(IENG)=SQRT(BENG(IENG)*FCEV)
 0010 CONTINUE
      DO 0020 IENG=0,NENG-1
        CVLC(IENG)=(BVLC(IENG)+BVLC(IENG+1))*0.5
        CENG(IENG)=CVLC(IENG)**2*FCVE
 0020 CONTINUE
      DO 0030 IANG=0,NANG
        BANG(IANG)=REAL(IANG)*DANG
        BSIN(IANG)=SIN(BANG(IANG))
        BCOS(IANG)=COS(BANG(IANG))
        CANG(IANG)=(REAL(IANG)+0.5)*DANG
        CSIN(IANG)=SIN(CANG(IANG))
        CCOS(IANG)=COS(CANG(IANG))
        CP00(IANG)=1.0
        CP01(IANG)=CCOS(IANG)
        CP02(IANG)=(CCOS(IANG)*CP01(IANG)* 3.0-CP00(IANG)* 1.0)/ 2.0
        CP03(IANG)=(CCOS(IANG)*CP02(IANG)* 5.0-CP01(IANG)* 2.0)/ 3.0
        CP04(IANG)=(CCOS(IANG)*CP03(IANG)* 7.0-CP02(IANG)* 3.0)/ 4.0
        CP05(IANG)=(CCOS(IANG)*CP04(IANG)* 9.0-CP03(IANG)* 4.0)/ 5.0
 0030 CONTINUE
* ---------- arrays for collisions -----------------------------------
      QDMY=SARMOM(0.0)+SAREXC(0.0)+SAREXM(0.0)+SARION(0.0)+QDMY
      DO 0040 IENG=0,NENG-1
        QMOM(IENG)=QARMOM(CENG(IENG))  *GPRS
        QEXM(IENG)=QAREXM(CENG(IENG))  *GPRS
        QEXC(IENG)=QAREXC(CENG(IENG))  *GPRS
        QION(IENG)=QARION(CENG(IENG))  *GPRS
 0040 CONTINUE
```

Constants and Variables

`NENG` the number of divisions for ϵ
`NANG` the number of divisions for θ

`EBYP` E/p ($\mathrm{Vcm^{-1}Torr^{-1}}$)
`GPRS` the gas pressure p (Torr)
`EMAX` ϵ_{max} (eV)

`TLIM` the simulation time (s)
`TSM0` the sampling interval (s) for $F(\epsilon)$
`TSM1` the sampling interval (s) for electron swarm parameters
`TUNT` the time step Δt (s)

`DENG` the cell width $\Delta\epsilon$ (eV)
`EEXC` ϵ_{ex} (eV)
`EEXM` $\epsilon_{ex,meta}$ (eV)
`EION` ϵ_{ion} (eV)
`KEXC` $\epsilon_{ex}/\Delta\epsilon$
`KEXM` $\epsilon_{ex,meta}/\Delta\epsilon$
`KION` $\epsilon_{ion}/\Delta\epsilon$
`NSUP` the number of divisions for ϵ with margin

`ECHG` $e = 1.602 \times 10^{-19}$ C
`EMAS` $m = 9.109 \times 10^{-28}$ g

`PI00` $\pi = 3.14159265\cdots$
`DANG` the cell width $\Delta\theta$ (rad)

`FCEV` $v_1 = 5.79 \times 10^7$ $\mathrm{cms^{-1}}$
`FCVE` $1/v_1$
`EFLD` the electric field E ($\mathrm{Vcm^{-1}}$)
`DACC` the acceleration $a\Delta t$ ($\mathrm{cms^{-1}}$)

`NIT0,NIT1,NIT2` iteration cycles

`IENG` subscript i of ϵ_i and v_i

`BENG` $\epsilon_i = i\Delta\epsilon$ (eV)
`BVLC` $v_i = \sqrt{2\epsilon_i/m}$ ($\mathrm{cms^{-1}}$)
`CVLC` $\bar{v}_i$ ($\mathrm{cms^{-1}}$)
`CENG` $\bar{\epsilon}_i$ (eV)

`IANG` subscript j of θ_j

`BANG` $\theta_j = j\Delta\theta$ (rad)
`BSIN` $\sin\theta_j$
`BCOS` $\cos\theta_j$
`CANG` $\bar{\theta}_j$ (rad)
`CCOS` $\cos\bar{\theta}_j$

`CP00,CP01,CP02,CP03,CP04,CP05` Legendre's polynomials $P_n(\cos\bar{\theta}_j)$ $(n = 0, \cdots, 5)$

`QDMY` a dummy variable for initialization of function subprograms

`QMOM` $Nq_{\mathrm{mom}}(\epsilon)$ ($\mathrm{cm^{-1}}$)
`QEXC` $Nq_{\mathrm{ex}}(\epsilon)$ ($\mathrm{cm^{-1}}$)
`QEXM` $Nq_{\mathrm{ex,meta}}(\epsilon)$ ($\mathrm{cm^{-1}}$)
`QION` $Nq_{\mathrm{ion}}(\epsilon)$ ($\mathrm{cm^{-1}}$)

```
      DO 0050 IENG=0,NENG-1
        QTTL(IENG)=QMOM(IENG)+QEXM(IENG)+QEXC(IENG)+QION(IENG)
        FNUL(IENG)=EXP(-QTTL(IENG)*CVLC(IENG)*TUNT)
        FCOL      =(1.0-FNUL(IENG))/QTTL(IENG)
        FMOM(IENG)=FCOL*QMOM(IENG)
        FEXM(IENG)=FCOL*QEXM(IENG)
        FEXC(IENG)=FCOL*QEXC(IENG)
        FION(IENG)=FCOL*QION(IENG)
        GION(IENG)=FION(IENG)/REAL(DIM(IENG,KION)*2+1)*2.0
 0050 CONTINUE
      DO 0060 IANG=0,NANG-1
        RSCT(IANG)=(BCOS(IANG)-BCOS(IANG+1))*0.5
 0060 CONTINUE
* ---------- arrays for acceleration ---------------------------------
      PI23=PI00*2.0/3.0
      DO 0070 IANG=0,NAHF-1
      DO 0070 IENG=0,NENG-1
        RCEL           =PI23 *(BVLC(IENG+1)**3-BVLC(IENG)**3)
     >                       *(BCOS(IANG)-BCOS(IANG+1))
        RAC1(IENG,IANG)=PI00 *(BVLC(IENG+1)**2-BVLC(IENG)**2)
     >                       *BSIN(IANG)**2                      *DACC/RCEL
        RAC2(IENG,IANG)=PI00 *BVLC(IENG+1)**2
     >                       *(BSIN(IANG+1)**2-BSIN(IANG)**2) *DACC/RCEL
        RAC0(IENG,IANG)=1.0-RAC1(IENG,IANG)-RAC2(IENG,IANG)
 0070 CONTINUE
      DO 0080 IANG=NAHF,NANG-1
      DO 0080 IENG=   0,NENG-1
        RCEL           =PI23 *(BVLC(IENG+1)**3-BVLC(IENG)**3)
     >                       *(BCOS(IANG)-BCOS(IANG+1))
        RAC1(IENG,IANG)=PI00 *(BVLC(IENG+1)**2-BVLC(IENG)**2)
     >                       *BSIN(IANG)**2                      *DACC/RCEL
        RAC2(IENG,IANG)=PI00 *BVLC(IENG)**2
     >                       *(BSIN(IANG)**2-BSIN(IANG+1)**2) *DACC/RCEL
        RAC0(IENG,IANG)=1.0-RAC1(IENG,IANG)-RAC2(IENG,IANG)
 0080 CONTINUE
      DO 0090 IANG=0,NANG-1
      DO 0090 IENG=0,NENG-1
        IF (RAC0(IENG,IANG) .LT. 0.0) THEN
          WRITE(6,*) 'ratio negative : cell No.(E,A) ',IENG,IANG
          WRITE(6,*) RAC0(IENG,IANG),RAC1(IENG,IANG),RAC2(IENG,IANG)
          STOP
        END IF
 0090 CONTINUE
* ---------- initial condition ----------------------------------------
      SPN0=1.0
      FET0(0,0)=0.5*SPN0
      WRITE(40,'(I5,X,I5)') 7,NIT0*NIT1+1
      WRITE(40,'(''time (ns)''                              )')
      WRITE(40,'(''electron number''                        )')
      WRITE(40,'(''ionization frequency (~ms^-^1)''         )')
      WRITE(40,'(''mean energy (eV)''                       )')
      WRITE(40,'(''drift velocity Wv (cm/~ms)''             )')
      WRITE(40,'(''diffusion coefficient Dv (cm^2/~ms)''    )')
      WRITE(40,'(''diffusion coefficient Dv_/_/ (cm^2/~ms)'')')
      WRITE(40,'(''diffusion coefficient Dv_T (cm^2/~ms)''  )')
      WRITE(40,'(    5(E12.6,X))') 0.0 , SPN0, 0.0 , 0.0 , 0.0
      WRITE(40,'(12X,3(X,E12.6))') 0.0 , 0.0 , 0.0
* ---------- passage of time ------------------------------------------
      DO 0280 IIT0=0,NIT0-1
      DO 0230 IIT1=0,NIT1-1
      DO 0160 IIT2=0,NIT2-1
* ---------- collision & scattering -----------------------------------
      DO 0100 IENG=0,NENG-1
        FEI0(IENG)=0.0
 0100 CONTINUE
      DO 0110 IANG=0,NANG-1
      DO 0110 IENG=0,NENG-1
        FEI0(IENG)=FEI0(IENG)+FET0(IENG,IANG)
 0110 CONTINUE
      FISM(NENG)=0.0
      DO 0120 IENG=NENG-1,0,-1
        FISM(IENG)=FISM(IENG+1)
     >            +FEI0(IENG+KION  )*GION(IENG+KION  )
     >            +FEI0(IENG+KION+1)*GION(IENG+KION+1)
        FEI1(IENG)=FEI0(IENG       )*FMOM(IENG       )
     >            +FEI0(IENG+KEXM  )*FEXM(IENG+KEXM  )
     >            +FEI0(IENG+KEXC  )*FEXC(IENG+KEXC  )
     >            +FISM(IENG)
 0120 CONTINUE
      DO 0130 IANG=0,NANG-1
      DO 0130 IENG=0,NENG-1
        FET1(IENG,IANG)=FET0(IENG,IANG)*FNUL(IENG)+FEI1(IENG)*RSCT(IANG)
 0130 CONTINUE
```

Constants and Variables

QTTL	$Nq_T(\epsilon)$ (cm^{-1})
FNUL	the probability of no collision
FMOM,FEXM,FEXC,FION	the ratios of colliding electrons
GION	the distribution ratio of electrons after ionization
RSCT	the scattering ratio $(1/2)\sin\theta\Delta\theta$
RCEL	the volume of a cell $(cms^{-1})^3$
RDR0	the ratio of electrons remaining in $C_{l,i,j}$
RDR1	the ratio of electrons flowing out of $C_{l,i,j}$ to $C_{l,i,j+1}$
RDR2	the ratio of electrons flowing out of $C_{l,i,j}$ to $C_{l\pm1,i\pm1,j}$
SPN0	the number of initial electrons
FET0	$F(\epsilon,\theta)$ before collision
FEI0	$F(\epsilon)$ before collision
FISM	the number of electrons after ionization
FEI1	$F(\epsilon)$ after collision
FET1	$F(\epsilon,\theta)$ after collision

```
* ---------- acceleration ------------------------------------------------
      DO 0140 IANG=0,NAHF-1
      DO 0140 IENG=0,NENG-1
        FET0(IENG,IANG)=FET1(IENG  ,IANG  )*RAC0(IENG  ,IANG  )
     >                 +FET1(IENG  ,IANG+1)*RAC1(IENG  ,IANG+1)
     >                 +FET1(IENG-1,IANG  )*RAC2(IENG-1,IANG  )
 0140 CONTINUE
      DO 0150 IANG=NAHF,NANG-1
      DO 0150 IENG=   0,NENG-1
        FET0(IENG,IANG)=FET1(IENG  ,IANG  )*RAC0(IENG  ,IANG  )
     >                 +FET1(IENG  ,IANG+1)*RAC1(IENG  ,IANG+1)
     >                 +FET1(IENG+1,IANG  )*RAC2(IENG+1,IANG  )
 0150 CONTINUE
 0160 CONTINUE
* ---------- sampling (interval TSM1) ------------------------------------
      DO 0170 IANG=0,NANG-1
      DO 0170 IENG=0,NENG-1
        FET1(IENG,IANG)=FET1(IENG,IANG)+FET0(IENG,IANG)
 0170 CONTINUE
      DO 0180 IENG=0,NENG-1
        FE00(IENG)=0.0
 0180 CONTINUE
      SPNE=0.0
      SPME=0.0
      SPWV=0.0
      SPDV=0.0
      SPDX=0.0
      SPDR=0.0
      DO 0190 IANG=0,NANG-1
      DO 0190 IENG=0,NENG-1
        FE00(IENG)=FE00(IENG)+FET1(IENG,IANG)
 0190 CONTINUE
      DO 0200 IENG=0,NENG-1
        SPNE=SPNE+FE00(IENG)
 0200 CONTINUE
      SPRI=ALOG(SPNE/SPN0)/TSM1
      DO 0210 IANG=0,NANG-1
      DO 0210 IENG=0,NENG-1
        SPWV=SPWV+FET1(IENG,IANG)* CVLC(IENG)*CCOS(IANG)
        SPDX=SPDX+FET1(IENG,IANG)*(CVLC(IENG)*CCOS(IANG))**2
     >           /(QTTL(IENG)*CVLC(IENG)+SPRI)
        SPDR=SPDR+FET1(IENG,IANG)*(CVLC(IENG)*CSIN(IANG))**2
     >           /(QTTL(IENG)*CVLC(IENG)+SPRI)
 0210 CONTINUE
      DO 0220 IENG=0,NENG-1
        SPME=SPME+FE00(IENG)*CENG(IENG)
        SPDV=SPDV+FE00(IENG)*CVLC(IENG)**2/(QTTL(IENG)*CVLC(IENG)+SPRI)
 0220 CONTINUE
      SPRI=SPRI           *1.0E-06
      SPN0=SPNE
      SPME=SPME/SPNE
      SPWV=SPWV/SPNE      *1.0E-06
      SPDV=SPDV/SPNE/3.0  *1.0E-06
      SPDX=SPDX/SPNE      *1.0E-06
      SPDR=SPDR/SPNE/2.0  *1.0E-06
      WRITE(40,'(    5(E12.6,X))') (IIT0*TSM0+(IIT1+1)*TSM1)*1.0E+09,
     >                             SPNE,SPRI,SPME,SPWV
      WRITE(40,'(13X,3(E12.6,X))') SPDV,SPDX,SPDR
 0230 CONTINUE
* ---------- sampling (interval TSM0) ------------------------------------
      DO 0240 IENG=0,NENG-1
        FE00(IENG)=0.0
        FE01(IENG)=0.0
        FE02(IENG)=0.0
        FE03(IENG)=0.0
        FE04(IENG)=0.0
        FE05(IENG)=0.0
 0240 CONTINUE
      DO 0250 IANG=0,NANG-1
      DO 0250 IENG=0,NENG-1
        FE00(IENG)=FE00(IENG)+FET1(IENG,IANG)*CP00(IANG)
        FE01(IENG)=FE01(IENG)+FET1(IENG,IANG)*CP01(IANG)
        FE02(IENG)=FE02(IENG)+FET1(IENG,IANG)*CP02(IANG)
        FE03(IENG)=FE03(IENG)+FET1(IENG,IANG)*CP03(IANG)
        FE04(IENG)=FE04(IENG)+FET1(IENG,IANG)*CP04(IANG)
        FE05(IENG)=FE05(IENG)+FET1(IENG,IANG)*CP05(IANG)
 0250 CONTINUE
      FNRM=1.0/(SPNE*DENG)
      DO 0260 IENG=0,NENG-1
        FE00(IENG)=FE00(IENG)*FNRM* 1.0
        FE01(IENG)=FE01(IENG)*FNRM* 3.0
        FE02(IENG)=FE02(IENG)*FNRM* 5.0
        FE03(IENG)=FE03(IENG)*FNRM* 7.0
        FE04(IENG)=FE04(IENG)*FNRM* 9.0
        FE05(IENG)=FE05(IENG)*FNRM*11.0
 0260 CONTINUE
```

Constants and Variables

SPNE	the number of electrons n
SPME	the mean electron energy $\bar{\epsilon}$ (eV)
SPWV	the drift velocity $W_{\rm v}$ (cmμs^{-1})
SPDV	the diffusion coefficient $D_{\rm v}$ (cm$^2\mu$s^{-1})
SPDX	the diffusion coefficient $D_{{\rm v},\parallel}$ (cm$^2\mu$s^{-1})
SPDR	the diffusion coefficient $D_{{\rm v},\perp}$ (cm$^2\mu$s^{-1})
SPRI	the ionization frequency $R_{\rm ion}$ (μs^{-1})

FE00,FE01,FE02,FE03,FE04,FE05
: Legendre's polynomial expansion terms of $F(\epsilon)$; $F_n(\epsilon)$ $(n = 0, \cdots, 5)$

```
      WRITE(41,'(I5,X,I5)') 6,NENG+1
      WRITE(41,'(''electron energy (eV) (t='',F8.3,''ns)'')')
     >     (IIT0+1)*TSM0*1.0E+09
      WRITE(41,'(''energy distribution F_0'')')
      WRITE(41,'(''energy distribution F_1'')')
      WRITE(41,'(''energy distribution F_2'')')
      WRITE(41,'(''energy distribution F_3'')')
      WRITE(41,'(''energy distribution F_4'')')
      WRITE(41,'(''energy distribution F_5'')')
      WRITE(41,'(  F12.6   )') 0.0
      WRITE(41,'(6(E12.6,X))') 0.0 , 0.0 , 0.0 , 0.0 , 0.0 , 0.0
      DO 0270 IENG=0,NENG-1
        WRITE(41,'(  F12.6   )') (REAL(IENG)+0.5)*DENG
        WRITE(41,'(6(E12.6,X))') FE00(IENG),FE01(IENG),FE02(IENG),
     >                           FE03(IENG),FE04(IENG),FE05(IENG)
 0270 CONTINUE
 0280 CONTINUE
      STOP
      END
* ========== momentum transfer cross section of Ar ====================
* Suzuki M, Taniguchi T and Tagashira H
* 1990 J.Phys.D: Appl.Phys. 23 842-50
      FUNCTION SARMOM(EV)
      REAL X(50),Y(50),A(50),B(50),C(50)
      DATA (X(I),Y(I),I=1,17) /
     >  0.3, 0.37 ,  0.4, 0.42 , 0.5, 0.49 ,  1.0,1.16 ,  2.0, 2.69 ,
     >  5.0, 7.52 ,  9.0,13.6  ,10.0,14.7  , 12.0,15.8 , 14.0,15.0  ,
     > 16.0,14.0  , 20.0,11.48 ,25.0, 9.33 , 30.0,7.92 , 40.0, 6.22 ,
     > 50.0, 5.09 , 62.5, 4.18 /
      DO 0010 I=3,17,2
        A(I)=(Y(I)-Y(I-1))/(X(I)-X(I-1))-(Y(I-1)-Y(I-2))/(X(I-1)-X(I-2))
        A(I)=A(I)/(X(I)-X(I-2))
        B(I)=(Y(I-2)-Y(I-1))/(X(I-2)-X(I-1))-A(I)*(X(I-2)+X(I-1))
        C(I)=Y(I)-X(I)*(A(I)*X(I)+B(I))
 0010 CONTINUE
      ENTRY QARMOM(EV)
      IF (EV .LT. X(1)) THEN
        QARMOM=(0.141/(EV+0.001)+(1.55*EV)-0.566)  *3.5355
        RETURN
      END IF
      DO 0020 I=3,17,2
        IF (EV .LT. X(I)) THEN
          QARMOM=(EV*(A(I)*EV+B(I))+C(I))  *3.5355
          RETURN
        END IF
 0020 CONTINUE
      QARMOM=261.25/EV  *3.5355
      RETURN
      END
* ========== excitation cross section of Ar (excitation) ===============
* Zetner P W, Westerveld W B, King G C and McConkey J W,
* 1986 J.Phys.B: At.Mol.Phys. 19 4205-13
      FUNCTION SAREXC(EV)
      REAL X(50),Y(50),A(50),B(50),C(50)
      DATA (X(I),Y(I),I=1,21) /
     >  12.9,0.0  , 13.0,0.8 , 13.1,0.84 , 13.2,0.88 , 13.5,1.0 ,
     >  14.0,1.15 , 14.5,1.3 , 15.0,1.4  , 16.0,1.5  , 18.0,1.8 ,
     >  20.0,2.7  , 23.0,4.1 , 25.0,4.65 , 27.0,5.1  , 30.0,5.6 ,
     >  32.0,5.7  , 36.0,5.7 , 40.0,5.5  , 50.0,4.8  , 60.0,4.2 ,
     >  70.0,3.6  /
      DO 0010 I=3,21,2
        A(I)=(Y(I)-Y(I-1))/(X(I)-X(I-1))-(Y(I-1)-Y(I-2))/(X(I-1)-X(I-2))
        A(I)=A(I)/(X(I)-X(I-2))
        B(I)=(Y(I-2)-Y(I-1))/(X(I-2)-X(I-1))-A(I)*(X(I-2)+X(I-1))
        C(I)=Y(I)-X(I)*(A(I)*X(I)+B(I))
 0010 CONTINUE
      ENTRY QAREXC(EV)
      IF (EV .LT. X(1)) THEN
        QAREXC=0.0
        RETURN
      END IF
      DO 0020 I=3,21,2
        IF (EV .LT. X(I)) THEN
          QAREXC=(EV*(A(I)*EV+B(I))+C(I))  *3.5355E-01
          RETURN
        END IF
 0020 CONTINUE
      QAREXC=256.376/(EV**1.004)  *3.5355E-01
      RETURN
      END
```

```
* ========== excitation cross section of Ar (metastable) ===============
* Sakai Y, Tagashira H and Sakamoto S,
* 1972 J.Phys.B: At.Mol.Phys. 20 1010-6
      FUNCTION SAREXM(EV)
      REAL X(50),Y(50),A(50),B(50),C(50)
      DATA (X(I),Y(I),I=1,23) /
     > 11.55,0.0   , 11.8,0.008 , 12.0,0.01 , 12.3,0.02 , 12.6,0.04 ,
     > 13.0 ,0.075 , 13.5,0.15  , 14.0,0.3  , 14.5,0.75 , 15.0,1.5  ,
     > 16.0 ,3.5   , 16.5,4.7   , 17.0,4.9  , 17.2,5.0  , 17.3,5.0  ,
     > 17.4 ,5.0   , 18.0,4.95  , 18.5,4.9  , 19.0,4.85 , 20.0,4.75 ,
     > 23.0 ,4.7   , 25.0,4.5   , 30.0,3.75 /
      DO 0010 I=3,23,2
        A(I)=(Y(I)-Y(I-1))/(X(I)-X(I-1))-(Y(I-1)-Y(I-2))/(X(I-1)-X(I-2))
        A(I)=A(I)/(X(I)-X(I-2))
        B(I)=(Y(I-2)-Y(I-1))/(X(I-2)-X(I-1))-A(I)*(X(I-2)+X(I-1))
        C(I)=Y(I)-X(I)*(A(I)*X(I)+B(I))
 0010 CONTINUE
      ENTRY QAREXM(EV)
      IF (EV .LT. X(1)) THEN
        QAREXM=0.0
        RETURN
      END IF
      DO 0020 I=3,23,2
        IF (EV .LT. X(I)) THEN
          QAREXM=(EV*(A(I)*EV+B(I))+C(I))  *3.5355E-01
          RETURN
        END IF
 0020 CONTINUE
      QAREXM=429.78/(EV**1.394)  *3.5355E-01
      RETURN
      END
* ========== ionization cross section of Ar ============================
* Montague R G, Harrison M F A and Smith A C H
* 1984 J.Phys.B: At.Mol.Phys. 17 3295-310
      FUNCTION SARION(EV)
      REAL X(50),Y(50),A(50),B(50),C(50)
      DATA (X(I),Y(I),I=1,23) /
     >  15.76,0.0 , 16.0,0.04 , 16.7,0.125 , 18.0,0.29 , 20.0,0.63 ,
     >  22.0 ,0.93, 24.0,1.18 , 26.0,1.41  , 28.0,1.6  , 30.0,1.8  ,
     >  34.0 ,2.11, 36.0,2.24 , 40.0,2.39  , 45.0,2.49 , 50.0,2.54 ,
     >  60.0 ,2.66, 70.0,2.77 , 80.0,2.84  , 90.0,2.86 ,100.0,2.85 ,
     > 120.0 ,2.8 ,150.0,2.68 ,300.0,1.98  /
      DO 0010 I=3,23,2
        A(I)=(Y(I)-Y(I-1))/(X(I)-X(I-1))-(Y(I-1)-Y(I-2))/(X(I-1)-X(I-2))
        A(I)=A(I)/(X(I)-X(I-2))
        B(I)=(Y(I-2)-Y(I-1))/(X(I-2)-X(I-1))-A(I)*(X(I-2)+X(I-1))
        C(I)=Y(I)-X(I)*(A(I)*X(I)+B(I))
 0010 CONTINUE
      ENTRY QARION(EV)
      IF (EV .LT. X(1)) THEN
        QARION=0.0
        RETURN
      END IF
      DO 0020 I=3,23,2
        IF (EV .LT. X(I)) THEN
          QARION=(EV*(A(I)*EV+B(I))+C(I))  *3.5355
          RETURN
        END IF
 0020 CONTINUE
      QARION=64.226/(EV**0.61)  *3.5355
      RETURN
      END
```

B.4 $F(\epsilon)$ in SF_6 in the Upstream Region

```
* ======================================================================
*  "Propagator Method" for steady-state Townsend conditions
*  (backward diffusion to the upstream region of an electron source)
*
*  Hirotake Sugawara 1994.01.07.-1994.04.10.
*  Applied Electricity Laboratory,
*  Dept.of Electrical Eng., Hokkaido Univ., N13 W8 Sapporo 060 Japan
*  TEL 011-706-6482, FAX 011-706-7890, sgwr@e5.hines.hokudai.ac.jp
* ======================================================================
* ---------- initial setting ---------------------------------------------
      PARAMETER ( NENG=3000                 , NANG=36                 ,
     >            NAHF=NANG/2               , NDIV=10                 ,
     >            EBYP=50.0                 , EMAX=30.0               ,
     >            TLIM=0050.000E-09         , TSM0=0050.000E-09       ,
     >            TSM1=0000.500E-09         , TUNT=0000.500E-12       ,
     >            GPRS=1.0                  )
      PARAMETER ( DENG=EMAX/(NENG*1.0)      ,
     >            EEXC= 9.8                 , NEXC=EEXC/DENG+0.5      ,
     >            EEXV= 0.095               , NEXV=EEXV/DENG+0.5      ,
     >            EION=15.8                 , NION=EION/DENG+0.5      ,
     >            NSUP=NENG+NION+1          ,
     >            ECHG=1.602E-19            , EMAS=9.109E-28          )
      PARAMETER ( ENBC=DENG*1.000E-05       , FEME=5.0                )
      REAL    FET0(-1:NENG,0:NANG),FET1(-1:NENG,0:NANG),
     >        RDR0(-1:NENG,0:NANG),RDR1(-1:NENG,0:NANG),
     >        RDR2(-1:NENG,0:NANG)
      REAL    FEI0(0:NSUP),FEI1(0:NSUP),RSCT(0:NANG),
     >        QMOM(0:NSUP),FMOM(0:NSUP),
     >        QEXC(0:NSUP),FEXC(0:NSUP),
     >        QEXV(0:NSUP),FEXV(0:NSUP),
     >        QION(0:NSUP),FION(0:NSUP),GION(0:NSUP),
     >        QATT(0:NSUP),FATT(0:NSUP),
     >        QTTL(0:NSUP),FNUL(0:NSUP),FCOL
      REAL    BENG(0:NSUP),CENG(0:NSUP),
     >        BVLC(0:NSUP),CVLC(0:NSUP),
     >        BANG(0:NANG),CANG(0:NANG),
     >        BSIN(0:NANG),
     >        BCOS(0:NANG),CCOS(0:NANG),
     >        CP02(0:NANG),CP03(0:NANG),CP04(0:NANG),CP05(0:NANG)
      REAL    FE00(0:NENG),FE01(0:NENG),FE02(0:NENG),
     >        FE03(0:NENG),FE04(0:NENG),FE05(0:NENG)
      REAL*8 RNEL,RFWD,RBWD,REFF,EAXP,EAXN
      REAL*8 RMOM,REXC,REXV,RION,RATT,RATE
      REAL*8 SPNE,SPME,SPVD,SPVE,SPDS,SPWS,SPV1,SPV2,SPAL
      REAL*8 FISM
* ---------- constants ---------------------------------------------------
      PI00=ATAN(1.0)*4.0
      DANG=PI00/REAL(NANG)
      FCEV=2.00*ECHG/EMAS*1.0E+07
      FCVE=0.50*EMAS/ECHG*1.0E-07
      EFLD=EBYP*GPRS
      DDRF=ECHG*EFLD/EMAS*1.0E+07  *TUNT
      DXIN=EFLD/DENG
      NIT0=NINT(TLIM/TSM0)
      NIT1=NINT(TSM0/TSM1)
      NIT2=NINT(TSM1/TUNT)
      DO 0010 IENG=0,NSUP
        BENG(IENG)=DENG*REAL(IENG)
        BVLC(IENG)=SQRT(BENG(IENG)*FCEV)
0010  CONTINUE
      DO 0020 IENG=0,NSUP-1
        CVLC(IENG)=(BVLC(IENG)+BVLC(IENG+1))*0.5
        CENG(IENG)=CVLC(IENG)**2*FCVE
0020  CONTINUE
      DO 0030 IANG=0,NANG
        BANG(IANG)=DANG*REAL(IANG)
        BSIN(IANG)=SIN(BANG(IANG))
        BCOS(IANG)=COS(BANG(IANG))
        CANG(IANG)=DANG*(REAL(IANG)+0.5)
        CCOS(IANG)=COS(CANG(IANG))
        CP02(IANG)=(CCOS(IANG)*CCOS(IANG)* 3.0-           1.0)/ 2.0
        CP03(IANG)=(CCOS(IANG)*CP02(IANG)* 5.0-CCOS(IANG)* 2.0)/ 3.0
        CP04(IANG)=(CCOS(IANG)*CP03(IANG)* 7.0-CP02(IANG)* 3.0)/ 4.0
        CP05(IANG)=(CCOS(IANG)*CP04(IANG)* 9.0-CP03(IANG)* 4.0)/ 5.0
0030  CONTINUE
```

Constants and Variables

`NENG` the number of divisions for ϵ
`NANG` the number of divisions for θ

`EBYP` E/p ($\mathrm{Vcm^{-1}Torr^{-1}}$)
`GPRS` the gas pressure p (Torr)
`EMAX` ϵ_{max} (eV)

`TLIM` the simulation time (s)
`TSM0` the sampling interval (s) for $F(\epsilon)$
`TSM1` the sampling interval (s) for electron swarm parameters
`TUNT` the time step Δt (s)

`DENG` the cell width $\Delta\epsilon$ (eV)
`EEXC` ϵ_{ex} (eV)
`EEXV` $\epsilon_{ex,v}$ (eV)
`EION` ϵ_{ion} (eV)
`KEXC` $\epsilon_{ex}/\Delta\epsilon$
`KEXV` $\epsilon_{ex,v}/\Delta\epsilon$
`KION` $\epsilon_{ion}/\Delta\epsilon$
`NSUP` the number of divisions for ϵ with margin

`ECHG` $e = 1.602 \times 10^{-19}$ C
`EMAS` $m = 9.109 \times 10^{-28}$ g

`ENBC` the boundary condition for $F(\epsilon_{max})$
`FEME` the mean electron energy (eV) for the initial electron distribution

`PI00` $\pi = 3.14159265\cdots$
`DANG` the cell width $\Delta\theta$ (rad)

`FCEV` $v_1 = 5.79 \times 10^7$ $\mathrm{cms^{-1}}$
`FCVE` $1/v_1$
`EFLD` the electric field E ($\mathrm{Vcm^{-1}}$)
`DDRF` the acceleration $a\Delta t$ ($\mathrm{cms^{-1}}$)
`DXIN` $1/\Delta x$ ($\mathrm{cm^{-1}}$)

`NIT0,NIT1,NIT2` iteration cycles

`IENG` subscript i of ϵ_i and v_i

`BENG` $\epsilon_i = i\Delta\epsilon$ (eV)
`BVLC` $v_i = \sqrt{2\epsilon_i/m}$ ($\mathrm{cms^{-1}}$)
`CVLC` $\bar{v}_i$ ($\mathrm{cms^{-1}}$)
`CENG` $\bar{\epsilon}_i$ (eV)

`IANG` subscript j of θ_j

`BANG` $\theta_j = j\Delta\theta$ (rad)
`BSIN` $\sin\theta_j$
`BCOS` $\cos\theta_j$
`CANG` $\bar{\theta}_j$ (rad)
`CCOS` $\cos\bar{\theta}_j$

`CP02,CP03,CP04,CP05` Legendre's polynomials $P_n(\cos\bar{\theta}_j)$ $(n = 2, \cdots, 5)$

```
* ---------- arrays for collisions ----------------------------------
      DO 0040 IENG=0,NENG-1
        QMOM(IENG)= QSF6MO(CENG(IENG))  *GPRS
        QEXC(IENG)= QSF6E1(CENG(IENG))  *GPRS
        QEXV(IENG)= QSF6E2(CENG(IENG))  *GPRS
        QION(IENG)= QSF6IO(CENG(IENG))  *GPRS
        QATT(IENG)=(QSF6A1(CENG(IENG))+QSF6A2(CENG(IENG))
     >             +QSF6A3(CENG(IENG))+QSF6A4(CENG(IENG))
     >             +QSF6A5(CENG(IENG))) *GPRS
 0040 CONTINUE
      DO 0050 IENG=0,NENG-1
        QTTL(IENG)=QMOM(IENG)+QEXC(IENG)+QEXV(IENG)
     >            +QION(IENG)+QATT(IENG)
        FNUL(IENG)=EXP(-QTTL(IENG)*CVLC(IENG)*TUNT)
        FCOL      =(1.0-FNUL(IENG))/QTTL(IENG)
        FMOM(IENG)=FCOL*QMOM(IENG)
        FEXC(IENG)=FCOL*QEXC(IENG)
        FEXV(IENG)=FCOL*QEXV(IENG)
        FION(IENG)=FCOL*QION(IENG)
        FATT(IENG)=FCOL*QATT(IENG)
        GION(IENG)=FION(IENG)/REAL(DIM(IENG,NION)*2+1)*2.0
 0050 CONTINUE
      DO 0060 IANG=0,NANG-1
        RSCT(IANG)=(BCOS(IANG)-BCOS(IANG+1))*0.5
 0060 CONTINUE
* ---------- arrays for acceleration --------------------------------
      PI23=PI00*2.0/3.0
      DO 0070 IANG=0,NAHF-1
      DO 0070 IENG=0,NENG-1
        RCEL           =PI23 *(BVLC(IENG+1)**3-BVLC(IENG)**3)
     >                       *(BCOS(IANG)-BCOS(IANG+1))
        RDR1(IENG,IANG)=PI00 *(BVLC(IENG+1)**2-BVLC(IENG)**2)
     >                       *BSIN(IANG)**2                    *DDRF/RCEL
        RDR2(IENG,IANG)=PI00 *BVLC(IENG+1)**2
     >                       *(BSIN(IANG+1)**2-BSIN(IANG)**2)  *DDRF/RCEL
        RDR0(IENG,IANG)=1.0-RDR1(IENG,IANG)-RDR2(IENG,IANG)
 0070 CONTINUE
      DO 0080 IANG=NAHF,NANG-1
      DO 0080 IENG=   0,NENG
        RCEL           =PI23 *(BVLC(IENG+1)**3-BVLC(IENG)**3)
     >                       *(BCOS(IANG)-BCOS(IANG+1))
        RDR1(IENG,IANG)=PI00 *(BVLC(IENG+1)**2-BVLC(IENG)**2)
     >                       *BSIN(IANG)**2                    *DDRF/RCEL
        RDR2(IENG,IANG)=PI00 *BVLC(IENG)**2
     >                       *(BSIN(IANG)**2-BSIN(IANG+1)**2)  *DDRF/RCEL
        RDR0(IENG,IANG)=1.0-RDR1(IENG,IANG)-RDR2(IENG,IANG)
 0080 CONTINUE
      DO 0090 IENG=0,NENG,NENG
      DO 0090 IANG=0,NANG-1
        IF (RDR0(IENG,IANG) .LT. 0.0) THEN
          WRITE(6,*) 'ratio negative : cell No. (E,A) ',IENG,IANG
          WRITE(6,*) RDR0(IENG,IANG),RDR1(IENG,IANG),RDR2(IENG,IANG)
          STOP
        END IF
 0090 CONTINUE
* ---------- initial condition --------------------------------------
      FMB0=2.0*PI00*(1.5/PI00/FEME)**1.5*DENG  *0.5
      FMB1=-1.5/FEME
      DO 0100 IENG=0,NENG-1
        FEI0(IENG)=FMB0*SQRT(CENG(IENG))*EXP(FMB1*CENG(IENG))
        DO 0100 IANG=0,NANG-1
          FET0(IENG,IANG)=FEI0(IENG)*RSCT(IANG)
 0100 CONTINUE
      FET1(NENG,NANG-1)=ENBC
*     DO 0110 IANG=NAHF,NANG-1
*       FET1(NENG,IANG)=RSCT(IANG)*ENBC
*0110 CONTINUE
      WRITE(40,'(I5,X,I5)') 18,NIT0*NIT1+1
      WRITE(40,'(''time (ns)''                              )')
      WRITE(40,'(''collision frequency Rmom (~ms^-^1)''  )')
      WRITE(40,'(''collision frequency Rexc (~ms^-^1)''  )')
      WRITE(40,'(''collision frequency Rexv (~ms^-^1)''  )')
      WRITE(40,'(''collision frequency Rion (~ms^-^1)''  )')
      WRITE(40,'(''collision frequency Ratt (~ms^-^1)''  )')
      WRITE(40,'(''collision frequency E*Ra (eV~ms^-^1)'')')
      WRITE(40,'(''mean energy (eV)''                       )')
      WRITE(40,'(''diffusion coefficient Ds (cm^2/~ms)'' )')
      WRITE(40,'(''drift velocity Ws (cm/~ms)''          )')
      WRITE(40,'(''drift velocity Vd (cm/~ms)''          )')
      WRITE(40,'(''drift velocity Ri/a (cm/~ms)''        )')
      WRITE(40,'(''drift velocity Ws-aDs (cm/~ms)''      )')
      WRITE(40,'(''number of electrons''                 )')
      WRITE(40,'(''graduation factor''                   )')
      WRITE(40,'(''graduation coefficient (cm^-^1)''     )')
      WRITE(40,'(''energy gain (Vd) (eVs^-^1)''          )')
      WRITE(40,'(''energy loss (eVs^-^1)''               )')
      WRITE(40,'(''energy gain (eVs^-^1)''               )')
```

Constants and Variables

`QMOM` $Nq_{\mathrm{mom}}(\epsilon)$ (cm^{-1})
`QEXC` $Nq_{\mathrm{ex}}(\epsilon)$ (cm^{-1})
`QEXV` $Nq_{\mathrm{ex,v}}(\epsilon)$ (cm^{-1})
`QION` $Nq_{\mathrm{ion}}(\epsilon)$ (cm^{-1})
`QATT` $Nq_{\mathrm{att}}(\epsilon)$ (cm^{-1})
`QTTL` $Nq_{\mathrm{T}}(\epsilon)$ (cm^{-1})

`FNUL` the probability of no collision
`FMOM,FEXC,FEXV,FION,FATT`
the ratios of colliding electrons
`GION` the distribution ratio of electrons after ionization

`RSCT` the scattering ratio $(1/2)\sin\theta\Delta\theta$

`RCEL` the volume of a cell $(\mathrm{cms}^{-1})^3$
`RDR0` the ratio of electrons remaining in $C_{l,i,j}$
`RDR1` the ratio of electrons flowing out of $C_{l,i,j}$ to $C_{l,i,j+1}$
`RDR2` the ratio of electrons flowing out of $C_{l,i,j}$ to $C_{l\pm1,i\pm1,j}$

`FMB0,FMB1`
factors to determine a Maxwellian distribution

```
      WRITE(40,'(F12.3    ))') 0.0
      WRITE(40,'(6(E12.6,X))') 0.0, 0.0 ,0.0 ,0.0 ,0.0 ,0.0
      WRITE(40,'(6(E12.6,X))') FEME,0.0 ,0.0 ,0.0 ,0.0 ,0.0
      WRITE(40,'(6(E12.6,X))') SPN0,0.0 ,0.0 ,0.0 ,0.0 ,0.0
* ---------- passage of time ----------------------------------------
      DO 0300 IIT0=0,NIT0-1
      DO 0250 IIT1=0,NIT1-1
      DO 0200 IIT2=0,NIT2-1
* ---------- collision & scattering ---------------------------------
      DO 0120 IENG=0,NENG
        FEI0(IENG)=0.0
 0120 CONTINUE
      DO 0130 IANG=0,NANG-1
      DO 0130 IENG=0,NENG-1
        FEI0(IENG)=FEI0(IENG)+FET0(IENG,IANG)
 0130 CONTINUE
      FISM=0.0
      REFF=0.0
      DO 0140 IENG=NENG-1,0,-1
        FISM=FISM+FEI0(IENG+NION  )*GION(IENG+NION  )
     >           +FEI0(IENG+NION+1)*GION(IENG+NION+1)
        FEI1(IENG)=FEI0(IENG     )*FMOM(IENG     )
     >             +FEI0(IENG+NEXC)*FEXC(IENG+NEXC)
     >             +FEI0(IENG+NEXV)*FEXV(IENG+NEXV)
     >             +FISM
        REFF=REFF+FEI0(IENG)*(FION(IENG)-FATT(IENG))
 0140 CONTINUE
      DO 0150 IANG=0,NANG-1
      DO 0150 IENG=0,NENG-1
        FET1(IENG,IANG)=FNUL(IENG)*FET0(IENG,IANG)+FEI1(IENG)*RSCT(IANG)
 0150 CONTINUE
* ---------- drift --------------------------------------------------
      RFWD=0.0
      DO 0160 IANG=0,NAHF-1
      DO 0160 IENG=0,NENG-1
        RFWD=RFWD+FET1(IENG,IANG)*RDR2(IENG,IANG)
 0160 CONTINUE
      RBWD=0.0
      DO 0170 IANG=NAHF,NANG-1
      DO 0170 IENG=   0,NENG
        RBWD=RBWD+FET1(IENG,IANG)*RDR2(IENG,IANG)
 0170 CONTINUE
      RNEL=RFWD+RBWD-REFF
      EAXP=(RNEL+SQRT(ABS(RNEL**2-4.0*RFWD*RBWD)))/RBWD*0.5
      EAXN=1.0/EAXP
      DO 0180 IANG=0,NAHF-1
      DO 0180 IENG=0,NENG
        FET0(IENG,IANG)=FET1(IENG  ,IANG  )*RDR0(IENG  ,IANG  )
     >                 +FET1(IENG  ,IANG+1)*RDR1(IENG  ,IANG+1)
     >                 +FET1(IENG-1,IANG  )*RDR2(IENG-1,IANG  )*EAXN
 0180 CONTINUE
      DO 0190 IANG=NAHF,NANG-1
      DO 0190 IENG=   0,NENG-1
        FET0(IENG,IANG)=FET1(IENG  ,IANG  )*RDR0(IENG  ,IANG  )
     >                 +FET1(IENG  ,IANG+1)*RDR1(IENG  ,IANG+1)
     >                 +FET1(IENG+1,IANG  )*RDR2(IENG+1,IANG  )*EAXP
 0190 CONTINUE
 0200 CONTINUE
* ---------- sampling (interval TSM1) -------------------------------
      DO 0210 IENG=0,NENG-1
        FE00(IENG)=0.0
        FE01(IENG)=0.0
 0210 CONTINUE
      DO 0220 IANG=0,NANG-1
      DO 0220 IENG=0,NENG-1
        FET1(IENG,IANG)=FET1(IENG,IANG)+FET0(IENG,IANG)
        FE00(IENG)=FE00(IENG)+FET1(IENG,IANG)
        FE01(IENG)=FE01(IENG)+FET1(IENG,IANG)*CCOS(IANG)
 0220 CONTINUE
      SPNE=0.0
      SPME=0.0
      SPVD=0.0
      SPVE=0.0
      SPDS=0.0
      RMOM=0.0
      REXC=0.0
      REXV=0.0
      RION=0.0
      RATT=0.0
      RATE=0.0
      DO 0230 IENG=0,NENG-1
        SPNE=SPNE+FE00(IENG)
        SPME=SPME+FE00(IENG)*CENG(IENG)
        SPVD=SPVD+FE01(IENG)*CVLC(IENG)
        SPVE=SPVE+FE01(IENG)*CVLC(IENG)*CENG(IENG)
        SPDS=SPDS+FE00(IENG)*CVLC(IENG)/QTTL(IENG)
        RMOM=RMOM+FE00(IENG)*FMOM(IENG)
        REXC=REXC+FE00(IENG)*FEXC(IENG)
        REXV=REXV+FE00(IENG)*FEXV(IENG)
        RION=RION+FE00(IENG)*FION(IENG)
        RATT=RATT+FE00(IENG)*FATT(IENG)
        RATE=RATE+FE00(IENG)*FATT(IENG)*CENG(IENG)
 0230 CONTINUE
```

Constants and Variables

FET0	$F(\epsilon,\theta)$ before collision
FEI0	$F(\epsilon)$ before collision
FISM	the number of electrons after ionization
FEI1	$F(\epsilon)$ after collision
FET1	$F(\epsilon,\theta)$ after collision
REFF	$n_{\rm ion}-n_{\rm att}$
RBWD	$n_{\rm b,out}$
RFWD	$n_{\rm f,out}$
EAXN	$\exp(-\bar{\alpha}\Delta x)$
EAXP	$\exp(+\bar{\alpha}\Delta x)$
SPNE	the number of electrons n
SPME	the mean electron energy $\bar{\epsilon}$ (eV)
SPVD	the drift velocity $v_{\rm d}$ (cmμs^{-1})
SPVE	the energy-weighted drift velocity $\tilde{v}_{\rm d}$ (eVcmμs^{-1})
SPDS	the diffusion coefficient $D_{\rm s}$ (cm$^2\mu$s^{-1})
SPAL	the effective ionization coefficient $\bar{\alpha}$ (cm^{-1})
RMOM	$R_{\rm mom}$ (μs^{-1})
REXC	$R_{\rm ex}$ (μs^{-1})
REXV	$R_{\rm ex,v}$ (μs^{-1})
RION	$R_{\rm ion}$ (μs^{-1})
RATT	$R_{\rm att}$ (μs^{-1})
RATE	$\tilde{R}_{\rm att}$ (eVμs^{-1})

```
      SPWS=CVLC(0)/QTTL(0)*(FE00(1)/DENG-FE00(0)/CENG(0))*0.5
      DO 0240 IENG=1,NENG-1
        SPWS=SPWS+CVLC(IENG)/QTTL(IENG)
     >           *(  (FE00(IENG+1)-FE00(IENG-1))/DENG
     >              -FE00(IENG)/CENG(IENG)  )*0.5
 0240 CONTINUE
      FNRM=1.0/SPNE/TUNT        *1.0E-06
      RMOM=RMOM*FNRM
      REXC=REXC*FNRM
      REXV=REXV*FNRM
      RION=RION*FNRM
      RATT=RATT*FNRM
      RATE=RATE*FNRM
      SPAL= LOG(EAXP)*DXIN
      SPME= SPME/SPNE
      SPDS= SPDS/SPNE/3.0       *1.0E-06
      SPWS=-SPWS/SPNE/3.0*EFLD  *1.0E-06
      SPVD= SPVD/SPNE           *1.0E-06
      SPVE= SPVE/SPNE           *1.0E-06
      SPV1=(RION-RATT)/SPAL
      SPV2= SPWS-SPAL*SPDS
      EBLS=REXC*EEXC+REXV*EEXV+RION*EION+RATE
      EBGN=EFLD*SPVD-SPAL*SPVE
      WRITE(40,'(F12.3     )') (IIT0*TSM0+(IIT1+1)*TSM1)*1.0E+09
      WRITE(40,'(6(E12.6,X))') RMOM,REXC,REXV,RION,RATT,RATE
      WRITE(40,'(6(E12.6,X))') SPME,SPDS,SPWS,SPVD,SPV1,SPV2
      WRITE(40,'(6(E12.6,X))') SPNE,EAXP,SPAL,SPVE,EBLS,EBGN
 0250 CONTINUE
*  ---------- sampling (interval TSM0) ---------------------------------
      DO 0260 IENG=0,NENG-1
        FE00(IENG)=0.0
        FE01(IENG)=0.0
        FE02(IENG)=0.0
        FE03(IENG)=0.0
        FE04(IENG)=0.0
        FE05(IENG)=0.0
 0260 CONTINUE
      DO 0270 IANG=0,NANG-1
      DO 0270 IENG=0,NENG-1
        FE00(IENG)=FE00(IENG)+FET1(IENG,IANG)
        FE01(IENG)=FE01(IENG)+FET1(IENG,IANG)*CC0S(IANG)
        FE02(IENG)=FE02(IENG)+FET1(IENG,IANG)*CP02(IANG)
        FE03(IENG)=FE03(IENG)+FET1(IENG,IANG)*CP03(IANG)
        FE04(IENG)=FE04(IENG)+FET1(IENG,IANG)*CP04(IANG)
        FE05(IENG)=FE05(IENG)+FET1(IENG,IANG)*CP05(IANG)
 0270 CONTINUE
      FNR0= 1.0/(SPNE*DENG)
      FNR1= 3.0/(SPNE*DENG)
      FNR2= 5.0/(SPNE*DENG)
      FNR3= 7.0/(SPNE*DENG)
      FNR4= 9.0/(SPNE*DENG)
      FNR5=11.0/(SPNE*DENG)
      DO 0280 IENG=0,NENG-1
        FE00(IENG)=FE00(IENG)*FNR0
        FE01(IENG)=FE01(IENG)*FNR1
        FE02(IENG)=FE02(IENG)*FNR2
        FE03(IENG)=FE03(IENG)*FNR3
        FE04(IENG)=FE04(IENG)*FNR4
        FE05(IENG)=FE05(IENG)*FNR5
 0280 CONTINUE
      WRITE(41,'(I5,X,I5)') 6,NENG/NDIV+1
      WRITE(41,'(''electron energy (eV) (t='',F8.3,''ns)'')')
     >     (IIT0*TSM0+IIT1*TSM1)*1.0E+09
      WRITE(41,'(''energy distribution F_0'')')
      WRITE(41,'(''energy distribution F_1'')')
      WRITE(41,'(''energy distribution F_2'')')
      WRITE(41,'(''energy distribution F_3'')')
      WRITE(41,'(''energy distribution F_4'')')
      WRITE(41,'(''energy distribution F_5'')')
      WRITE(41,'(F8.4,6(X,E11.5))') 0.0, 0.0, 0.0, 0.0, 0.0, 0.0, 0.0
      DO 0290 IENG=0,NENG-NDIV,NDIV
        WRITE(41,'(F8.4,6(X,E11.5))')
     >    CENG(IENG),FE00(IENG),FE01(IENG),FE02(IENG),
     >               FE03(IENG),FE04(IENG),FE05(IENG)
 0290 CONTINUE
 0300 CONTINUE
      STOP
      END
```

Constants and Variables

`SPWS` the drift velocity W_s ($\mathrm{cm}\mu\mathrm{s}^{-1}$)

`EBLS,EBGN` the energy balance terms

`FE00,FE01,FE02,FE03,FE04,FE05` Legendre's polynomial expansion terms of $F(\epsilon)$; $F_n(\epsilon)$ $(n = 0, \cdots, 5)$

```
*  ======================================================================
*   collision cross sections of SF6
*     (QSF6A1,QSF6A2,QSF6A3,QSF6A4,QSF6A5,QSF6E1,QSF6E2,QSF6IO,QSF6MO)
*   H.Itoh, Y.Miura, N.Ikuta, Y.Nakao and H.Tagashira
*     J.Phys.D: Appl.Phys. 21 (1988) 922-930
*   H.Itoh, T.Matsumura, K.Satoh, H.Date, Y.Nakao and H.Tagashira
*     J.Phys.D: Appl.Phys. 26 (1993) 1975-1979
*  ======================================================================
* attachment ( SF6- ) QSF6A1 ----------------------------------------
      FUNCTION QSF6A1(EV)
      IF (EV .LE. 0.14) THEN
*       QSF6A1=(6.17E-02/SQRT(EV)*EXP(-(EV/4.5E-03)**2)
        QSF6A1=(6.17E-02          *EXP(-(EV/4.5E-03)**2)
     >                            +EXP(-EV/5.59E-02))*4.36E+02
      ELSE IF (EV .LE. 0.9746) THEN
        QSF6A1=EXP(1.183*EV**2-20.91*EV+6.477)
      ELSE
        QSF6A1=0.0
      END IF
      QSF6A1=QSF6A1  *3.5355
      RETURN
      END
* attachment ( SF5- ) QSF6A2 ----------------------------------------
      FUNCTION QSF6A2(EV)
      IF (EV .LE. 0.312) THEN
        QSF6A2=2.85*EV+5.419*EV**2+30.49*EV**3
      ELSE IF (EV .LE. 0.425) THEN
        QSF6A2=-34.75+268.1*EV-624.3*EV**2+468*EV**3
      ELSE IF (EV .LE. 1.05) THEN
        QSF6A2=8.751-22.15*EV+19.08*EV**2-5.592*EV**3
      ELSE
        QSF6A2=EXP(-10.42*EV+8.054)
      END IF
      QSF6A2=QSF6A2  *3.5355
      RETURN
      END
* attachment ( F- ) QSF6A3 ------------------------------------------
      FUNCTION QSF6A3(EV)
      IF (EV .LT. 2.19) THEN
        QSF6A3=0.0
      ELSE IF (EV .LE. 2.9) THEN
        QSF6A3=-0.1069+0.08552*EV-0.01676*EV**2
      ELSE IF (EV .LT. 3.32) THEN
        QSF6A3=0.0
      ELSE IF (EV .LE. 4.27) THEN
        QSF6A3=-0.2016+0.2133*EV-0.07421*EV**2+0.00851*EV**3
      ELSE IF (EV .LE. 5.59) THEN
        QSF6A3=0.7777-0.6913*EV+0.1856*EV**2-0.0153*EV**3
      ELSE IF (EV .LE. 7.95) THEN
        QSF6A3=0.9885-0.3216*EV+0.03252*EV**2-0.0009533*EV**3
      ELSE IF (EV .LE. 9.73) THEN
        QSF6A3=-0.3504+0.08087*EV-0.0045*EV**2
      ELSE IF (EV .LE. 11.1) THEN
        QSF6A3=1.397-0.2724*EV+0.01335*EV**2
      ELSE IF (EV .LE. 11.8) THEN
        QSF6A3=-3.3+0.5801*EV-0.02533*EV**2
      ELSE
        QSF6A3=EXP(-1.264*EV+10.91)
      END IF
      QSF6A3=QSF6A3  *3.5355
      RETURN
      END
* attachment ( SF4- ) QSF6A4 ----------------------------------------
      FUNCTION QSF6A4(EV)
      IF ((EV .GE. 3.92) .AND. (EV .LE. 8.25)) THEN
        QSF6A4=EXP(-0.3033*EV**4+7.573*EV**3-71.09*EV**2+296.4*EV-466.8)
      ELSE
        QSF6A4=0.0
      END IF
      QSF6A4=QSF6A4  *3.5355
      RETURN
      END
* attachment ( F2- ) QSF6A5 -----------------------------------------
      FUNCTION QSF6A5(EV)
      IF (EV .LE. 1.5) THEN
        QSF6A5=0.0
      ELSE IF (EV .LE. 3.27) THEN
        QSF6A5=EXP(2.932*EV**3-22.91*EV**2+56.52*EV-53.37)
      ELSE IF (EV .LE. 7.45) THEN
        QSF6A5=EXP(0.5554*EV**3-9.613*EV**2+52.82*EV-100.3)
      ELSE IF (EV .LE. 10.6) THEN
        QSF6A5=EXP(0.1216*EV**2-1.035*EV-9.723)
      ELSE IF (EV .LE. 11.7) THEN
        QSF6A5=EXP(-1.114*EV**2+25.12*EV-148.0)-0.00012
      ELSE
        QSF6A5=EXP(-0.9386*EV**2+21.0*EV-123.9)
      END IF
      QSF6A5=QSF6A5  *3.5355
      RETURN
      END
```

```
* excitation ( SF6 ) QSF6E1 ------------------------------------------
      FUNCTION QSF6E1(EV)
      IF (EV .LE. 9.8) THEN
        QSF6E1=0.0
      ELSE IF (EV .LE. 20.3) THEN
        QSF6E1=-735.6/EV**2+83.24/EV-0.8345
      ELSE
        QSF6E1=34.74*EV**(-1.048)
      END IF
      QSF6E1=QSF6E1*1.08  *3.5355
      RETURN
      END
* vibration ( SF6 ) QSF6E2 -------------------------------------------
      FUNCTION QSF6E2(EV)
      IF (EV .LE. 0.095) THEN
        QSF6E2=0.0
      ELSE IF (EV .LE. 0.247) THEN
        QSF6E2=-0.5472/EV**2+4.425/EV+14.06
      ELSE IF (EV .LE. 0.505) THEN
        QSF6E2=EXP(11.19*EV**3-13.91*EV**2+4.663*EV+2.664)
      ELSE IF (EV .LE. 1.03) THEN
        QSF6E2=EXP(0.3166*EV**2-1.341*EV+3.509)
      ELSE
        QSF6E2=22.0*10**(-0.2645*EV)
      END IF
      QSF6E2=QSF6E2  *3.5355
      RETURN
      END
* ionization ( SF6 ) QSF6IO ------------------------------------------
      FUNCTION QSF6IO(EV)
      IF (EV .LE. 15.8) THEN
      QSF6IO=0.0
      ELSE IF (EV .LE. 38.9) THEN
        QSF6IO=4.715-0.6943*EV+0.0306*EV**2-3.508E-4*EV**3
      ELSE IF (EV .LE. 122.0) THEN
        QSF6IO=6.986-EXP(-1.4E-4*EV**2-0.0145*EV+2.07)
      ELSE IF (EV .LE. 201.0) THEN
        QSF6IO=4.364+0.0323*EV-9.987E-5*EV**2
      ELSE
        QSF6IO=EXP(-1.15E-3*EV+2.151)
      END IF
      QSF6IO=QSF6IO  *3.5355
      RETURN
      END
* momentam transfer ( SF6 ) QSF6MO -----------------------------------
      FUNCTION QSF6MO(EV)
      IF (EV .LE. 1.61) THEN
        QSF6MO=16.02-17.7*EV+11.55*EV**2-2.258*EV**3
      ELSE IF (EV .LE. 10.1) THEN
        QSF6MO=4.481+2.417*EV-0.1563*EV**2+0.001238*EV**3
      ELSE IF (EV .LE. 74.0) THEN
        QSF6MO=EXP(0.000153*EV**2-0.0305*EV+2.952)
      ELSE
        QSF6MO=7.722*10**(-0.003*EV)
      END IF
      QSF6MO=QSF6MO  *3.5355
      RETURN
      END
```

B.5 Moment Equations for Wr in a Model Gas

```
* ======================================================================
*  "Propagator Method" for Wr (the centroid drift vellocity)
*                      from moment equations
*
*  Hirotake Sugawara 1996.02.24.
*  Applied Electricity Laboratory,
*  Dept. of Electrical Eng., Hokkaido Univ., N13 W8 Sapporo 060 Japan
*  TEL 011-706-6482, FAX 011-706-7890, MAIL sgwr@e5.hines.hokudai.ac.jp
* ======================================================================
* ---------- initial setting -------------------------------------------
      PARAMETER ( NENG=8000       , NANG=72         , NAHF=NANG/2     ,
     >            KENG=400        ,
     >            EBYP=100.0      , GPRS=1.0        , EMAX=040.0      ,
     >            TLIM=10.000D-09 , TSM0=10.000D-09 ,
     >            TSM1=01.000D-09 , TUNT=00.100D-12 ,
     >            DENG=EMAX/(NENG*1.0)              ,
     >            EFLD=EBYP*GPRS  , DXXX=DENG/EFLD  ,
     >            EEXC= 9.0       , KEXC=EEXC/DENG+0.5              ,
     >            EION= 1.0       , KION=EION/DENG+0.5              ,
     >            NSUP=NENG+KEXC+1                  ,
     >            ECHG=1.602D-19  , EMAS=9.109D-28  )
      REAL   FET0(-1:NENG,0:NANG),FET1(-1:NENG,0:NANG),
     >       FCM0(-1:NENG,0:NANG),FCM1(-1:NENG,0:NANG),
     >       RAC0(-1:NENG,0:NANG),RAC1(-1:NENG,0:NANG),
     >       RAC2(-1:NENG,0:NANG)
      REAL   FEI0(0:NSUP),FEI1(0:NSUP),FISM(0:NSUP),RSCT(0:NANG),
     >       FCI0(0:NSUP),FCI1(0:NSUP),FICM(0:NSUP),
     >       FNEI(0:NENG),FNEA(0:NENG),
     >       FCMI(0:NENG),FCMA(0:NENG),
     >       QMOM(0:NSUP),RMOM(0:NSUP),FMOM(0:NSUP),
     >       QEXC(0:NSUP),REXC(0:NSUP),FEXC(0:NSUP),
     >       QATT(0:NSUP),RATT(0:NSUP),
     >       QION(0:NSUP),RION(0:NSUP),FION(0:NSUP),GION(0:NSUP),
     >       QTTL(0:NSUP),FNUL(0:NSUP)
      REAL   BENG(0:NSUP),CENG(0:NSUP),
     >       BVLC(0:NSUP),CVLC(0:NSUP),
     >       BANG(0:NANG),CANG(0:NANG),
     >       BSIN(0:NANG),
     >       BCOS(0:NANG),CCOS(0:NANG),
     >       CP00(0:NANG),CP01(0:NANG),CP02(0:NANG),
     >       CP03(0:NANG),CP04(0:NANG),CP05(0:NANG)
      REAL   FE00(0:NENG),FE01(0:NENG),FE02(0:NENG),
     >       FE03(0:NENG),FE04(0:NENG),FE05(0:NENG)
* ---------- constants -------------------------------------------------
      PI00=ATAN(1.0)*4.0
      DANG=PI00/REAL(NANG)
      FCEV=2.0*ECHG/EMAS*1.0D+07
      FCVE=0.5*EMAS/ECHG*1.0D-07
      DACC=ECHG*EFLD/EMAS*1.0D+07  *TUNT
      NIT0=NINT(TLIM/TSM0)
      NIT1=NINT(TSM0/TSM1)
      NIT2=NINT(TSM1/TUNT)
      DO 0010 IENG=0,NENG
        BENG(IENG)=DENG*REAL(IENG)
        BVLC(IENG)=SQRT(BENG(IENG)*FCEV)
 0010 CONTINUE
      DO 0020 IENG=0,NENG-1
        CVLC(IENG)=(BVLC(IENG)+BVLC(IENG+1))*0.5
        CENG(IENG)=CVLC(IENG)**2*FCVE
 0020 CONTINUE
      DO 0030 IANG=0,NANG
        BANG(IANG)=REAL(IANG)*DANG
        BSIN(IANG)=SIN(BANG(IANG))
        BCOS(IANG)=COS(BANG(IANG))
        CANG(IANG)=(REAL(IANG)+0.5)*DANG
        CCOS(IANG)=COS(CANG(IANG))
        CP00(IANG)=1.0
        CP01(IANG)=CCOS(IANG)
        CP02(IANG)=(CCOS(IANG)*CP01(IANG)* 3.0-CP00(IANG)* 1.0)/ 2.0
        CP03(IANG)=(CCOS(IANG)*CP02(IANG)* 5.0-CP01(IANG)* 2.0)/ 3.0
        CP04(IANG)=(CCOS(IANG)*CP03(IANG)* 7.0-CP02(IANG)* 3.0)/ 4.0
        CP05(IANG)=(CCOS(IANG)*CP04(IANG)* 9.0-CP03(IANG)* 4.0)/ 5.0
 0030 CONTINUE
* ---------- arrays for collisions -------------------------------------
      DO 0040 IENG=0,NENG-1
        CALL CASE3(CENG(IENG),QM,QE,QI,QT)
        QMOM(IENG)= QM  *GPRS
        QEXC(IENG)= QE  *GPRS
        QION(IENG)= QI  *GPRS
        QATT(IENG)= 0.0
        QTTL(IENG)= QT  *GPRS
 0040 CONTINUE
```

Constants and Variables

NENG	the number of divisions for ϵ
NANG	the number of divisions for θ
EBYP	E/p (Vcm^{-1}Torr^{-1})
GPRS	the gas pressure p (Torr)
EMAX	$\epsilon_{\max}$ (eV)
TLIM	the simulation time (s)
TSM0	the sampling interval (s) for $F(\epsilon)$
TSM1	the sampling interval (s) for electron swarm parameters
TUNT	the time step Δt (s)
DENG	the cell width $\Delta\epsilon$ (eV)
EFLD	the electric field E (Vcm^{-1})
DXXX	$\Delta x = \Delta\epsilon/(eE)$ (cm)
EEXC	ϵ_{ex} (eV)
EION	ϵ_{ion} (eV)
KEXC	$\epsilon_{ex}/\Delta\epsilon$
KION	$\epsilon_{ion}/\Delta\epsilon$
NSUP	the number of divisions for ϵ with margin
ECHG	$e = 1.602 \times 10^{-19}$ C
EMAS	$m = 9.109 \times 10^{-28}$ g
PI00	$\pi = 3.14159265\cdots$
DANG	the cell width $\Delta\theta$ (rad)
FCEV	$v_1 = 5.79 \times 10^7$ cms^{-1}
FCVE	$1/v_1$
DACC	the acceleration $a\Delta t$ (cms^{-1})
NIT0,NIT1,NIT2	iteration cycles
IENG	subscript i of ϵ_i and v_i
BENG	$\epsilon_i = i\Delta\epsilon$ (eV)
BVLC	$v_i = \sqrt{2\epsilon_i/m}$ (cms^{-1})
CVLC	$\bar{v}_i$ (cms^{-1})
CENG	$\bar{\epsilon}_i$ (eV)
IANG	subscript j of θ_j
BANG	$\theta_j = j\Delta\theta$ (rad)
BSIN	$\sin\theta_j$
BCOS	$\cos\theta_j$
CANG	$\bar{\theta}_j$ (rad)
CCOS	$\cos\bar{\theta}_j$
CP00,CP01,CP02,CP03,CP04,CP05	Legendre's polynomials $P_n(\cos\bar{\theta}_j)$ $(n = 0,\cdots,5)$
QMOM	$Nq_{\mathrm{mom}}(\epsilon)$ (cm^{-1})
QEXC	$Nq_{\mathrm{ex}}(\epsilon)$ (cm^{-1})
QION	$Nq_{\mathrm{ion}}(\epsilon)$ (cm^{-1})
QTTL	$Nq_{\mathrm{T}}(\epsilon)$ (cm^{-1})

```
      DO 0050 IENG=0,NENG-1
*       QTTL(IENG)=QMOM(IENG)+QEXC(IENG)+QION(IENG)+QATT(IENG)
        FNUL(IENG)=EXP(-QTTL(IENG)*CVLC(IENG)*TUNT)
        FCOL      =(1.0-FNUL(IENG))/QTTL(IENG)
        FMOM(IENG)=FCOL*QMOM(IENG)
        FEXC(IENG)=FCOL*QEXC(IENG)
        FION(IENG)=FCOL*QION(IENG)
        GION(IENG)=FION(IENG)/REAL(DIM(IENG,KION)*2+1)*2.0
        RMOM(IENG)=QMOM(IENG)*CVLC(IENG)
        REXC(IENG)=QEXC(IENG)*CVLC(IENG)
        RATT(IENG)=QATT(IENG)*CVLC(IENG)
        RION(IENG)=QION(IENG)*CVLC(IENG)
 0050 CONTINUE
      DO 0060 IANG=0,NANG-1
        RSCT(IANG)=(BCOS(IANG)-BCOS(IANG+1))*0.5
 0060 CONTINUE
* ---------- arrays for acceleration ---------------------------------
      PI23=PI00*2.0/3.0
      DO 0070 IANG=0,NAHF-1
      DO 0070 IENG=0,NENG-1
        RCEL           =PI23 *(BVLC(IENG+1)**3-BVLC(IENG)**3)
     >                       *(BCOS(IANG)-BCOS(IANG+1))
        RAC1(IENG,IANG)=PI00 *(BVLC(IENG+1)**2-BVLC(IENG)**2)
     >                       *BSIN(IANG)**2                    *DACC/RCEL
        RAC2(IENG,IANG)=PI00 *BVLC(IENG+1)**2
     >                       *(BSIN(IANG+1)**2-BSIN(IANG)**2)  *DACC/RCEL
        RAC0(IENG,IANG)=1.0-RAC1(IENG,IANG)-RAC2(IENG,IANG)
 0070 CONTINUE
      DO 0080 IANG=NAHF,NANG-1
      DO 0080 IENG=   0,NENG-1
        RCEL           =PI23 *(BVLC(IENG+1)**3-BVLC(IENG)**3)
     >                       *(BCOS(IANG)-BCOS(IANG+1))
        RAC1(IENG,IANG)=PI00 *(BVLC(IENG+1)**2-BVLC(IENG)**2)
     >                       *BSIN(IANG)**2                    *DACC/RCEL
        RAC2(IENG,IANG)=PI00 *BVLC(IENG)**2
     >                       *(BSIN(IANG)**2-BSIN(IANG+1)**2)  *DACC/RCEL
        RAC0(IENG,IANG)=1.0-RAC1(IENG,IANG)-RAC2(IENG,IANG)
 0080 CONTINUE
      DO 0090 IANG=0,NANG-1
      DO 0090 IENG=0,NENG-1
        IF (RAC0(IENG,IANG) .LT. 0.0) THEN
          WRITE(6,*) 'ratio negative : cell No.(E,A) ',IENG,IANG
          WRITE(6,*) RAC0(IENG,IANG),RAC1(IENG,IANG),RAC2(IENG,IANG)
          STOP
        END IF
 0090 CONTINUE
* ---------- initial condition ----------------------------------------
      SPN0=1.0
      SPC0=0.0
      FEME=4.0
      FMB0=2.0*PI00*(1.5/PI00/FEME)**1.5*DENG  *0.5
      FMB1=-1.5/FEME
      DO 0100 IENG=0,NENG-1
        FEI0(IENG)=FMB0*SQRT(CENG(IENG))*EXP(FMB1*CENG(IENG))
        DO 0100 IANG=0,NANG-1
          FET0(IENG,IANG)=FEI0(IENG)*RSCT(IANG)
 0100 CONTINUE
      WRITE(40,'(I5,X,I5)') 15,NIT0*NIT1+1
      WRITE(40,'(''time (ns)''                          )')
      WRITE(40,'(''number of electrons (a.u.)''         )')
      WRITE(40,'(''ionization frequency (~ms^-^1)''     )')
      WRITE(40,'(''mean energy (eV)''                   )')
      WRITE(40,'(''drift velocity Wv (cm/~ms)''         )')
      WRITE(40,'(''center of mass G (cm)''              )')
      WRITE(40,'(''drift velocity Wr (cm/~ms)''         )')
      WRITE(40,'(''diffusion coefficient Dv (cm^2/~ms)'')')
      WRITE(40,'(''collision frequency (~ms^-^1) (mom)'')')
      WRITE(40,'(''collision frequency (~ms^-^1) (ion)'')')
      WRITE(40,'(''collision frequency (~ms^-^1) (att)'')')
      WRITE(40,'(''collision frequency (~ms^-^1) (exc)'')')
      WRITE(40,'(''moment generation (cm/~ms) (ion)''   )')
      WRITE(40,'(''moment loss       (cm/~ms) (att)''   )')
      WRITE(40,'(''moment variation  (cm/~ms) (i-a)''   )')
      WRITE(40,'(''Wr-Wv (cm/~ms)''                     )')
      WRITE(40,'(4(E12.6,X))') 0.0 , SPN0, 0.0 , 0.0
      WRITE(40,'(4(E12.6,X))') 0.0 , SPC0, 0.0 , 0.0
      WRITE(40,'(4(E12.6,X))') 0.0 , 0.0 , 0.0 , 0.0
      WRITE(40,'(4(E12.6,X))') 0.0 , 0.0 , 0.0 , 0.0
* ---------- passage of time ------------------------------------------
      DO 0270 IIT0=0,NIT0-1
      DO 0220 IIT1=0,NIT1-1
      DO 0170 IIT2=0,NIT2-1
```

Constants and Variables

FNUL the probability of no collision

FMOM,FEXM,FEXC,FION the ratios of colliding electrons

GION the distribution ratio of electrons after ionization

RMOM $R_{\mathrm{mom}}(\epsilon)$ (s^{-1})

REXC $R_{\mathrm{ex}}(\epsilon)$ (s^{-1})

RATT $R_{\mathrm{att}}(\epsilon)$ (s^{-1})

RION $R_{\mathrm{ion}}(\epsilon)$ (s^{-1})

RSCT the scattering ratio $(1/2)\sin\theta\Delta\theta$

RCEL the volume of a cell $(\mathrm{cms}^{-1})^3$

RDR0 the ratio of electrons remaining in $C_{l,i,j}$

RDR1 the ratio of electrons flowing out of $C_{l,i,j}$ to $C_{l,i,j+1}$

RDR2 the ratio of electrons flowing out of $C_{l,i,j}$ to $C_{l\pm1,i\pm1,j}$

SPN0 the number of initial electrons

SPC0 the initial value of the 1st order moment (cm)

FEME the initial value of the mean electron energy (eV)

```
* ---------- collision & scattering ----------------------------------
      DO 0110 IENG=0,NENG-1
        FEIO(IENG)=0.0
        FCIO(IENG)=0.0
 0110 CONTINUE
      DO 0120 IANG=0,NANG-1
      DO 0120 IENG=0,NENG-1
        FEIO(IENG)=FEIO(IENG)+FETO(IENG,IANG)
        FCIO(IENG)=FCIO(IENG)+FCMO(IENG,IANG)
 0120 CONTINUE
      FISM(NENG)=0.0
      DO 0130 IENG=NENG-1,0,-1
        FISM(IENG)=FISM(IENG+1)
     >            +FEIO(IENG+KION  )*GION(IENG+KION  )
     >            +FEIO(IENG+KION+1)*GION(IENG+KION+1)
        FICM(IENG)=FICM(IENG+1)
     >            +FCIO(IENG+KION  )*GION(IENG+KION  )
     >            +FCIO(IENG+KION+1)*GION(IENG+KION+1)
        FEI1(IENG)=FEIO(IENG       )*FMOM(IENG       )
     >            +FEIO(IENG+KEXC  )*FEXC(IENG+KEXC  )
     >            +FISM(IENG)
        FCI1(IENG)=FCIO(IENG       )*FMOM(IENG       )
     >            +FCIO(IENG+KEXC  )*FEXC(IENG+KEXC  )
     >            +FICM(IENG)
 0130 CONTINUE
      DO 0140 IANG=0,NANG-1
      DO 0140 IENG=0,NENG-1
        FET1(IENG,IANG)=FETO(IENG,IANG)*FNUL(IENG)+FEI1(IENG)*RSCT(IANG)
        FCM1(IENG,IANG)=FCMO(IENG,IANG)*FNUL(IENG)+FCI1(IENG)*RSCT(IANG)
 0140 CONTINUE
* ---------- acceleration --------------------------------------------
      DO 0150 IANG=0,NAHF-1
      DO 0150 IENG=0,NENG-1
        FETO(IENG,IANG)=FET1(IENG  ,IANG  )*RACO(IENG  ,IANG  )
     >                 +FET1(IENG  ,IANG+1)*RAC1(IENG  ,IANG+1)
     >                 +FET1(IENG-1,IANG  )*RAC2(IENG-1,IANG  )
        FCMO(IENG,IANG)=FCM1(IENG  ,IANG  )*RACO(IENG  ,IANG  )
     >                 +FCM1(IENG  ,IANG+1)*RAC1(IENG  ,IANG+1)
     >                 +FCM1(IENG-1,IANG  )*RAC2(IENG-1,IANG  )
     >                 +FET1(IENG-1,IANG  )*RAC2(IENG-1,IANG  )*DXXX
 0150 CONTINUE
      DO 0160 IANG=NAHF,NANG-1
      DO 0160 IENG=   0,NENG-1
        FETO(IENG,IANG)=FET1(IENG  ,IANG  )*RACO(IENG  ,IANG  )
     >                 +FET1(IENG  ,IANG+1)*RAC1(IENG  ,IANG+1)
     >                 +FET1(IENG+1,IANG  )*RAC2(IENG+1,IANG  )
        FCMO(IENG,IANG)=FCM1(IENG  ,IANG  )*RACO(IENG  ,IANG  )
     >                 +FCM1(IENG  ,IANG+1)*RAC1(IENG  ,IANG+1)
     >                 +FCM1(IENG+1,IANG  )*RAC2(IENG+1,IANG  )
     >                 -FET1(IENG+1,IANG  )*RAC2(IENG+1,IANG  )*DXXX
 0160 CONTINUE
 0170 CONTINUE
* ---------- sampling (interval TSM1) --------------------------------
      DO 0180 IENG=0,NENG-1
        FEOO(IENG)=0.0
        FCIO(IENG)=0.0
 0180 CONTINUE
      SPNE=0.0
      SPME=0.0
      SPWV=0.0
      SPDV=0.0
      SPCM=0.0
      PMOM=0.0
      PEXC=0.0
      PION=0.0
      PATT=0.0
      UION=0.0
      UATT=0.0
      DO 0190 IANG=0,NANG-1
      DO 0190 IENG=0,NENG-1
        FET1(IENG,IANG)=FET1(IENG,IANG)+FETO(IENG,IANG)
        FCM1(IENG,IANG)=FCM1(IENG,IANG)+FCMO(IENG,IANG)
        FEOO(IENG)=FEOO(IENG)+FET1(IENG,IANG)
        FCIO(IENG)=FCIO(IENG)+FCM1(IENG,IANG)
        SPWV=SPWV+FET1(IENG,IANG)*CVLC(IENG)*CCOS(IANG)
0190 CONTINUE
      DO 0200 IENG=0,NENG-1
        SPNE=SPNE+FEOO(IENG)
        SPCM=SPCM+FCIO(IENG)
        PMOM=PMOM+FEOO(IENG)*RMOM(IENG)
        PEXC=PEXC+FEOO(IENG)*REXC(IENG)
        PION=PION+FEOO(IENG)*RION(IENG)
        PATT=PATT+FEOO(IENG)*RATT(IENG)
        UION=UION+FCIO(IENG)*RION(IENG)
        UATT=UATT+FCIO(IENG)*RATT(IENG)
0200 CONTINUE
      SPRN=LOG(SPNE/SPNO)/TSM1
      DO 0210 IENG=0,NENG-1
        SPME=SPME+FEOO(IENG)*CENG(IENG)
        SPDV=SPDV+FEOO(IENG)*CVLC(IENG)**2/(QTTL(IENG)*CVLC(IENG)+SPRN)
0210 CONTINUE
```

Constants and Variables

FETO	$F(\epsilon,\theta)$ before collision
FEIO	$F(\epsilon)$ before collision
FCMO	$M_x(\epsilon,\theta)$ before collision
FCIO	$M_x(\epsilon)$ before collision
FISM	the number of electrons after ionization
FICM	the moment generation (cm) at ionization
FEI1	$F(\epsilon)$ after collision
FET1	$F(\epsilon,\theta)$ after collision
FCI1	$M_x(\epsilon)$ after collision
FCM1	$M_x(\epsilon,\theta)$ after collision
SPNE	the number of electrons n
SPCM	the centroid G (cm)
SPME	the mean electron energy $\bar{\epsilon}$ (eV)
SPWV	the drift velocity $W_{\rm v}$ (cmμs^{-1})
SPWR	the drift velocity $W_{\rm r}$ (cmμs^{-1})
SPDV	the diffusion coefficient $D_{\rm v}$ (cm$^2\mu$s^{-1})
SPRN	$R_{\rm ion}$ (μs^{-1})
PMOM	$R_{\rm mom}$ (μs^{-1})
PEXC	$R_{\rm ex}$ (μs^{-1})
PION	$R_{\rm ion}$ (μs^{-1})
PATT	$R_{\rm att}$ (μs^{-1})
UION	$R_{\rm ion}M_x$ (cmμs^{-1})
UATT	$R_{\rm att}M_x$ (cmμs^{-1})

```
      SPRN=SPRN                *1.0D-06
      SPME=SPME/SPNE
      SPWV=SPWV/SPNE           *1.0D-06
      SPCM=SPCM/SPNE
      SPWR=(SPCM-SPC0)/TSM1    *1.0D-06
      SPDV=SPDV/SPNE/3.0       *1.0D-06
      SPN0=SPNE
      SPC0=SPCM
      PMOM=PMOM/SPNE           *1.0D-06
      PEXC=PEXC/SPNE           *1.0D-06
      PION=PION/SPNE           *1.0D-06
      PATT=PATT/SPNE           *1.0D-06
      UION=UION/SPNE           *1.0D-06  -PION*SPCM
      UATT=UATT/SPNE           *1.0D-06  -PATT*SPCM
      WRITE(40,'(4(E12.6,X))') (IIT0*TSM0+(IIT1+1)*TSM1)*1.0D+09,
     >                          SPNE,SPRN,SPME
      WRITE(40,'(4(E12.6,X))') SPWV,SPCM,SPWR,SPDV
      WRITE(40,'(5(E12.6,X))') PMOM,PION,PATT,PEXC
      WRITE(40,'(4(E12.6,X))') UION,UATT,UION-UATT,SPWR-SPWV
 0220 CONTINUE
* ---------- sampling (interval TSM0) ---------------------------------
      DO 0230 IENG=0,NENG-1
        FE00(IENG)=0.0
        FE01(IENG)=0.0
        FE02(IENG)=0.0
        FE03(IENG)=0.0
        FE04(IENG)=0.0
        FE05(IENG)=0.0
 0230 CONTINUE
      DO 0240 IANG=0,NANG-1
      DO 0240 IENG=0,NENG-1
        FE00(IENG)=FE00(IENG)+FET1(IENG,IANG)*CP00(IANG)
        FE01(IENG)=FE01(IENG)+FET1(IENG,IANG)*CP01(IANG)
        FE02(IENG)=FE02(IENG)+FET1(IENG,IANG)*CP02(IANG)
        FE03(IENG)=FE03(IENG)+FET1(IENG,IANG)*CP03(IANG)
        FE04(IENG)=FE04(IENG)+FET1(IENG,IANG)*CP04(IANG)
        FE05(IENG)=FE05(IENG)+FET1(IENG,IANG)*CP05(IANG)
 0240 CONTINUE
      FNRM=1.0/(SPNE*DENG)
      DO 0250 IENG=0,NENG-1
        FE00(IENG)=FE00(IENG)*FNRM* 1.0
        FE01(IENG)=FE01(IENG)*FNRM* 3.0
        FE02(IENG)=FE02(IENG)*FNRM* 5.0
        FE03(IENG)=FE03(IENG)*FNRM* 7.0
        FE04(IENG)=FE04(IENG)*FNRM* 9.0
        FE05(IENG)=FE05(IENG)*FNRM*11.0
        FCI0(IENG)=FCI0(IENG)*FNRM-FE00(IENG)*SPCM
        FNEI(IENG)=FE00(IENG)*RION(IENG)  *1.0D-06
        FNEA(IENG)=FE00(IENG)*RATT(IENG)  *1.0D-06
        FCMI(IENG)=FCI0(IENG)*RION(IENG)  *1.0D-06
        FCMA(IENG)=FCI0(IENG)*RATT(IENG)  *1.0D-06
 0250 CONTINUE
      WRITE(41,'(I5,X,I5)') 13,KENG+1
      WRITE(41,'(''electron energy (eV) (t='',F8.3,''ns)'')')
     >     (IIT0+1)*TSM0*1.0D+09
      WRITE(41,'(''energy distribution F_0'')')
      WRITE(41,'(''energy distribution F_1'')')
      WRITE(41,'(''energy distribution F_2'')')
      WRITE(41,'(''energy distribution F_3'')')
      WRITE(41,'(''energy distribution F_4'')')
      WRITE(41,'(''energy distribution F_5'')')
      WRITE(41,'(''generation/loss of Ne (ion)''     )')
      WRITE(41,'(''generation/loss of Ne (att)''     )')
      WRITE(41,'(''generation/loss of Ne (net)''     )')
      WRITE(41,'(''generation/loss of Mx (ion)''     )')
      WRITE(41,'(''generation/loss of Mx (att)''     )')
      WRITE(41,'(''generation/loss of Mx (net)''     )')
      WRITE(41,'(''1st-order moment distribution Mx'')')
      WRITE(41,'(  F12.6   )') 0.0
      WRITE(41,'(6(E12.6,X))') 0.0 , 0.0 , 0.0 , 0.0 , 0.0 , 0.0
      WRITE(41,'(6(E12.6,X))') 0.0 , 0.0 , 0.0 , 0.0 , 0.0 , 0.0
      WRITE(41,'(1(E12.6,X))') 0.0
      DO 0260 IENG=0,NENG-NENG/KENG,NENG/KENG
        WRITE(41,'(  F12.6   )') (REAL(IENG)+0.5)*DENG
        WRITE(41,'(6(E12.6,X))') FE00(IENG),FE01(IENG),FE02(IENG),
     >                           FE03(IENG),FE04(IENG),FE05(IENG)
        WRITE(41,'(6(E12.6,X))') FNEI(IENG),FNEA(IENG),
     >                           FNEI(IENG)-FNEA(IENG),
     >                           FCMI(IENG),FCMA(IENG),
     >                           FCMI(IENG)-FCMA(IENG)
        WRITE(41,'(1(E12.6,X))') FCI0(IENG)
 0260 CONTINUE
 0270 CONTINUE
      STOP
      END
```

Constants and Variables

`FE00,FE01,FE02,FE03,FE04,FE05`
: Legendre's polynomial expansion terms of $F(\epsilon)$; $F_n(\epsilon)$ $(n = 0, \cdots, 5)$

`FNEI` $R_{\rm ion}(\epsilon)$ $(\mu{\rm s}^{-1})$
`FNEA` $R_{\rm att}(\epsilon)$ $(\mu{\rm s}^{-1})$
`FCMI` $R_{\rm ion}(\epsilon)M(\epsilon)$ $({\rm cm}\mu{\rm s}^{-1})$
`FCMA` $R_{\rm att}(\epsilon)M(\epsilon)$ $({\rm cm}\mu{\rm s}^{-1})$

```
* MODEL CROSS-SECTIONS QT(V)=1/V : CASE-3
      SUBROUTINE CASE3 ( EV, QM, QE, QI, QT )
* Q-TOTAL
      QT=47.5/SQRT(EV)
* Q-IONISATION [THRESHOLD=1.0 eV]
      IF ((EV .LT. 1.0) .OR. (EV .GT. 4.0)) THEN
        QI=0.0
      ELSE IF (EV .LE. 2.016) THEN
        QI=-21.69145+33.58734*SQRT(EV)-11.895894*(SQRT(EV))**2
      ELSE
        QI=-9.59606+16.45165*SQRT(EV)-5.8268102*(SQRT(EV))**2
      END IF
      QI=MAX(QI,0.0)
* Q-EXCITATION [THRESHOLD=9.0 eV]
      IF (EV .LT. 9.0) THEN
        QE=0.0
      ELSE IF (EV .LE. 43.56) THEN
        QE=-14.694+7.005*(SQRT(EV)+.02)-0.76*(SQRT(EV)+.02)**2
     >           +0.017*(SQRT(EV)+.02)**3
      ELSE IF (EV .LE. 108.16) THEN
        QE=52.02*(SQRT(EV)+.024)**(-1.458)
      ELSE
        QE=14.75*(SQRT(EV)+.033)**(-0.92)
      END IF
      QE=MAX(QE,0.0)
* Q-MOMENTUM TRANSFER
      QM=QT-QE-QI
      QM=QM*3.5355
      QE=QE*3.5355
      QI=QI*3.5355
      QT=QT*3.5355
      RETURN
      END
```

inches 1 2 3 4 5 6 7 8

cm 1 2 3 4 5 6 7 8 9 10 11 12 13 14 15 16 17 18 19

Kodak Color Control Patches

Blue Cyan Green Yellow Red Magenta White 3/Color Black

Kodak Gray Scale

C Y M

A 1 2 3 4 5 6 **M** 8 9 10 11 12 13 14 15 **B** 17 18 19